WYOMING STATE GEOLOGICAL SURVEY
Gary B. Glass, State Geologist

Proceedings of the First International Soda Ash Conference Volume II

edited by

John R. Dyni and Richard W. Jones



Public Information Circular No. 40

1998

Laramie, Wyoming

WYOMING STATE GEOLOGICAL SURVEY

Gary B. Glass, *State Geologist*

GEOLOGICAL SURVEY BOARD

Ex Officio

Jim Geringer, *Governor*
Philip L. Dubois, *President, The University of Wyoming*
Don J. Likwartz, *Oil and Gas Supervisor*
Gary B. Glass, *State Geologist*

Appointed

Ronald A. Baugh, *Casper*
Nancy M. Doelger, *Casper*
Victor R. Hasfurther, *Laramie*
Charles M. Love, *Rock Springs*
Stephen L. Payne, *Casper*

STAFF

Computer Services Unit
Susan McClendon - *Manager*

Geologic Sections
James C. Case, *Staff Geologist - Geologic Hazards*
Rodney H. De Bruin, *Staff Geologist - Oil and Gas*
Ray E. Harris, *Staff Geologist - Industrial Minerals and Uranium*
W. Dan Hausel, *Senior Economic Geologist - Metals and Precious Stones*
Robert M. Lyman, *Staff Geologist - Coal*
Alan J. Ver Ploeg, *Senior Staff Geologist - Geologic Mapping*

Publications Section
Richard W. Jones - *Editor*
Janet A. Van Nuys - *Editorial Assistant*
Kathryn S. Hastreiter - *Sales Manager*
Fred H. Porter - *Cartographer*
Phyllis A. Ranz - *Cartographer*

Laboratory Unit
Robert W. Gregory - *Laboratory Technician*

Supportive Services Section
Susanne G. Bruhnke - *Office Manager*
Vacant - *Administrative Secretary*

People with disabilities who require an alternative form of communication in order to use this publication should contact the Editor, Wyoming State Geological Survey at (307) 766-2286. TTY Relay Operator 1(800) 877-9975.

This and other publications available from:

Wyoming State Geological Survey
P.O. Box 3008
Laramie, Wyoming 82071-3008
(307) 766-2286 • FAX (307) 766-2605
E-mail: sales@wsgs.uwyo.edu

Text and cover printed on 50% recycled fiber paper. First printing of 750 copies by Vision Graphics, Incorporated, Cheyenne, Wyoming.

Proceedings of the First International Soda Ash Conference–Volume II, edited by John R. Dyni and Richard W. Jones.

ISBN 1-884589-14-6

Front cover: Photomicrograph of clean trona particles from sieve concentrates. Diameter of particles is not more than 0.5 millimeter (35-mesh screen). Photograph by Wayne Hazen; see article by Hazen (this volume), p. 177-183, for details.

WYOMING STATE GEOLOGICAL SURVEY
Gary B. Glass, State Geologist

Public Information Circular No. 40

PROCEEDINGS OF THE FIRST INTERNATIONAL SODA ASH CONFERENCE VOLUME II

Utilization of natural resources of sodium carbonate into the next century

Meeting in Rock Springs, Wyoming, June 10-12, 1997

edited by

John R. Dyni and Richard W. Jones

Laramie, Wyoming

1998

STATE OF WYOMING
1933
GEOLOGICAL SURVEY

Contents

Page

Introduction to Volume II v

Editors' preface to Volume II vii

Geology, exploration, and resources

Wyoming trona: An overview of the geology
R. Terry Leigh 1

Origin of the Green River trona deposit (from a chemical and other saline mineral perspective)
Donald E. Garrett 15

A mineralogic and stratigraphic profile of trona bed 17 in the Solvay trona mine near Green River, Wyoming
Paul L. Boni and William W. Atkinson, Jr. 21

The anomalous zone in bed 17
Michael Weller 33

Prospecting for Green River-type sodium carbonate deposits
John R. Dyni 37

Trona crystallization processes–Observations at Owens Lake, California, 1970-77
George I. Smith and Irving Friedman 49

The natural soda deposits of China
Chending Zhang 57

The Beypazari trona deposit, Ankara Province, Turkey
Cahit Helvaci 67

Leasing

Acquiring trona leases on Wyoming state lands
Harold D. Kemp and Ray E. Harris 105

Leasing federal sodium lands
Ted Murphy 109

The history of leasing sodium minerals on the Union Pacific land grant
Bob See and Neil Brown 113

Solution mining

Solution mining of Colorado nahcolite
Roger L. Day 121

Feasibility of trona solution mining
Edward C. Rosar and Wolfram H. Kube 131

A new technology for the soda ash deposits near Trona, California
James L. Fairchild, Michael E. Lovejoy, and Gail F. Moulton, Jr. 143

A model for solution mining trona
Henry W. Haynes, Jr. and Animesh Ukidwe 153

Processing and refining

Process selection criteria for refining trona to commercial products
Roger Aitala and Mark Aitala 163

Evolution of Wyoming soda ash processes
William Ramon (Ray) Frint 173

The Wold Benetron® process
Wayne Hazen 177

Microwave-induced wet calcination of trona
Robert D. Streuber and Chang Yul Cha 185

Environmental issues

Overview of air pollution issues facing the trona industry
David Gaige 195

Tailings disposal methods
David H. Scriven 201

Conference events

Road log for the geology field trip of June 13, 1997
Geology and outcrops of the trona-bearing rocks of the Green River Formation
William C. Culbertson 205

Luncheon talk of June 11, 1997
A new entrant's perspective of the Wyoming soda ash industry
John Wold 213

Frontispieces

Aerial view of Tg Soda Ash, Incorporated's trona mine and refinery viii
Aerial view of Solvay Minerals, Incorporated's trona mine and processing plant 36
Aerial view of General Chemical Corporation's trona mine and processing plant 104
Aerial view of White River Nahcolite Company's mine and processing plant 120
Aerial view of the trona mine and processing plant operated by FMC Wyoming Corporation 172
Aerial view of the trona mine and processing plant operated by OCI Wyoming, L.P. 212

Selected conversion factors ..... Inside Back Cover

Introduction to Volume II

The First International Soda Ash Conference (ISAC) was held in Rock Springs, Wyoming, June 10-12, 1997 under the auspices of the U.S. Geological Survey, the Wyoming State Geological Survey, and the U.S. Bureau of Land Management. The conference marked the 50th anniversary of the start-up of the Wyoming trona mining industry. The conference brought together technical experts in the soda ash industry including those involved in the economic geology, mining, and ore processing of soda ash together with soda ash information specialists. The purpose of the conference was to examine the state of the natural soda ash industry and trends and directions of the natural and synthetic soda ash industries as we approach the 21st century.

Volume I of the conference proceedings contains papers on the history of the soda ash industry in the United States and papers that discuss market trends in different parts of the world. Volume II contains technical papers on the geology and exploration for natural soda ash deposits, on conventional and new methods of mining and processing trona, and on environmental issues.

We had hoped to discuss several technical problems faced by the Wyoming trona industry. These include an analysis of the collapse at Solvay trona mine in February 1995 and the potential conflict between trona mining and petroleum exploration within the trona district. Neither of these problems had been resolved by the date of the conference, therefore, papers on these subjects could not be included. Another issue not discussed was air and water quality as related to mining and processing trona. We would like to see papers on these topics included in future conferences.

We wish to thank those who helped make this First ISAC a success. Our technical committee included Ray Harris (Wyoming State Geological Survey), Ted Murphy (U.S. Bureau of Land Management), Terry Leigh (Tg Soda Ash), and Neil Brown (Union Pacific Resources). We also wish to thank those who presented papers at the conference and who provided written texts for these two volumes of the conference proceedings.

The logistics of the conference were ably handled by Wil Radosevich and his staff (University of Wyoming Office of Conferences and Institutes). The staff at Western Wyoming College, where the technical sessions of the conference were held, provided quality support with projectionists, ushering, and catering of luncheons. We also thank the college staff for providing emergency evacuation of the conferees to the basement during a tornado warning as the meeting was in progress. Lastly, we would like to express our appreciation to the Wyoming Science, Technology, and Energy Authority, FMC Corporation, North American Chemical Company, Tg Soda Ash, Inc., and the U.S. Geological Survey for their financial contributions that helped make this conference a success.

We hope that this conference will be a beginning in a series of similar conferences on the natural and synthetic soda ash industries of the world and that we can meet again to discuss new ideas and examine other parts of the industry elsewhere in the world.

Dennis S. Kostick,
U.S. Geological Survey

John R. Dyni
U.S. Geological Survey, Emeritus

Conference Co-chairmen

STATE OF WYOMING
1933
GEOLOGICAL SURVEY

Editors' preface to Volume II

The editors of proceedings volume II for the first ISAC would like to thank all the authors that contributed to this publication. We hope the papers in this volume reflect the authors' high degree of professionalism and their hard work. We would also like to thank those unnamed people that reviewed the manuscripts before they were submitted for this volume. Their comments and suggestions certainly improved the overall quality of the papers and saved us much work.

The papers were reviewed first for technical and scientific content and then edited for style, language, and consistency. In some cases, word slides and speakers' notes from the oral presentations were transcribed into text manuscript and headings. The paper on the Beypazari trona deposit in Turkey was converted entirely to English language conventions, with apologies to the author. All the special characters, accents, and diacritical marks were dropped for clarity and consistency with other papers in this volume.

Units of measurement as used by the authors were retained; conversions from one system to another are included only when furnished by the author. The inside back cover of this publication contains conversion factors for the different units.

We acknowledge the assistance of Fred H. Porter and Phyllis A. Ranz, cartographers with the Wyoming State Geological Survey (WSGS), for their work in drafting, redrafting, or revising many of the illustrations. We are especially grateful to Janet A. Van Nuys, Editorial Assistant with the WSGS, for word processing, design and layout of the publication, and proofreading of the manuscripts. Ray E. Harris of the WSGS is acknowledged for his encouragement, guidance, and support throughout the production of both ISAC proceedings volumes. We also appreciate the assistance of Robert J. Machacek, who piloted the aircraft for the aerial photographs of the Wyoming trona mines and processing plants (used as frontispieces for various articles in this volume). Finally, we thank the organizers and committees of the First International Soda Ash Conference for the funding support necessary to produce the proceedings volumes.

John R. Dyni
U.S. Geological Survey, Emeritus

Richard W. Jones
Wyoming State Geological Survey



Frontispiece: Aerial view of Tg Soda Ash, Incorporated's trona mine and refinery northwest of Green River, Wyoming. In 1997, this operation produced about 2.5 million net short tons of trona from the underground mine and refined about 1.2 million short tons of soda ash (data from Wyoming State Inspector of Mines, Annual Report for 1997). Photograph by John R. Dyni, July, 1998.

Wyoming trona: An overview of the geology

R. Terry Leigh
Tg Soda Ash, Incorporated
Granger, Wyoming 82934

Abstract

Wyoming is often referred to as the "Soda Ash Capital of the World" because of the enormous world-class trona reserves found in the Green River Basin. Trona, sodium sesquicarbonate ($Na_2CO_3 \cdot NaHCO_3 \cdot 2H_2O$), was precipitated in a lacustrine environment during the restrictive stages of the Wilkins Peak Member of the Eocene Green River Formation in southwestern Wyoming. Textural variations of the bedded trona deposits are suggestive of multiple depositional scenarios.

Because it is composed of 70% sodium carbonate, trona is referred to as natural soda ash. The single major industrial product obtained from refining trona is soda ash. Over 90% of the United States soda ash is produced by five Wyoming trona companies. This equates to over 30% of the world's soda ash production.

The total resource of Wyoming trona deposits is estimated at 122 billion tonnes (metric tons), or 122 gigatonnes (Gt). Of this, 36 Gt of economical trona reserves are mineable by current technology, including conventional "hard rock" methods, mechanized extraction (drum-miner and boring machines), and hydraulically supported longwall shearing.

Introduction

The trona deposits of the Green River Basin in southwestern Wyoming are the world's largest resource of natural soda ash. The total resource in 22 persistent trona beds is estimated at 115.6 Gt [gigatonnes or billion metric tons (tonnes)] or 127.0 billion short tons of which 68.7 Gt (75.7 billion short tons) are bedded trona deposits and 46.9 Gt (51.7 billion short tons) are interbedded or intermixed trona and halite (Wiig and others, 1995). Economically mineable trona reserves are estimated at 36 Gt (40 billion short tons) of refined sodium carbonate (Kostick, 1991). The five trona companies annually produce over 90% of the domestic supply of soda ash, which equates to over 30% of the world's soda ash production.

The enormous trona deposits are associated with a saline facies within the Wilkins Peak Member of the Eocene Green River Formation. The accumulation of sediments from the surrounding tectonically active uplifts occurred in a large, subsiding, intermontane basin. Extensive alluvial plains of the Wasatch and Bridger Formations intertongued with and graded laterally into lacustrine sequences of the Green River Formation. These lacustrine deposits collected in a series of lakes (Lake Gosiute), which oscillated in size and depth in response to tectonic activity and climatic changes.

Thick deposits of evaporite minerals in the Wilkins Peak Member represent the only restrictive saline stage of the lakes. A cyclic pattern of oil shale development, followed by evaporite accumulation of trona, halite, or shortite, within marlstones and altered tuffs, is suggestive of their depositional relationship.

Of the 42 known trona beds, 25 exceed 1 meter (3 feet) in thickness and 300 km^2 (100 square miles) in areal extent (Culbertson, 1971). Identified in ascending order, these thicker trona beds are numbered 1 through 25 from the oldest (stratigraphically lowest) to the youngest (stratigraphically highest). Textural variations of the trona beds are indicative of multiple depositional scenarios. Situated in the southern three-quarters of the resource area, beds 1 through 18 are composed predominantly of light brown, fine-grained (1 mm to microcrystalline), "maple sugar" type trona. Halite is also common in these beds. In contrast, beds 19 through 25 are halite free and consist of amber (light to very dark), translucent, coarse-crystalline

(5 mm to 30 cm), fibrous, random to radiating bladelike crystal forms, commonly referred to as "root beer" type trona.

The mineral trona or sodium sesquicarbonate ($Na_2CO_3 \cdot NaHCO_3 \cdot 2H_2O$) is composed of over 70% sodium carbonate. Soda ash is the major industrial product refined from trona. Soda ash is utilized predominantly by the glass industry and as a component in the manufacture of various sodium compounds including sodium bicarbonate, caustic soda, sodium cyanide, sodium phosphates, and others. Approximately 40% of the soda ash production is exported (Breunig, 1998).

Geologic setting

Located in southwestern Wyoming during the early Tertiary Period, a large subsiding intermontane basin accumulated sediments derived from surrounding tectonically active uplifts: Rawlins uplift, Uinta, Granite, and Sierra Madre mountains and Wyoming, Gros Ventre, and Wind River ranges (**Figure 1**). Between 3000 and 6000 meters (10,000 to 20,000 feet) of continuous successions of predominantly fluvial and lacustrine deposits accumulated. Sediments eroded from the peripheral mountains created extensive alluvial plains and broad, flat pediments. Clastic wedges of the Wasatch and Bridger-Washakie Formations intertongue and grade laterally with the lacustrine sequences of the Green River Formation (**Figure 2**). The lacustrine sequences were deposited in a series of lakes (Lake Gosiute, **Figure 3**), which oscillated in size and depth in response to tectonic activity and climatic variation. Within the hydrogeographic basin of approximately 77,300 km² (48,500 square miles), the greatest expanses of Lake Gosiute and surrounding mud flats occurred during the Tipton and Laney stages. Bradley (1964) estimated that the lake expanded to over 24,000 km² (15,000 square miles) during the Laney stage. Total evaporation of Lake Gosiute during the restrictive phases of the Wilkins Peak stage is only speculated.

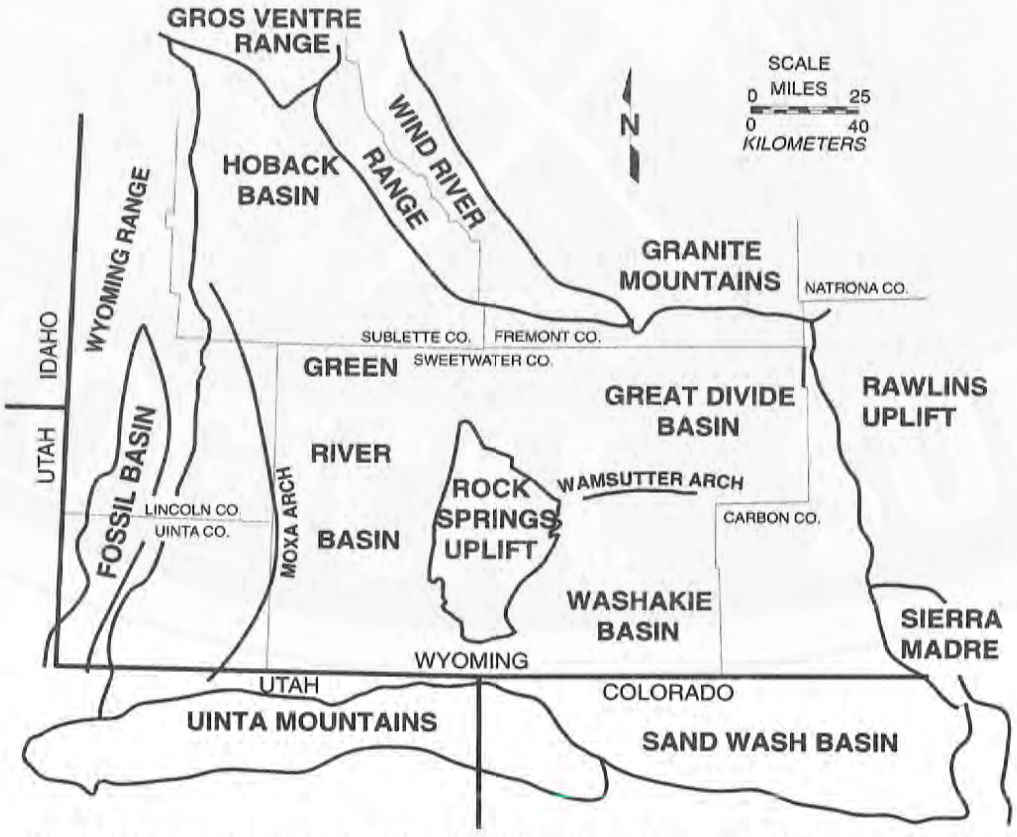


Figure 1. Structural features of southwestern Wyoming and portions of Utah and Colorado.

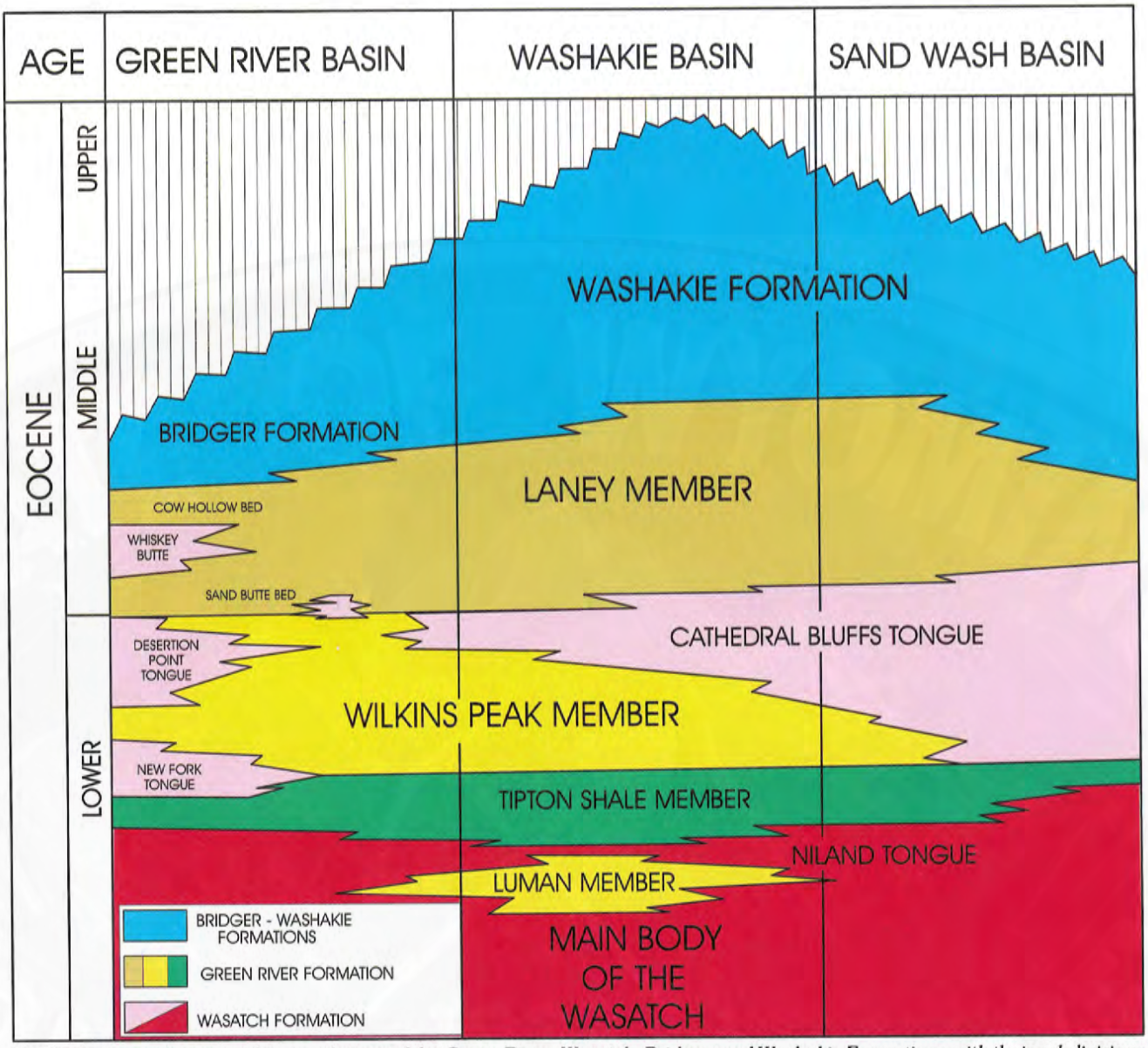


Figure 2. General stratigraphic correlations of the Green River, Wasatch, Bridger, and Washakie Formations with their subdivisions in southwestern Wyoming (after Sullivan, 1980).

Figure 4 illustrates the stratigraphic relationships of these formations within the Green River Basin. Fluvial sediments composing the Niland, Cathedral Bluffs, Desertion Point, and Whiskey Butte Tongues (Sullivan, 1980) of the Wasatch Formation (see **Figure 2**) transgressed into the basin. Additional fluvial sequences identified by Roehler (1991a, b; 1992a, b, c) include the Farson and Sand Butte beds. The Wilkins Peak Member of the Green River Formation in **Figure 4** is characterized by two distinct subdivisions. The lower Wilkins Peak is composed of primarily gray-green marlstones, oil shales, and tuffaceous marlstones. An increase in silicious detrital sediments and an increase in dolomitization distinguishes the upper Wilkins Peak. A third subdivision, the mid-Wilkins Peak, is suggested for the strata associated with trona beds 18 through 22, which contain increased amounts of detrital sediments with less dolomitization. A change in depositional environment is indicated for this third subdivision. Intertonguing with the Wilkins Peak at these subdivisional breaks are sequences of fluvial sediments of the Desertion Point Tongue of the Wasatch, which thickens to the west and south.

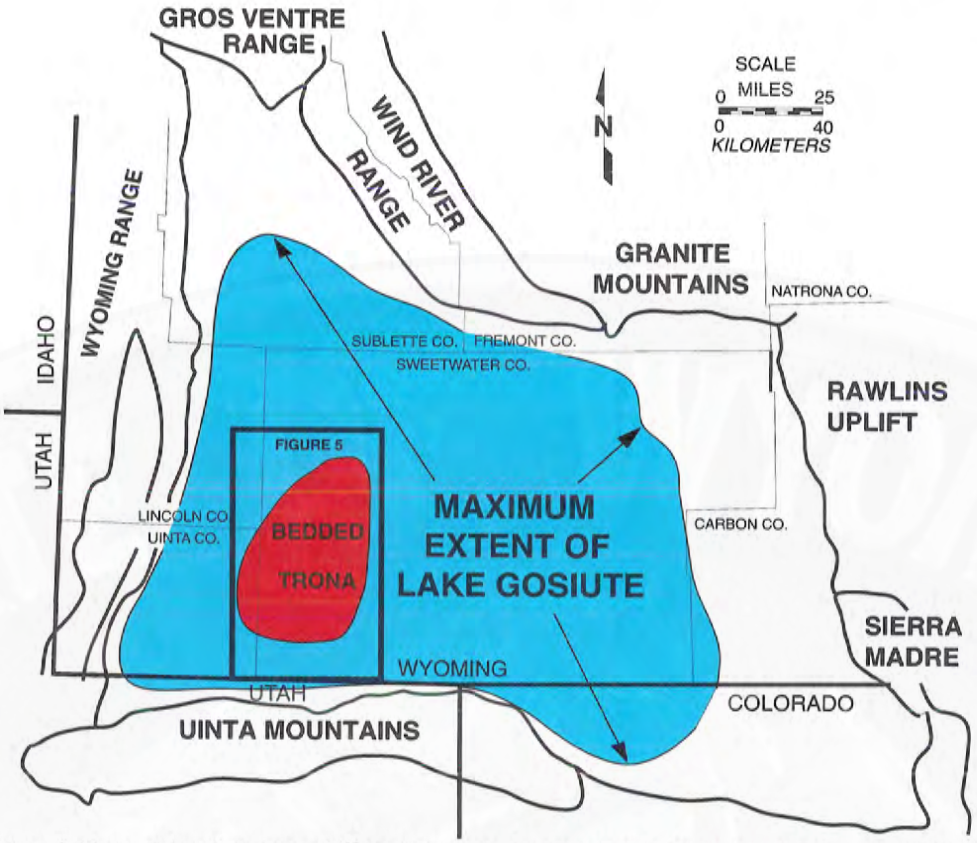


Figure 3. General location map of Wyoming trona deposits in relation to maximum extent of Lake Gosiute (modified from Sullivan, 1980).

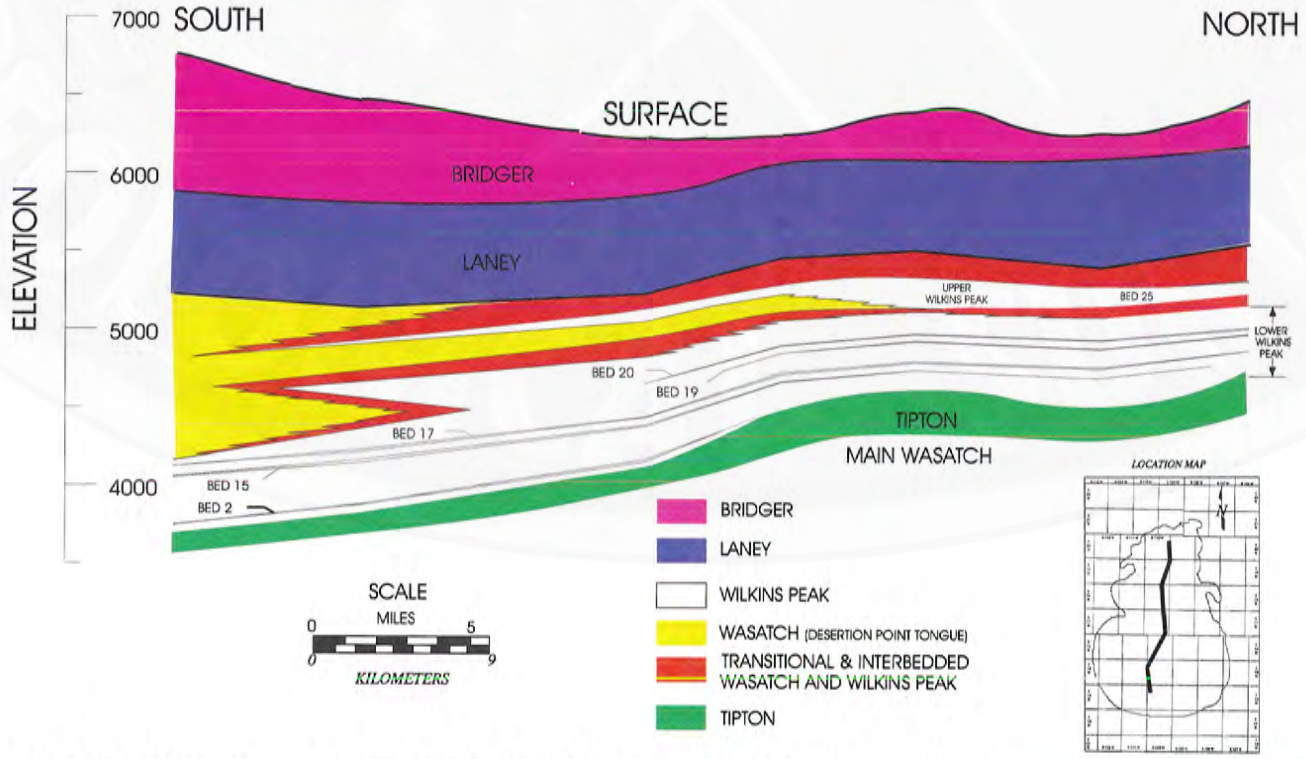


Figure 4. Stratigraphic south-north cross section through the Green River Basin, illustrating the transgression of the 25 major trona beds in relation to the fluvial influx of the Desertion Point Tongue of the Wasatch Formation. Location of section is shown on inset map. Outlined area on inset map is the BLM Known Sodium Leasing Area.

Physical characteristics of trona

Trona is a non-metallic industrial mineral of the compound sodium sesquicarbonate ($Na_2CO_3 \bullet NaHCO_3 \bullet 2H_2O$), which is a partially hydrated double salt of sodium carbonate (commonly known as soda ash) and sodium bicarbonate (commonly known as baking soda).

The following mineral characteristics of trona have been identified by Dana (1966):

crystal form – monoclinic, prismatic;

crystal habit – elongated, flattened with faces striated, parallel;

cleavage – perfect along {100} plane; fractures are uneven to subconchoidal;

color – clear to dark amber depending upon organic impurities;

luster – vitreous, glistening, translucent;

hardness – 2.5-3;

specific gravity – 2.14 g/cc;

taste – alkaline.

Trona deposits

Abundant saline minerals occur within the Wilkins Peak Member, which underlies an area of 3370 km^2 (1300 square miles) of the Green River Basin (Culbertson, 1971). Twenty-five trona and trona-halite beds, exceeding 1 meter (3 feet) in thickness and 300 km^2 (100 square miles) in areal extent, have been recognized along with 17 minor beds (Culbertson, 1966). **Figure 4** illustrates the correlation of selected trona beds.

The location map showing the extent of trona beds 1, 17, 20, and 25 (**Figure 5**), depicts the movement of the trona depocenter through time. Beds 1 through 18, which are located in the southern three-quarters of the resource area, have the greatest potential for mineral development with bed 1 reaching the greatest indicated thickness of 11.3 m (37 feet) and bed 17 occupying the greatest area of 2253 km^2 (870 square miles) (Burnside and Culbertson, 1979). Mixed trona and halite is common. A stable tectonic regime is indicated by the "layer cake" appearance of the depocenters for beds 1 through 18. Depocenter movement (from tectonic activity and/or climatic changes) during deposition of beds 19 through 25 is indicated. Located within the northern third of the resource area, these beds have limited areal extent, are halite free, and reach local thicknesses exceeding 4 m (13 feet). Stratigraphically younger than trona bed 25 are "black trona water" brines located north of the resource area at Eden, Wyoming. This suggests further depocenter movement to the north.

Wiig and others (1995) have reevaluated the trona resources within the Federal Government's Known Sodium Leasing Area (KSLA) (called the resource area throughout this paper) from the increased database since Burnside and Culbertson's (1979) estimate and have determined that only 22 of the original 25 major trona beds exceed four feet in thickness. Trona beds 13, 22, and 23 were deleted from the analysis. The total resources of the 22 persistent major trona beds have been revised to 115.6 Gt (127.4 billion short tons) or approximately 68.7 Gt (75.7 billion short tons) of bedded trona and 46.9 Gt (51.7 billion short tons) of interbedded or intermixed trona and halite. The U.S. Bureau of Mines (Kostick, 1991) estimated sodium carbonate reserves of 20 Gt (22 billion short tons), which equates to 36 Gt (40 billion short tons) of economically mineable trona reserves, assuming a conversion factor of 1.8 short tons of trona yielding 1 short ton of refined soda ash. Reserves represent only that quantity recoverable based on an average extraction-rate efficiency of 60% from room-and-pillar, longwall, and shortwall methods of underground mining, with a mining height restriction limiting the minimum total trona thickness to 1.8 m (6 feet). Secondary recovery of the remaining trona by liquid feed methods, and recovery of sodium carbonate from interbedded or intermixed trona and halite deposits, were excluded from the reserve calculations.

Depositional theories

The Wilkins Peak Member contains evaporite-rich cycles of saline minerals (trona, halite, and shortite) alternating with organic-rich oil shales within marlstones with abundant altered tuffs, which suggests a depositional relationship. Oil shales developed from preservation of aquatic organisms including algae

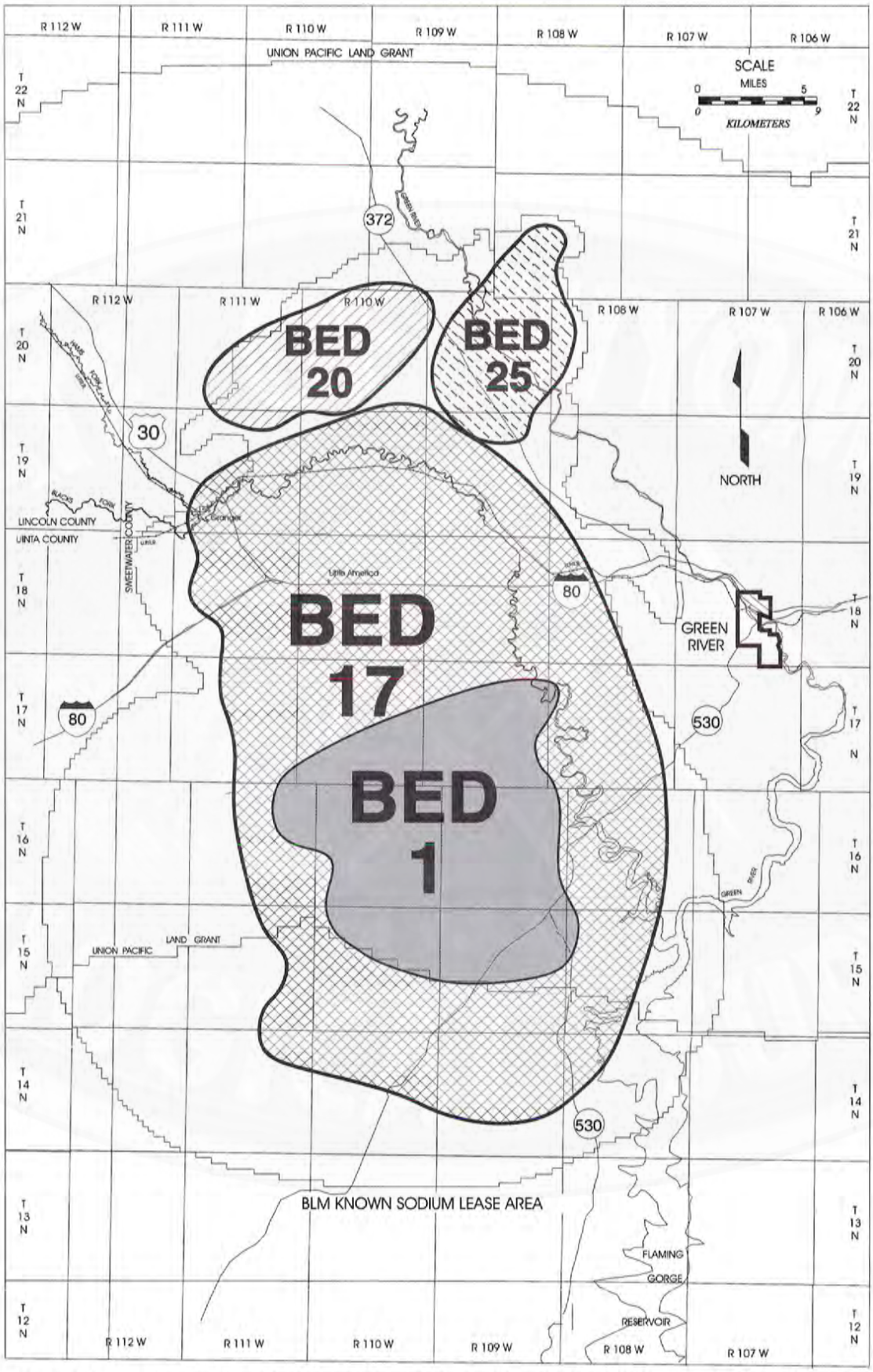


Figure 5. Location map of trona beds 1, 17, 20, and 25 within (greater than) their respective 6-foot isopach lines illustrating depocenter changes (modified from Burnside and Culbertson, 1979).

which flourished when lake conditions were favorable. As evaporation exceeded recharge, the lake became more saline. A release of carbon dioxide from these decaying organisms elevated its concentration, exceeding the partial pressure with respect to the atmosphere. Trona precipitation was triggered when saturation conditions were reached. A large source of sodium was supplied by the continual rain of volcanic ash which may have acted as nutrient for these organisms.

Other processes that could yield large quantities of carbonates and bicarbonates include: bacterial reduction of sulfates with bicarbonate production, hydrolysis of silicate minerals and volcanic ash, ammonia generation and reaction with carbonic acids and halite, and bicarbonate enriched springs and streams discharging from the margins of the basin.

Depositional models

Trona precipitation requires a specific range of weight% sodium and carbon dioxide in solution, a specific range of temperatures, and a specific range of relative concentration of other ions (calcium, magnesium, chlorides, sulfates, etc.). Two divergent theories have been proposed for the concentration of brines that lead to trona deposition: the stratified lake model and the playa-lake model.

The stratified lake model (**Figure 6**) of Bradley and Eugster (1969) suggested brines were concentrated by evaporation in closed sub-basins of the larger Lake Gosiute. Continuous trona precipitation followed as a result of evaporation and saturation of the denser trona brines within the basal portions of sub-basins. Algal plumes and other life-forms were possible in the less saline regions of the lake waters. Evaporation to complete dryness is not postulated in this model.

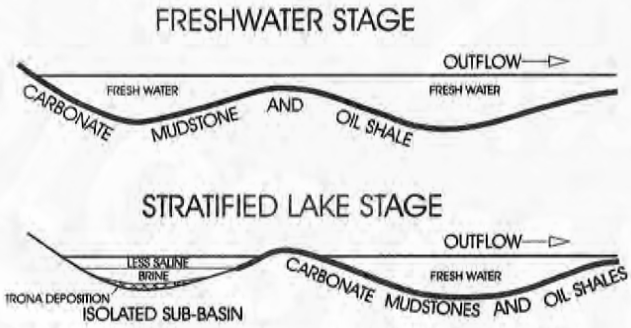


Figure 6. Stratified lake model (after Bradley, 1964).

In contrast, Eugster and Surdam (1973) and Surdam and Wolfbauer (1975), proposed the playa-lake model for trona deposition (**Figure 7**). In this model, a shallow, closed basin fringed with a large playa mud flat existed during regressive stages of the lake. Through capillary pumping and evaporation, alkaline brines were concentrated and precipitated as an efflorescent crust on the playa mud flats. Storm events and sheet wash transported the salts into the basin interior for final deposition.

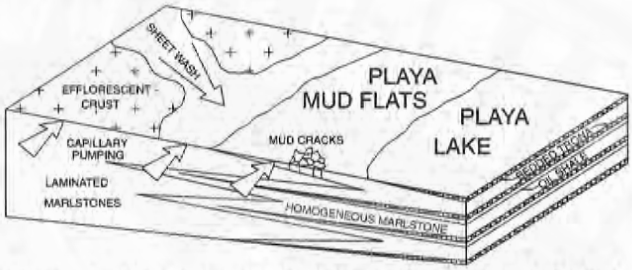


Figure 7. Playa-lake model (after Birnbaum and Radlick, 1982; Eugster and Surdam, 1973).

Boyer (1982) and Sullivan (1985) combined aspects of both models to form the perennial ectogenic-meromictic lake model (**Figure 8**). In this composite model, fluctuations of lake size occurred in response to climatic and tectonic events influencing the freshwater inflows. During transgressive expansions, the lake became stratified and deposited oil shales. Trona deposition occurred during regressive constrictions, as proposed in the playa-lake model.

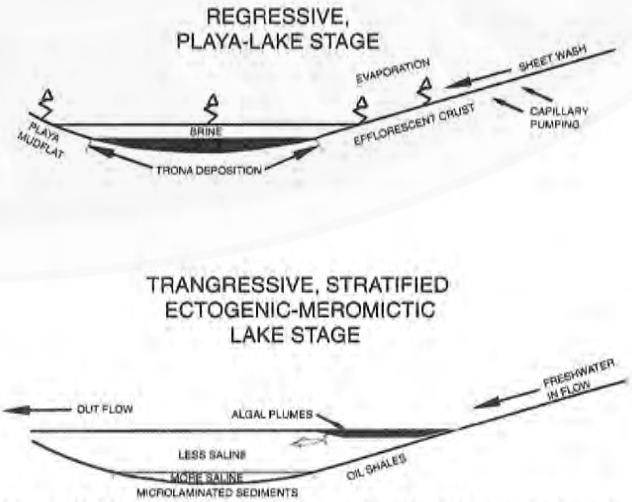


Figure 8. Perennial ecotegenic-meromictic lake model (modified from Boyer, 1982; Sullivan, 1985).

Trona textures

Textural analyses of trona in drill core and exposures within underground mine workings suggest multiple depositional scenarios. Three textural forms of trona are common within the Wilkins Peak Member:

1. Light brown, fine-grained (1 mm to microcrystalline) aggregated masses commonly referred to as "maple sugar" trona (**Figure 9**).

2. Amber (light to very dark), translucent, coarse-crystalline (5 mm to 30 mm), fibrous masses with random to radiating bladelike euhedral crystals forming individual nodules to massive beds commonly called "root beer" trona (**Figure 10**).

3. Vertically oriented, clear crystalline, columnar vein-filling trona commonly called "spar" trona or "3c" trona (**Figure 11**).

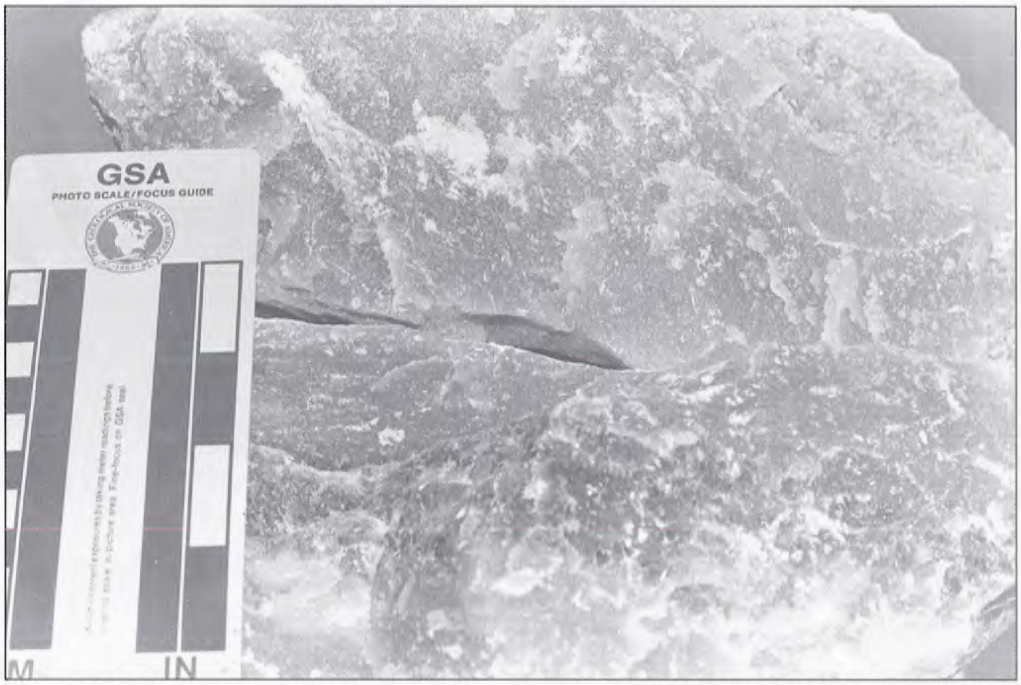


Figure 9. Microcrystalline "maple sugar" type trona is common to trona beds 1 through 18.

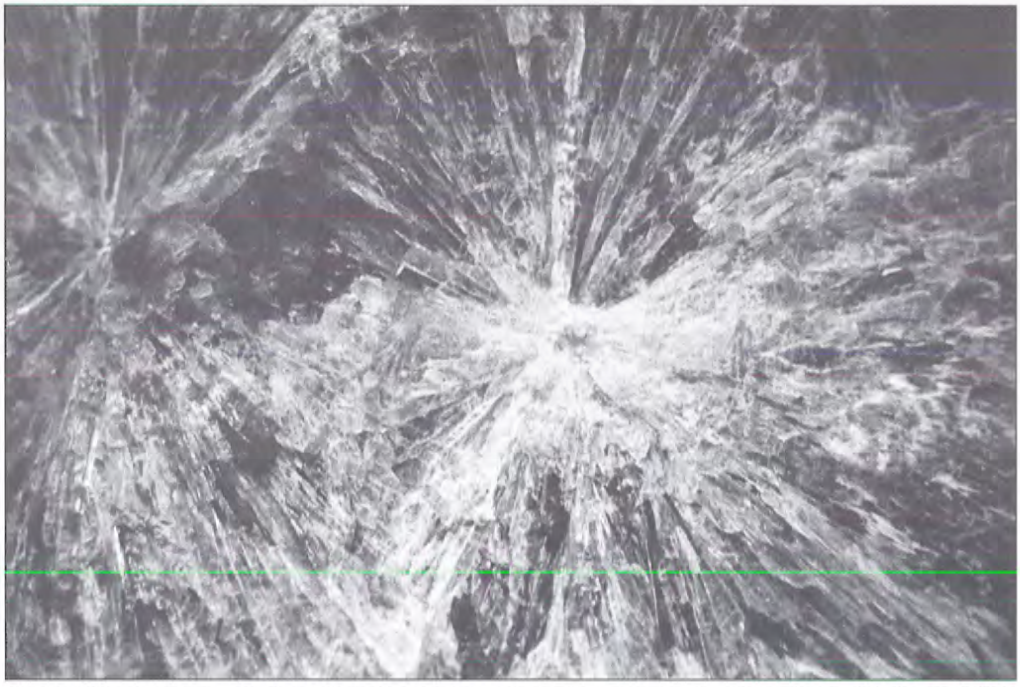


Figure 10. Coarse-crystalline "root beer" type trona is common to trona beds 19 through 25. (Photograph scale approximately 30 cm wide.)



Figure 11. Clear, crystalline, columnar "spar" trona.

Depositional history as interpreted from trona textures

Initial deposition

Trona beds 1 through 18, primarily composed of "maple sugar" type trona with locally large quantities of intermixed or interlayered halite, are located predominantly in the southern three-quarters of the trona resource area. Little variation in the depocenter suggests a stable tectonic regime (see **Figure 5**). Strong stratification features are observed in these beds, including layering of trona by textural characteristics, occasionally separated by marlstone laminae that extend for great distances; graded bedding; and brecciation (See **Figures 12, 13**, and **14**).

A modified ectogenic-meromictic lake model best depicts the possible trona deposition for beds 1 through 18. During low lake stands, capillary pumping of brines precipitated trona crust along the peripheral mud flats. Transportation as trona grains or concentrated brines into a shallow saline lake followed by rapid deposition is indicated by the fine texture of these deposits. The widespread distribution of marl laminae indicates subaqueous deposition in an undisturbed environment and may represent sediment transported during storm events. The bedding features and brecciation occurrences could represent fluvial transportation of trona by sheet erosion from the peripheral mud flats or erosion by wave action and redeposition. Halite precipitation occurred in response to saturation with respect to high sodium chloride concentrations during more intense evaporation.



Figure 12. Sedimentary features found in trona bed 17. a. Brecciation (upper half of photograph), b. graded bedding (central portion), and c. bedding by textural characteristics (lower portion).



Figure 13. Brecciation in trona bed 17.



Figure 14. Sedimentary bedding features common to trona beds 1 through 18.

Closing deposition

Depositional and/or climatic changes are indicated by the deposition features of beds 19 through 25, which are composed of "root beer" type trona. Polygonal desiccation structures, remobilization, dissolution/recrystallization of trona crystals, and a general lack of stratification are more suggestive of the classic playa-lake model (see **Figures 15** and **16**).



Figure 15. Vertical desiccation feature common to trona beds 19 through 25. Photograph is of underground mine rib approximately 3 meters high.



Figure 16. Vertical desiccation feature. Symmetry of clay partings (light bands) implies multiple episodes of development. Post-depositional compression during trona solidification has deformed this feature. Scale of photograph approximately 2 meters high.

The coarse-crystalline trona with bladelike crystals forming "rosette" features grew in the undisturbed areas of the lake from slow precipitation of the rich brines while the geochemical formation of trona brines may have occurred along the peripheral margins. Trona rosettes partially destroyed by wave action and/or by dissolution by fresher brines, were later redeposited as aggregated masses of broken crystals. Repeatedly, the playa completely evaporated, as indicated by polygonal desiccation structures (see **Figures 17**, **18**, and **19**). Intense evaporation and a warmer climate may have kept the lake in a state of trona saturation, which could have contributed to the slow crystal growth and coarse texture of the deposits. Marl laminations do occur within these beds but are highly disturbed by the crystal growth and depositional processes.



Figure 17. Trace of polygonally patterned desiccation feature observed in the roof of an underground mine entry.

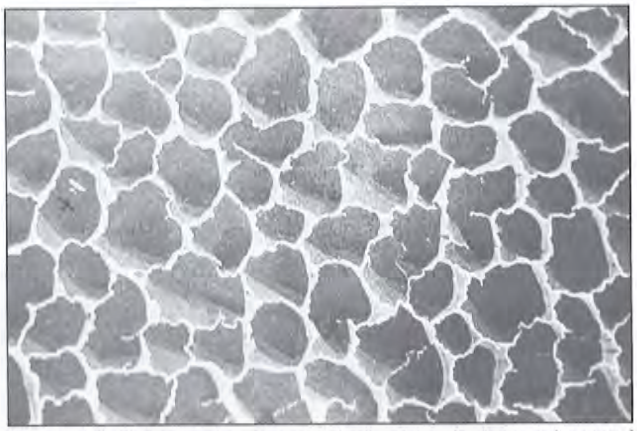


Figure 18. Polygonal pattern of desiccation features observed on Lake Magadi, Kenya, composed of "root beer" type trona. Airplane at left for scale. Photograph provided by R.C. Surdam.

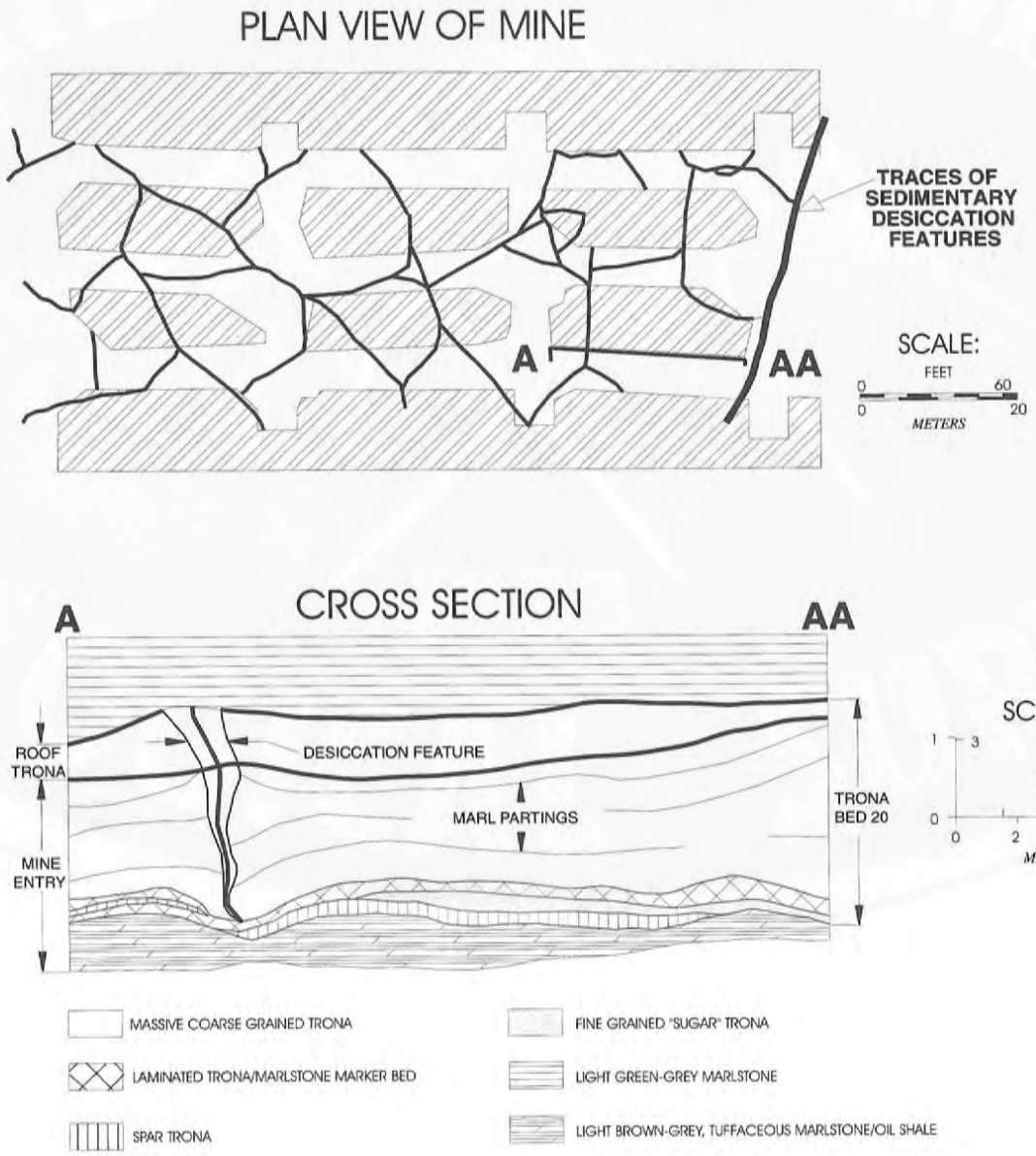


Figure 19. Polygonally patterned desiccation feature of trona bed 20 mapped from actual mine workings.

Post-deposition

"Spar" trona (**Figure 20**) is a post-depositional vein-filling feature occurring within marlstone. Saturated brines precipitated trona in voids created by hydro-fracturing of the marlstones during dewatering and compaction. The vertical orientation of the crystal structure is an indication of compressional stresses of the overburden at the time of crystallization. "Spar" trona occurs anywhere within the saline Wilkins Peak Member and is not necessarily associated with a trona bed.



Figure 20. "Spar" trona exhibiting vertical crystal orientation. Multiple episodes of development are inferred by the banding of impurities. Photograph scale approximately 30 cm high.

Mining history

The first sodium carbonate discovery within the district occurred in 1896, when a 38-meter (125-foot)-deep water well encountered soda brines west of Green River. By 1907, these brines were being pumped to solar ponds for evaporation and concentration into a crude soda ash.

Trona was first discovered in 1938, when Mountain Fuel Supply Company drilled a wildcat oil well, the John Hay Jr. No. 1, and encountered what was later determined to be 3 meters (10 feet) of trona bed 17. Subsequent exploration by Westvaco Company and the Union Pacific Railroad showed the trona bed to be uniform and laterally persistent. From 1946 to 1948, Westvaco (predecessor of FMC Corporation) sank a 456-meter (1500-foot) shaft to mine trona bed 17 and started a pilot plant with a daily capacity of 181 tonnes (200 short tons) of crude soda ash. FMC began full-scale production of refined soda ash in 1953. Subsequent exploration by numerous companies further delineated the Green River Basin trona resources.

Today five Wyoming companies produce soda ash from various trona beds (**Figure 21**). Three companies mine trona bed 17. One company operates in beds 19 and 20 and the remaining company mines beds 24 and 25. All activities are currently in the northern third of the resource area. A solution mine pilot facility to extract brines from beds 1 through 5 by vertical wells, is in operation in the central portion of the resource area.

All dry mining is accessed through vertical shafts sunk to various trona beds. Mining is performed by conventional "hard rock" methods, mechanical extraction (drum miners, boring machines), and hydraulically supported longwall shearing or modified shortwall methods (**Figures 22** through **25**). These dry mining methods extract up to 75% by volume of the trona within a limited area of a mine. The average extraction rate is less than 50% and is dependent upon depth and mechanical properties of the ore and overburden. Therefore, greater than 50% of the trona is left behind as pillars and barriers. Enhanced trona recovery by solution mining the remaining ore will eventually be attempted by all the companies in the area.

References cited

Birnbaum, S.J., and Radlick, T.M., 1982, A textural analysis of trona and associated lithologies, Wilkins Peak Member, Eocene Green River Formation, southwestern Wyoming, *in* Depositional and Diagenetic Spectra of Evaporites - A Core Workshop: SEPM Core Workshop no. 3, p. 75-99.

Boyer, B.W., 1982, Green River laminates: does the playa-lake model really invalidate the stratified-lake model?": Geology, v. 10, p. 321-324.

Bradley, W.H., 1964, Geology of Green River Formation and associated Eocene rocks in southwestern Wyoming and adjacent parts of Colorado and Utah: U.S. Geological Survey Professional Paper 496-A, 88 p.

Bradley, W.H., and Eugster, H.P., 1969, Geochemistry and paleolimnology of the trona deposits and associated authigenic minerals of the Green River Formation of Wyoming: U.S. Geological Survey Professional Paper 496-B, 71 p.

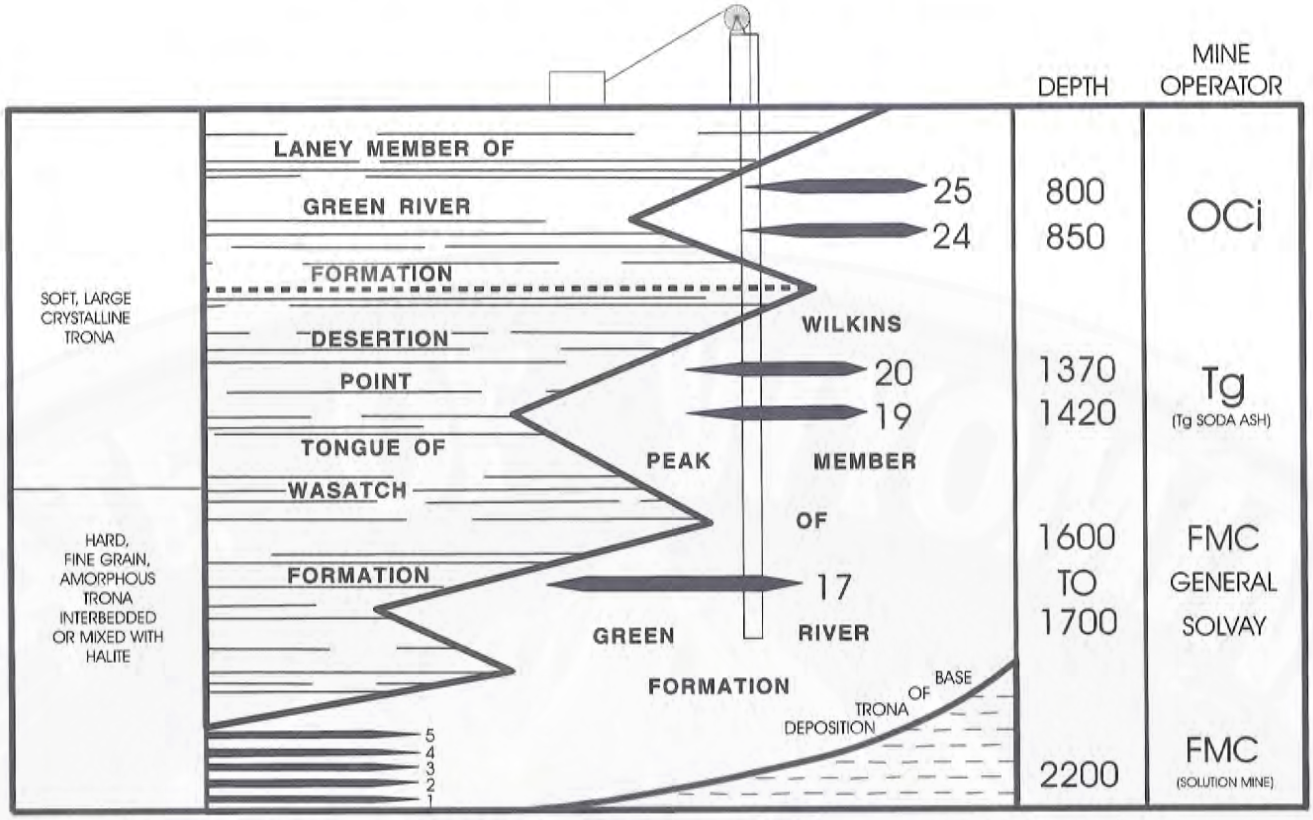


Figure 21. Schematic geological section identifying the five major trona/soda ash producers and the trona beds they are mining.



Figure 22. Drum-type continuous miner, about 5.6 meters wide.



Figure 23. Three-meter-high bore miner.

Breunig, W., 1998, Soda ash: Engineering and Mining Journal, March, 1998, p. 64-65.

Burnside, M., and Culbertson, W., 1979, Trona deposits in the Green River Basin, Sweetwater, Uinta and Lincoln Counties, Wyoming: U.S. Geological Survey Open File Report 79-737, 10 p.

Culbertson, W.C., 1966, Trona in the Wilkins Peak Member of the Green River Formation, southwestern Wyoming: U.S. Geological Survey Professional Paper 550-B, p. 159-164.

Culbertson, W.C., 1971, Stratigraphy of the trona deposits in the Green River Formation, southwest Wyoming: University of Wyoming Contributions to Geology, v. 10, p. 15-23.

Eugster, H.P., and Surdam, R.C., 1973, Depositional environments of the Green River Formation of Wyoming: a preliminary report: Geological Society of America Bulletin, v. 84, p. 1115-1120.

Kostick, D.S., 1991, 1991 Soda ash annual report: U.S. Bureau of Mines (November, 1992), 22 p.

Roehler, H.W., 1991a, Revised stratigraphic nomenclature for the Wasatch and Green River Formations of Eocene age,



Figure 24. Shortwall mining method. Note two men standing to left of mining machine for scale.



Figure 25. Longwall mining method with 1-meter shearing head.

Wyoming, Utah, and Colorado: U.S. Geological Survey Professional Paper 1506-B, 38 p.

Roehler, H.W., 1991b, Godiva Rim Member - A new stratigraphic unit of the Green River Formation in southwest Wyoming and northwest Colorado: U.S. Geological Survey Professional Paper 1506-C, 17 p.

Roehler, H.W., 1992a, Introduction to greater Green River Basin geology, physiography, and history of investigations: U.S. Geological Survey Professional Paper 1506-A, 14 p.

Roehler, H.W., 1992b, Description and correlation of Eocene rocks in stratigraphic reference sections for the Green River and Washakie Basins, southwest Wyoming: U.S. Geological Survey Professional Paper 1506-D, 83 p.

Roehler, H.W., 1992c, Correlation, composition, areal distribution, and thickness of Eocene stratigraphic units, greater Green River Basin, Wyoming, Utah, and Colorado: U.S. Geological Survey Professional Paper 1506-E, 49 p.

Sullivan, R., 1980, A stratigraphic evaluation of the Eocene rocks of southwestern Wyoming: Wyoming State Geological Survey Report of Investigations 20, 50 p.

Sullivan, R., 1985, Origin of lacustrine rocks of Wilkins Peak Member, Wyoming: American Association of Petroleum Geologists Bulletin, v. 69, no. 6, p. 913-922.

Surdam, R.C., and Wolfbauer, C.A., 1975, Green River Formation, Wyoming: a playa lake complex: Geological Society of America Bulletin, v. 86, p. 335-345.

Wiig, S.V., Grundy, W.D., and Dyni, J.R., 1995, Trona resources in the Green River Basin, southwest Wyoming: U.S. Geological Survey Open File Report 95-476, 88 p.

Origin of the Green River trona deposit
(from a chemical and other saline mineral perspective)

Donald E. Garrett
Saline Processors, Incorporated
Ojai, California 93024

Abstract

The carbonate source and reason(s) for the purity of the Green River trona deposit is unknown. Quite likely river and runoff water, even with sulfate-reducing bacteria, could not have formed it. High-carbonate springs could have formed the deposit, primarily because most trona deposits exhibit a somewhat different brine chemistry before, during, and after the depositing period. The trona deposit's purity is similar to other large saline mineral deposits, and in marine formations partial leaching, followed by seepage and/or periodic flushing of the end liquor, accounts for their composition and purity. The Green River and Farson-Eden brines may represent end liquors that originated in a similar manner.

Introduction

There have been many articles written on the origin of the Green River trona deposit from the point of view of whether it formed in a deep stratified lake, a shallow lake, a playa, or a combination of all three. Many observations have been made on physical aspects of the deposit to help answer this question, as recently summarized by Leigh (1991). From the data presented to date there appears to be strong evidence that during the time the Wilkins Peak Member of the Green River Formation was deposited, the basin alternated between all three lake forms. This conclusion will be further considered later in this article.

There has been little speculation on the brine or water source that caused this unique deposit to form, and why the trona and trona-halite minerals are so pure and free from other soluble salts. There is no other buried trona deposit in the world of a comparable size or purity, although the adjacent Uinta and Piceance Basins contain very large and pure deposits of nahcolite and dawsonite, along with some wegscheiderite. There are also four other similar trona deposits of a smaller size (i.e., 50 to 200 million short tons), and with a somewhat higher insolubles content (two in China, and one each in Turkey and Kenya). There are three massive surface or near-surface soda ash deposits of the hundreds of millions to billions of short tons in size, but which contain only small-to-major amounts of other soluble salts (Searles, Magadi, and Natron Lakes). Then there are literally hundreds of smaller trona or sodium carbonate-containing deposits, with most of them being mixtures with other soluble salts.

Carbonate sources

Carbonate from oil shale

Initially it was proposed, and it is still commonly inferred, that the carbonate source for the Green River trona deposits was the companion oil shale in the formations. Presumably a high CO_2 content existed in the lake waters from decaying organic matter, and this precipitated the trona. However, this has to be a misconception, since large oil shale deposits are common throughout the world, and none of the others are associated with trona deposits. Also, carbon dioxide that was absorbed in neutral (non-sodium carbonate-containing) water would produce an acidic solution (with carbonic acid) that would merely degas and lose its CO_2 as the water evaporated, or occasionally form dawsonite. Thus, any water with more Ca+Mg than CO_3+HCO_3 and SiO_2 would soon precipitate essentially all of its CO_3 (and HCO_3 after it

converted to CO_3 according to the CO_2-HCO_3-CO_3 versus concentration equilibrium) upon evaporation. The remaining solution would be a neutral NaCl-Na_2SO_4 mixture with some calcium, magnesium, chloride, and sulfate ions and would not precipitate trona or nahcolite upon carbonation. Waters with an excess of CO_3+HCO_3+SiO_2 over Ca+Mg could evaporate to form a nahcolite or trona deposit, but the excess of carbonates would usually be somewhat equal to the other salts in the solution, and a mixture of salts would crystallize, giving a very impure deposit. Furthermore, the CO_2 from decaying organic matter is an unnecessary factor in forming trona deposits, since the carbon dioxide in the atmosphere is ample to establish the CO_2-HCO_3-CO_3 equilibrium and form trona by itself.

The oil shale, decaying organics, and CO_2 absorption, however, undoubtedly does help to explain the presence of nahcolite rather than trona in deposits where the carbonates were already present, but not why the carbonates were originally there. On the other hand, the reverse of this oil shale-to-trona assumption is true, since carbonate-containing waters do provide a very favorable environment for algae, brine shrimp, and other lake organisms. Over two-thirds of the world's flamingos feed off the prolific algae and brine shrimp in the Rift Valley's soda ash lakes. Also, the algae grew so heavily in their solar evaporation ponds that Texcoco in Mexico harvested it as a valuable by-product to their soda ash production. Thus, the presence of oil shale in and under trona beds is not an unexpected occurrence, but it has little to do with how the trona deposits formed.

Carbonate from sulfate conversion

Others have further speculated that sulfate-reducing bacteria acting on ordinary water, such as in the current Green River, have supplied the carbonate for the deposit. The bacteria were known to be present in the lake muds because of the presence of considerable pyrite and other sulfides with an abnormally high ^{34}S content. Consequently, some-to-much of the sulfate in the lake waters must have been converted to carbonates, and some undoubtedly survived the Ca, Mg precipitation period:

$$\underset{\text{organics}}{H_2O+2C+SO} \rightarrow \underset{\text{bacteria}}{H_2S+CO_3^{*}+CO_2}$$

However, in all of the known examples of this conversion, either at present or within several million years, the reaction has never been complete, and considerable sodium sulfate has always been left behind and buried with the carbonate minerals. In modern lakes a sulfate conversion of 20 to 40% is the most that has ever been observed (i.e., the Wadi Natron in Egypt, where the bacteria have almost certainly produced about 1000 tons per year of trona that has been harvested for the past 5500 years), but in most deposits the conversion has only been about 1%. This can be demonstrated in the laboratory where the bacteria's vigor is strongly dependent upon the sulfate concentration, making even moderately high conversions (i.e., 10%) difficult in short periods, and 20 to 40% the maximum with many years residence time. With Green River water it would have taken a 100% conversion during the trona deposit's 800,000- to 1,000,000-year formation time to have formed the deposit. As an additional factor, the complex mechanism of all of the lake water repeatedly sinking down through the mud to the sulfate-reducing anaerobic bacterial zone and then back up is difficult to imagine, and has never been observed in modern lakes. Also, if this very common reaction for most stagnant or evaporating bodies of water was capable of forming large, pure trona deposits there should be many more of them, including perhaps some in the adjacent Tipton and Laney Members of the Green River Formation.

Carbonate from leaching

Finally, the present Green River water is not typical of that from most volcanic rock leaching, and it is known that the Wilkins Peak period was quite volcanically active. At least part of the basin's drainage area should have been composed of volcanic-type rocks, as indicated by the numerous tuff beds and the arkosic (decomposed granite) nature of the deposit's various insoluble layers and "tongues." Runoff water that leached granite, basalt, or tuff would have far more sodium and carbonate, and less SO_4, Ca, and Mg than the current Green River, but based upon modern waters they would still not have had enough excess carbonate, even with sulfate reduction, to have formed this deposit. Essentially no drainage waters are known today, except perhaps in the Rift Valley of Africa, that could have formed such a large or pure deposit, and even there Lake Magadi's trona contains 5 to 15% impurities (NaF, NaCl, Na_2SO_4, Na_3SiO_3, etc.). Since the rock formations in the Green River drainage basin are not of the strong-alkali, ultra-basic, or carbonatite type of the Rift Valley, this would appear to eliminate the possibility of groundwater and sulfate reduction being the deposit's carbonate source, missing by a factor of 5 to 10 fold. Almost certainly most of the carbonate in the deposit had to have entered from another source.

High-carbonate geothermal springs

The above considerations lead to the alternative of a high-carbonate, low-other-salts spring being the source of the trona. To help support this theory, most of the world's nahcolite or trona deposits experienced a pronounced change in brine chemistry with the beginning of the sodium carbonate deposition. For instance, the immediately underlying rocks in the Piceance Creek and Anpeng deposits were entirely siliceous with some gypsum (gypsum cannot form when soluble carbonates are present). Then they changed to being carbonates with trona or nahcolite, and after the carbonate period they changed back. Similar, but less dramatic changes occurred with the other trona deposits, also indicating that they originated from waters with a changed chemical composition. In the Green River deposit, the underlying Tipton Member was predominantly calcitic, and the Wilkins Peak Member became dolomitic. Also, as with several of the deposits, there was a sudden change from halite being deposited to being absent. This type of change would be expected from springs opening or closing, but would be hard to explain with other carbonate sources. There are many springs known in the world today that meet the requirement of having a high carbonate, low-other-salts content, and almost certainly an equal number existed during Eocene time. If the modern springs flowed into a closed basin with reasonably low-Ca and Mg groundwaters, and remained open for a long time they might be capable of forming a large trona deposit. High-carbonate springs are known to be the major carbonate source in the Rift Valley trona deposits and Searles Lake, and locally considered to be the source in Turkey and China.

In considering high-carbonate springs as the source of the Green River trona deposit, it is interesting to compare the large, high purity trona deposits with similar borate deposits. Almost all high carbonate springs contain some-to-much boron, and many of the high-boron springs contain some-to-much carbonate. Alonso (1986) fairly well established that essentially all of the borate deposits in Argentina originated from thermal springs that opened at a time of considerable volcanic activity. He has shown that many closed basins with fossil or active geothermal springs contain borate deposits; similar basins with comparable groundwater leaching, but no springs, do not contain borate deposits. Since these observations were made, quite strong cases for many spring-originated borate deposits in the world have been made, and it is now almost universally accepted. There are four large, very pure buried borax deposits, and five similar trona deposits. All were formed in periods of intense volcanic activity, with interbedded tuff, and all were near, over, or under volcanic magma flows. The similarity of these deposits in size, purity, scarcity, brine chemistry, and being formed during periods of intense volcanic activity makes a strong (but certainly not conclusive) case for a similar mode of origin.

Purity of the trona deposit

The second major question about the Green River trona deposit is its amazing purity; it contains essentially no other soluble salts, and only 5 to 20% insolubles. Part of the answer to this was the result of three of the factors discussed above: 1) the primary carbonate source was a high-carbonate, low-other-salts geothermal spring; 2) considerable sulfate reduction by bacteria did occur to produce more carbonate; and 3) the entering river and groundwater was also comparatively low in other salts. Thus, the loading of the very soluble sulfate, chloride, borate, fluoride, bromide, excess sodium, potassium, lithium, etc. into the basin would still have been extremely large, but not as high as with "Green River-type" water.

Ion removal mechanism

Some of these ions entering the basin would have removal mechanisms, such as the sulfate-reducing bacteria. When the concentrations became high enough, the fluorine and boron would compete with the carbonate to be precipitated as calcium and magnesium compounds, or would replace some of the carbonate in calcite and dolomite. Some of the potassium leaves with the early-precipitated silica, and is co-precipitated with calcium and magnesium carbonates. Later, as it becomes more concentrated it enters the tuff-zeolite-analcime-K feldspar-searlesite reaction chain, as does some of the boron. However, even with considerable removal, all of these ions would normally have crystallized with the trona-halite or trona beds. The removal mechanisms, and the reduced input, would allow them to only become saturated about the time, or soon after, the first halite would have crystallized (if present). This is what happens in most of the world's current soda ash playas, leaving the question of why didn't at least some of the other salts crystallize in the large trona deposits.

Leaching/seepage mechanism

Marine evaporites

With the question of trona deposits lacking other salts, there is strong support from the world's other large buried saline mineral deposits, since most of them are as pure as the trona formations. For instance, there are a very large number (many hundreds) of marine halite deposits, and fewer but still many sylvinite (a NaCl-KCl mixture) deposits. Most of them are as pure as the Green River trona, and many are much larger. It is also known that they all crystallized from concentrated multicomponent brines, that for halite should have at least co-crystallized epsomite ($MgSO_4 \cdot 7H_2O$). The final 25% of the halite (with evaporation going on to crystallize potash) should contain about 20% epsomite, and yet only one cycle of one deposit anywhere in the world has reported magnesium sulfate being present. With sylvinite there is no possible way for KCl to crystallize directly from sea water, and yet it is by far the most common potash salt. However, during sea water's evaporation the final potash salt is carnallite ($KCl\ MgCl_2 \cdot 6H_2O$), and when the brine has concentrated to over 16% $MgCl_2$ it can convert all of the previously deposited potash salts to carnallite and kieserite ($MgSO_4 \cdot H_2O$). It is now felt that this is exactly what happened in all of the sylvinite deposits. The addition of a little water (or a more dilute solution) can then convert the carnallite to sylvinite by dissolving the magnesium chloride and recrystallizing the KCl in about an 80-90% yield. It is also now generally agreed that the sylvinite resulted from this leach-conversion of carnallite soon after deposition, and the leaching of the magnesium sulfate (kieserite) therefore also had to occur.

The explanation of the purity of the marine deposits is thus twofold. First, all of them experienced some-to-considerable fairly immediate magnesium sulfate leaching (and for the carnallite, leach-conversion) while they were still permeable, but had been covered by mud and/or precipitates and a less saturated brine. Second, all of the residual precipitating brine (end liquor), and the leach solution was either (or both) flushed away from the deposit, or seeped down to lower formations (Garrett, 1995). This latter fact is demonstrated by the large number of sea water end liquor-type brines that are now under or near halite or sylvinite deposits. Also, sea water contains far more $MgCl_2$ and $MgSO_4$ than KCl, but little ($MgCl_2$ and $MgSO_4$) is now present in any deposits, so the end liquor and leach liquor must have escaped before it could further crystallize. Much or all of the escape had to have been by seepage in these low permeability closed basins.

The dilute brine for the leaching was formed by the successive incursions of fresh sea or terrestrial water into a well-stratified lake. With each more dilute inflow there would be some mixing with the dense bottom brine, and in time some water diffusion and further mixing would occur to reduce the brine's concentration to a point where, when it seeped through the deposit it could leach-convert the carnallite and leach the epsomite. This repeated inflow is well verified by the bromine analysis of the halite, or cesium and rubidium analyses of the potash salts. Each of these minor components crystallizes with the halite or potash salts, respectively, in exact proportion to their concentration in the brine. A plot of the Br, Cs, or Rb concentration in the salts with the height of the deposit shows a steady increase as the brine is evaporating and crystallizing, and then a sudden drop as the brine is diluted by the next inflow of sea or terrestrial water. This cycle is repeated countless times for all of the deposits.

Trona deposits

With trona deposits the seepage theory is less clear, but at the Green River deposit there are two extensive areas of carbonate brines nearby that perhaps could represent the seepage and end liquors of the trona deposit. Both have large ratios of CO_3/HCO_3 (2:1 to 5:1), which is typical of highly evaporated carbonate brines, and very unusual for water from totally leached trona or groundwater. There are also no extensive nahcolite areas in the deposit to indicate partial leaching. Both brines are fairly concentrated, such as end or seepage liquor somewhat diluted by groundwater. The Farson-Eden "black water" brines to the northeast of the deposit are very low in chloride, such as from brines that may have produced the pure trona. The Green River brines to the southeast of the deposit have a more normal high chloride content, as would end liquor from the trona-halite beds. In both cases the sulfate is highly variable, as would be expected with extensive sulfate reduction. Finally, the "black water" brine has a high kerogen-type organic content, as might be expected from this area's oil shale brines. It also has a comparatively high fluorine and boron content, elements usually found in geothermal brines but not in groundwater. Simple ^{18}O and deuterium isotopic analyses could help to determine the source of these brines.

This strong brine seepage, and/or periodic flushing out of the end liquor, combined with some-to-considerable leaching soon after the initial sediment deposition on its surface (and more dilute water flooding) appears to be a general phenomena for most of

the world's large, pure saline mineral deposits (halite, potash, borax, sodium sulfate, etc.). It is the only way to explain their purity when it is known that they all crystallized late in the evaporative sequence of multi-component brines. With the pure trona deposits, probably only a very small amount of leaching was required to remove some halite and burkeite; with the halite beds in the trona, more leaching would have been needed to remove trona, burkeite, and perhaps some potassium, fluorine, and borate salts. However, it would have been the seepage phenomena that primarily determined the deposit's purity by keeping the concentration of the other ions below their saturation point. Most basins, no matter how low the permeability in much of the strata, do undergo significant seepage over long geologic periods, particularly before deep burial and compaction. Since the more concentrated brines are the heaviest, they sink to the bottom, fill the porosity voids, and are the principal ones that ultimately seep away. The seepage is more intense through higher permeability zones in the basin floor, and at depth it can also be a horizontal flow through the "tongues," marker beds, or other more porous strata in the deposit. The escaping brine is then either trapped in underlying or adjacent aquifers, or more commonly is eventually diluted and flows away from the basin.

Origin of trona deposits

Modern trona deposition

To test the leeching/seepage theory of origin, and to consider the playa-deep lake question, it is interesting to examine modern trona deposits. There are a large number of playas that contain trona and other sodium carbonate minerals, and many of these have been studied to at least some extent. In most of them trona occurs as a mixed-salt efflorescent coating on portions of the playa surface. With a continuing carbonate supply these surface zones can become quite thick, and would appear to have been impossible to leach-purify by the dilute seepage brine. The same would be true of other trona forms that are occasionally present, such as "trona reefs," or zones of natron or burkeite. In none of the playas are there massive beds of trona that could be leach-purified. Often there are zones of other fairly pure individual salts (NaCl, sodium sulfate, borates, burkeite, etc.) in sections of the playa and at various depths (i.e., Rhodes and Fish Lake Marshes, Nevada, and many others), but trona is never one of these salts. In the modern playas that only flood periodically and/or briefly (the definition of a playa), trona is always impure, and never in a massive or bedded form. On the other hand, in soda ash deposits where a perennial or longer term lake has existed, relatively pure bedded trona may occur.

A graphic example of this action occurred with Borax Lake in central California (Vonsen and Hanna, 1936). It normally was 400 to 600 acres (150 to 250 hectares) in size, and 3 to 6 feet (1 to 2 m) deep in the spring, and about half that at the end of summer. It had been fed by a recently extinct high-carbonate, low-total-salts spring ("Little Sulfur Bank," which was still giving off "sulfurous gases"), and runoff water from a very small volcanic rock drainage basin. The spring's mantle was identical to that of the still-flowing Sulfur Bank geothermal spring 1.5 miles (2.5 km) away. The lake's brine was very similar to these water sources, except for proportionately less of the more soluble salts. This indicated that there had been sufficient seepage over the years to maintain the salts just below their saturation point. The presence of the large clusters of borax crystals in the lake's mud at depths of 2 to 6 feet (0.7 to 2 m) was also a clear indication of brine seepage. The lake waters had a high organic content (it was a favored migrating duck resting stop), and prolific sulfate-reducing bacteria. Borax crystals were harvested (as the first, and sole U.S. source) from 1864 to 1868. In 1934 the lake evaporated down to its lowest level in recorded history, about 1 acre (0.25 hectare) in size, and a few inches (cm) deep. In reaching this level a 3- to 4-inch (8 to 10 cm)-thick bed of almost pure trona (in a radiating crystal form) was deposited from its multi-component brine, and disseminated trona crystals were formed in the underlying mud. Then, at its edges and above the trona a fairly pure halite bed was formed. The trona bed experienced compressional cracks, and formed ridges in a polygonal pattern. One of these polygons, 60 feet (20 m) across, buckled and one side rose slightly above the surface of the brine. During the next winter both beds dissolved, and in the intervening years there has been sufficient seepage so that the lake and its salts have disappeared.

This deposit appears to be a very close analogy to the Green River trona formation, except for not being in a deep basin where a stratified brine layer could form. Here, as at Lakes Magadi and Natron, the basins did not deeply flood to allow the leach-purification step to occur. It does, however, show that relatively pure bedded trona, followed by pure halite, can form from a very complex brine, and that the brine can seep sufficiently to prevent complete satura-

tion. Even while still a shallow lake, compression cracks in the trona bed, disseminated trona in the mud, bird tracks in the mud, and mud cracks could all be formed.

Green River trona deposition

In summary, it is speculated that the Green River trona deposit, and others like it, formed in closed basins that usually maintained a shallow, perennial lake. It periodically flooded to form a chemically stratified lake (stable stratification can occur in lakes over 10 to 15 feet (3 to 5 m) deep, as indicated by detailed surveys of the Dead Sea and the Great Salt Lake) that could support fresh water life forms in its upper zone. As the lake evaporated in dryer periods it also reached brine concentrations (up to 16% Na_2CO_3) at its shores or throughout the lake that were favorable to the growth of algae, brine shrimp, and other alkali-lake biotic life forms, thus increasing the bottom sediment's organic (and eventually oil shale) content over a much larger area than the trona. It was fed by one or more high-carbonate, low-other-salts hot springs, and the runoff water from the surrounding drainage basin did not have a comparatively high SO_4, Ca, Mg, or total salts content (i.e., there was much volcanic rock in the drainage basin).

When the lake became shallow enough (based upon solar ponds, this would be <1 to 3 feet (<0.3 to 1 m) deep to have a uniformly saturated brine composition that could warm rapidly with each day's period of sunshine, trona crystallized rapidly on the surface, settled, and formed the "maple sugar," or "sucrosic" textured trona beds. When the lake level was higher (i.e., 2 to 9 feet, or 1 to 3 m deep), so that there was still some stratification, the heating cycle was averaged, and only evening cooling (and crystallization)-day time heating (with some dissolving) could occur and the radiating crystal-type trona beds were formed. The initial springs contained some chloride, so halite crystallization periods followed some of the trona beds, but after bed 18 was formed the high chloride-containing springs were shut off, and only high-carbonate springs remained. Only rarely did the lake totally dry up (to become a playa) and form thick, mixed salt trona masses, but when it did dry up it reflooded soon to continue forming trona beds and minimize the amount of other salts crystallized.

Thus, the basin normally contained a lake with a highly variable depth and size, and strong end-liquor continually seeped through its floor to prevent the minor components in the brine from becoming saturated. Each time the lake re-flooded, enough of the strong brine remained stratified at its base to protect the deposit from dissolving until mud and sediments had deposited to more completely protect the beds. However, during these reflooded periods some brine dilution did occur and the deposit was mildly leached by the descending seepage brine. The water entering the lake had most of its metal, Ca, Mg, and SiO_2 content precipitated as it first mixed with the alkaline, high-carbonate brine. Similar precipitation occurred throughout the basin during the lake's net evaporation periods, and considerable sulfate reduction also took place. When the high-carbonate springs finally shut off, the lake returned to its non-trona cycle (the Luman Member).

It is possible that the reason for shortite ($NaCO_3 \cdot 2CaCO_3$) being the dominant Na-Ca carbonate mineral in the deposit, instead of the more common gaylussite or pirssonite, is because of the entering brine having a disproportionately higher bicarbonate than carbonate content, which is not unusual in many geothermal springs. Also, the geothermal waters may have given the shallow lake a slightly elevated temperature (as with many of the borax and all of the colemanite-depositing lakes). These conditions would then favor the anhydrous, higher-calcium-than-carbonate shortite over the other Na-Ca carbonates.

References cited

Alonso, R.N., 1986, Occurrences, stratigraphic position and genesis of the borate deposits of the Puna region of Argentina: Ph.D. dissertation, University Nacional de Salta, Department of Natural Sciences, Argentina, 196 p.

Garrett, D.E., 1995, Potash: Deposits, processing, properties and uses: Chapman and Hall, London, 734 p.

Leigh, R.T., 1991, Wyoming trona: an overview of the geology and economic utilization: Wyoming Geological Association 42nd Field Conference Guidebook, p. 103-120.

Vonsen, M., and Hanna, G.D., 1936, Borax Lake, California: California Journal of Mines and Geology, v. 32, no. 1, p. 99-108.

A mineralogic and stratigraphic profile of trona bed 17 in the Solvay trona mine near Green River, Wyoming

Paul L. Boni
and
William W. Atkinson, Jr.
Department of Geological Sciences
University of Colorado at Boulder
Boulder, Colorado 80309

Abstract

A detailed study of trona bed 17, using techniques of petrography and x-ray diffraction, was undertaken in the Solvay trona mine, near Green River, Wyoming. A continuous, vertical channel sample was taken from near the production shaft for this study. At this location bed 17 is 12.6 feet thick and includes several easily recognizable stratigraphic markers within bed 17 which can be correlated throughout the mine.

The mineralogy and stratigraphy of trona bed 17 evolved throughout the life of its depositional history in cyclic and linear patterns. Data indicate that this region of bed 17 was deposited subaqueously during its early and late history and may have undergone periods of subaerial deposition. The lower 4 feet of bed 17 exhibit couplets of sparry and laminated trona capped with a thin layer of microscopic dolomite rhombs and dark organic matter (algae?) which are likely controlled by periods of cooler air temperatures and rainfall in the Green River Basin. If these cyclic textures represent annual climatic cycles, then trona accumulated at an annual rate of two to four inches per year.

The lower 8 to 8.5 feet of bed 17 are relatively free of insoluble and trace minerals whereas the upper 4 feet contain increased accumulations of dolomite, nahcolite, shortite, trace searlesite, and other unidentified minerals. The upper 4 feet were deposited from brines modified by the influx of waters from marginal areas during an overall re-wetting of the basin at the close of the bed 17 evaporative stage.

Introduction

The trona deposits of southwestern Wyoming are contained within the Wilkins Peak Member of the lacustrine Green River Formation. Lake Gosiute occupied a closed subsiding forethrust basin to the east of the Wyoming overthrust belt during the Eocene. Sedimentary rocks of the Green River Formation, deposited as sediments in Lake Gosiute, are designated in ascending order, the Tipton Shale, Wilkins Peak, and Laney Shale Members. The Tipton and Laney Members were deposited in fresh water, during periods of maximum extension of Lake Gosiute. The Wilkins Peak Member was deposited in a much reduced and saline Lake Gosiute, which evaporated to playa conditions during periods of trona and trona/halite deposition (Bradley and Eugster, 1969; Culbertson, 1966; Deardorff, 1963; Sullivan, 1985; and others). Periodicity of playa events was controlled by Earth's precessional and eccentricity orbital cycles and their effects on regional weather patterns. Elapsed time between trona playas is approximately 20,000 years (Fischer and Roberts, 1991).

Trona beds which exceed 3 feet in thickness and 100 square miles in areal extent are numbered upwards from 1 through 25. Together these beds contain an estimated 36 billion tons of trona and mixed

trona and halite (Culbertson, 1966). The subject of this study is bed 17, also referred to as the Westvaco bed. Bed 17 reaches a maximum thickness of 20 feet (Deardorff and Mannion, 1971) and underlies approximately 1000 square miles. Approximately 640 square miles of the bed are trona facies (with a minimum thickness of 3 feet) and 210 square miles are mixed trona and halite (Culbertson, 1966). Bed 17 is the most widespread of the trona beds and is accessible by underground workings in three of the five underground trona mines operating in the Green River Basin.

Joseph Fahey (1962) published some invaluable information concerning the mineralogy, crystal chemistry, and paragenesis of many saline minerals found in the Green River Formation. Included in Fahey's work is a section by Mary Mrose on powder diffraction data for many of the minerals. Deardorff and Manion (1971) published a good overall stratigraphy of beds 17, 24, and 25, with good mineralogic information for beds 24 and 25. Charles Milton (1971) published a comprehensive listing of the known authigenic minerals of the Green River Formation. These papers provide many useful comparisons with the present article. What is missing in the literature, however, is a systematic treatment of the specific trona beds, integrating stratigraphy, mineralogy, and chemistry on a small and detailed scale. The trona beds have been considered so uniform in consistency of ore grade and flat-lying stratigraphy that there has been little economic need to learn more of the geological details involved. As mining operations expand and expose new and anomalous portions of the trona beds, more questions are being asked concerning the occurrence of trona specific to the Green River Basin and in general. This study attempts to document and explain the details of trona bed 17 for future reference and comparison.

Samples for this study were taken from Solvay Mineral's trona mine, located about 15 miles west of Green River, Wyoming (**Figure 1**). The study area is located in the trona facies of bed 17 along the north-

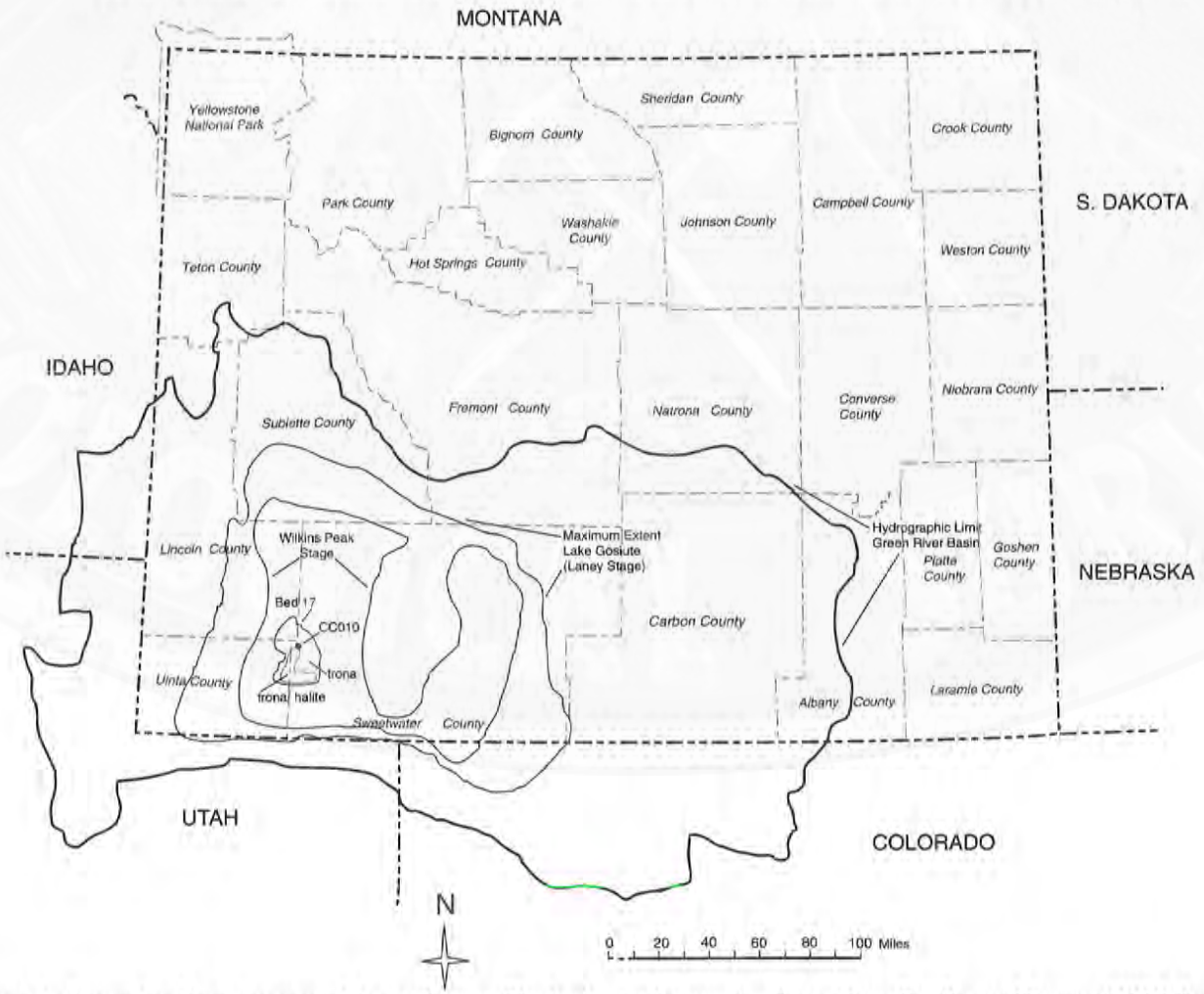


Figure 1. Generalized location map of the study area. The hydrographic map is adapted from Bradley and Eugster (1969, figure 3) and the lithologic map of bed 17 is from Deardorff and Mannion (1971, figure 5).

ern edge of the mixed trona and halite facies (Deardorff and Mannion, 1971).

A 7 1/4-inch circular saw, fitted with a diamond blade, was used to cut five channel samples from ribs of the underground mine. These channel samples extend from the floor shale upward to the roof shale and sample recovery was complete at each location. The channel samples are spaced on roughly one mile centers. Sample CC010, located near the production shaft, was chosen for this study, as it best represents the most commonly observed features of bed 17 in this region. Bed 17 at this location is 12.6 feet thick.

A continuous suite of thin sections, covering 13 vertical feet, was cut from CC010, studied with a petrographic microscope, and documented. X-ray diffraction studies are ongoing in support of thin section observations and identification of unidentified and submicroscopic minerals. Stratigraphic measurements are given in vertical feet above the base contact of bed 17 with the floor shale.

Three depositional stages of bed 17

Bed 17 can be divided into three depositional stages, early, middle, and late, based upon stratigraphic, microscopic, and mineralogical features (**Figures 2** and **3**). Each stage was deposited under environmental conditions which were recorded in the texture and mineralogy of the deposit.

Early Stage

The early stage extends upward 4.75 feet from the floor shale to the pilot bands (**Figures 2** and **3**) It is characterized by repetitions of sparry and laminated trona. The mineralogy is dominantly trona [$Na_3(CO_3)(HCO_3) \cdot 2H_2O$] with trace to minor dolomite [$CaMg(CO_3)_2$] and trace shortite [$Na_2Ca_2(CO_3)_3$] and pyrite (FeS_2). Dolomite occurs scattered in trace amounts; in association with very fine-grained trona or in thin-bedded layers termed "partings," which are 1 to 2 mm thick; and as a laminated layer, 1/2 inch thick (pilot band 1). Dolomite occurs as very fine-grained subrounded rhombic crystals 0.006 to 0.05 mm across. Pyrite and shortite are scattered through-

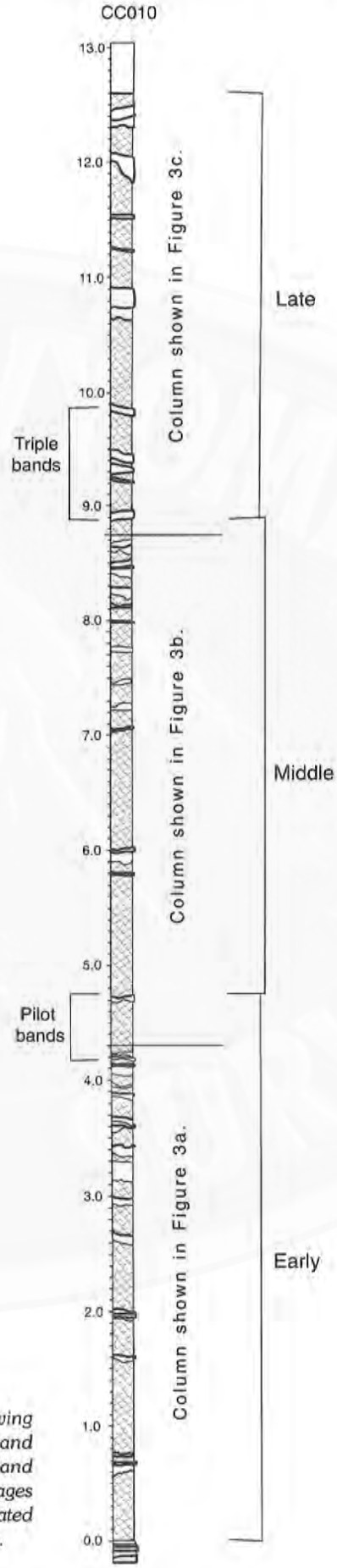


Figure 2. Generalized stratigraphic column from sample locality CC010, showing relative positions of the early, middle, and late depositional stages of bed 17 and approximate positions of columns shown in Figure 3. Dolomitic partings and bands are outlined by bold lines. Hatched areas in the early and middle stages are sparry trona. Hatched areas in the late stage are sparry, massive, and brecciated trona. Unmarked areas are laminated trona. Refer to Figure 3 for more details.

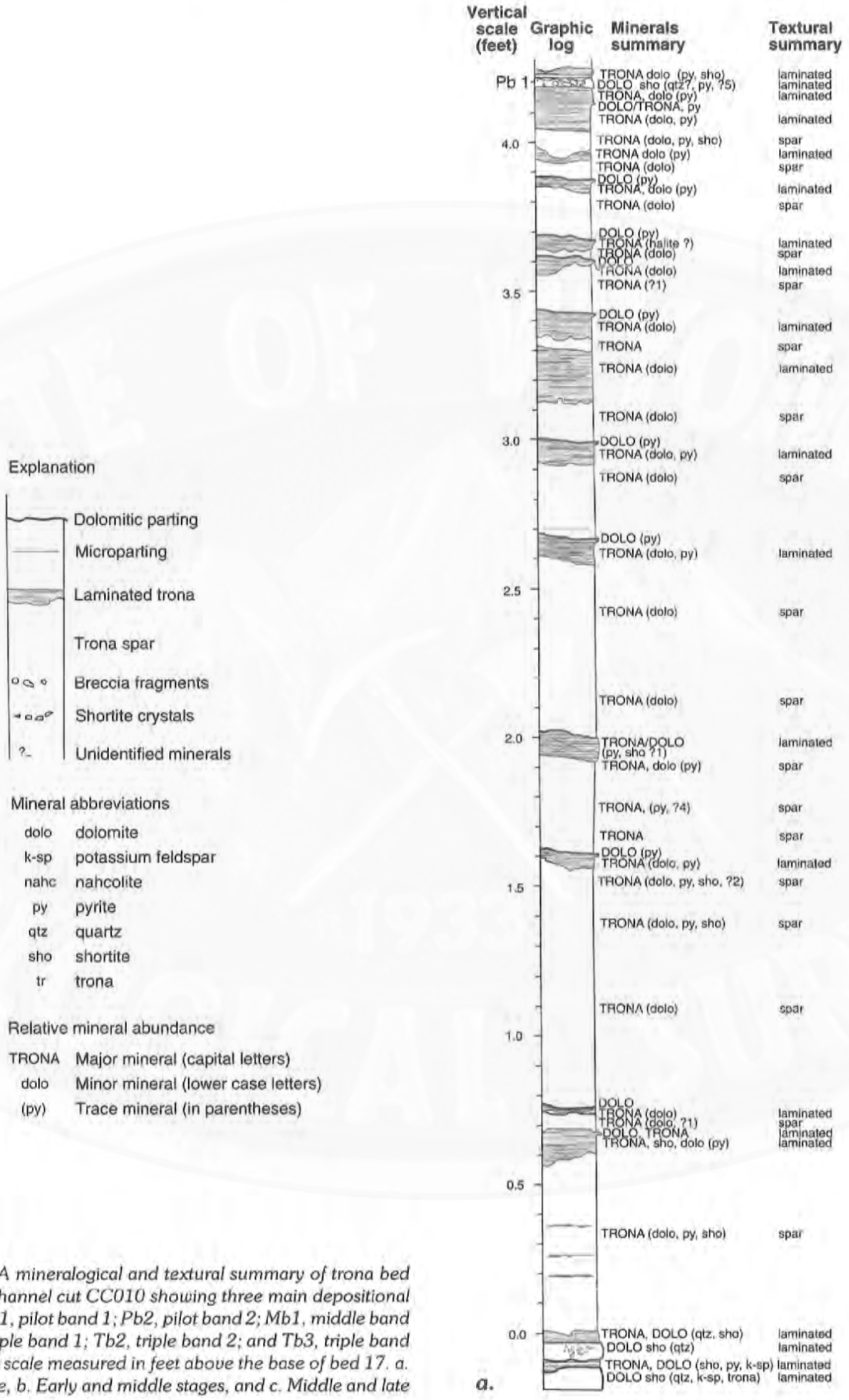


Figure 3. A mineralogical and textural summary of trona bed 17 from channel cut CC010 showing three main depositional stages. Pb1, pilot band 1; Pb2, pilot band 2; Mb1, middle band 1; Tb1, triple band 1; Tb2, triple band 2; and Tb3, triple band 3. Vertical scale measured in feet above the base of bed 17. a. Early stage, b. Early and middle stages, and c. Middle and late stages.

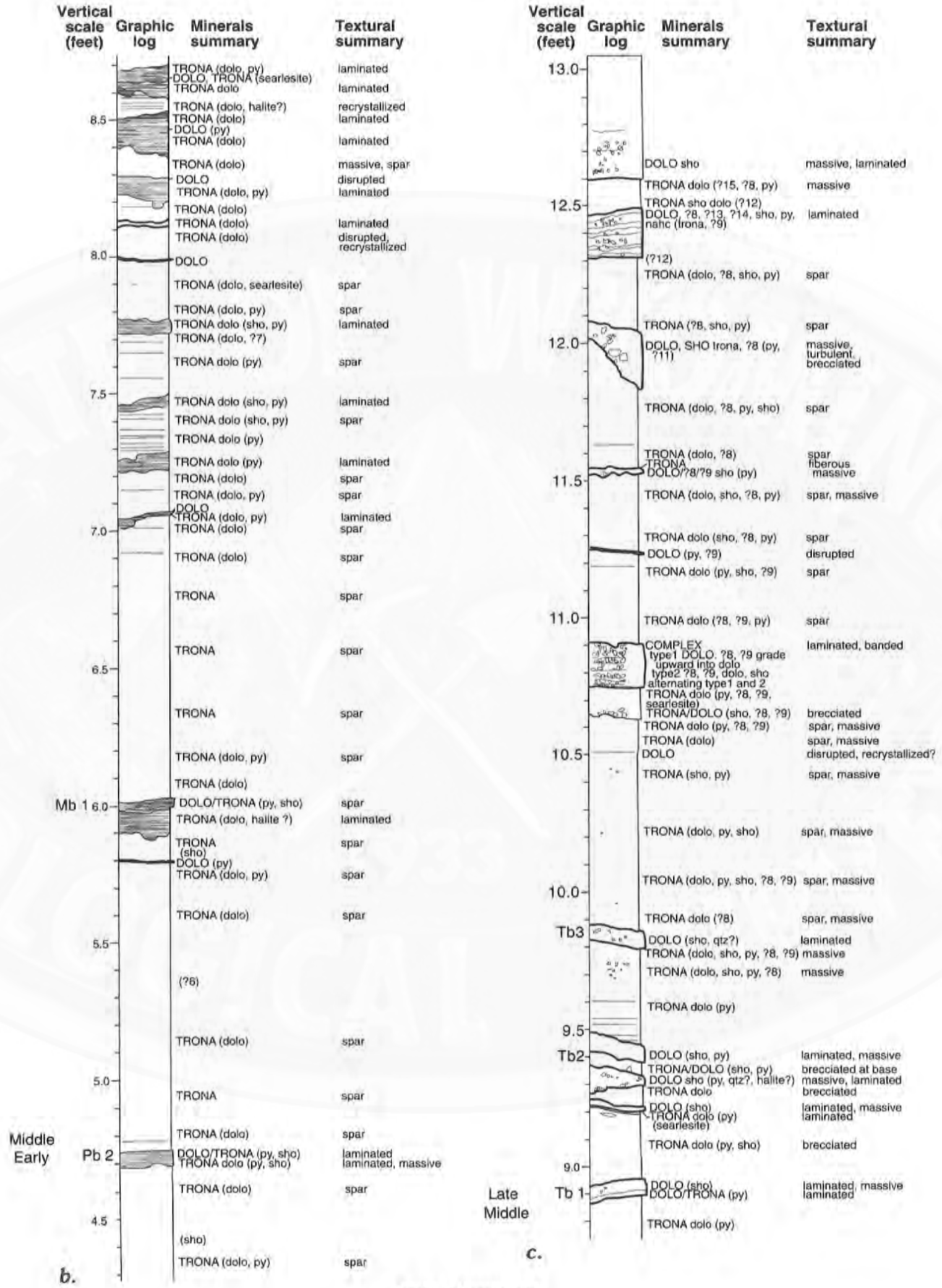


Figure 3 (continued)

out bed 17 with an increased frequency in or near dolomitic layers. Pyrite occurs as euhedral single crystals and crystal clusters 0.05 to 0.5 mm across. Shortite crystals range in size from 0.5 to 1.25 mm and often include fragments of trona crystals. Wherever shortite has been observed in trona, it is corroded and replaced along crystal edges by trona. Conversely, where shortite occurs in dolomitic layers it is euhedral and unaltered.

Trona spar is composed of medium-grained (approximately 3 to 4 mm) trona crystals, in association with intercrystalline accumulations of very fine-grained (approximately 0.05 to 0.2 mm) trona (**Figure 4**). Crystal growth habits of the coarse fraction range from intergrown and randomly oriented to water-laid and parallel to bedding. Some crystals grew in place while others settled through the water column onto the playa lake bottom. The very fine-grained component is randomly oriented and is accompanied by trace amounts of microscopic dolomite and trace pyrite.

The change in trona crystal size and texture from sparry to laminated trona, and back again, is abrupt. In the laminated layers, very fine trona (0.05 to 0.2 mm) lies conformably on top of sparry trona, filling in crystal-sized depressions, becoming sub-parallel and finally parallel to bedding (**Figure 5**). This texture is in contrast to the random orientation of the same size of trona crystals with a sparry texture.

Each laminated layer is capped by a dolomitic parting, composed of microscopic dolomite crystals, dark organic matter, an increased occurrence of pyrite, and rare shortite. Preliminary observations of the dark organic matter suggest it is algae. Similar organic matter from the base of bed 17 was separated from trona in the laboratory by dissolution of the soluble minerals in clear water. When examined under magnification (20x dissection microscope), the insoluble residue appeared to be fossil algae. Elongated and somewhat flexible fibers appeared to be organic in origin and entangled very fine pyrite and dolomite crystals. Trona spar was deposited on top of the parting layers and does not penetrate the parting surface.

The relationship between laminated trona and spar is cyclic. Each cycle is composed of a layer of spar, followed by a layer of laminated trona, which is capped by a thin layer of dolomite and dark organic matter. Trona spar overlies the dolomitic parting and begins the next cycle.

Micropartings are microscopically thin, bedded accumulations of dolomite and dark organic material, with trace pyrite. Unlike the dolomitic partings associ-

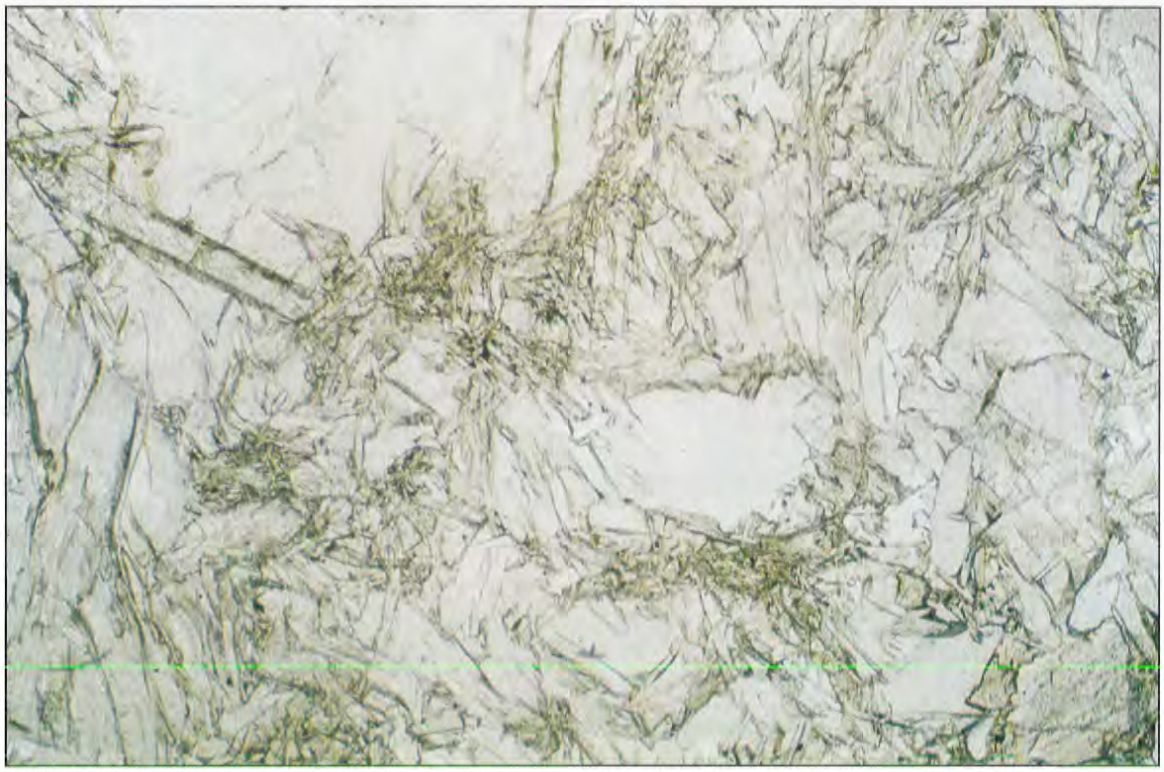


Figure 4. Photomicrograph of trona spar showing typical segregation of crystal size. Trona is the only mineral visible in this view. This is a thin section from 6.68 feet and photographed at 25x in plane light.



Figure 5. Photomicrograph of a single lamination cycle. The dark layer is a dolomitic parting composed of dolomite and organic matter. Note the contrast of crystal size and texture above and below the dolomitic parting. Below the parting, trona is very fine grained and bedded. Above the parting, trona is considerably coarser and randomly oriented. This is a thin section from 2.68 feet and photographed at 25x in plane light.

ated with lamination cycles, micropartings are not associated with definable textural features. They occur in both laminated and sparry trona of the early and middle stages and are significantly disrupted or absent in the late stage.

Middle stage

The middle stage begins at the upper contact of pilot band 2 (4.75 feet) and extends upward to the base of the triple bands, at 8.88 feet (**Figures 2** and **3**). Between pilot band 2 and 7.2 feet, the trona is mostly spar with only one significant laminated layer at about 6 feet. Trona spar in this interval is nearly pure (mineralogically) containing only trace amounts of scattered dolomite. Lamination cycles begin again at 7.2 feet and continue upwards to triple band 1. Dolomite increases in this interval, though still only in trace to minor amounts. Also observed are occurrences of trona recrystallization and disruption of dolomitic partings, which increase in frequency upward.

The upper contact with the late stage is transitional, in terms of observed textures and an increased occurrence of dolomite, from 7.2 feet to the triple bands at 8.88 feet. From about 8 feet and upward, late trona crystal growth was observed to displace primary depositional textures in laminated trona and dolomitic partings. At 8.54 feet, recrystallized trona was observed. Very large (to 2 cm) trona crystals grew in very fine-grained, laminated trona. The recrystallized trona incorporated dolomite and pyrite of micropartings during growth.

Late stage

The late stage includes the triple bands (at 8.88 feet) and extends upward to the roof shale at 12.6 feet (**Figures 2** and **3**). This is the most variable part of bed 17, stratigraphically and mineralogically, and contains the lowest ore grades. The late stage does include layers of high grade trona ore, but the increased frequency and thickness of dolomitic bands renders selective mining difficult. The mineralogy is complex in places and includes a number of as yet unidentified minerals. Two classifications of breccia have been observed: the first is formed from high energy, turbulent, depositional waters, and the second is the product of post-depositional remobilization of dolomitic muds. Recrystallization of trona and disruption of dolomitic bands was also observed. Mineral impurities include dolomite (greatly increased over the early and middle stages), increased shortite, trace pyrite, two searlesite ($NaBSi_2O_6 \cdot H_2O$) crystals, and the majority of unidentified minerals.

Depositional breccia fragments are rip-up clasts of previously deposited trona in a dolomitic trona or dolomitic matrix, and are overlain by a dolomitic

band. Clasts are 1.5 mm to 1 cm across and are subangular to subrounded. Dissolution likely contributed to rounding in addition to physical transport. Matrix minerals are either dolomite or a mixture of dolomite and trona. Depositional breccias are located beneath pilot band 1 (4.19 feet); from the top of triple band 1 through triple band 2 (8.94 to 9.40 feet); 10.64 to 10.66 feet; and 11.49 feet (**Figure 3**). Mineral and stratigraphic relationships indicate that these breccias are produced when a volume of water enters the playa under high energy, turbulent conditions. Torrential rainfall and flash flooding are a possible cause, as is overflow from peripheral basins due to increased rainfall basin-wide.

Post-depositional breccias are deposited on top of textural features locally termed "mud squirts" (**Figure 6**) and are characterized by turbulent textures with breccia fragments from buried strata, to a depth of a few feet, in a dolomitic "muddy" matrix. Mud squirts are scattered throughout the mine workings, scarce in some areas, common in others. These features usually originate in middle stage bed 17 and fill a sinuous vertical suture which is topped by an associated breccia, deposited in the late stage. Bedded trona at the margins of these squirts is deformed upward, indicating upward flow under force. A breccia formed from this process (at 12.6 feet) was found to contain breccia fragments that originated from 10.8 feet, which supports upward movement of sediment. Terry Leigh (this volume) has mapped "mud squirts" in bed 17 in the Tg Soda Ash mine and linked them to large scale desiccation cracks. In most geological occurrences of desiccation cracks, sediment fills the vertical crack from above. In this case, sediment fill is definitely from below. It may be that desiccation cracking originated the vertical features which were later injected from underneath by liquefied and pressurized muds from underlying dolomitic layers. Sufficient lithostatic pressure could have been produced by the loading of crystallized trona above unconsolidated dolomitic muds.

Post-depositional changes in mineralogy and textures occur in the late stage and the upper part of the middle stage. Included are recrystallization of trona, disruption of dolomitic partings by late trona crystal growth, and replacement of shortite by nahcolite. An occurrence at 11.25 feet demonstrates increased disruption of a dolomitic parting adjacent to a fracture (**Figure 7**). The undisturbed parting measures $^{1}/_{16}$ inch in thickness and thins to extinction where it contacts the fracture. Disruption of the parting layer increases as the fracture is approached. The fracture is filled with trona satin spar and contains petroleum inclusions. Petroleum inclusions can also be observed spreading out along the degraded parting layer. Post-burial fluids moving along fractures are indicated, as



Figure 6. A "mud squirt" exposed in the western portion of Solvay Mineral's underground mine. Note the roof bolts and wire mesh for scale.

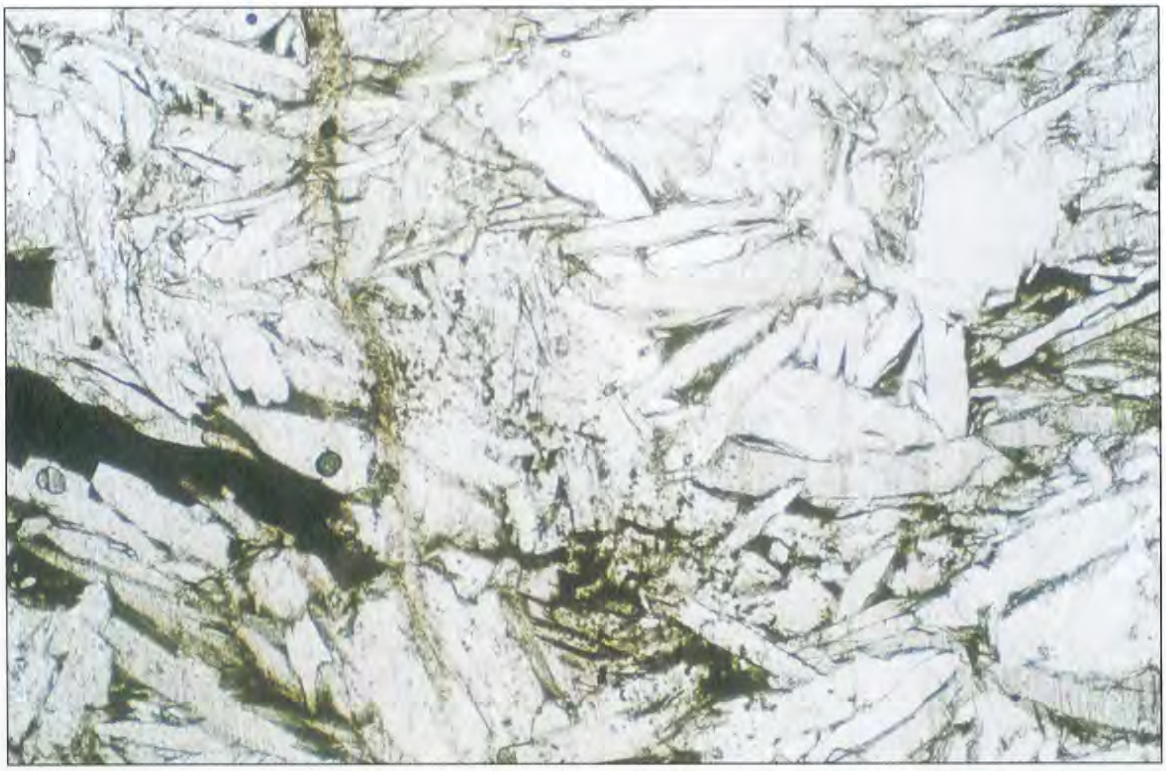


Figure 7. Photomicrograph of a healed fracture cutting a dolomitic band (dark material). The dolomitic band is disrupted by secondary trona crystal growth to the right of the fracture and is truncated to the left. This is a thin section from 11.25 feet and photographed at 25x in plane light.

kerogens in underlying and surrounding oil shales required time and temperature to mature, before petroleum fluid inclusions were possible. Timing of post-depositional mineral activity is unclear. However, at least some of it took place after burial. Halite-bearing stalactites, which deposit along fractures in abandoned mine workings, indicate that chlorine-rich brines are actively moving along fractures. It is possible that these mobile solutions are diagenetically altering the lacustrine deposits at the present time.

Deardorff and Manion (1971) noted trona recrystallization and disruption of original depositional textures in beds 24 and 25. This is in agreement with observations of this study. Recrystallization and disruption of depositional textures is limited to an interval of 8 feet (above floor shale) to the upper contact of bed 17 at 12.6 feet. Below 8 feet, original depositional textures are well preserved.

Discussion

Drever (1982), using data from Garrels and Mackenzie (1967) demonstrated that dolomite should theoretically precipitate from evaporating Sierra Nevada spring water in a closed system at a concentration factor of approximately 10. As evaporation continues, dolomite will continue to precipitate until magnesium and calcium are depleted. Trona does not precipitate until past a concentration factor of 1000. By the time trona begins to precipitate, the solution will be relatively depleted in calcium and magnesium, thus dolomite precipitation will become infrequent to impossible. Thin section observations reveal that dolomite is present as rare submicroscopic and euhedral crystals, even in the purest trona layers of the middle stage. Some calcium and magnesium must therefore be present and available, but relative concentrations are insignificant. Thin section observations also reveal trona and dolomite to be co-depositional at times and to fluctuate between dolomite and trona in specific layers. A flow of water, bearing fresh supplies of calcium and magnesium, is required to precipitate a new dolomite layer under the inferred chemical conditions. Due to the extreme concentrations of trona brines, calcium and magnesium should precipitate dolomite immediately upon entering the playa. Dolomite therefore represents addition of new water into the playa and can be used as a marker for such.

The sudden change in crystal size and texture, from spar to laminated trona in the early stage, indicates a rapid shift in the playa brine conditions toward supersaturation with respect to trona, causing fine crystals of trona to precipitate rapidly in the water column and settle on the playa bottom (**Figures 8** and **5**). Subaqueous deposition is indicated as a volume of water is required to allow crystals to orient and settle parallel to the bedding surface.

A likely factor controlling solution equilibrium is temperature. A rapid drop in temperature of just a few degrees could force a solution close to equilibrium to supersaturation. Such a drop in temperature would occur during winter or a cool and wet season. Lake brine temperatures are the likely controlling factor over grain size variations in sparry trona as well.

If the lamination cycles are the result of annual weather patterns, then dividing the total accumulated thickness of trona by the number of cycles present will produce an average annual rate of accumulation for this stage of bed 17. For the entire thickness of the early stage this rate is 4.75 feet per 14 cycles = .34 feet per year, or 4 inches (10.2 cm) per year. In the upper part of the early stage, where lamination cycles are the dominant stratigraphic feature, this rate is 2 inches (5.1 cm) per year. Lamination cycles in the upper part of the middle stage yield an accumulation rate of 2.6 inches (6.6 cm) per year. Using rates of 2 to 4 inches per year, the entire 12.6 feet of bed 17 could have been deposited in 76 to 38 years.

Micropartings are the result of minor influxes of new water, as described above, which are not associ-

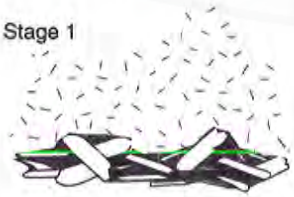
Summary of thin section observations	Interpretation	Inferred causes
Stage 4 	Water temperature warms again. Evaporation condenses the lake brine until the lake is again saturated with respect to trona. Coarser trona crystals grow on the new lake bottom (composed of dolomite and algae). A new layer of trona spar accumulates.	Warm and dry weather patterns return with summer. Evaporation in the basin exceeds rainfall.
Stage 3 	As new waters continue to enter the lake, its brines become undersaturated with respect to trona, which ceases to precipitate. Dolomite continues to accumulate until new waters cease to enter the lake and calcium and magnesium are depleted. Algae flourishes briefly in conjunction with dolomite.	Rainfall ceases or tapers off towards the end of the cooling weather cycle. Waters already enroute to the basin continue until surface aquifers and streams begin to dry up.
Stage 2 	Water temperature remains relatively low and small trona crystals continue to accumulate. Rain water falling in surrounding highlands arrives carrying fresh supplies of calcium and magnesium. Calcium and magnesium precipitate as dolomite and accumulate with fine trona.	Rain (or possibly snow) falls on the mountain ranges surrounding the basin. The new water travels toward the basin center in surface aquifers and ephemeral streams. As the water travels it accumulates an ionic load from the weathering of local rocks.
Stage 1 	Water temperature drops resulting in supersaturation of lake brine and rapid precipitation of small trona crystals in the water column. Small trona crystals settle on the lake bottom. In this example the bottom is composed of trona spar.	Regional weather patterns cool, possibly resulting from a winter or monsoon season. Cooling air temperatures cause a corresponding cooling of water temperatures in the playa lake.

Figure 8. Diagram interpreting the formation of a sequence of laminated trona. The diagram is synthesized from thin section observations from all of the laminated trona layers in sample CC010 and represents a single lamination cycle.

ated with seasonal changes. They may, however, be indicative of storm events in the surrounding mountain ranges.

If the proposed scenario for the formation of lamination cycles is accurate, then a similar scenario for the deposition of trona spar is likely: when cool, wetter, weather patterns begin, trona rapidly precipitates very fine-grained crystals in interstitial spaces between coarser trona crystals. As the fine-grained crystals are confined to the interstitial spaces between the coarser crystals they do not have the space to settle and orient. They remain in the random positions in which they form. Concurrent new water influx carries ionic components for dolomite and pyrite, which crystallize with the fine-grained trona.

If the occurrence of dolomite can be used as an indicator of new water influx, then an absence of dolomite in the middle stage indicates a corresponding lack of new water influx. The interval between pilot band 2 and 7.2 feet therefore may have been deposited under conditions of maximum desiccation in the basin. Furthermore, the relative lack of textures that would indicate subaqueous deposition leaves open the possibility that trona may have been deposited at the brine surface or a marshy environment during accumulation of this interval. The above noted desiccation cracks are strong evidence that the playa did indeed undergo subaerial exposure. Lamination cycles, similar to those found in the early stage, between 7.2 feet and triple band 1 were likely deposited under conditions which prevailed during the early stage, with periodic influxes of new water and seasonal temperature fluctuations.

The increased concentrations of dolomite in the late stage of bed 17 indicate increased influx of new water into the playa lake towards the close of trona deposition. The late stage also contains the majority of unidentified minerals and the greatest diversity of mineral phases. Re-wetting of the hydrographic basin at the close of bed 17 deposition likely washed in dissolved efflorescent saline (trona) crusts from the surrounding surface sediments and smaller basins peripheral to the main central playa. The additional input of sodium from dissolved and remobilized efflorescent trona crusts and accumulations from peripheral playas kept sodium concentrations at a point where trona could still precipitate while the additional water influx into the playa transported elements for the formation of dolomite and other minerals. Thus the final stage of bed 17 takes place under conditions of net water increase into the basin and not under conditions of maximum desiccation of the basin.

Summary and conclusions

The mineralogy and stratigraphy of bed 17 evolved through three stages of trona deposition. The early stage contains cycles of sparry and laminated trona which record annual fluctuations in seasonal weather conditions within the Green River Basin. During this stage trona deposited subaqueously with annual accumulation rates of 5.1 cm (2 inches) to 10.2 cm (4 inches). The mineralogy of the early and middle stages is dominantly trona with very minor dolomite and traces of pyrite and shortite. The middle stage was deposited subaqueously during times of laminated trona accumulation, and may have undergone periods of trona precipitation at the brine surface and/or subaerial exposure where lamination textures are absent for a foot or more of trona accumulation. The third stage represents the beginning of refilling of Lake Gosiute at the end of bed 17 deposition. This final stage is composed of alternating trona and dolomitic layers. Although many layers are dominantly trona with only minor dolomite and other impurities, the overall quality of the ore is diminished due to the frequency and thickness of dolomitic bands. The third stage was also subject to post-depositional recrystallization of trona and original depositional textures are often disrupted.

Acknowledgments

The authors wish to thank Tenneco Minerals (now Solvay Minerals) for sponsoring and supporting this study, with special thanks to D.R. Delling, Ted Eggleston, Larry Refsdal, and Mike Weller. Also thanks to John Dyni and all those whose hard work made this conference a reality.

References cited

Bradley, W.H., and Eugster, H.P., 1969, Geochemistry and paleolimnology of the trona deposits and associated authigenic minerals of the Green River Formation of Wyoming: U.S. Geological Survey Professional Paper 496-B, p. B1-B68.

Culbertson, W.C., 1966, Trona in the Wilkins Peak Member of the Green River Formation, southwestern Wyoming: U.S. Geological Survey Professional Paper 525-D, p. 159-164.

Deardorff, D.L., 1963, Eocene Salt in the Green River Basin, Wyoming, *in* Symposium on Salt: Northern Ohio Geological Society, Cleveland, Ohio, p. 176-195.

Deardorff, D.L., and Mannion, L.E., 1971, Wyoming trona deposits: University of Wyoming Contributions to Geology, v. 10, no. 1, p. 25-37.

Drever, J.I., 1982, The geochemistry of natural waters: Prentice-Hall, Inc., Englewood Cliffs, New Jersey, p. 200-202.

Fahey, J.J., 1962, Saline minerals of the Green River Formation: U.S. Geological Survey Professional Paper 405, 50 p.

Fischer, A.G., and Roberts, L.T., 1991, Cyclicity in the Green River Formation (lacustrine Eocene) of Wyoming: Journal of Sedimentary Petrology, v. 61, no. 7, p. 1146-1154.

Garrels, R.M., and Mackenzie, F.T., 1967, Origin of the chemical compositions of some springs and lakes, *in* Equilibrium concepts in natural water systems: American Chemical Society Advances in Chemistry Series 67, p. 222-242.

Leigh, R.T., 1998, Wyoming trona: A geological overview, *in* Dyni, J.R., and Jones, R.W., editors, Proceedings of the First International Soda Conference, Vol. II: Wyoming State Geological Survey Public Information Circular 40, p. 1-14.

Milton, C., 1971, Authigenic minerals of the Green River Formation: University of Wyoming Contributions to Geology, v. 10, no. 1, p. 57-63.

Sullivan, R., 1985, Origin of lacustrine rocks of Wilkins Peak Member, Wyoming: American Association of Petroleum Geologists Bulletin, v. 69, no. 6, p. 913-922.

The anomalous zone in bed 17

Michael Weller
Solvay Minerals, Incorporated
Green River, Wyoming 82935

Abstract

The anomalous zone is an area of mineralogical and physical changes in bed 17 between an area of mixed halite and trona mineralization and "normal" trona. The principal changes (from normal trona) in the anomalous zone are: 1) the presence of major quantities of wegscheiderite and nahcolite in the bed; 2) changes in the roof and upper insoluble bands of the bed to a rock consisting of northupite, shortite, and quartz; and 3) thinning of the bed. This paper examines the nature of the anomalous zone from core and underground workings and discusses its effect on mechanical mining.

Introduction

The anomalous zone is an area of mineralogical and physical change in bed 17 between the mixed halite and trona zone and "normal" trona. The anomalous zone differs from normal bed 17 by having the following characteristics:

1) Sodium carbonate minerals within the bed change from trona ($Na_2CO_3 \cdot NaHCO_3 \cdot 2H_2O$) to nahcolite ($NaHCO_3$) and/or wegscheiderite ($Na_2CO_3 \cdot 3NaHCO_3$) plus trona. Besides loss of molecular water, the changes consist of increased sodium bicarbonate, hence the term "excess bicarbonate mineralization."

2) The mineral content of the roof, insoluble bands in the trona, and, to a lesser extent, floor rocks, change from dolomite ($CaCO_3 \cdot MgCO_3$) and clay minerals plus shortite ($Na_2CO_3 \cdot 2CaCO_3$) to northupite ($Na_2CO_3 \cdot MgCO_3 \cdot NaCl$) plus shortite and quartz. Broken, disrupted, and/or contorted bands are common in the thinner anomalous bed 17 intersected in drill holes.

3) The thickness of bed 17 decreases.

4) Tar-like hydrocarbons are present in some fractures, in some of the wegscheiderite mineralization, and impregnated in trona.

5) A few cavities filled with high pressure gas are present.

Nahcolite/wegscheiderite mineralization

Excess bicarbonate mineralization is the easiest feature of the anomalous zone to map underground so its presence is used as the boundary of the anomalous zone. Mineralization starts as scattered, small, thin pods of nahcolite at the top of the bed. As one proceeds into the anomalous zone the nahcolite pods become more numerous and slightly thicker. Still farther into the anomalous zone excess bicarbonate mineralization moves to the middle of the bed and wegscheiderite begins to appear. In some of the core holes west of Solvay's mine workings, the bulk of the excess bicarbonate mineralization is at the bottom of the bed and wegscheiderite content greatly increases over that found to the east.

Almost all exposures of excess bicarbonate mineralization observed in Solvay's mine workings were discontinuous lenses. In the 1S 12W panel, a large portion of the mineralization occurred next to subvertical shale seams. In a few other places the mineralization was next to northwest-trending fractures. However, most of the occurrences were lenses that graded laterally to "normal" trona. The only place where excess bicarbonate mineralization showed any continuity was the extreme west end of the 1S 11W exploration entries where the floor rolled up and bed 17 was very thin.

Changes in roof, insoluble bands, and floor rocks

In the normal trona area of Solvay's mine the immediate roof and the upper insoluble bands of bed 17 consist of marlstone with an earthy texture. Estimates from acid soluble analyses indicate a dolomite content of 27 to 46%. In the anomalous zone, the roof and some of the bands are much harder rock with more crystalline texture. Chemical and X-ray diffraction analyses (XRD) show these rocks to consist of up to 50% northupite ($Na_2CO_3 \cdot MgCO_3 \cdot NaCl$), 30% shortite ($Na_2CO_3 \cdot 2CaCO_3$), and 16% quartz. As the term marlstone infers 25 to 75% claystone, the new term "narlstone" was established by Solvay to differentiate these rocks from normal roof and bands. Water soluble NaCl analyses of the roof and bands are excellent indicators of narlstone–northupite is 27% NaCl, although an acid soluble analysis of the water insoluble residue is required to liberate all of its NaCl.

Several core holes through the anomalous zone show a consistent pattern of 0.5 to several feet of narlstone in the immediate roof overlain by a zone of thinly interbedded narlstone, marlstone, and mudstone. XRD analyses of the interbedded zone show the presence of up to 20% dolomite with a corresponding decrease of northupite. Several core holes contain lenses of narlstone above this interbedded zone and thicker lenses at the stratigraphic equivalent of bed 18. Most core holes in the anomalous zone also contain thin lenses of narlstone above beds 16 and 15.

Chemical and XRD analyses of floor rocks in the anomalous zone show a few intervals that contain up to 27% northupite.

Tar-like hydrocarbons

Tar-like hydrocarbons have been encountered in at least one other place besides the anomalous zone in the Solvay and other mines. The greatest concentration of this material has been found in the southern portion of the 1S bleeders in the anomalous zone. The tar occurs as seeps in northwest-trending fractures, in pore spaces of wegscheiderite lenses, and impregnated in trona. At least one core hole also intersected tar in a horizontal fracture in the roof. A sample sent to the U.S. Geological Survey was characterized as "identical to immature Green River oil shale."

High pressure gas cavities

At least ten gas-filled cavities were intersected by mining in the anomalous zone. All but two were encountered at the intersection of the 1S bleeders and the 1S 10W entries. Of the cavities observed, all but one were at the same stratigraphic horizon (between the single and double bands or about 5½ feet above the base of the bed) and had very pure, fine-grained bleached or recrystallized trona to the sides. The largest cavity was about 25 feet long, 15 feet wide, and about 1 foot thick. The roofs of all but one were very smooth with a waterworn look. The cavity floors were covered with small angular pieces of trona. When intersected by mining, the cavities had sufficient gas pressure to hurl rocks up to several hundred feet away and contained a small amount of ammonia.

Cross section

Figure 1 is a cross section of bed 17 through the anomalous zone in core holes passing from normal trona to mixed halite and trona. Insoluble bands less than 0.1 foot thick are not shown.

Starting with the normal trona in DH #1 (right side of section), the top is dirty but the bed is generally high-grade trona, low in NaCl. Moving near the margin of the anomalous zone (as defined by excess bicarbonate mineralization) at DH #2, the number and thickness of the bands increases and a narlstone band is present at the top of the bed. The content of water-soluble NaCl has increased in both the roof and trona bed. Since the bed thickness at both DH #1 and DH #2 is more than 10 feet, most of the bands and the higher NaCl content are above Solvay's normal 9-foot mining height. Just into the anomalous zone at DH #3 is a nahcolite lens at the top of the bed; the narlstone bands are lower and more numerous. The bed has thinned to 9 feet here so the narlstone bands are now within the mining height. Due to the hardness of the narlstone bands, mining productivity begins to decrease away from the normal. At DH #4 excess bicarbonate mineralization has thickened, moved to

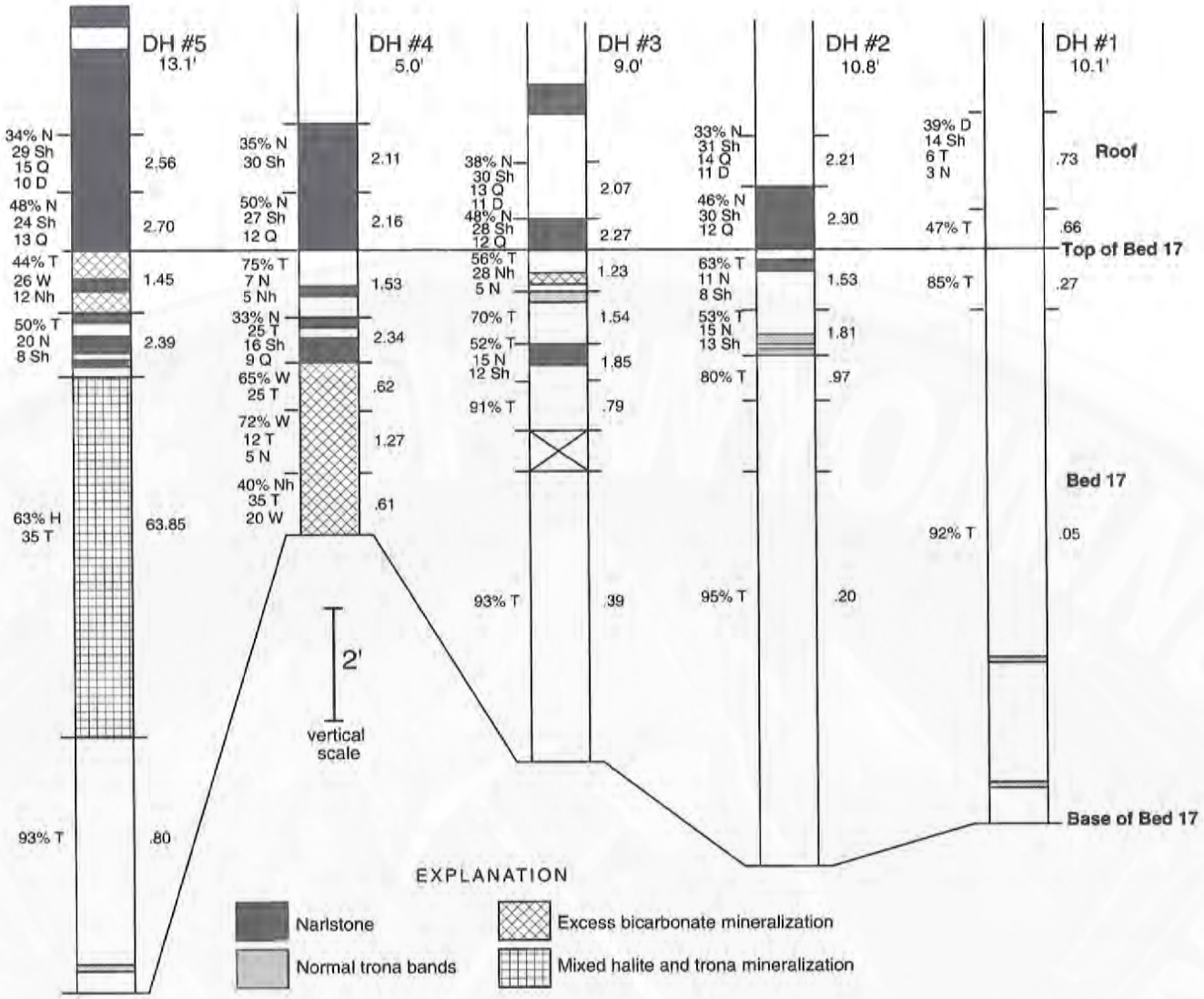


Figure 1. Cross section of bed 17 across the anomalous zone. Datum is the top of bed 17. Figures to left of the core columns are XRD analyses and mineral estimates from water and acid soluble analyses. Abbreviations are: D, dolomite; H, halite; N, northupite; Nh, nahcolite; Q, quartz; Sh, shortite; T, trona; and W, wegscheiderite. Numbers to the right of the core columns are percentages of water soluble NaCl.

the bottom of the bed, and is predominantly wegscheiderite. The floor has rolled up and the bed is now only 5 feet thick. Mining the 1S 11W exploration entries through this material was very slow and required bit changes in as little as 20 feet of advance. At DH #5 the bed has thickened to 13 feet but the middle is now predominantly halite. Excess bicarbonate mineralization has moved back to the top of the bed.

The mineralogical content of the narlstone roof is fairly consistent in and past the anomalous zone on the cross section. Note the presence of dolomite at the expense of northupite at some of the second intervals above the trona. On the cross section, the thickest narlstone roof is above the halite mineralization and generally thins towards and past the margin of the anomalous zone. This contradicts the roof bolters' experience of locally harder and softer drilling. Perhaps anomalous roof conditions are more pod-like than the cross section suggests.



Frontispiece: Aerial view of Solvay Minerals, Incorporated's trona mine and processing plant west of Green River, Wyoming. Production of trona, from both the underground mine and solution mining, was about 3.7 million net tons in 1997; production of refined soda ash and other products was about 2.3 million tons in 1997 (data from Wyoming State Inspector of Mines, Annual Report for 1997). Photograph by John R. Dyni, July, 1998.

Prospecting for Green River-type sodium carbonate deposits

John R. Dyni
U.S. Geological Survey
Denver, Colorado 80225

Abstract

Large economic deposits of sodium carbonate minerals, such as the trona ($Na_2CO_3 \cdot NaHCO_3 \cdot 2H_2O$) and nahcolite ($NaHCO_3$) deposits of the Eocene Green River Formation in the western United States, are rare in the geologic record. Most sodium carbonate deposits are found in lacustrine and playa-lake environments in closed continental basins. The carbonates were deposited episodically with other evaporites during periods of dry climatic conditions. Most deposits range in age from Tertiary to Recent, although older deposits are not out of the question.

The sources of soluble salts include the rocks and sediments exposed in the hydrographic basin of the lake; springs; and air-borne volcanic ash carried into the basin. In addition to the sources of the salts, the relative purity of a sodium carbonate deposit depends upon a variety of factors. Some of these factors include the paleohistory of the lake–whether it existed for long periods of time or repeatedly evaporated to dryness; the structure and hydrology of the basin; and perhaps of key importance, the role of algae and sulfate-reducing bacteria in the lake and sediment waters.

Guides to discovery of sodium carbonate deposits in relatively unexplored regions of the world include geologic mapping and measurement of surface sections with attention paid to sedimentary evaporite structures, mineralogical and geochemical analyses of outcrop samples, analyses of surface and subsurface waters, seismic profiles of basin sediments, and ultimately, core drilling.

Areas favorable for exploration of buried sodium carbonate deposits include the Basin and Range Province of western United States and northern Mexico. Elsewhere, continental basins in Turkey and nearby regions, in large areas of China and adjacent regions, and in the East African Rift where there are present-day soda lakes, such as Lake Magadi, have potential for the discovery of large buried deposits of sodium carbonate.

Introduction

Many of the largest known buried deposits of sodium carbonate were discovered during exploratory drilling for fossil fuels. For example, the Wyoming trona deposit in the Eocene Green River Formation in southwestern Wyoming, was discovered during exploratory drilling for oil and gas in 1937 (Kostick, 1998). Similarly, the nahcolite deposit in the same formation in the Piceance Creek Basin in northwestern Colorado, was discovered in the 1950s during exploratory drilling for oil shale. Elsewhere, the Beypazari trona deposit in western Turkey was discovered during exploratory drilling for coal. Similar discoveries of buried sodium carbonate deposits were made during exploration for oil and gas in the Uinta Basin, Utah, and in Railroad Valley, Nevada.

A model for deposition of sodium carbonate minerals is presented in this paper that may help in exploration for trona and other sodium carbonate minerals in other areas. The model is developed from geochemical studies of modern closed-basin waters as reported in the literature as well as from studies of the sodium carbonate deposits of the Green River Formation in Colorado, Utah, and Wyoming made by the author and other researchers. Some geologic controls on the origin of sodium carbonate deposits are briefly discussed, especially those that resulted in the deposition of the high-purity Wyoming trona deposits. Exploration guides and areas having economic potential for resources of sodium carbonate are presented.

Basic concepts of sodium carbonate deposition

Most sodium carbonate deposits are of lacustrine origin. No marine deposits are known to the author. The geologic setting for most deposits is a closed hydrographic basin in which waters accumulate in a lake or playa (**Figure 1**). Water inflow and evaporation vary widely over time in such an environment. A closed-basin lake may be ephemeral, seasonally evaporating to dryness, or it may be a perennial lake that exists for tens of thousands or even millions of years such as the Eocene Green River lake system in Colorado, Wyoming, and Utah.

Topography can have a strong effect on precipitation. A closed basin on the lee side of a mountain range may receive little precipitation owing to the rain shadow effect. If topographic relief is high, precipitation may accumulate as snow in the mountains during the cool months and contribute melt waters to the closed basin in warmer weather. If the topographic relief is low, the closed lake can expand its borders for many miles during periods of increased water inflow into the basin, and conversely, the lake can contract to a small area, or even evaporate to dryness, during periods of little or no inflow.

The sediments deposited in a closed basin can offer clues as to topographic relief. For example, lacustrine sediments deposited on broad shallow mudflats during lake expansions may form laterally extensive stratigraphic units that can be traced for miles. Conversely, where topographic relief is locally high, coarse clastics from highlands adjacent to the lake may intertongue abruptly with finer-grained sediments basinward.

Climate obviously plays an important role in deposition of closed-basin sediments. A moist climate with a high rate of precipitation would lead to rapid filling of the closed basin and eventually overflow with loss of solutes. If evaporation keeps pace with, or exceeds precipitation, the lake waters will increase in solute content, form a brine, and when it reaches salting stage, precipitate salts.

Some of the largest deposits of sodium carbonate (for example, the Green River deposits, the Beypazari deposit, and some Chinese deposits) are Tertiary in age. Climatic conditions during the Tertiary seemed to favor thicker and purer deposits of sodium carbonate commonly in association with fine-grained organic marlstone and oil shale, perhaps owing to warmer temperatures and moderate to low precipitation at least in those areas where these deposits are found. Many sodium carbonate deposits were also deposited during the Pleistocene, but these are commonly smaller deposits that are typically contaminated with sulfate salts and intermingled with abundant clastic sediments.

Many closed basins in which evaporites accumulated are of tectonic origin, often graben or block-faulted structures (Hutchinson, 1957, chapter 1). Tectonism was probably a critical factor in controlling sedimentation in the Green River lakes. The rate of basin downwarping was commensurate with the rate of sedimentation, permitting the lakes to persist for a period of 10 or so million years during the Eocene.

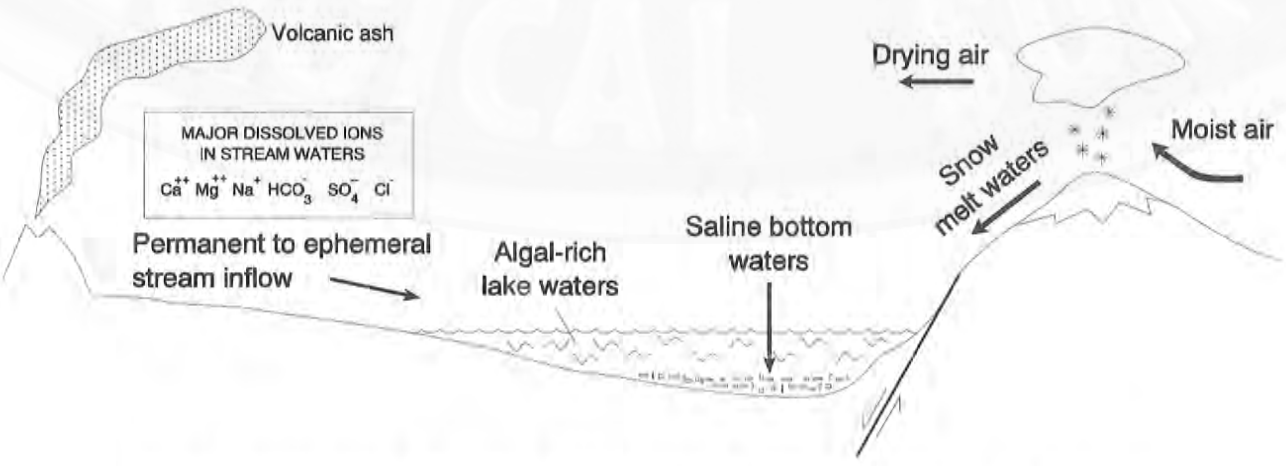


Figure 1. Simple model of deposition of sodium carbonate minerals in a continental closed basin.

Sources of closed-basin sediments and solutes

The source for clastic sediments in a closed-basin lake is limited to its hydrographic basin with one major exception. Airborne volcanic ash from volcanic fields lying beyond the hydrographic basin adds substantial amounts of ash to some lakes and their surrounding hydrographic basins. Glassy tuffaceous material, which decomposes readily in some environments, may add substantial quantities of solutes to the lake.

Numerous, thin, airfall, water-laid, tuff beds are found in the Green River Formation. For example, in a 953-meter-thick lacustrine section of upper Green River rocks measured southwest of Duchesne, Utah, a total of 11.53 meters, or 1.2% of the total thickness of measured sequence, is volcanic ash (author's field notes). Additional tuffaceous material deposited in upland areas of the hydrographic basin would have added considerably more detritus as well as solutes to the lake.

In addition to volcanic tuff, other sources of clastic sediments and solutes that entered the Green River lakes include a wide variety of older Cenozoic, Mesozoic, Paleozoic, and even Precambrian rocks, that were exposed in the hydrographic basins (**Figure 2**).

Springs are another important source of solutes in many closed basin lakes. Lakes Magadi and Little Magadi, in the Rift Valley, Kenya, for example, receive as much 3900 metric tons of sodium carbonate per day via springs (Baker, 1958). The sodium carbonate in these springs may have been derived from nearby carbonatites or possibly from trona-bearing rocks at depth within or near the hydrographic basin of the Magadi lakes.

Spring deposits have been noted in the Green River Formation along the south and east sides of the Green River Basin in southwestern Wyoming (Bradley and Eugster, 1969, p. B29-B30). These springs, and probably others, may have contributed substantial amounts of water to the Green River lakes. However, in contrast to the Lake Magadi springs, it seems doubtful that springs supplied large quantities of sodium carbonate to the Green River lakes because the rocks known to underlie the Green River Formation are unlikely sources of large quantities of sodium carbonate salts.

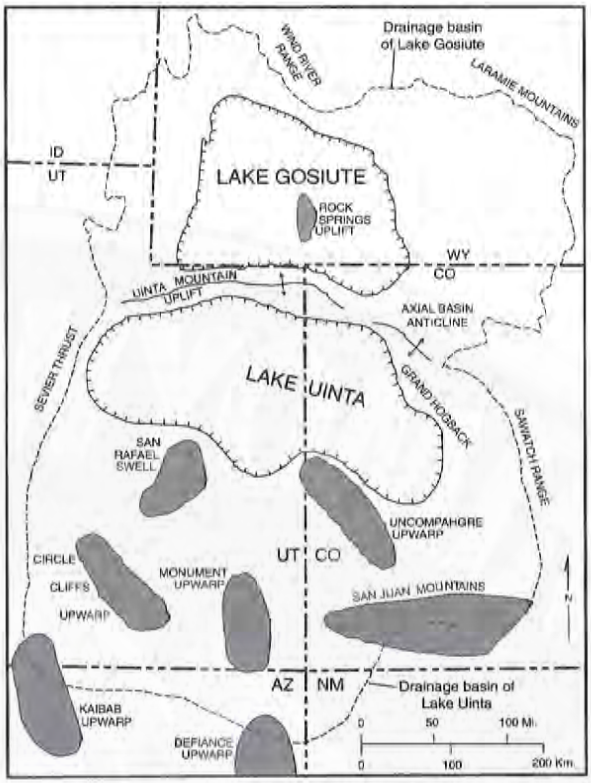


Figure 2. Map of the Green River lakes during their estimated maximum expansion in Eocene time in Wyoming, Colorado, and Utah. The hydrographic basins of the lakes and the major tectonic features of the region are shown. Adapted from Bradley and Eugster (1969, figure 3) and Dyni (1981, figure 1).

Much carbonate entered closed-basin lakes by dissolution of carbonate source rocks and by hydrolysis of silicate minerals in source rocks within the hydrographic basin. Additionally, large amounts of carbonate may have also been introduced by biogenic processes including carbonate-secreting algae, and by bacterial sulfate reduction.

Sedimentation rates

Sedimentation rates in closed-basin lakes vary widely depending upon the type of sediment and mode of deposition. Sedimentation rates for sandstone, marlstone and related rocks, and oil shale of varied grades in the Green River Formation estimated by Bradley (1929, p. 99) are given in **Figure 3**. Fahey (1962, p. 44-45) assumed that the insoluble material in trona was deposited at the same rate as the sediments of the Wilkins Peak Member in the Green River Basin, which was estimated by Bradley to be about 3000 years per foot (Fahey, 1962, p. 44). On this basis, Fahey determined that trona bed 17 was de-

posited at variable rates of 3 to 877 years per foot, depending upon the amounts of insoluble material distributed vertically through the bed. Boni and Atkinson (1998, this volume) noted cyclic sedimentary structures and textures in the lower 4 feet of trona bed 17 that suggested an average depositional rate of 2 to 3 inches per year (4 to 6 years to deposit one foot of trona). Fahey (1962, table 17) also noted a rapid rate of deposition in the lower part of bed 17 as compared with the upper part. Compared with deposition of other Green River sediments, deposition of bedded evaporites was much more rapid (**Figure 3**).

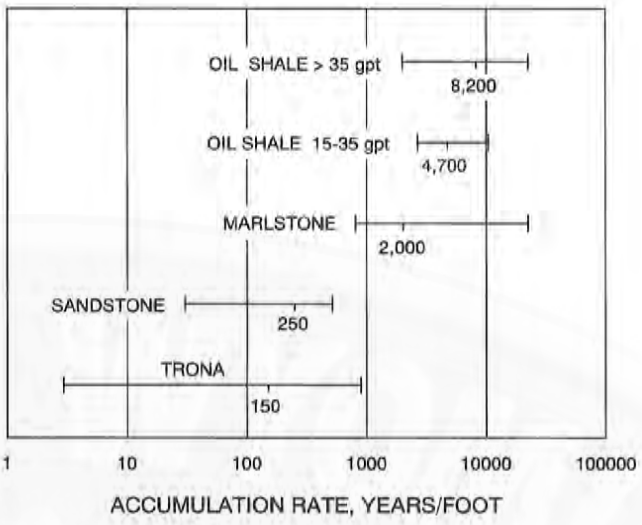


Figure 3. Rates of deposition, in years per foot, of lacustrine rocks in the Green River Formation. Data from Bradley (1929), Fahey (1962), Boni and Atkinson (1998), and the author's unpublished notes. The range and average for each rock type is shown. Depositional rates for rocks of turbiditic and storm origin are not included. gpt, gallons of shale oil per short ton of rock.

Evolution of closed-basin waters

Hardie and Eugster (1970) modeled the system Ca-Mg-Na-K-(CO_3+HCO_3)-SO_4-Cl in closed-basin brines and for the evaporation paths of fresh waters from varied source rocks. They found that natural brines in closed basins range widely in composition. Generally, the ratio of Na to Ca+Mg is high owing to early precipitation of Ca and Mg as relatively insoluble alkaline earth carbonates. The anions show a much wider diversity in their relative abundances (**Figure 4**).

Theoretical evaporation paths calculated for dilute waters sourced by a variety of rock types show a general evolution of Ca+Mg in most waters toward Na as a function of precipitation of Ca and Mg carbonates and depletion of CO_3+HCO_3 with the anion path moving toward SO_4 and Cl. These paths are based on physical chemistry alone and do not account for biochemical processes such as bacterial sulfate reduction.

The evaporation path for average North American river water calculated by Hardie and Eugster (1970, figure 2e), is plotted with a second path suggested for Green River water entering the Eocene Green River lakes in which the sulfate is removed (**Figure 5**) by sulfate-reducing bacteria according to the generalized reaction:

$$2CH_2O + SO_4^{-2} \rightarrow 2HCO_3^{-1} + H_2S.$$

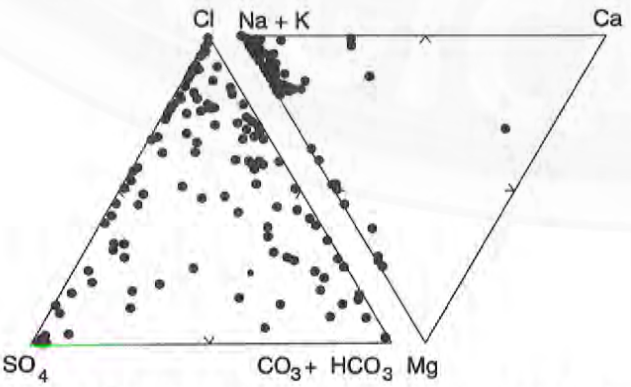


Figure 4. Composition of over 100 natural closed-basin brines in the system Ca-Mg-Na-K-(CO_3+HCO_3)-SO_4-Cl from Hardie and Eugster (1970, figure 1 reproduced with permission). Note the great diversity of especially the anionic compositions.

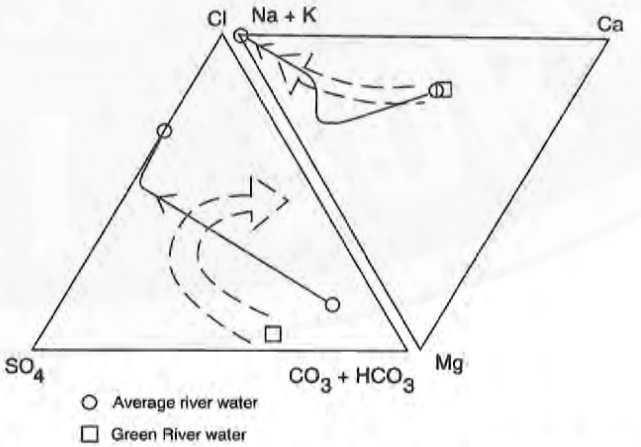


Figure 5. Calculated evaporation path of average North American river water modified from Hardie and Eugster (1970, figure 2e) and a suggested evaporation path for modern Green River water, assuming total reduction of sulfate by sulfate-reducing bacteria. Composition of Green River water is from Bradley and Eugster (1969, table 7).

Note that two moles of bicarbonate are produced for each mole of sulfate reduced which would move the anion path toward the (CO_3+HCO_3)-Cl line. The H_2S could react with available divalent iron and precipitate as sulfides or it could escape the system as a gas.

Bacterial sulfate reduction

Most models of the chemistry of closed lake systems such as that proposed by Hardie and Eugster (1970) do not account for biochemical reactions, yet closed basin sediments commonly contain abundant organic matter including algae and, no doubt, large colonies of bacteria including sulfate reducers. Few of the earlier studies of the Green River sedimentary rocks and sodium carbonate deposits have considered the importance of bacteria in mineral-forming processes, most likely because of the difficulty of identifying bacterial remains and the products of bacterial processes in the sediments. Indirect evidence, however, points to such processes as being of prime importance in the evolution of solutes in closed-basin waters and to the precipitation of sodium carbonate deposits free of sulfate salts.

In an earlier paper, Dyni (1983) has shown that the vertical distribution of sulfur through the nahcolite-bearing Green River oil shale in the Piceance Creek Basin, Colorado, is cyclic and that many of these cycles can be traced between core holes. Maximum sulfur values, reaching as much as 5 wt.% of the oil shale on a nahcolite-free basis, are found near the top of, or just above, a zone of nahcolite. Several of these sulfur cycles are shown in **Figure 6**.

Dyni (1983) originally interpreted the maximum increase in sulfur in a sulfur cycle to represent a low stand of the Eocene lake, but compelling isotopic sulfur and other data published by Tuttle and Goldhaber (1993) suggests the reverse may be true; that the sulfur maxima of these cycles represent high stands of the lake. In one of Dyni's numbered sulfur cycles (cycle 21) through a thickness of about 33 feet of oil shale, Tuttle and Goldhaber (1993, their figure 4) show strong inverse associations between total sulfur (organic plus mineral sulfur) and $\delta^{34}S_{di}$ (**Figure 7**) where S_{di} represents sulfur in divalent pyrite and marcasite, and between total sulfur and the ratio of dolomite to calcite. The decreases in $\delta^{34}S_{di}$ and in the dolomite to calcite ratio through sulfur cycle 21 suggest freshening of the lake waters rather than increasing salinity. In either case, the important point is that the distribution of sulfur in organic-rich sediments may be an indicator of the relative importance of bacterial reduction of sulfate in closed lake-basin sediments. Large amounts of sulfide minerals in such

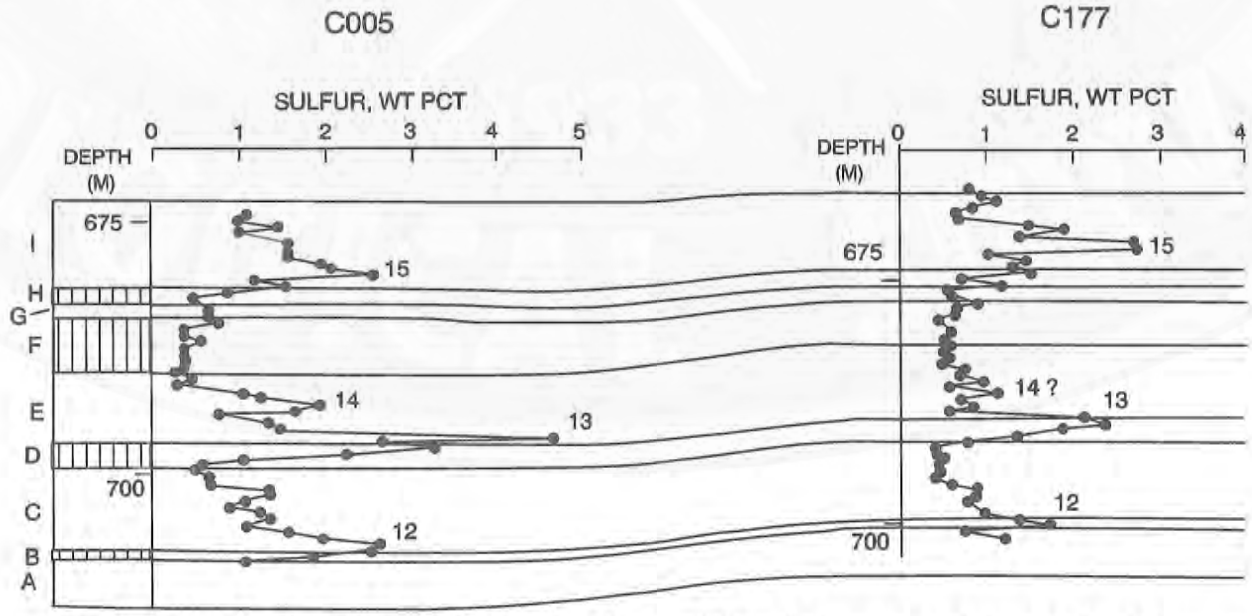


Figure 6. Vertical profiles of total sulfur in weight percent in two core holes in the Piceance Creek Basin, Colorado. Samples are composites of approximately 0.6-meter increments of drill core. The unpatterned parts of the drill core are nahcolite-bearing oil shale and the vertically ruled bands (B, D, F, and H) are units of nahcolite. The numbered sulfur cycles are from Dyni (1983, figure 8).

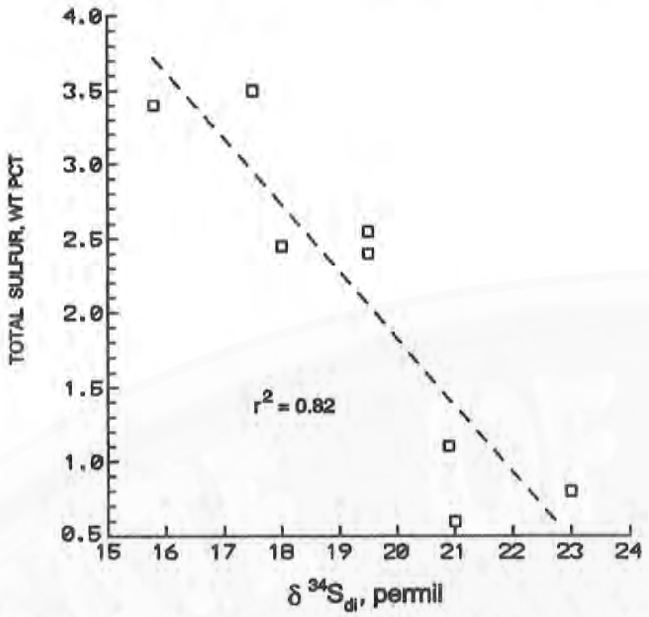


Figure 7. Plot of total sulfur in weight percent against $\delta^{34}S$ permil through sulfur cycle 21 of Dyni (1983) in the Juhan core hole 4-1, Piceance Creek Basin, Colorado. Sulfur data from Tuttle and Goldhaber (1993, figure 4c). A strong negative association of total sulfur with $\delta^{34}S$ is indicated by a coefficient of determination, r^2, of 0.82.

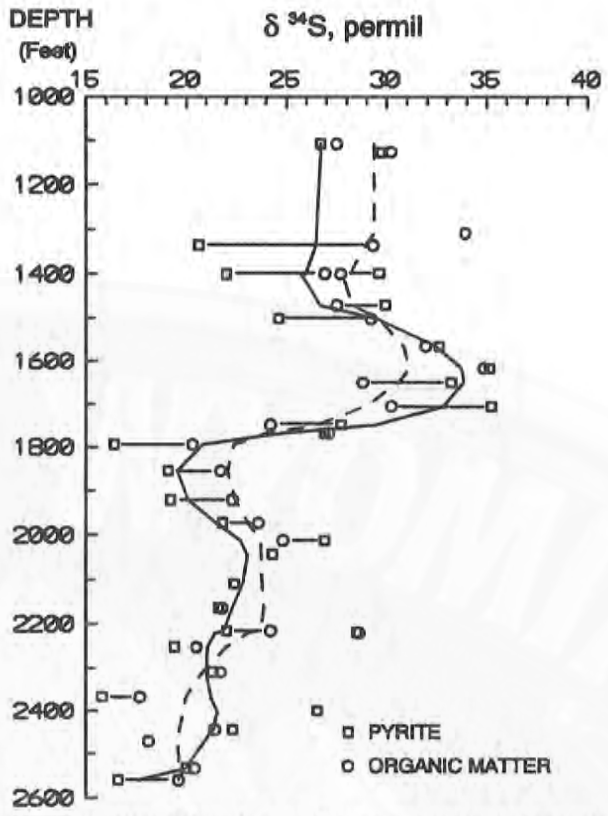


Figure 8. Vertical distribution of $\delta^{34}S$ permil values for organic matter and pyrite through a 1453-foot-thick sequence of nahcolite-bearing Green River oil shale in U.S. Bureau of Mines Colorado core hole 1, Piceance Creek Basin, Colorado. The horizontal lines connect analyses made on the same sample. The solid black line is statistically smoothed through the $\delta^{34}S$ values for pyrite and the dashed line is smoothed through the $\delta^{34}S$ determinations for organic matter.

sediments suggest that large amounts of biogenic carbonate were generated.

Isotopic sulfur values may also provide clues as to the history of a closed-basin lacustrine environment. Smith and Young (1983) determined $\delta^{34}S$ values in organic matter and in iron sulfide minerals in 32 samples from a core hole drilled through a 1450-foot-thick sequence of Green River oil shale in the Piceance Creek Basin (**Figure 8**). A statistically smoothed profile of their $\delta^{34}S$ values for the organic sulfur and for the iron sulfide minerals (labeled pyrite on figure) plotted against depth clearly shows an overall upward increase toward more positive values from the base to the top of the analyzed sequence, ranging from about 17 to 35 permil (per 1000). Similar vertical trends in $\delta^{34}S$ were found by Cole (1975), Tuttle (1988), and Tuttle and Goldhaber (1993).

The upward increase in $\delta^{34}S$ may have been caused by the preferential utilization of the lighter sulfur istope ^{32}S by sulfate-reducing bacteria in their metabolic processes. Because of this preference, the heavier sulfur isotope ^{34}S would tend to increase in the closed-basin waters relative to ^{32}S as the sulfate is reduced to sulfides. With influx of fresh water having lower $^{34}S/^{32}S$ ratios, the trend would be reversed. The large upward increase in $\delta^{34}S$ in Smith and Young's (1993) data beginning at a depth of about 1800 feet and reaching a maximum at about 1670 feet suggests a strong regressive lake stage followed by a period of freshening waters up to a depth of 1400 feet. This decrease in $\delta^{34}S$ is somewhat puzzling, because it occurs in the leached upper part (leached zone) of the nahcolite facies in the basin. However, secondary sulfide minerals with lower $^{34}S/^{32}S$ ratios may have been introduced by surface waters that dissolved the water-soluble salts in the leached zone. Isotopic sulfur data above 1400 feet appear to be too sparse to determine a clear trend in this part of the sequence.

The stratigraphically lowest $\delta^{34}S$ value of 16.6 permil as determined by Smith and Young (1983) was of a sample of oil shale close to the base of the carbonate-bearing oil shale sequence in the basin below which are fresher-water illitic oil shales. It would be of interest to determine if the $\delta^{34}S$ values in the illitic oil shales remain low. If so, it might be possible to predict where sodium carbonate mineralization might be expected in a sequence of organic-rich sediments on the basis of $\delta^{34}S$ values.

Further work on the geochemistry of sulfate-reducing bacteria in the Green River Formation is needed. There may be specific geochemical biomarkers that could help identify sulfate-reducing bacteria and the role they played in the origin of sodium carbonate deposits.

Summary of the Green River model

Five sodium carbonate/chloride evaporite facies are known in the Green River Formation in Wyoming, Colorado, and Utah (**Figure 9**). Although they differ from one another in mineral composition and other details, they all share the following attributes:

(1) all of the Green River evaporite deposits are free of sulfate minerals, presumably because of effective and total reduction of sulfate by sulfate-reducing bacteria;

(2) all are associated with organic-rich host rocks (organic marlstone and oil shale);

(3) they occur in a very large lake system whose hydrographic basins occupied thousands of square miles;

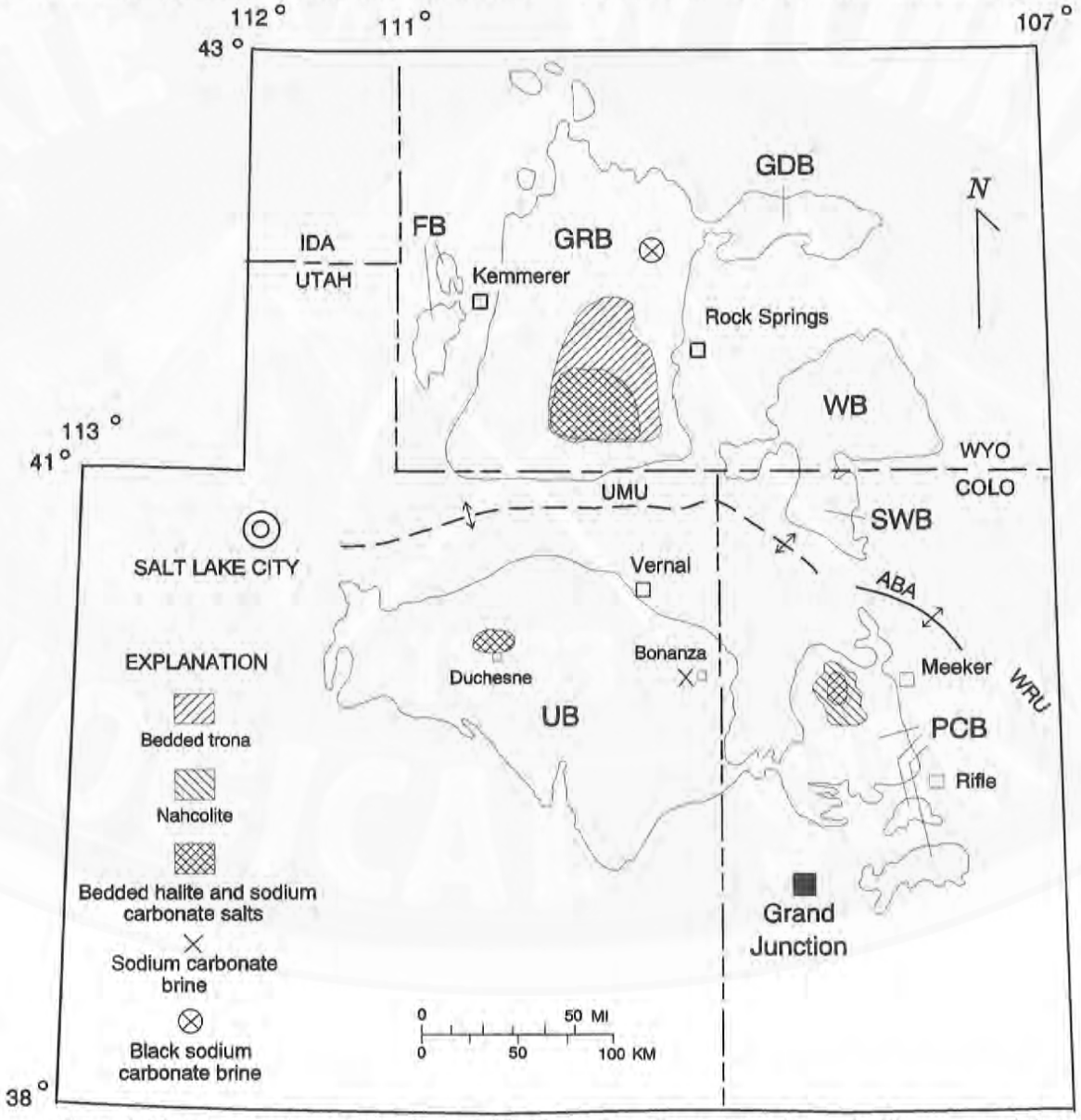


Figure 9. Map showing the areal distribution of the Green River Formation in Colorado, Wyoming, and Utah and the location of three deposits of bedded sodium carbonate and two sodium carbonate brine fields. FB, Fossil Basin; GRB, Green River Basin; GDB, Great Divide Basin; WB, Washakie Basin; UMU, Uinta Mountain uplift; SWB, Sand Wash Basin; ABA, Axial Basin anticline; PCB, Piceance Creek Basin; UB, Uinta Basin; WRU, White River uplift.

(4) they were deposited in closed lakes in structural-sedimentary basins that existed for millions of years in regions of generally low precipitation; and

(5) the sources of sediments and solutes included a variety of rock types including marine, continental, and volcanic.

Exploration guides

Prospecting for sodium carbonate deposits should focus on closed basins in which thick accumulations of organic-rich lacustrine rocks are found. Probably the most favorable areas would be basins containing lacustrine rocks of Tertiary age, as these may offer the best possibility of finding high-purity sodium carbonate deposits like those in the Green River Formation.

Younger lacustrine and playa sediments of Quaternary age may also host economically significant resources of sodium carbonate, such as those at Searles Lake, California. Sulfate-reduction in the younger deposits may be less effective than in older Tertiary deposits; therefore, the younger deposits may contain significant quantities of sulfate as gangue minerals which would lessen their economic value. Some additional guides for exploring for sodium carbonate deposits follow.

Sedimentary structures

The most obvious evidence of evaporite deposition may be found in outcrops of fine-grained lacustrine sedimentary rocks. Sedimentary structures such as crystal and crystal-aggregate cavities, pseudomorphic minerals after evaporite minerals, and solution breccias all point to deposition of evaporites (**Figures 10** and **11**). The euhedral shapes of some crystal cavities may be sufficiently diagnostic to identify the dissolved mineral.

Water chemistry

Analyses of springs and groundwaters may provide clues to the presence of evaporite minerals or the discovery of sodium carbonate brines at depth within a closed basin. Spring waters in contact with buried evaporitic rocks via faults may provide direct evidence of a buried sodium carbonate deposit. Water chemistry data plotted on a map might show trends in concentrations of sodium, carbonate, and bicarbonate that would point toward buried sodium carbonate minerals or brine.



Figure 10. Evaporite structures in an outcrop of Green River oil shale. The oval cavities were once filled with coarse-crystalline rosettes of water-soluble nahcolite. The cavity being measured is about 32 cm across and 23 cm high.



Figure 11. Close-up of a nahcolite cavity in the ledge shown in Figure 10. The knife in the cavity is about 8 cm long. The cavity is lined with organic-rich papery layers that originally separated individual blades of nahcolite in the rosette.

Mineralogy

Because the most favorable host rocks for sodium carbonate are commonly fine-grained lacustrine rocks including marlstones, oil shales, and claystones, determination of the mineralogy of these rocks is best accomplished by X-ray diffraction analysis. Mineral facies trends, such as those noted in the Green River Formation may indicate evaporitic conditions in parts of the lacustrine sequence.

Mineral trends in Green River rocks from basin edge to basin center show progressive changes from typical clastic minerals such as feldspars, quartz, and detrital clays; to calcite and probable authigenic smectite and illite; to dolomite, siderite, Na-Ca carbonates; and at basin center to evaporites including nahcolite, trona, and other salts.

A somewhat similar relationship to that above is also noted in vertical sequences of Green River sediments in the Piceance Creek Basin: from low-carbonate, illitic oil shale at the base of the sequence progressing upward into non-clayey dolomitic marlstone containing dawsonite, nahcolite, and, locally, halite (Hite and Dyni, 1967, figure 4). In the Piceance Creek Basin, this change in mineralogy is abrupt, signalling a change in water chemistry of the lake from a relatively fresh initial stage progressing to highly saline waters at a later time (**Figure 12**).

Changes in mineral facies and lithofacies, abundance of organic matter, trends in $\delta^{34}S$ as related to salinity, and depositional environments of the lacustrine rocks of the Green River Formation are summarized in **Figure 13**.

Ultimately, core drilling would be required to co firm the presence of a buried sodium carbonate deposit. Seismic lines could aid in delineating the areal extent of a deposit. Detailed core logs (and identification of minerals) are imperative to determine modes of occurrence of the evaporite minerals (bedded, vein, disseminated crystals, crystal aggregates, etc.), and grade of ore.

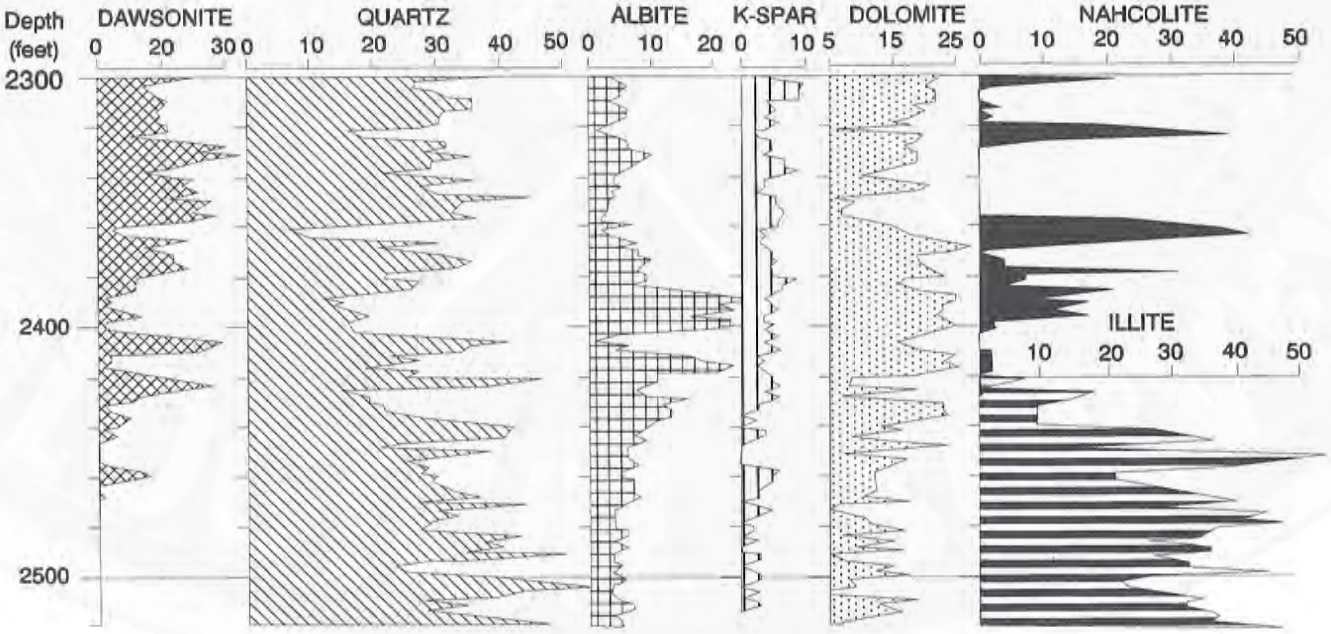


Figure 12. Changes in mineralogy through the lower part of the Green River oil shale sequence in the Juhan 4-1 core hole in the Piceance Creek Basin, Colorado. In the interval between the depths of about 2380 and 2480 feet, note the upward decrease then disappearance of illite as the first sodium carbonate minerals, nahcolite and dawsonite, appear in the sequence. Dolomite and albite increase upward through this interval, and quartz decreases. The relative abundances of dawsonite and quartz through the dawsonite-bearing sequence of oil shale track one another, suggesting a common aluminosilicate precursor (illite?). These mineralogical changes are related to the change from fresh or brackish waters to saline waters as these rocks were being deposited.

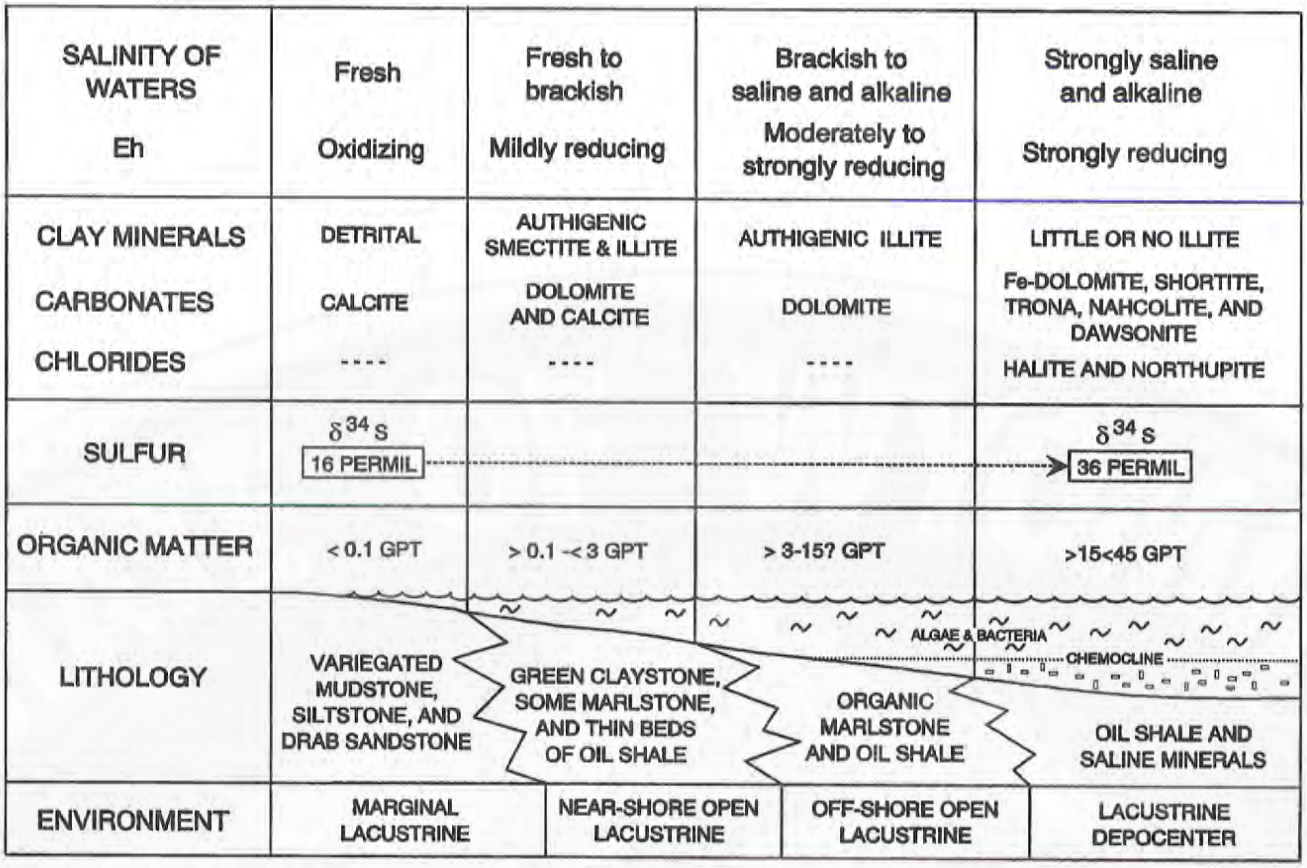


Figure 13. Schematic summary of changes in lithofacies, sulfur geochemistry, and mineral facies from basin margin to depocenter of the the Green River lakes. gpt = gallons of shale oil per short ton of rock. Sulfur isotope values (δ^{34}s) are expressed in permils (per 1000).

Areas favorable for sodium carbonate exploration

Although sodium carbonate deposits of high purity and size similar to those of the Green River Formation are rare in the geologic column, there are numerous areas in the world where large deposits might yet be found. The Basin and Range Province in western United States and northern Mexico, still little explored for sodium carbonate deposits, offers good possibilities. Large continental basins in China containing thick sequences of lacustrine rocks could host sizable deposits of sodium carbonate. Elsewhere in Asia, lacustrine oil shale is present in Tertiary basins in Thailand and Myanmar (Burma). The mineralogy and organic matter of the Thai oil shale near Mae Sot, for example, is quite similar to that of the Green River Formation, suggesting an alkaline depositional environment. These basins offer some possibility of hosting sodium carbonate deposits.

Numerous continental basins containing lacustrine rocks are found in Turkey and in nearby regions of the Near East and may be favorable sites for sodium carbonate deposition. In eastern Africa the Rift Valley is noted for numerous soda lakes, including Lake Magadi, where soda ash has been produced in past years. The Rift Valley has been little explored by core drilling, yet the potential for buried deposits of sodium carbonate minerals and brines seems to be good.

Conclusions

An understanding of the conditions controlling the deposition of bedded sodium carbonate minerals in the Eocene Green River Formation provides a model that may be useful in the search for similar deposits elsewhere in the world. Deposits of high purity, like those of the Green River Formation which lack sulfate minerals, suggest a highly efficient process of removing sulfate from the system, probably by sulfate-reducing bacteria. This biogenic oxidation-reduction process also produces significant quantities of bicarbonate-carbonate to closed-basin lacustrine waters. Lacustrine sedimentation in a warm Tertiary climate

during a period of relatively low precipitation in a stable downwarping tectonic basin that persisted for hundreds of thousands to millions of years probably provided optimum conditions for the deposition of organic-rich sediments and high-purity sodium carbonate deposits.

References cited

Baker, B.H., 1958, Geology of the Magadi area: Kenya Geological Survey Report 42, 81 p.

Boni, P., and Atkinson, W.W., Jr., 1998, A mineralogic and stratigraphic profile of trona bed 17 in the Solvay trona mine near Green River, Wyoming, *in* Dyni, J.R., and Jones, R.W., editors, Proceedings of the First International Soda Ash Conference, Volume II: Wyoming State Geological Survey Public Information Circular 40, p. 21-32.

Bradley, W.H., 1929, The varves and climate of the Green River Epoch: U.S. Geological Survey Professional Paper 158, p. 87-110.

Bradley, W.H., and Eugster, H.P., 1969, Geochemistry and paleolimnology of the trona deposits and associated authigenic minerals of the Green River Formation of Wyoming: U.S. Geological Survey Professional Paper 496-B, 71 p.

Cole, R.D., 1975, Sedimentology and sulfur isotope geochemistry of Green River Formation (Eocene), Uinta Basin, Utah, Piceance Creek Basin, Colorado: Ph.D. dissertation, University of Utah, Salt Lake City, 274 p.

Dyni, J.R., 1981, Geology of the nahcolite deposits and associated oil shales of the Green River Formation in the Piceance Creek Basin, Colorado: Ph.D. dissertation, University of Colorado, Boulder, 144 p.

Dyni, J.R., 1983, Distribution and origin of sulfur in Colorado oil shale deposits [abstract], *in* Gary, J.H., editor, Proceedings of 16th Oil Shale Symposium: Colorado School of Mines Press, Golden, Colorado, p. 144-159.

Fahey, J.J., 1962, Saline minerals of the Green River Formation: U.S. Geological Survey Professional Paper 405, 50 p.

Hardie, L.A., and Eugster, H.P., 1970, The evolution of closed-basin brines: Mineralogical Society of America Special Paper 3, p. 273-290.

Hite, R.J., and Dyni, J.R., 1967, Potential resources of dawsonite and nahcolite in the Piceance Creek Basin, northwest Colorado *in* Fourth Symposium on Oil Shale: Quarterly Colorado School of Mines, v. 62, p. 25-38.

Hutchinson, G.E., 1957, A Treatise on Limnology, volume I, Geography, Physics, and Chemistry: John Wiley and Sons, New York, New York, 1015 p.

Kostick, D.S., 1998, The origin of the U.S. natural and synthetic soda ash industries, *in* Dyni, J.R., and Jones, R.W., editors, Proceedings of the First International Soda Ash Conference, Volume I: Wyoming State Geological Survey Public Information Circular 39, p. 11-33.

Smith, J.W., and Young, N.B., 1983, Stratigraphic variation of sulfur isotopes in Colorado corehole number 1, *in* Gary, G.H., editor, Proceedings of 16th Oil Shale Symposium: Colorado School of Mines Press, Golden, Colorado, p. 176-188.

Tuttle, M.L., 1988, Geochemical evolution and depositional history of sediment in modern and ancient saline lakes: evidence from sulfur geochemistry: Ph.D. dissertation, Colorado School of Mines, Golden, 312 p.

Tuttle, M.L., and Goldhaber, M.B., 1993, Sedimentary sulfur geochemistry of the Paleogene Green River Formation, western USA: implications for interpreting depositional and diagenetic processes in saline alkaline lakes: Geochimica et Cosmochimica Acta, v. 57, p. 3023-3039.



Aerial view of trona mining and processing facilities and tailings disposal ponds operated by FMC Wyoming Corporation in the Green River Basin, Wyoming.

Trona crystallization processes– Observations at Owens Lake, California, 1970-77

George I. Smith
U.S. Geological Survey
Menlo Park, California 94025
and
Irving Friedman
U.S. Geological Survey
Denver, Colorado 80225

Abstract

For most of the time since about 1920, Owens Lake in southeastern California has been dry, capped by a 1- to 3-m-thick layer of sodium carbonate, sulfate, and chloride salts. Because of an uncommonly wet 1968-69 winter, the lake was flooded during the spring and summer of 1969, and about 20% of the pre-existing salt body was dissolved. Evaporation led to re-deposition of those salts, starting in late summer 1970, and eventually to desiccation in late summer 1971.

The lake's compositional and isotopic chemistry, mineralogy, depth, and temperature were monitored during 15 visits over a 17-month period. We collected samples of the salts when they began to recrystallize, and cored both the "new" and the underlying "old" salts, testing both sample sets for their mineralogic and isotopic (Deuterium/Hydrogen or D/H) composition. The sodium carbonate salts all contain H^+, allowing any post-depositional recrystallization to be identified and partially reconstructed on the basis of their changed D/H values. With the passage of the hot and cold seasons, the lake water and its salt layer warmed and cooled, causing the mineral assemblages to change as a result of dissolution of some minerals and crystallization of others from the brines; they continued to change for the six years following desiccation. Observations of the crystallization processes showed that salts having a large decrease in solubility at lower temperatures crystallized on the lake surface during cold nights, and that salts with little change in solubility at lower temperatures crystallized most rapidly on the surface during mid-day.

The D/H values of the "new" salts showed less scatter each year, and they eventually approached the minimal scatter and absolute values of the "old" salts, suggesting that the mineralogic and isotopic composition of the "new" salts, through diagenetic processes, was evolving the same way as the "old" salts did following the post-1913 period of salt deposition.

Introduction

Owens Lake, in southeastern California immediately east of the Sierra Nevada (**Figure 1**), began to shrink shortly after 1913 when its water supply was diverted into an aqueduct leading to Los Angeles. By about 1920, it had completely desiccated, leaving the former lake floor covered by a 0- to 3-m-thick bed of mixed Na-bearing salts and interstitial brines that had a density of ~1.3 and a pH of ~11.

Following the exceptionally wet winter of 1968-69, runoff from melting snow in the adjoining Sierra Nevada exceeded the capacity of the aqueduct, causing fresh water to flood Owens Lake and dissolve the top ~0.6 m of the salt layer, leaving about ~0.6 m (at our sample site) of the "old" salts that were deposited earlier this century. Maximum lake depth of ~2.7 m was reached in August, 1969, and evaporation then

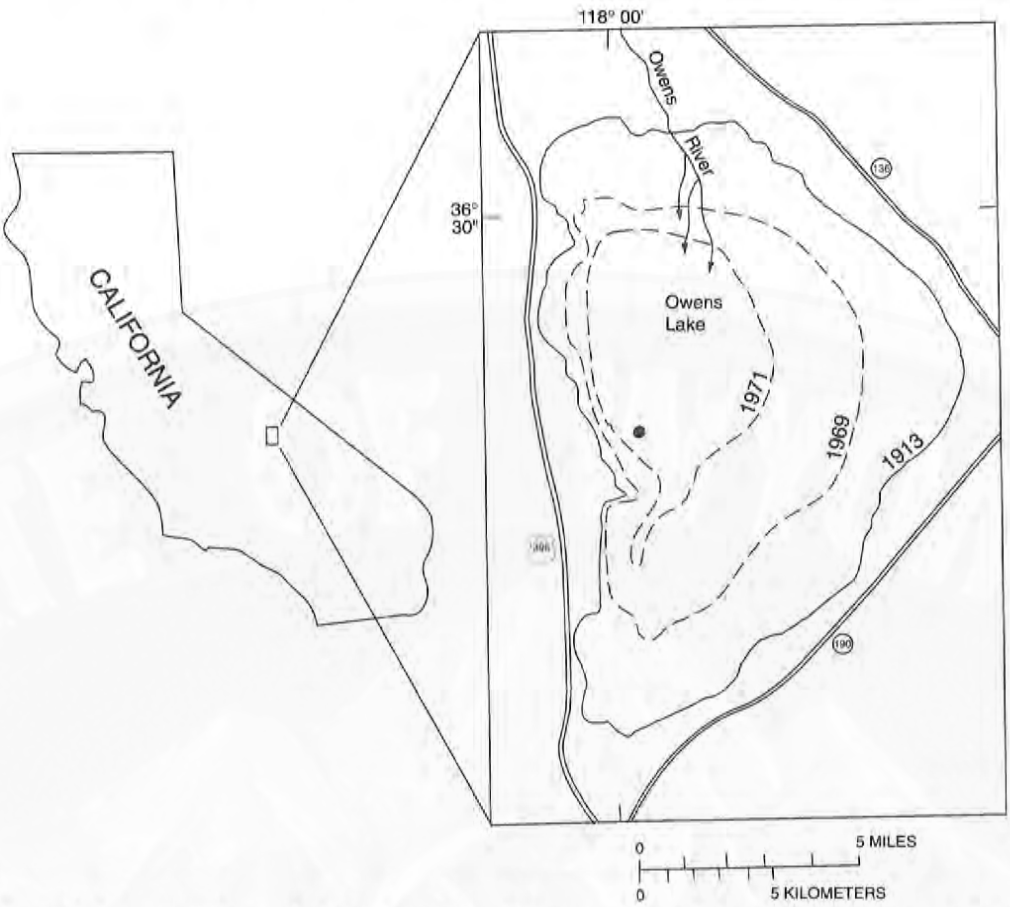


Figure 1. Location of Owens Lake and positions of lake shorelines in February, 1913 (prior to its first desiccation), August, 1969 (maximum area following 1969-70 flooding), and April, 1971 (four months prior to desiccation). Sample site (black circle) is near lowest point in lake floor.

lowered lake level to a depth of ~1.2 m by early September, 1970, when salt crystallization began; its salinity at that time was ~25 wt.%. By August, 1971, desiccation was complete, and lake salinity was 36%.

This paper is a brief summary of our studies of crystallization processes that were carried out to understand them better, hopefully allowing us to use the isotopic compositions of saline minerals as a geothermometer. These studies (see papers by Friedman and others, 1976; Smith and Friedman, 1986; Smith and others, 1987) describe the processes observed as Owens Lake first was flooded in January, 1969, then evaporated over a 34-month period, and finally desiccated, leaving a 0.6-m layer of "new" salts resting on the "old" salts. We described the assemblages of re-deposited minerals as they, and the hydrogen isotope compositions of the minerals, interstitial brines, and lake waters, changed after initial salt deposition–and for six additional years after desiccation. The isotopic composition of the "old" salts changed little.

Table 1 lists the names of the most common saline minerals in Owens Lake, their chemical formulas, and their abbreviations as used in diagrams herein. **Table 2** lists the composition of the lake waters as evaporation caused the lake depth to decrease and the lake salinity to increase.

Deuterium (D) analyses in the following section are expressed in δD units (permil or per 1000), where:

$$\delta D = \frac{(D/H)_{sample} - (D/H)_{standard}}{(D/H)_{standard}} \times 1000.$$

The standard is Standard Mean Ocean Water (SMOW) as defined by Craig (1961).

Table 1. Names, abbreviations, and compositions of major saline minerals from Owens Lake.

Name	Abbreviation used in this paper	Chemical composition
Burkeite	Bk	$2Na_2SO_4 \cdot Na_2CO_3$
Halite	Ha	NaCl
Mirabilite	Mb	$Na_2SO_4 \cdot 10H_2O$
Nahcolite	Nh	$NaHCO_3$
Natron	Nt	$Na_2CO_3 \cdot 10H_2O$
Thenardite	Tn	Na_2SO_4
Trona	Tr	$Na_2CO_3 \cdot NaHCO_3 \cdot 2H_20$

Table 2. Major components and pH, Owens Lake surface brine. Data from Friedman and others (1976, table 1); expressed as grams per liter (g/l).

Date	pH	Na	HCO_3	CO_3	SO_4	Cl
February, 1970	9.6	51.5	16.1	29.0	12.5	25.4
August	9.6	95.5	11.1	66.7	24.4	49.3
September[1]	9.62	114.0	17.3	70.9	30.2	60.2
January, 1971	9.31	92.5	7.95	31.9	12.8	89.2
April	9.5	150.0	3.66	70.8	39.6	116.0
July	10.5	172.0	[2]	99.3[2]	37.3	129.0
August	11.0	179.0	[2]	132.0[2]	26.6	113.0

[1] Bottom brine.
[2] Total carbonate expressed as CO_3.

Primary-salt crystallization processes

Crystallization of the dissolved salts began in late August, 1970. The salts included species of Cl-, SO_4-, and CO_3-bearing phases (halite, burkeite, mirabilite, and thenardite), but tracing the deposition of, and seasonal changes in, the CO_3- and HCO_3-minerals (natron, nahcolite, and trona) best illustrates how complex crystallization and recrystallization processes can be. These detailed changes can be followed by hydrogen-isotope measurements because all of these Na-carbonate minerals contain hydrogen (H^+), allowing variations its two stable isotopes ($^1H+$ and D or $^2H^+$) to be used as an indictor of changes even when the mineralogy did not appear to change.

Lake-water salinity and temperature largely controlled the mineralogy of the original precipitates. Lake-water salinity depended primarily on the amount of time that had passed since the evaporation rates exceeded inflow plus the amount of rain or snow falling on its surface. Temperatures, which greatly influenced the process because they change rapidly, depended on the season, day-to-day weather variations, and the time of day when precipitation occurred. Cooler conditions promoted crystallization of high-hydrate mineral species (i.e., natron and mirabilite), and warm conditions promoted crystallization of lower- or un-hydrated species (i.e., trona, nahcolite, and thenardite). Measured mid-day surface-water temperatures during the year ranged from 8.0° to 29.5°C, but daily fluctuations probably resulted in 10° to 20°C variation. Measured lake-floor temperatures ranged from 4.5° to 27.0°C and closely approximated mean monthly air temperatures (**Figure 2**). Lake-water compositions and salinities, and

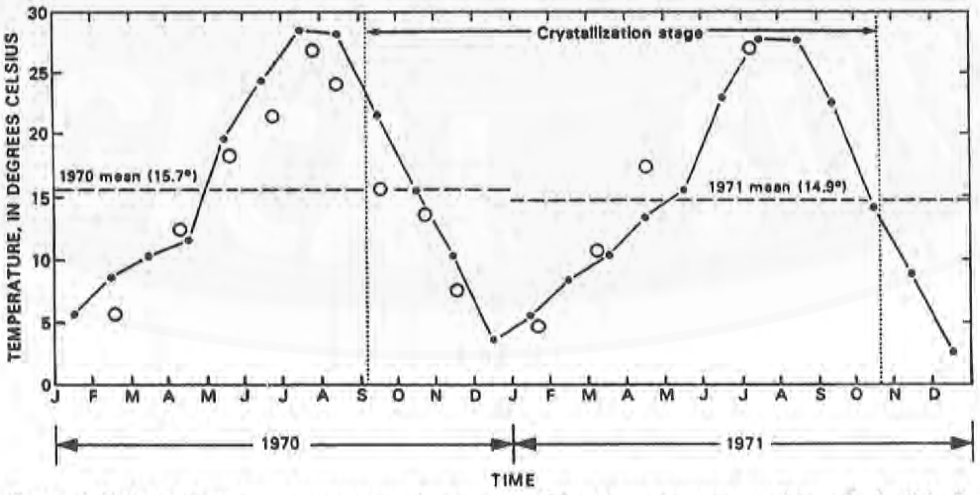


Figure 2. Relation between reconstructed mean-monthly air temperatures at Owens Lake (black dots connected by line) and Owens Lake bottom-water temperatures (circles), 1970 through 1971. Air temperatures calculated from Haiwee National Weather Service station, 25 km south of, and 80 m higher (~0.5 °C cooler) than, the Owens Lake sample site. After Smith and others (1987, figure 5).

water temperatures at the lake surface, where all primary crystallization appeared to take place, determined what minerals formed. Water temperatures at the lake-floor then determined what happened to those primary minerals after they sank–where they survived, dissolved, or recrystallized as a different mineral.

The following account of the phenomena observed during the crystallization of the salts that had been dissolved earlier from the floor of Owens Lake shows that it was a process that changed–even reversed itself–daily, monthly, and seasonally. To illustrate the importance of temperature, note the changes in the positions of the several mineral-stability-field boundaries at different water temperatures as they change in 5°C increments between 0° and 25°C (**Figure 3**). The diagram is constructed so that if the brine at any point contains the plotted weight percentages of the three components represented by its corners, it will precipitate the mineral in the field it occupies if the brine salinity is high enough. If it is not high enough, and if the temperature changes enough to move a field boundary across the point representing the brine composition, then a different mineral will precipitate when the salinity becomes high enough. If, however, the solubility of this different mineral is low enough at this new temperature, it will precipitate without any increase in brine salinity.

In the following, we summarize our observations during visits to the lake during the crystallization period of two minerals, natron (whose solubility in water changes markedly with temperature) and halite (whose solubility changes very little with temperature). In November, 1970, when the lake-water salinity was ~25%, no crystals were seen on the surface of Owens Lake late in the afternoon of the 18th when the surface water was at 10.2°C. According to a nearby U.S. Weather Bureau station, air temperatures fell during the next night to 2°C. At sunrise on the 19th, the lake surface was nearly covered by "rafts" of natron crystals, floating on the surface because of surface tension. The cold night-time temperature caused them to form and the lack of wind allowed them to remain floating on the surface and be observed the next day. Early that morning, the surface-water temperature was 6.2°C and the air temperature was 5°C. Later, however, the surface water warmed and the crystals began to dissolve. About that time, a light wind started to produce small waves, causing some of the remaining crystal rafts to break up, founder, and sink, possibly to be preserved on the bottom where the water was 7.8°C. By noon, no crystals remained on the surface.

In July, 1971, when the lake water salinity was ~35%, only a few crystals of halite were seen on the lake surface at sunrise. By 10:30 AM, however, the lake surface was largely covered by 1- to 5-m wide crystal rafts, products of the warming air and surface-waters which increased the evaporation rate. By noon, the lake surface appeared to be entirely covered by aggregates of rafts composed of interlocked radial crystals, 1 to 5 mm across. When breezes came up, small waves and swells developed and some rafts broke up, foundered, and sank. Inasmuch as halite solubilities in water are little changed with temperature, most of the crystals that sank were preserved on the bottom. By August, 1971, crystallization of the "new" salts was complete.

Prior to the first period of precipitation, we established a precipitated-salt collector near the deepest part of the lake, a vertical, 20-cm-diameter tube that was open on the top, closed at its base, and suspended from a 3-m-high tripod. This permitted the collection of samples of the salts as they precipitated and sank below the lake surface. Every collection thus represented the total accumulation of precipitated salts during a collection period, minus those salts that re-dissolved because of unfavorable temperatures at the depth of the collector which was kept near lake-floor level. Each collection thus approximated the precipitates that would have reached, and survived, on the floor of the lake since the last collection. In addition to samples of the lake water that were routinely collected for chemical and deuterium-isotope ($^2H+$ or D) analysis, we determined the mineralogy of the collected samples by microscope and X-ray diffraction, and determined the hydrogen isotope content of the interstitial brines and the hydrated salts.

Primary salt recrystallization

Intermittent coring of the "new" salt bed between November, 1970 and July, 1971 showed that the mineral assemblages commonly differed from the assemblages found previously at the same stratigraphic position (**Figure 4**). This was most clearly shown by the isotopic analyses that showed that the hydrogen-isotope balance of the salt minerals and their interstitial brines had changed because they had undergone mineral-species transformations, with the hydrogen in the minerals, in the interstitial brines, and in the lake brines interacting. Possible chemical reactions involved in these changes are listed in **Table 3** and the

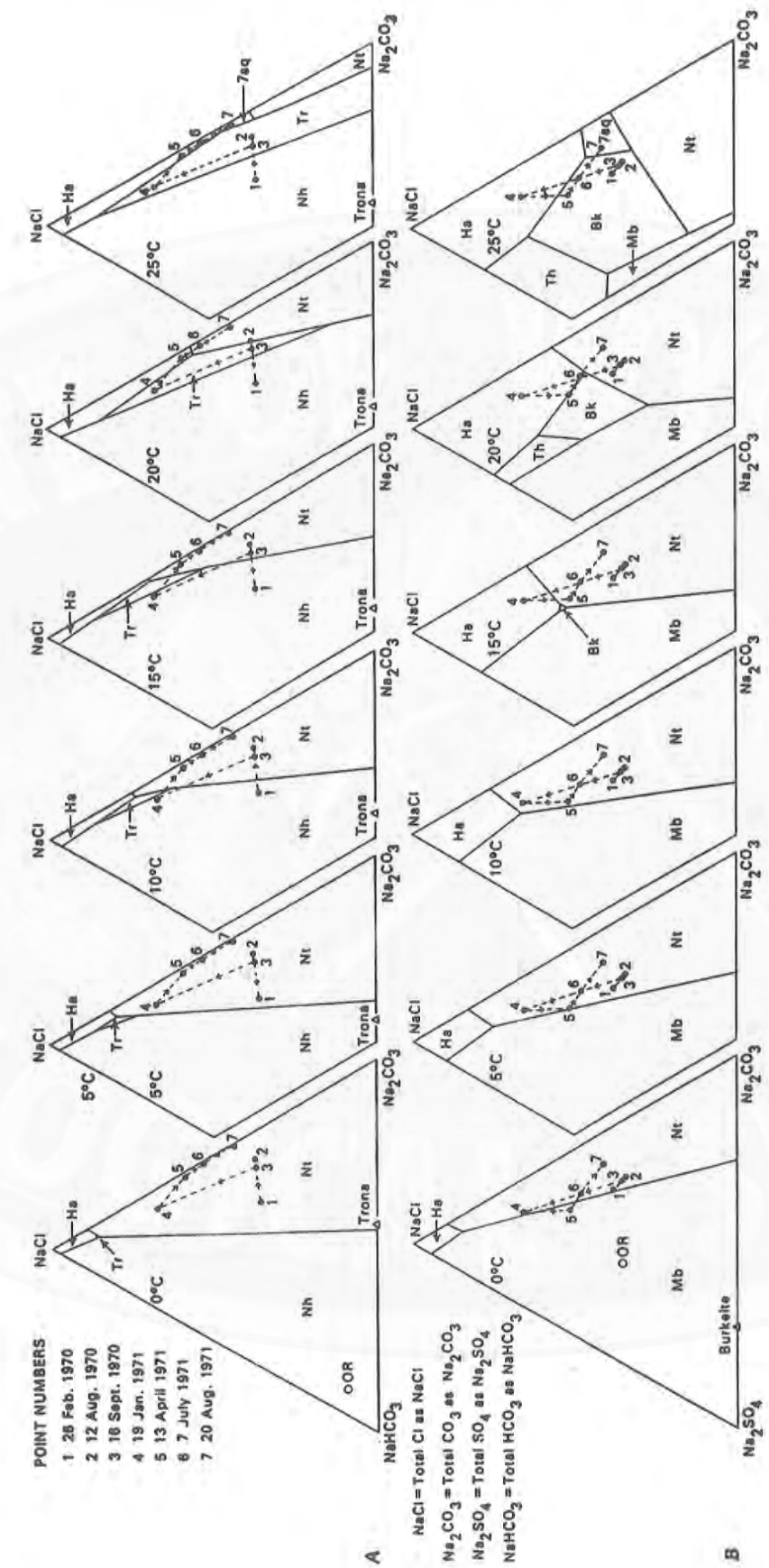


Figure 3. Four-component phase diagrams relating saline minerals in the five-component $NaHCO_3$-Na_2CO_3-Na_2SO_4-NaCl-H_2O systems at 0°, 5°, 10°, 15°, 20°, and 25°C. The $NaHCO_3$-Na_2CO_3-NaCl-H_2O system diagrams (A) are constructed or interpolated linearly from weight-percentage data of Freeth (1923, tables 49-52) and Makarov and Sedelnikov (1940, table 2); the Na_2CO_3-Na_2SO_4-NaCl-H_2O system diagrams (B) are constructed or interpolated from data of Makarov and Bliden (1938, tables 2-5, 8, and figure 5). Except at 0°C, diagrams are truncated at 50% $NaHCO_3$ or Na_2SO_4. Owens Lake brine composition points calculated from anion weight-percentages by assuming equivalent Na; the presumed path followed between these points shown by dashed lines. OR, Owens River water composition. See Table 1 for abbreviations. After Smith and others (1987, figure 2).

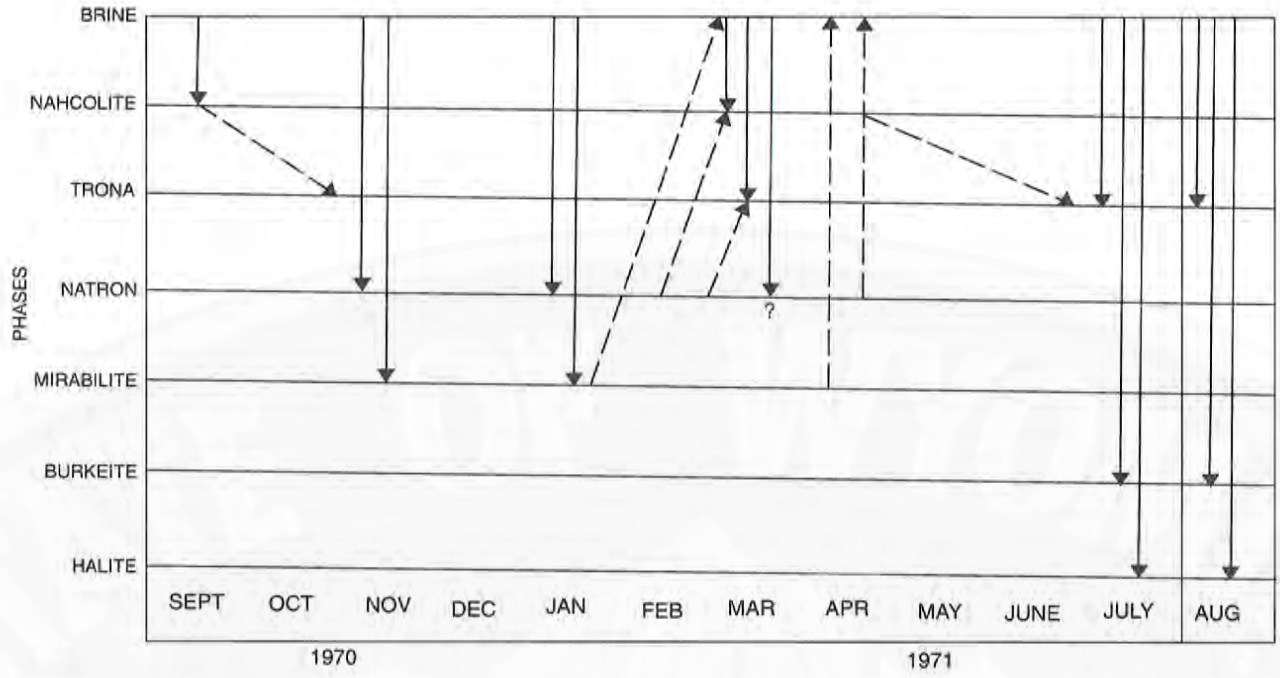


Figure 4. Changes observed in salts on the floor of Owens Lake between September, 1970 (when "new" salts first crystallized) and August, 1971 (when lake desiccated). Crystallization and deposition of listed mineral phases from brine phase shown by solid-line arrows; re-solution or re-crystallization to another mineral by diagenetic proceses within the salt body shown by dashed-line arrows. From Smith and Friedman (1986, figure 2A).

resulting observed assemblages and δD values are listed in **Table 4**.

Table 3. Reactions between minerals, CO_2, and H_2O that can occur during phase transformations of common minerals in Owens Lake. Abbreviations for minerals as in Table 1; CO_2 and H_2O are conventional chemical symbols.

(1)	$3Nt + {}_2 = 2Tr + 25H_2O$
(2)	$Nt + CO_2 = 2Nh + 9H_2O$
(3)	$Tr + CO2 = 3Nh + H_2O$
(4)	$Tr + 8H_2O = Nt + Nh$
(5)	$2Bk + 30H_2O = Nt + 2Mb$
(6)	$3Bk + 65H_2O + CO_2 = 2Tr + 6Mb$
(7)	$2Bk + 21H_2O + CO_2 = 6Nh + 2Mb$

Between September, 1970 and January, 1971, brine temperatures decreased by ~11°C and large amounts of Na, CO_3, and SO_4 were precipitated, presumably as natron and mirabilite, as shown by the decreases in the amounts of those components remaining in the lake brine by January (**Table 2**). Between mid-January and mid-April, 1971, however, additional changes in the mineralogy of the salts caused a 15-cm (27%) decrease in the thickness of the "new" salt layer, the result of a ~6°C warming of lake-floor waters and the solution of most or all of the natron and mirabilite present in the January core. The

Table 4. Carbonate minerals and δD values of hydrated salts and interstitial brines of "new" salts deposited after late August, 1970, but since prior date of coring. Successive changes in mineral assemblages and in δD values resulted from new deposition and/or diagenetic reactions between pre-existing assemblages. Multiple data sets and ranges of values from one core represent visibly different horizons that were sampled separately. Data from Smith and others (1987, table 2, figure 5).

Date of coring	Mean Monthly temperature (°C)	Na-CO_3 minerals[1]	δD (per mil, SMOW) Hydrated salts	δD (per mil, SMOW) Interstitial brine
November, 1970	12	Nt	+5	-11
		Tr	-106	-26
January, 1971	5	Nt	-6 to -13	—
		Tr+Nh	-89	—
		Tr	-106 to -121	—
April	11	Tr+Nh	-56 to -101	-14 to -16
		Tr+Nh+Nt	-26 to -89	-9 to -30
July	26	Tr	-55 to -103	-9 to +3

[1]See Table 1 for abbreviations.

major change was the loss of salt volume by recrystallization of natron to trona or nahcolite, releasing H_2O into the interstitial or lake brines according to equations 1 and 2 (**Table 3**), plus the dehydration of mirabilite to thenardite. Evidence of this change is documented in **Table 2** which shows increases in Na, CO_3, and SO_4 in the brine between January and April of 1971.

Converting the salt formulas (**Table 1**) to gram molecular weights in those equations, and then to volumes using mineral densities (and assuming sufficient CO_2 was dissolved in the brine), approximates the changes in the volumes of solids during these transformations:

$$3\ \text{Natron} + CO_2 \longrightarrow 2\ \text{Trona} + 25\ H_2O$$

[580.9 ml] [211.2 ml] [450.0 ml]

and

$$\text{Natron} + CO_2 \longrightarrow 2\ \text{Nahcolite} + 9\ H_2O$$

[193.6 ml] [76.0 ml] [162.0 ml].

Applying the same method to mirabilite, one gets:

$$\text{Mirabilite} \longrightarrow \text{Thenardite} + 10\ H_2O$$

[216.2 ml] [53.3 ml] [180 ml].

During the changes that occurred from January to April, 1971, the natron-to-trona reaction reduced the volume of the solid phases to 36% of the original volume, the natron-to-nahcolite reaction reduced the volume to 39% of the original, and the conversion of mirabilite to thenardite reduced the volume to 25% of the original. The change in the thickness of the "new" salt layer, which was 56 cm thick in January but only 41 cm thick in April (73% of its January volume), probably means either that the diagenetically produced trona, nahcolite, and thenardite were more porous than their predecessors had been, or that the diagenesis was incomplete. The released water presumably migrated upward into the lake.

If the lake had not desiccated in late summer, then the above reactions would have reversed during the following winter, and the cool-season mineral assemblages would have increased in volume by 275, 255, and 406%, respectively, of the summer assemblage. The volume of interstitial water would probably not have been enough to permit these reactions to be completed, and lake, rain, or melted-snow water would have been required for their completion. That these reactions took place is corroborated by the observation of workers on the lake that the surface was "hard and workable" in the winter but "soft mush" in the summer (Alderman, 1983, p. 81).

Post-desiccation diagenesis of the salts

In 1974 and 1977, three to six years after desiccation was "complete," new cores were collected to monitor changes in the mineralogy and the isotopic values of the hydrated salts and interstitial brines. We used the isotopic and mineralogic properties of the 46 to 60 cm of pre-1969 "old" salts and their interstitial brines that were also recovered in each of our four cores, as a record of what the mineralogy and isotopic character of the deposit was like before the 1969 flooding. This appeared reasonable for two reasons: (1) The mineralogy of those parts of the cores seemed not to have been affected by that flooding, and (2) the hydrogen-isotope balance of the hydrated minerals varied over a small range (average range in δD, any one core: 15) as did the values in the interstitial brines (average range in δD, any one core: 11). The mineralogy and isotopic character of this "old" zone apparently remained about the same throughout the year during its recrystallization stage (Smith and others, 1987, table 2), possibly because the lake water partially insulated the salt bed from changing atmospheric temperatures. However, Dub (1947) and Alderman (1983) reported seasonal diagenesis in the Owens Lake salt layers when the lake was dry during periods over a third of a century apart; our 1974 and 1977 cores were collected in November and September, respectively, giving us no samples representing 10 months of the post-desiccation mineralogy. This means that we do not have data on their mineral and isotopic character during other parts of the year, but the similarity in the range of isotopic values in the "old" salts, before and after the lake dried (Smith and Friedman, 1986, figure 3), suggests that our inferred trend caused by seasonal diagenesis is valid.

In contrast, the range of isotopic values from the first samples of the "new" hydrated minerals in the post-1970 salts, cored in November, 1970, ranged from δD = +5 to -106, a range of 111 permil. By July, 1971, when the lake had nearly desiccated, their δD range had decreased to 48 permil, extending from -55 to -103. In the cores taken in November, 1974 and September, 1977, the hydrated "new" salts had reduced their δD range to 38 permil, from -87 to -125, and by 1977 their range had decreased to 20 permil, -90 to -110–which was not far from that of the hydrated "old" salts which at that time ranged from -87 to -75.

By November, 1974, the interstitial brines in the "new" salts, had a δD spread of 15 permil (from -45 to -30), and by September, 1977, they had a spread of 17 permil (from -50 to -33). The δD range of the interstitial brines in the "old" salt part of the section was -42 to -33, virtually identical to the values found in the "new" salts in 1977, -50 to -33.

This progression diminished the spread in δD values from the "new" salts to ~15% of the scatter found in the first samples collected in November, 1970, and their absolute values had migrated toward the isotopic values of the "old" salts that crystallized sometime after 1913 but were not dissolved during the 1969 flooding of the lake. The interstitial brines followed the same trend. This suggests that this process of seasonal recrystallization, driven by seasonal changes in temperatures, causes the minerals, interstitial brines, and their hydrogen-isotope contents to evolve by processes too complex to reconstruct in detail but approaching the same end-point.

Annual changes in mineralogic compositions and δD values will only end when the salt layer is buried to a depth where seasonal temperature shifts are too small to drive the annual mineral transformations. The D/H fractionation factor for trona is temperature sensitive (Matsuo and others, 1972). Therefore, if the interstitial brines were not contaminated by groundwater, and if the hydrated Na-carbonate mineral was trona, the isotopic ratios in the interstitial brine and trona would record the mean annual temperature, the one normally found at the base of the seasonal-temperature fluctuation zone.

References cited

Alderman, S.S., Jr., 1983, Geology of the Owens Lake evaporite deposit, *in* Schreiber, B.C., and Herner, H.L., editors, Sixth International Symposium on Salt: The Salt Lake Institute, Alexandria, Virginia, v. 1, p. 75-83.

Craig, H., 1961, Standard for reporting concentrations of deuterium and oxygen-18 in natural waters: Science, v. 133, p. 1833-1834.

Dub, G.D., 1947, Owens Lake–source of sodium minerals (California): American Institute of Mining, Metallurgical, and Petroleum Engineers Technical Publication 2235, p. 1-13.

Freeth, F.A., 1923, The system Na_2O-CO_2-NaCl-H_2O, considered as two four-component systems: Philosophical Transactions of the Royal Society of London, v. A223, p. 35-87.

Friedman, I., Smith, G.I., and Hardcastle, K.G., 1976, Studies of Quaternary saline lakes—II. Isotopic and compositional changes during the desiccation of brines in Owens Lake, California, 1969-1971: Geochimica et Cosmochimica Acta, v. 40, p. 501-511.

Makarov, S.Z., and Blidin, V.P., 1938, The polytherm of the quaternary system Na_2O-Na_2SO_4-NaCl-H_2O and solid solutions of the burkeite type: Izvestiaya Akademii Nauk SSSR, Chemistry, p. 865-890 (in Russian, English summary).

Makarov, S.Z., and Sedelnikov, G.S., 1940, A study of the system Na_2CO_3-$NaHCO_3$-NaCl-H_20 in the domain crystallization of trona: Izvestiaya Akademii Nauk SSSR, Chemistry, p. 835-863 (in Russian, English summary).

Matsuo, S., Friedman, I., and Smith, G.I., 1972, Studies of Quaternary saline lakes–I. Hydrogen isotope fractionation in saline minerals: Geochimica et Cosmochimica Acta, v. 36, p. 427-435.

Smith, G.I., and Friedman, I., 1986, Seasonal diagenetic changes in Owens Lake, California, 1970-77, *in* Bodine, M.W., Jr., editor, Studies in diagenesis: U.S. Geological Survey Bulletin 1578, p. 21-29.

Smith, G.I., Friedman, I., and McLaughlin, R.J., 1987, Studies of Quaternary saline lakes–III. Mineral, chemical, and isotopic evidence of salt solution and crystallization processes in Owens Lake, California, 1969-1971: Geochimica et Cosmochimica Acta, v. 51, p. 811-827.

Additional references

Bischoff, J.L., Stafford, T.W., Jr., and Rubin, M., 1997, A time-depth scale for Owens Lake sediments of core OL-92: Radiocarbon dates and constant mass-accumulation rate, *in* Smith, G.I., and Bischoff, J.L., editors, An 800,000-year paleoclimatic record from core OL-92, Owens Lake, southeast California: Geological Society of America Special Paper 317, Boulder, Colorado, p. 91-98.

Eugster, H.P., and Smith, G.I., 1965, Mineral equilibria in the Searles Lake evaporites: Journal of Petrology, v. 6, no. 3, p. 473-522.

The natural soda deposits of China

Chending Zhang[1]
Department of Chemical Engineering
Inner Mongolia Polytechnic University
Hohhot, 010062, China

Abstract

The total production of Chinese soda ash in 1996 was about 6.5 Mt (million metric tons or tonnes). Exports accounted for about 8.5% of the total output. Synthetic soda ash always dominates the soda ash industry in China. The synthetic soda ash production of China has expanded rapidly in the last twenty years, and the natural soda deposits of China have been developed simultaneously. Four natural soda deposits are introduced in this paper, two in Henan Province and two in Inner Mongolia Autonomous Region. The characteristics of the deposits, sodium carbonate-bearing minerals, and reserves are described; the mining methods, refining processes, and research studies are also discussed; and the current status of Chinese synthetic soda ash plants and markets is summarized.

Natural sodium carbonate-bearing minerals occur widely in China. Approximately thirty alkali lakes and natural soda mines have been exploited. Some of the larger natural soda deposits are concentrated in the Nanyang basin and on the Inner Mongolia plateau. Proven total sodium carbonate reserves are 154 Mt. About 83.5% of these reserves is contained in the Henan Province, and 15.5% of the reserves is contained in the Inner Mongolia Autonomous Region. Present annual production of the principal recovered products includes 100 Kt (thousand tonnes) from soda ash, 110 Kt from caustic soda, and 170 Kt of sodium bicarbonate.

Character of natural soda deposits

Wucheng trona deposit

The Wucheng trona deposit was discovered in 1971 during petroleum exploration. It is located in southern Henan Province, 18 km west of Tongbai County at latitude 32.4°N, longitude 113.5°E. The deposit occurs in the central part of the Paleogene faulted Wucheng basin and was formed in the Eocene Epoch. The trona beds occupy an area of 4.66 km^2 at depths of 643 to 974 m. The "upper structure" consists of 21 salt-bearing trona beds with thicknesses ranging from 1 to 3 m. The beds of the upper structure contain an average of 34.0% total sodium carbonate and 45.6% sodium chloride. The "lower structure" consists of 15 trona beds of low salt content with thickness ranging from 0.5 to 1.5 m. The ore (trona beds) of the lower structure contains an average of 55.0% total sodium carbonate and less than 0.3% sodium chloride. Resources of the Wucheng trona deposit total 36.8 Mt sodium carbonate and 17.8 Mt sodium chloride. The sodium carbonate-bearing minerals include mainly trona and nahcolite associated with shortite, northupite, and $NaCl \cdot Na_2CO_3 \cdot (MgFe)CO_3$. Halite is a commingled mineral. The floor and roof strata and gangue interbeds are oil shale, dolomite, and marl. A cross section containing three boreholes through the trona deposit is presented in **Figure 1**. The sodium carbonate and sodium chloride content varies with layers of the Tong #13 borehole **(Figure 2)**.

Anpeng nahcolite deposit

The Anpeng nahcolite deposit was discovered in 1976 during petroleum exploration. It is located 60 km southwest of the Wucheng trona deposit at latitude 32.3°N, longitude 113.2°E. The deposit occurs

[1]Current address: CAMI International Company, 9460 Telstar Avenue No. 6, El Monte, California 91731

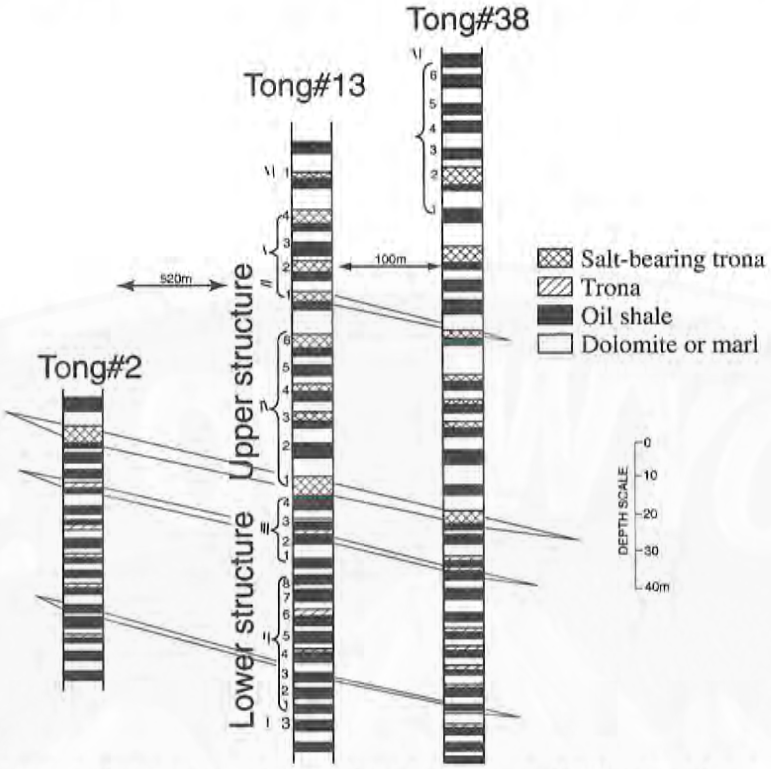


Figure 1. Cross section through three boreholes in the Wucheng trona deposit.

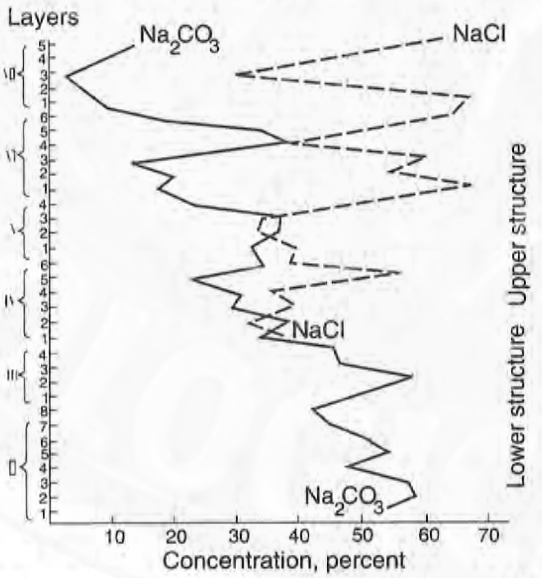


Figure 2. Composition of evaporite beds in Tong #13 borehole, Wucheng trona deposit.

in the southeastern part of the faulted Paleogene Biyang basin and was formed in the Eocene Epoch. The nahcolite beds occupy an area of 8 km² at depths of 1310 to 2520 m. The deposit consists of 17 nahcolite beds with thicknesses ranging from 0.6 to 3.6 m. Northwest of the area of the nahcolite beds, some solutions (brines) containing sodium bicarbonate and sodium carbonate occur in porous and permeable dolomite in five layers with thicknesses ranging from 1 to 5 m. The mean composition of nahcolite beds is shown in **Table 1**. The Anpeng nahcolite deposit has a reserve of 55 Mt sodium carbonate, of which about 2 to 3% occurs in brine.

Table 1. Average composition of the Anpeng nahcolite deposit (in weight percent).

		$NaHCO_3$	Na_2CO_3	NaCl
Solid	range	48-95	0-40	< 1
		77	16	
Brine*		13.48	4.88	

* At pressure of about 20 MPa, temperature 85°C.

The solid minerals include mainly nahcolite and wegschiderite ($Na_2CO_3 \cdot 3NaHCO_3$). The floor and roof strata and evaporite interbeds consist of dolomite, oil shale, and sandstone. **Figure 3** is a cross section showing two boreholes in the Anpeng nahcolite deposit.

Chaganor soda deposit

The Chaganor natural soda deposit was discovered by exploration in 1966. It is located in the central part of the Inner Mongolia Autonomous Region, 80 km southeast of Erlianhot, latitude 43.2°N, longitude

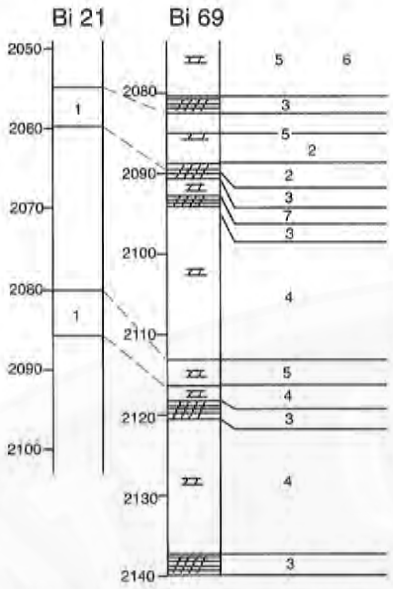


Figure 3. Cross section through two boreholes in Anpeng nahcolite deposit. Numbers to left of columns are depths, in meters. Numbers in columns identify lithologies: 1, nahcolite brine; 2, solid mineral (nahcolite and wegschiderite); 3, oil shale; 4, marl-bearing dolomite; 5, porous dolomite; 6, sandy dolomite; 7, dolomite and sandstone.

112.9°E. The deposit occurs in an arid denuded basin of the Inner Mongolia plateau. It was deposited as a lacustrine facies in sediments deposited in Pleistocene time. The deposit is surrounded by arid steppe at an elevation of 1000 meters. Annual evaporation is ten times that of precipitation. The natural soda beds occupy an area of 21 km² and are underlain by 20 m of sandy clay. The deposit consists of nine soda beds with interstitial brine. Lithologic logs of two boreholes in this deposit are shown in **Figure 4**. The chemical components and average contents of three principal soda beds and interstitial brine are presented in **Table 2**.

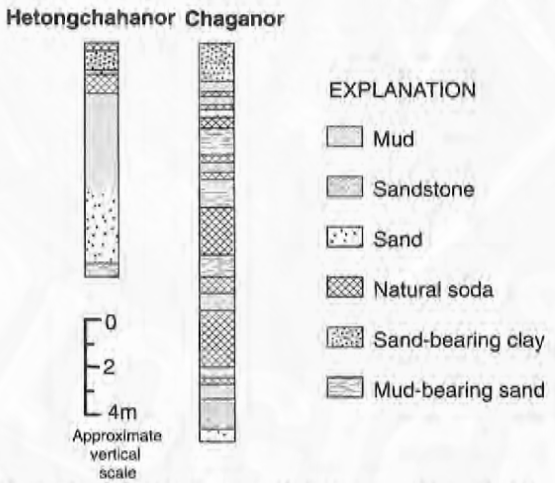


Figure 4. Lithologic logs of two boreholes of the Inner Mongolia natural soda lakes.

The Chaganor natural soda deposit has a reserve of 11.3 Mt of sodium carbonate. The main minerals are natron and trona and associated mirabilite and halite, with small amounts of northupite and gaylussite. The floor and roof strata and interbeds of the soda beds are black mud.

Ordus alkali lakes

The Ordus alkali lakes are located on Ordus Plateau, in the southwestern part of the Inner Mongolia Autonomous Region. Some of these alkali lakes are among the earliest worked natural soda deposits in China. There are two deserts, called Kubuqi and Maowusu, in the Ordus Plateau region at an elevation of 1268 to 1412 m. The climate is arid and the annual evaporation is seven times that of precipitation. About ten alkali lakes are distributed over the deserts. The largest–Hetongchahanor–is located in the northern part of the Maowusu desert, 110 km southwest of Dongsheng, at latitude 39.2°N, longitude 109°E. Hetongchahanor alkali lake occurs in an arid denuded basin, has an area of 29 km², and contains 0.4 to 1.0 m of alkaline surface water. The deposit consists of one natural soda bed, interstitial brine, and alkaline water. The soda bed covers an area of 6.14 km², has an average thickness of 1 m, and is underlain by 1 to 1.5 m of sandy clay. A lithologic log of a borehole in this deposit is shown in **Figure 4**. The composition of this deposit is presented in **Table 3**. The Hetongchahanor alkali lake contains a reserve of 1.7 Mt sodium carbonate. The principal minerals are natron and trona with associated mirabilite and halite, and a small amount of gaylussite. The floor strata of the soda bed is mud.

Table 2. Composition (in weight percent) of three soda beds and associated interstitial brines in the Chaganor soda deposit. Dashes indicate no data.

Bed	Average thickness (meters)	Na_2CO_3+ $NaHCO_3$	Na_2SO_4	NaCl	KCl	Insoluble matter	Crystalline water
I	1.39	26.10	11.90	1.38	–	3.22	56.86
II	2.44	27.34	11.13	1.21	–	3.51	56.46
III	2.46	28.91	10.00	1.19	–	3.77	55.53
I brine	–	6.30	2.27	14.86	0.33	–	–
II brine	–	6.39	2.11	13.80	0.41	–	–
m brine	–	6.08	2.30	16.17	0.58	–	–

Table 3. Composition of Hetongchahanor natural soda deposit.

Form (basis)	Na_2CO_3+ $NaHCO_3$	Na_2SO_4	NaCl	Insoluble matter	KCl
Soda bed (%)	16-24	0.2-0.5	0.3-0.7	35-45	-
Brine (grams/liter)	63.4	25.7	130.8	-	19.6
Alkaline water (grams/liter)	30.3	6.9	28.5	-	3.3

Mining methods

Solution mining

A trona vein of the lower structure of the Wucheng trona deposit is being dissolved. This trona vein consists of 38.63% Na_2CO_3, 47.72% $NaHCO_3$, 0.53% NaCl, and 13.12% H_2O (without insoluble matter). The calculated optimum concentration and consumption of caustic soda for solution mining at various temperatures based on a stability diagram of Na_2CO_3-$NaHCO_3$-NaOH-H_2O system is shown in **Table 4**. This trona vein is separated by 450 m of impermeable

Table 4. Optimum concentration and consumption of caustic soda for solution mining the Wucheng trona deposit.

Temperature °C	Optimum concentration NaOH%	Consumption of caustic soda per ton of trona ore
30	4.22	0.140
35	4.05	0.133
45	3.69	0.114
60	3.41	0.095
75	3.12	0.078

dolomite, marl, and oil shale in the upper aquifer strata; the floor strata are also impermeable. The Wucheng trona deposit shows no obvious faults. Rock strengths (**Table 5**) indicate that the floor or roof strata have higher strengths than the trona. To conclude, the conditions for solution mining are fairly good.

The surface distance between the injection and production wells is about 100 to 150 m. A scheme for the solution mining wells (**Figure 5**) shows that the

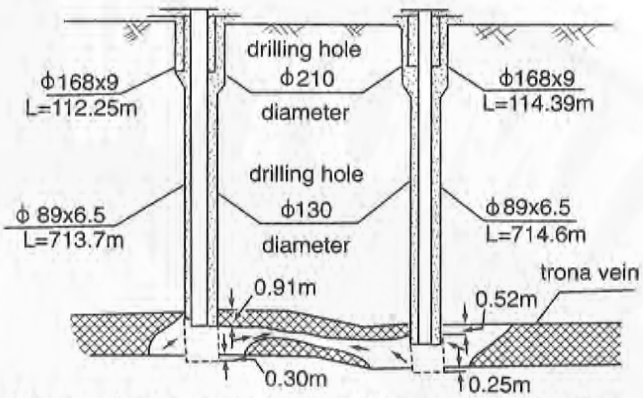


Figure 5. A scheme of solution mining wells of the Wucheng trona deposit.

position for fracturing the trona bed was located at the interface between the trona and floor stratum in an attempt to expand a crevice along the interface to achieve the maximum recovery rate. The trona vein was cracked through at an injection pressure of 15 megapascals (MPa), and the operating pressure was kept at about 2.5 MPa. Under normal conditions, solvent is injected with a caustic soda concentration of 4 to 5%. The solution obtained at the production well has a sodium carbonate content of 14 to 16%. The flow rate proportion of produced solution to injected solvent is about 0.85.

Solution mining of the Anpeng nahcolite deposit is similar to that of the Wucheng trona deposit. The surface distance between injection and production wells is about 168 to 215 m. **Table 6** shows that the dolomitic floor or roof stratum has a higher strength than nahcolite, so that solution mining is possible. With injection of a 3% caustic soda solution as a solvent, the produced solution has a sodium carbon-

Table 5. Rock strengths in the Wucheng trona deposit, in megapascals (MPa).

Rock type	Occurrence	Compressive strength	Shearing strength	Tensile strength
Dolomite	Roof stratum	49.88-59.49	2.94-3.92	0.49-1.08
Trona	Vein	25.97-33.02	3.03-5.19	0.78-1.57
Oil shale	Floor stratum	55.66-60.66	3.03-5.39	1.86

Table 6. Rock strengths in the Anpeng nahcolite deposit.

Rock type	Occurrence	Compressive strength (MPa)	Tensile strength (MPa)
Nahcolite	Vein	23.38	1.82
Dolomite	Floor or roof stratum	142.66	9.75

ate content of 8.5 to 10.1%. The flow rate proportion of produced solution to injected solvent is about 0.82. Some nahcolite ore is contaminated by petroleum which influences the dissolving effect. With respect to mining the primary liquid mineral (brine), the solution pumped from the production well has a composition as shown in **Table 7**. The pumped solution contains some sodium carbonate crystals.

Opencast mining

With a mining output capacity of 500 Kt (thousand tonnes) per annum, the Chaganor soda mine is the largest of those being operated in China at present. The method of the mining is similar to an opencut coal mine–stripping the topsoil and mud and excavating the natural soda bed step-by-step. The interstitial brine is drained off in advance by pumping it to solar ponds to recover salt in summer and burkeite in autumn. The possibility of invasion of the deposit by surface water and underground water must be prevented. Solar ponds have been used in Hetongchahanor for evaporation of alkaline water to recover trona in summer, and natron and mirabilite in autumn. The solid bed is excavated during the winter when the mud is frozen.

Table 7. Composition of pumped solution from the Anpeng deposit (g/l = grams per liter).

Component	Content (g/l)	Component	Content (g/l)
Na^+	51.90	Cl^-	1.02
K^+	0.27	Br^-	0.29
CO_3^{2-}	19.72	B_2O_3	0.51
HCO_3^-	96.28	pH	9.01

Processing methods

Dense soda ash

The monohydrate process has been adopted by the Wucheng, Anpeng, and Hetongchahanor processing plants. Their aggregate production is 100 Kt per annum. According to a phase diagram of the stability field for this system, crystals should be obtained in the sodium carbonate monohydrate region. Since the clarified raw sodium carbonate solution is the feed to the triple effect evaporators system, the individual content of sodium bicarbonate, sodium chloride, and sodium sulfate in the feed solution must be controlled. The separated monohydrate crystals are calcined to produce dense soda ash. Besides recycling, the mother liquor can be partly used to produce caustic soda for mining. The quality contrast of natural to synthetic product (**Table 8**) indicates that the quality of natural dense soda ash is quite good.

Table 8. The quality standard of synthetic dense soda ash of China (GB210-92) compared to the achieved quality of natural dense soda ash.

Quality index		Synthetic dense soda ash	Natural dense soda ash
Total sodium carbonate (calculated in Na_2CO_3)	% ≥	99.2	99.2-99.7
Chloride (calculated in NaCl)	% ≤	0.50	0.12-0.22
Ferrous (calculated in Fe)	% ≤	0.004	0.002-0.005
Weightlessness (200°C)	% ≤	0.8	0.1-0.3
Bulk density	g / ml	0.90	0.95-1.02
Particle size (180μm sieving residue)	≥	75	79

Caustic soda

Caustic soda is being produced by Chaganor, Hetongchahanor, and several other Ordus alkali lakes processing plants. Their aggregate production is 110 Kt per annum. The causticizing natural soda solution of Inner Mongolia belongs to a $NaOH$-Na_2CO_3-Na_2SO_4-$NaCl$-H_2O five-component system. According to the phase diagram for this system, the individual amount of water evaporating and crystals separating out can be calculated during evaporation. **Figure 6**

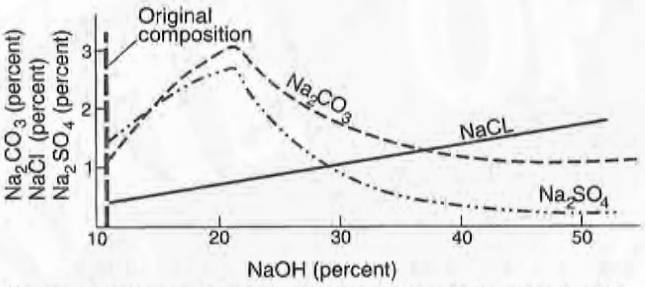


Figure 6. Concentration of the causticizing natural soda solution varies during evaporation. Original composition NaOH, 11.53%; Na_2CO_3, 1.08%; Na_2SO_4, 1.41%; NaCl, 0.41%; and specific gravity, 1.147.

shows that the concentration of three components varies with the sodium hydroxide concentration. It indicates that at a sodium hydroxide concentration ranging from 20 to 40%, most of the sodium sulfate and sodium carbonate precipitate out as burkeite and thenardite, but the sodium chloride is enriched. The NaCl is then precipitated from the high sodium hydroxide concentration liquor by cooling to 30°C, obtaining a concentration of less than 1.5% sodium chloride.

The clear caustic liquor is passed through a cocurrent, triple effect evaporator system, where it is concentrated to the required product concentration of 46% NaOH. Some individual separating equipment is associated with the second and third effect. Liquor and crystals drawn from the evaporator body are separated by settling tanks, centrifuges or filters; the liquor is returned to the same or succeeding effect; and the crystals are then dried as a by-product. The final liquor is cooled to 30°C to remove the salt. Moreover, by using an ascending film evaporator at high vacuum, the caustic soda liquor with a concentration of 46% NaOH can be further evaporated to a concentration of 70% NaOH. Then it is fed into the direct-fired units, and after the water has been driven off, the molten caustic soda is pumped to a drum-loading station to produce anhydrous caustic soda with a concentration of 96% NaOH .

Sodium bicarbonate

There are many carbonation units in Chaganor, Hetongchahanor, and several Ordus alkali lakes that produce sodium bicarbonate and utilize the limestone-kiln gas with a carbon dioxide concentration of more than 30%. The aggregate production is 170 Kt per annum. A phase diagram of the Na_2CO_3-$NaHCO_3$-Na_2SO_4-$NaCl$-H_2O system at corresponding temperature can be used to study the carbonation process of a natural soda solution. The original composition of the solution must ensure that the crystals are separated out in the sodium bicarbonate region. Based on phase diagram analysis and production experience, the solution with a composition of total $Na_2CO_3 \geq 15\%$, $Na_2SO_4 \leq 6\%$, and $NaCl \leq 8\%$ may be appropriate to produce sodium bicarbonate. In addition, the natural soda minerals of Inner Mongolia contain some mud which is suspended in solution, and must be removed by flocculation and filtration. The quality of sodium bicarbonate produced from natural soda deposits complies with the sodium bicarbonate quality standard of China, GB 1887-90, whereby $NaHCO_3 \geq 99.0\%$, $As \leq 0.0001\%$, $pH \leq 8.6$, etc.

Experimentation and research

In the last twenty years, a number of special works were published in China to report on pilot experimental results of solution mining, solar ponds, flocculent clarification, and filtration, etc. More than a hundred papers were presented in periodicals and at conferences in China, covering two major topics, listed below.

Geology and mineralization of natural soda deposits

These works dealt with characteristics of regional and deposit geology and discussed mineralization based on sources of mineral matter, ancient geographical features and paleoclimate, and lithofacies. They also discussed physical and chemical conditions based on phase equilibrium of mineral substances.

Natural soda polycomponent systems, phase equilibrium, and solubilities

Studies of 150°C and 10°C Na_2CO_3-$NaHCO_3$-Na_2SO_4-$NaCl$-H_2O systems, 150°C $NaOH$-Na_2CO_3-Na_2SO_4-$NaCl$-H_2O systems, 35°C $Na^+NH_4^+//Cl, SO_4^{2-}, HCO_3^-$-$H_2O$ systems. These studies attempted to pre-

dict solubilities of some five-component systems. A database of solubilities of natural soda systems was established and phase diagrams were displayed.

Development of China's natural soda deposits

Competition capability in the domestic market

Three principal recovered products, dense soda ash, caustic soda, and sodium bicarbonate, as mentioned above, have a ready domestic market. Sodium bicarbonate not only occupied 60% of the domestic market, but also entered the Asian market.

Advances in the local economy

The development of Chaganor and Ordus natural soda deposits has promoted local economic prosperity, and has increased local income and employment.

Problems with the economic benefit

Reserves of the main natural soda deposits are insufficient to fulfill the domestic market. The deposits of Wucheng and Anpeng comprise thin beds and are deeply buried, resulting in higher mining costs. The natural soda mines of China must improve their technical level to reduce the consumption of resources and energy.

Production outlook in the near future

The predicted total production of products from natural soda is about 480 Kt per annum by 2000, which includes 160 Kt of dense soda, 120 Kt of caustic soda, and 200 Kt of sodium bicarbonate, from expansions of existing natural soda mines.

Summary of the synthetic soda ash industry of China

Review of the development of synthetic soda ash

The first synthetic soda ash plant utilizing the Solvay process began construction in 1917. The location was selected on a coast of Tonggu, about 40 km east of Tianjin. The plant, originally named Yongli, surmounted many difficulties. High quality soda ash was produced in 1926 and won a gold prize at the international fair in Philadelphia. By 1936, the capacity of the plant was about 50 Kt per annum. This achievement was attributed to the success of Dr. Tepang Huo (1890-1974). He received the Ph.D. degree from Columbia University in 1921, then returned to China to take up an appointment as the director combined with the chief engineer of Yongli soda ash plant in 1922. His well-known book "Manufacture of Soda" was published in 1933 in New York. Henceforth, he engaged in the soda ash industry the remainder of his life. Besides the Yongli soda ash plant, the Dalian soda ash plant using the Solvay process was built in 1937. Its capacity was about 60 Kt per annum. Since the founding of the Peoples Republic of China (PRC) in 1949, the development of the synthetic soda ash industry can be reviewed in several stages as follows:

1949-1959. Restored and expanded the capacity of Tianjin and Dalian plants. Production increased from 88 Kt to 808 Kt per annum.

1960-1978. Continuous expansions of the capacity of the Tianjin and Dalian plants. Three plants located in Qingdao, Zigong, and Hubei entered the soda ash industry. Several small soda ash plants emerged. Production increased to 1.32 Mt per annum.

1979-1988. Expanded the capacity of the five plants mentioned above. A number of small soda ash plants entered the soda ash industry. Production increased to 2.61 Mt per annum, among which 0.69 Mt per annum was from small plants.

1989-1993. Three plants located in Tangshan, Weifang, and Lianyungang entered the soda ash industry, each with a capacity of 0.6 Mt per annum. Production increased to 5.28 Mt per annum, among which 1.46 Mt per annum was from small plants.

1994-1996. The Jilantai and Nanfang plants entered the soda ash industry. Production increased to 6.539 Mt per annum.

Expansion of the soda ash industry of China in the last twenty years is shown in **Figure 7**. Among the

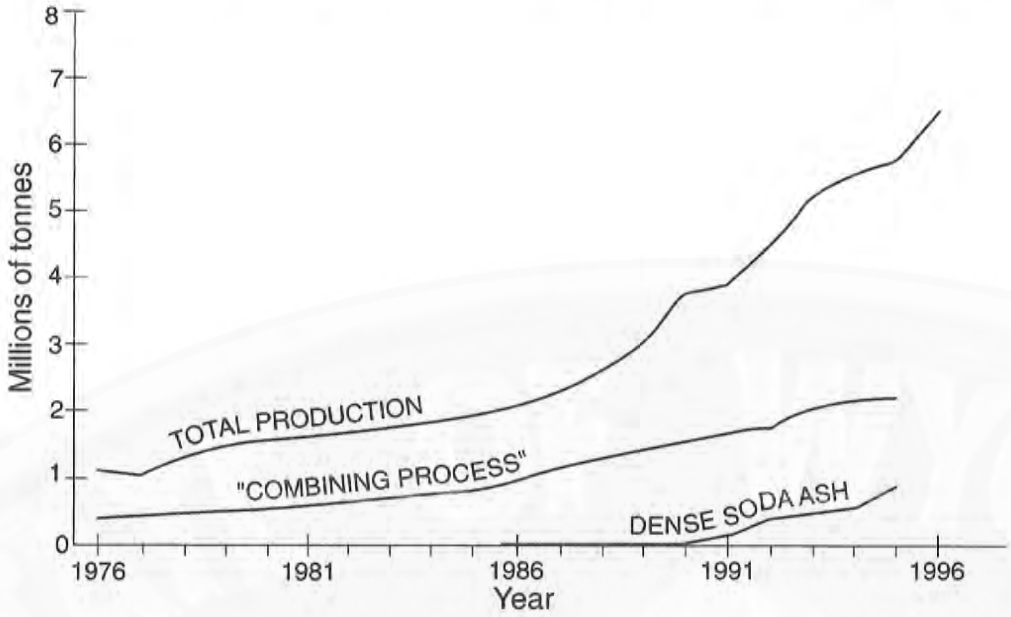


Figure 7. Production of soda ash in China from 1976 to 1996.

increasing total production, the production of the soda ash from the combining process and production of dense soda ash have obviously increased. In 1995, the total production of soda ash was 5.82 Mt, of which about 60% was provided by the Solvay process, 38.4% was provided by the combining process, and only 1.6% by the natural soda process. In addition, 16.1% of the total production was dense soda ash. At present, about sixty soda ash plants are being operated in PRC, of which eight plants with the largest capacity provided about 75% of the total production. The largest, the Weifang soda ash plant, has a capacity of 0.8 Mt per annum.

Imports and exports of soda ash in China in the last twenty years is shown in **Figure 8**. The demand of the domestic market exceeded the supply of soda ash products during the period of 1983-1988, which caused a great quantity of soda ash to be imported, reaching a maximum of 1.27 Mt in 1986. Since 1991, the growth of domestic market demand fell short of the increase in soda ash production. Exports have been increasing year by year. In 1996, the domestic market demand was about 5.6 Mt and exports amounted to 0.56 Mt. As to the domestic consumption of soda ash, flat glass consumes 21.43%, light industry (bottle glass, detergents, etc.) consumes

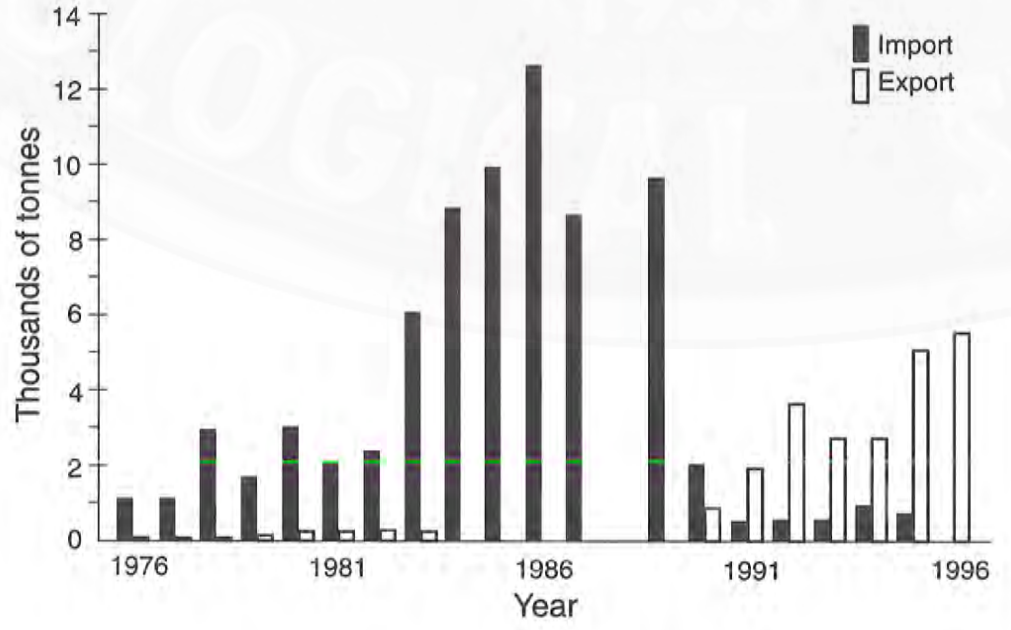


Figure 8. Imports and exports of soda ash in China from 1976 to 1996.

27.68%, the chemical industry consumes 20.54%, and miscellaneous uses (ferrous and nonferrous metallurgy, petroleum, medicine, edible, etc.) consume 30.35%.

Technical advantage of soda ash plants using the Solvay process

Equipment and installations move towards large-scale, high efficiency operation with consumption of less energy. China is now able to design and build a soda ash plant of 0.6 Mt per annum capacity on its own, and is capable of manufacturing 3.2 m-diameter carbonation and distillation towers, steam tube rotary dryers of 3.2 m diameter by 30 m long, vacuum filters with 20 m^2 of filtration area, the carbon dioxide turbine compressor, and the large plate heat exchangers. A number of advanced techniques introduced by several foreign companies include vacuum distillation, distillation with dried lime, dense soda ash with lower salt content, a steam tube rotary dryer 3.6 m in diameter, and an automatic packing facility. As a result of adopting new techniques, the energy consumption per tonne of soda ash produced by the Solvay process ranges from 12.895 to 15.212 GJ (gigajoules) in China.

Technological innovation has lead to improved quality of products, reduced consumption of raw materials, and decreased pollution. At present, salt consumption ranges from 1.37 to 1.50 tonnes per tonne of soda ash produced by the Solvay process, and ammonia consumption ranges from 5.7 to 11.4 kg per tonne. After passing through flash vaporization and recovering a certain quantity of heat, the liquid waste from distillation continuously goes through neutralization and sedimentation. Mostly clear waste liquor is pumped to the sea and the precipitate is shipped to the nearest coast or island and disposed of in a desolate site. At the Weifang soda ash plant, the waste distillation liquor is pumped to solar evaporation ponds of a sea salt plant to harvest high quality salt by simultaneously adding the salt brine. It is called "soda ash combined with salt." The Tianjin soda ash plant uses the waste distillation residue to produce building materials.

The combining process technique

Dr. Tepang Huo was successful in his development of the combining process by 1942, and obtained a patent in 1943. In this process, the soda ash plant is combined with the synthetic ammonia plant, using the carbon dioxide discharged and the ammonia produced to process the ammonia absorption and carbonation of salt brine, so that the limestone kiln, the distillation tower, and its liquid waste can be eliminated. According to the Na^+, NH_4^+ //HCO_3^-, Cl^- -H_2O phase diagram of a four-component cross-reacting system, the dual products soda ash and ammonium chloride can be obtained with a higher salt and ammonia use ratio. The first combining process facility with capacities of 80 Kt per annum soda ash and 80 Kt per annum ammonium chloride was built at the Dalian soda ash plant by 1962. Afterwards, several larger combining process facilities were built in Tianjin, Zigong, and Houbei soda ash plants, respectively, and a number of techniques were developed such as: applying the shift gas in carbonation, using a jet in ammonia absorption, and vacuum crystallization of ammonium chloride. About 40 small soda ash plants using the combining process are being operated and its production has been increasing yearly. Salt consumption ranges from 1.14 to 1.22 tonnes per tonne of soda ash in the combining process, and energy consumption ranges from 5.97 to 9.56 GJ per tonne of soda ash.

Future development of synthetic soda ash

In the near future, domestic growth rates for soda ash in light industry, flat glass, and the chemical industry is estimated to be 4%, 5%, and 6%, respectively. Total production of soda ash is projected to reach 6.8 Mt per annum by the end of 1997, and will exceed 7.2 Mt per annum by the end of 2000. It is probably impossible to construct a larger soda ash plant in the next several years, so increases in production would be mainly from plant capacity expansions. The export of soda ash should increase gradually and reach 0.6 Mt per annum in 1997. The import of dense soda ash with less salt and ferrous content will be in demand in the China market. As to production of soda ash by the combining process, it is predicted that there will be no significant increase in the near future because the ammonium chloride price is lower than that of urea with the same nitrogen content in the domestic market, which will lead to reduced income for the combining process plants. Henceforth, China is reducing the import of nitrogenous fertilizer to encourage a better selling price for ammonium chloride and a stable yield of soda ash. Since 1996, China is reducing the tariff from 35.9 to 15% by the end of 1997. This may stimulate increased imports of soda ash. On the other hand, China is still reducing the drawback rate of export commodities, which may impair export enthusiasm.

Conclusions

Synthetic soda ash will always dominate the soda ash industry of China. Synthetic soda ash production expanded rapidly in the last twenty years due to construction of a number of new plants. Although the current supply of soda ash products temporarily exceeds the demand of the domestic market, the total production of soda ash will steadily increase in the near future, and it appears that an increase in the production of dense soda ash will be rapid. Natural soda ash products share only a small portion of the total production of soda ash in China, but the products of natural soda deposits sell well in the domestic market, thereby improving the general welfare of the local economy and providing employment. The mining and exploitation of natural soda deposits of China is also predicted to show steady expansion. Compared with the advanced techniques of developed countries, the level of synthetic and natural soda ash technology in China still lags behind.

References cited

Cao, Jilin, and others, 1992, Phase equilibrium of minerogenetic substances in Chaganor natural soda deposit: Soda Ash Industry (China), v. 3, p. 10-16.

Di, Tongli, 1995, The circumstances of production and management of soda ash industry in 1994 and the predict situation of 1995: Soda Ash Industry (China), v. 3, p. 2-6.

Di, Tongli, 1996, The circumstances of production and management of soda ash industry in 1995 and the predict situation of 1996: Soda Ash Industry (China), v. 3, p. 1-8.

Inner Mongolia Geological Survey, 1966, 1986, Reports of the exploration of natural soda lakes (deposits) in the Inner Mongolia region.

Rong, Shou Chang, 1984-1994, Soda ash, *in* Yearbook of chemical industry of China: Chemical Industry Publishing House, Beijing.

Tian, Zhigao, 1994, Current situation and prospect on the development of Anpeng nahcolite deposit: Soda Ash Industry (China), v. 4, p. 34-37.

Wu, Deyun, and others, 1995, The dissolving characteristic and increasing mining solution concentration of Anpeng nahcolite vein: Soda Ash Industry (China), v. 5, p. 39-43.

Wu, Peiwen, 1986, Soda ash industry, *in* The chemical industry of China at the present age: Social Sciences Publishing House, Beijing, p. 118-131.

Zhang, Chending, 1979, The development of natural soda industry of China: Soda Ash Industry (China), v. 3, p. 53-64.

Zhang, Youxun, 1980, The geological characters and origin of Wucheng natural soda deposit: Chemical Industry Geology (China), v. 3.

Zhang, Youxun, and others, 1983, The geological characters and mineralizing conditions of Anpeng nahcolite deposit: Soda Ash Industry (China), v. 4, p. 1-6.

Zhao, Jilai, 1985, Report of fracturing experiment on Wucheng trona vein: Henan Chemical Industry (China), v. 2.

The Beypazari trona deposit, Ankara Province, Turkey

Cahit Helvaci
Dokuz Eylul University
Bornova-Yzmir, Turkey

Abstract

The Beypazari district is a large area of volcano-sedimentary rocks in the interior of central Anatolia, Turkey approximately 100 kilometers northwest of Ankara. Trona, lignite, and bituminous shale occur in the lower part, and sodium sulfate and gypsum occur in the upper part of the sedimentary sequence in the Miocene Beypazari basin.

The Miocene sequence rests with angular unconformity on basement, which consists of metamorphic, ophiolitic, carbonate, and clastic rocks ranging in age from Paleozoic to Eocene. The sequence has been subdivided into seven sedimentary formations with 11 members and the Teke Volcanics. These sedimentary rock units are, in ascending order: the Coraklar, Hirka, Akpinar, Cayirhan, Bozbelen, and Kirmir Formations, and Sariyar Limestone.

The trona deposit located north of the Zaviye village is associated with shale in the lower part of the Hirka Formation and alternates with bituminous shale and claystones. Based on borehole data, the areal extent of the trona deposit is estimated to be approximately 8 square kilometers. The trona beds were deposited as two lensoidal bodies within a 70- to 100-meter-thick zone in the lower part of the shale unit. A total of 33 trona beds are known: 16 in the lower trona lens and 17 in the upper lens. The total thickness of the lower trona sequence ranges from 40 to 60 meters and the total thickness of the upper trona sequence is about 40 meters. The interval between the lower and the upper trona sequence varies from 30 to 35 meters. The total thickness of the trona beds in both lenses varies between 21 and 34 meters in the central parts, and between 2.5 and 12 meters in the marginal parts of the ore bodies. The thickness of individual trona beds in both trona horizons ranges from 0.4 to 2 meters. Isopach lines of both trona sequences are restricted by the Zaviye fault. The central part of the trona deposit is generally thicker than the marginal parts. The trona beds grade laterally into dolomitic mudstones and claystones toward the edges of the basin.

The principal sodium carbonate minerals are trona and minor nahcolite (the latter occurring in the marginal parts of the trona deposits); trace amounts of pirssonite and thermonatrite occur sporadically. Trona and dolomite are associated with one another throughout the trona zone. Calcite, zeolites, feldspar, and clays are the most common minerals within the associated rocks of the trona deposit. The trona crystals, which are generally white and occasionally grayish due to the presence of impurities, formed in massive beds and as disseminated crystals in claystone and shale. Zeolitization, dolomitization, and chloritization are rather common within the associated rock units of the trona deposit and probably occurred shortly after deposition, or during diagenesis.

The Beypazari basin was affected by extensional tectonics during middle and upper Miocene time. This extensional regime became a single-direction compressional regime during the late Miocene and early Pliocene. The sediments now containing trona, lignite, and bituminous shale were formed within fluvial, lacustrine, and playa-lake (perennial and ephemeral) environments. The Beypazari Neogene basin is mainly filled by clastics and penecontemporaneous products of adjacent volcanic activity which was centered northeast of the basin. The most likely sources of sodium for the formation of the trona and other sodium carbonate salts are thermal springs, tuffs interbedded with the sediments, and extensive Neogene volcanic rocks interfingering with the sedimentary rocks in the northeastern part of the basin.

Introduction

A sedimentary sequence approximately 1200 meters (m) thick, ranging in age from middle to late Miocene crops out in the Beypazari-Cayirhan district situated 100 kilometers (km) northwest of Ankara (**Figure 1**). The stratigraphy, sedimentology, and tectonic evolution of this basin are different from other parts of Central Anatolia as is the presence of economic resources including lignite, bituminous shale, trona, sodium sulfates, gypsum, and clay minerals. The basin is approximately 65 km across and occupies 1500 km^2 between the Sariyar Dam and Beypazari.

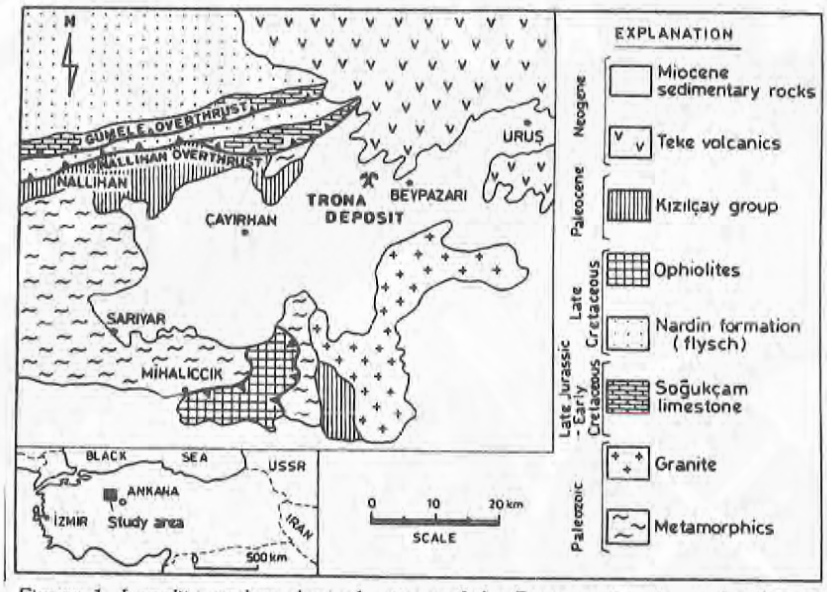


Figure 1. Locality and geological setting of the Beypazari basin and adjacent areas.

Ziegler and Onen (1936), Stephenisky (1941), Breue (1954), Gokmen (1965), Wedding (1965), Goktunali (1965), Ciculic (1969), Gokisik (1973), Oz (1976, 1977), Biron and others (1979), Narin (1980), and other previous workers have studied the geology of the lignite- and bituminous-shale-bearing basin, and many workers have studied the utilization of the bituminous shales.

The Neogene Beypazari basin is one of the most economically important basins in Turkey, containing lignite, bituminous shale, and trona deposits. This basin is mainly filled by fluvial, lacustrine, and volcano-sedimentary rocks. The Neogene sedimentary sequence in this basin is divided into eight formations (Inci and others, 1988; Helvaci and Inci, 1989). In the region between Beypazari and Nallihan, geological maps at a scale of 1:25,000 have been prepared. Stratigraphic sections were measured at different locations to determine the distribution of rock units and the locations of facies changes and tectonic features of the basin, as well as for determining the geological setting of the trona deposit.

The Neogene Beypazari basin is limited on the north by the West Pontid mountain belts. This part of the Pontids consists of metamorphic, volcanic, and sedimentary rocks, which are Paleozoic to Tertiary in age (Ketin, 1966; Saner, 1979). The Middle Sakarya massif consists mainly of metamorphic, acid-plutonic, and ultrabasic rocks, and occurs on the south edge of the Beypazari basin (Saner, 1979). Tertiary volcanic rocks are distributed in both the northeastern part of the basin and between the Beypazari and Kizilcahamam areas (**Figure 1**). Pre-Neogene sedimentary rocks ranging from Paleocene to Eocene in age limit the Neogene basin to the west.

Trona was discovered incidentally by the General Directorate of the Mineral Research and Exploration (MTA) while carrying out a drilling project of the lignite deposits in the summer of 1982. An extensive exploratory drilling program was undertaken by MTA during the period 1983-1985 on behalf of the Etibank Company. Some 64 drill holes have been completed in the area to date. The Beypazari area was mapped and sampled by the author in the summers of 1985, 1986, 1987, and 1988. Proven trona reserves are 210 Mt [million metric tons (tonnes)] and total reserves are estimated as 240 Mt (Kayakiran and others, 1986; Helvaci and others, 1989). In addition, there are approximately 400 Mt of lignite, 340 Mt of bituminous shale, and 1 Mt of Na-sulfate in the same basin (Siyako, 1984; Helvaci and Inci, 1989).

The aim of this paper is to report geological, mineralogical, and geochemical aspects of the trona deposit and associated rocks.

Sample collection and analytical methods

All samples used in this study were collected from drill cores and a series of sample traverses. Approximately 2 kilograms (kg) of material was collected from sample traverses to ensure a representative sample.

Na-carbonates and other minerals were characterized by direct-recording X-ray diffractometer (XRD) analysis with standard powder and oriented sample techniques. Debye-Scheuer and Guinier cameras were also used for mineral identification. Mineral fractions were purified by handpicking, heavy liquids, and magnetic separation.

Ca, Mg, Na, Li, and Sr from the trona samples were determined by atomic absorption (AA) and Induction-Coupled Plasma (ICP) methods. All the other major and trace elements of the trona samples were analyzed by the X-ray fluorescence (XRF) analysis method which is basically similar to that described by Leake and others (1969/1970). All samples were run in duplicate.

The major elements of volcanic, granite, tuff, and sediment samples were determined by a Philips 1410 XRF® spectrometer, using fused glass beads and G-2 and BCR-1 standard rocks for calibration. Trace elements were analyzed using pressed powder pellets and G-2 and BCR-1 standard rocks for calibration. All samples were run in duplicate. Cations and anions from the water samples were determined by AA. The K-Ar age dating method used in this study was published by Damon and others (1983).

Stratigraphy

The rock units of the study area are divided into two main groups: pre-Neogene basement rocks and Neogene rock units (**Figures 2** and **3**). The pre-Neogene basement rocks are Paleozoic to Eocene in age and consist of metamorphic, plutonic, volcanic, and sedimentary rocks. The Neogene sedimentary units generally consist of clastic, clayey, calcareous, bituminous, evaporitic, and silicified sediments.

The Neogene sedimentary sequence is divided into eight formations (**Figures 2b** and **3b**). These are, in ascending stratigraphic order, the Coraklar, Hirka, Akpinar, Cayirhan, Bozbelen, and Kirmir Formations; Teke Volcanics; and Sariyar Limestone (Inci and others, 1988; Helvaci and Inci, 1989).

Pre-Neogene rock units

The pre-Neogene basement consists chiefly of metamorphic rocks, granite, ultramafic rocks, the Sogukcam Limestone, Nardin Formation, and the Kizilcay Group–ranging in age from pre-Permian to middle Eocene (**Figures 2a** and **3a**).

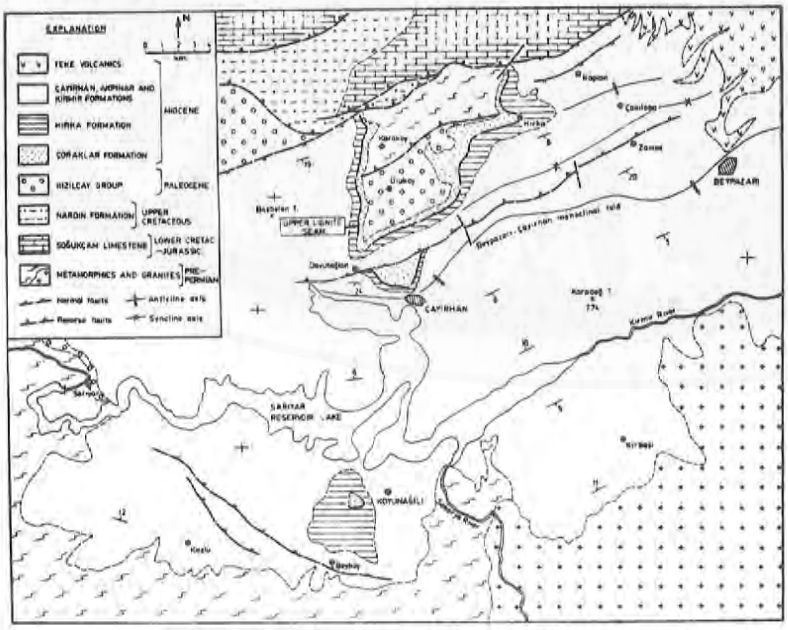


Figure 2a. Generalized geologic map of the Beypazari basin.

The oldest rocks observed in the study area are Paleozoic metamorphic rocks, which consist of mica schist, chlorite schist, amphibolite schist, quartzite, and marble. The inferred age of the metamorphic rocks is pre-Permian along the Middle Sakarya River (Altinli, 1976, 1977). These rocks were intruded by granite.

The granites intruded into the metamorphic rocks during post-Permian time. Amphibole from the granitic rocks has been dated by Rb-Sr as 48±7.4 Ma (Mega-annum or million years) with an initial $^{87}Sr/^{86}Sr$ ratio of 0.70579 (University of Tubingen, Germany, personal communication). Granitic rocks cover a wide area south of Beypazari (**Figure 1**). Aplite and pegmatite veins are dominant

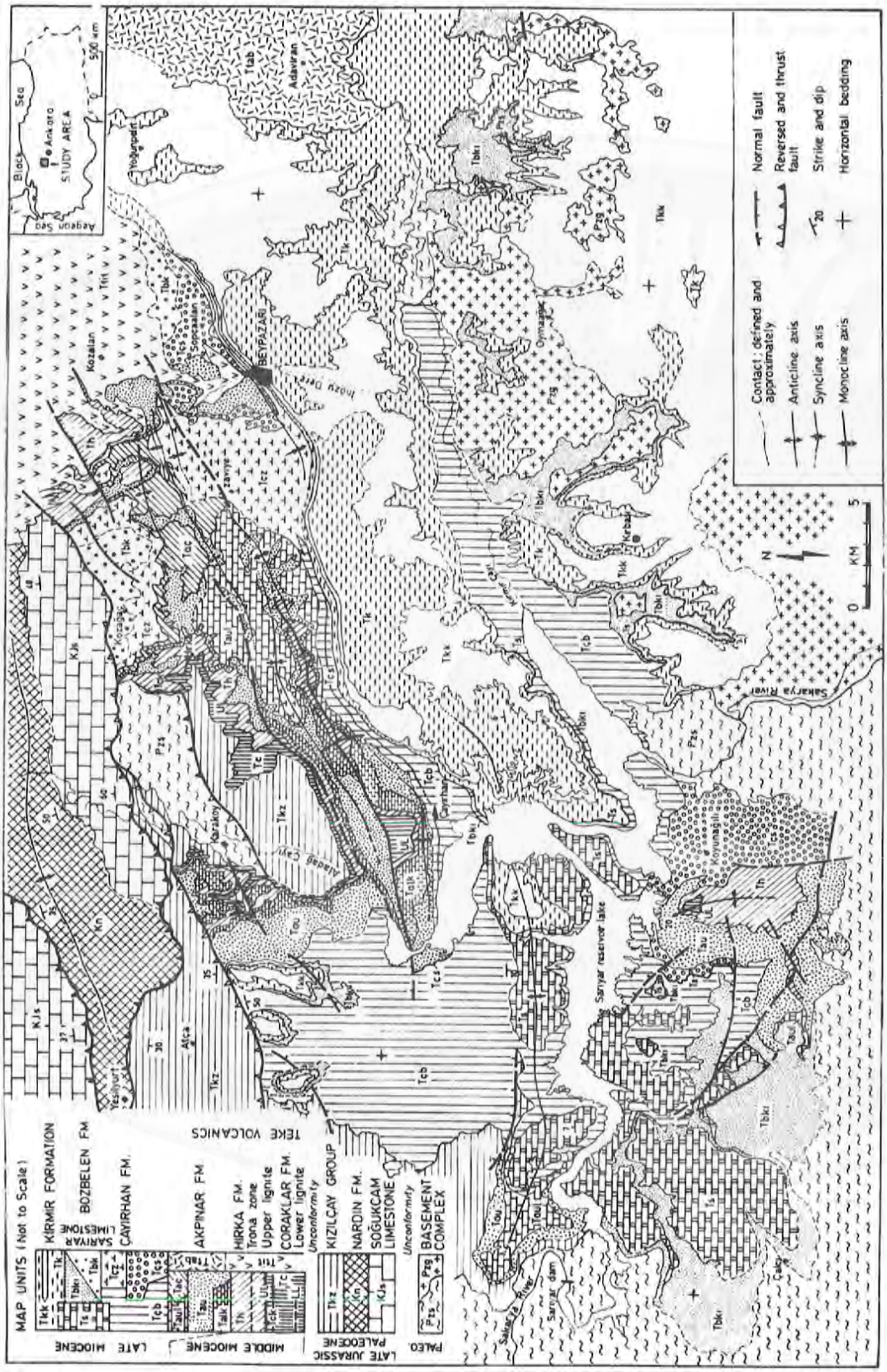


Figure 2b. Detailed geologic map of the Beypazari basin. Coraklar Formation (Tc): Karakoy Member (Tck); Hirka Formation (Th); Akpinar Formation (Ta): Lower Limestone Member (Talk), Uykudere Member (Tau), Upper Limestone Member (Taul), Cakiloba Member (Tac); Cayirhan Formation (Tc): Sopcalan Member (Tcs), Bozcayir Member (Tcb), Zavuye Member (Tcz); Bozbelen Formation (Tb): Kozagac Conglomerate Member (Tbk), Kiztepe Sandstone Member (Tbki); Kirmir Formation (Tk): Karabayir Gypsum Member (Tkk); and Teke Volcanics: Inozu Tuff (Titi), Adaviran Basalt (Tab).

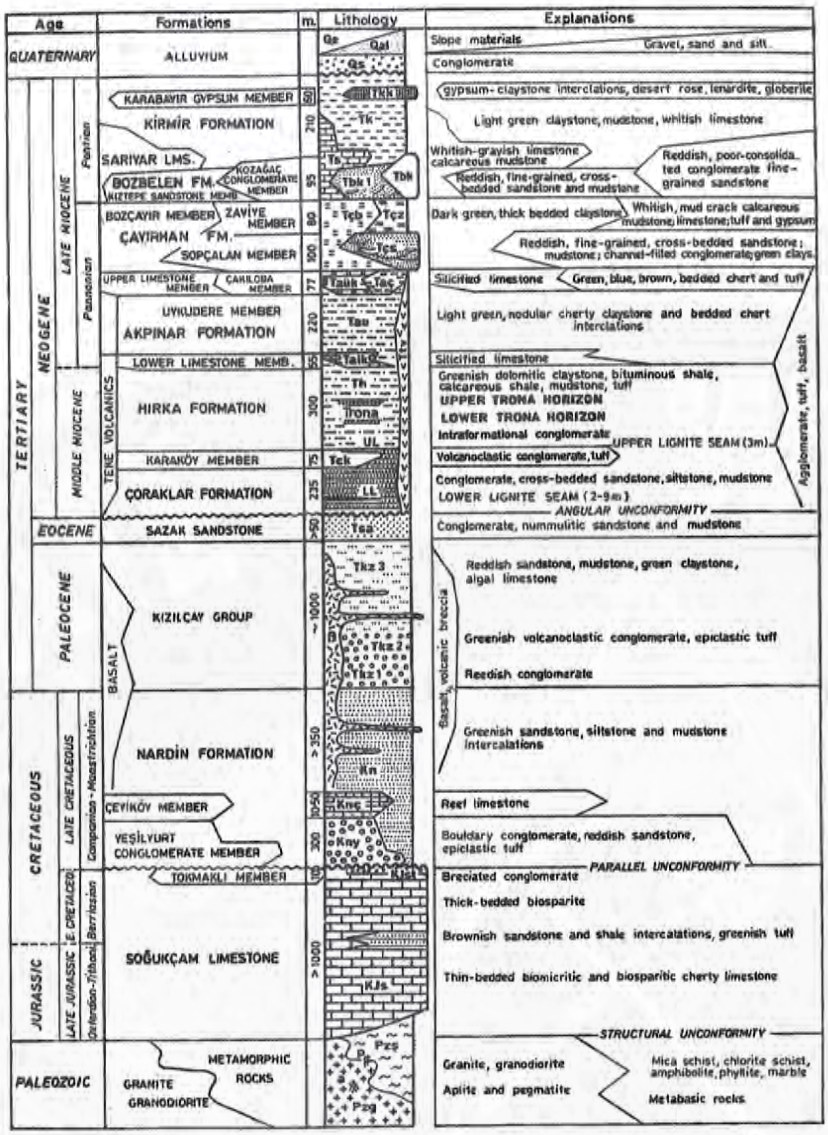


Figure 3a. Stratigraphic section of the Beypazari trona basin with details of underlying Neogene and older basement rocks.

in the granites, strike NE-SW and NW-SE, and dip to the south (Helvaci and Bozkurt, 1994). **Table 1** gives chemical analyses of granitic rocks from the region.

The ultramafics are mainly composed of serpentinite, metabasite, red chert, and gabbroic components. The ultramafics were placed on the metamorphic rocks with a tectonic (fault) contact during Late Cretaceous time (Cogulu, 1967).

Jurassic rocks are represented by thin-bedded, micritic, sparitic, and ammonite-bearing fossiliferous limestones alternating with sandstone, shale, and chert layers, and are named the "Bilecik Limestone" by Altinli (1973, 1976, 1977). The Bilecik Limestone grades into a Lower Cretaceous limestone named the "Sogukcam Limestone" by earlier workers in the area under investigation and in the area west of Nallihan.

In the region, the Upper Cretaceous sequence is represented by turbiditic clastic rocks of the Nardin Formation and rests concordantly on Lower Cretaceous limestones (Onal and others, 1988).

The Paleocene sequence consists mainly of reddish and grayish conglomerate, sandstone, siltstone, mudstone, thin-bedded limestone, and greenish to brownish volcaniclastic rock units. These rock units are named "Kizilcay Group" by Altinli (1976, 1977) and Saner (1979). The Kizilcay Group was deposited in fluvial and lacustrine environments and its total thickness exceeds 2000 m (Onal and others, 1988).

Eocene rocks in the area are mostly limestones and sandstones with a total thickness of approximately 250 m. Due to extensive post-Eocene erosion, these rocks are not widespread and only occur locally.

In the northern part of the area (**Figures 1** and **2**), Jurassic and Cretaceous units are in tectonic contact with the other rock units and are thrust to the south over the Paleozoic metamorphic complex and the Paleocene clastic rocks (Altinli, 1976; Yagmurlu and others, 1988).

Neogene rock units

Coraklar Formation

Sedimentary rocks of the Coraklar Formation consist of volcaniclastic conglomerates, sandstones, siltstones, and mudstones, and were deposited as alluvial facies in braided-meandering river and floodplain environments. A lower lignite bed occurs in the lower part of the Coraklar Formation and formed in channel-controlled swamps of a river system (**Figure 3b**). An upper lignite bed occurs in the uppermost part of the Coraklar Formation, was deposited in a lake-margin mud-flat environment, and is overlain and in sharp contact by the Hirka Formation (Yagmurlu and others, 1988; Helvaci and Inci, 1989).

Table 1. Whole-rock analyses of major oxides and selected trace elements in granites from the Beypazari basin. Oxide analyses in weight percent; elemental analyses in parts per million (ppm); LOI=loss on ignition.

Oxide (%)	1	2	3	4	5	6	7
SiO_2	57.60	74.97	65.04	52.64	59.17	65.35	67.52
Al_2O_3	17.59	12.33	16.28	18.38	21.67	15.75	14.96
Fe_2O_3	3.49	0.22	2.09	4.8	0.42	2.11	1.21
FeO	3.88	0.26	2.34	5.33	0.47	2.35	1.34
MgO	2.51	0.27	1.12	3.41	1.25	1.22	0.64
CaO	7.46	0.85	5.04	8.0	7.74	5.19	2.97
Na_2O	3.0	3.27	3.54	2.96	7.0	3.32	3.55
K_2O	2.71	4.95	4.29	2.28	0.3	3.97	3.8
TiO_2	1.1	0.7	0.52	1.6	1.2	0.7	0.7
P_2O_5	0.3	0.19	0.15	0.3	0.2	0.2	0.2
LOI	0.57	0.42	0.33	0.69	0.23	0.39	0.55
TOTAL	99.64	99.87	100.41	100.39	99.63	100.55	97.44
Elements (ppm)							
Rb	75	333	134	62	8	126	72
Sr	509	61	728	410	676	633	610
Y	31	34	53	25	30	51	22
Zr	115	66	150	74	135	144	148
Nb	12	16	13	17	6	23	6

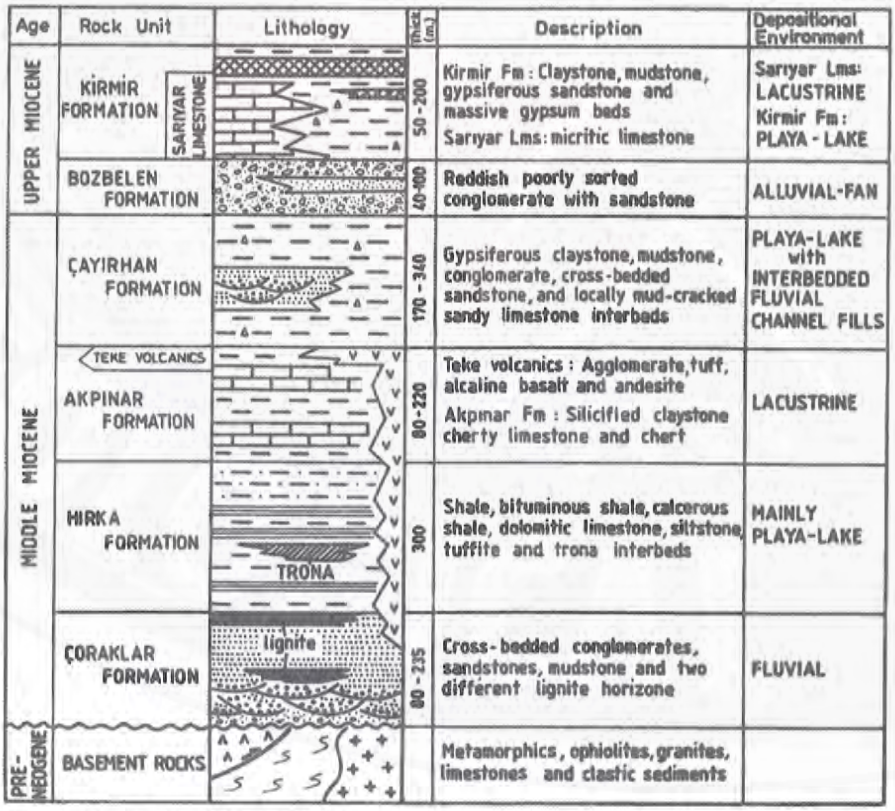


Figure 3b. Stratigraphic columnar section of middle and upper Miocene rocks in the Beypazari trona basin.

Conglomerates are dominant in the lowermost part of the alluvial sequence of the Coraklar Formation; the sequence continues to the top as sandstone-mudstone alternations. Also, channel-fill conglomerates occur locally in the uppermost part of the sandstone-mudstone sequence. Drilling information indicates that this unit is approximately 150 m thick, increases in thickness from north to south, and reaches 250 m in the Cayirhan area. The Coraklar Formation rests with angular unconformity on the pre-existing rock units older than Neogene, and grades laterally into the Hirka Formation to the northeast (**Figures 2** and **4**).

Conglomerates of the Coraklar Formation are yellowish, medium consolidated, poorly sorted, well-drained, trough-shaped and large-scale (75 to 125 cm) cross-bedded, and generally fining-upward, graded beds. Moderate size clasts range between 3 and 6 cm up to a maximum size of 10 to 12 cm. The conglomerates contain locally imbricated clasts, mudstone and sandstone intercalations, and rip-up clasts, all within the lower parts. Sandstones are locally trough-shaped and cross-bedded. Grains generally are angular to

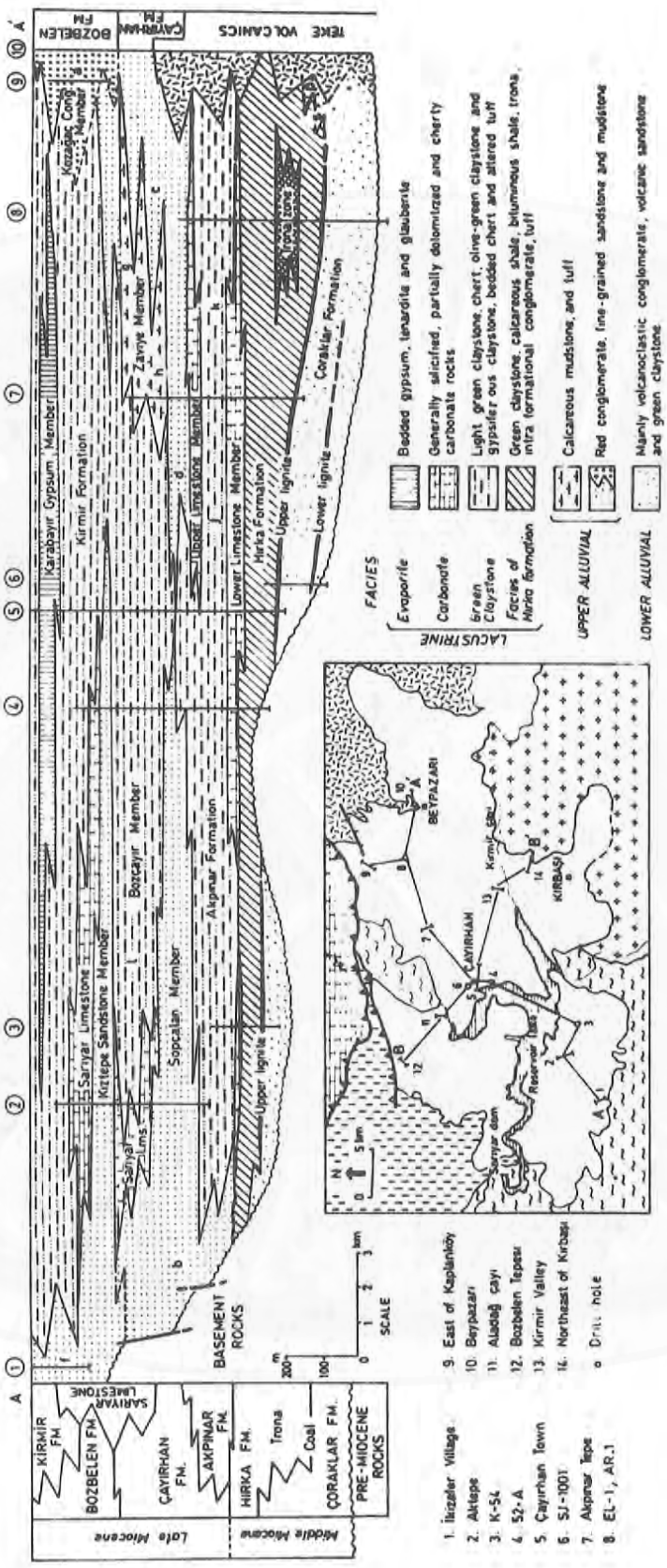


Figure 4. Stratigraphic section showing the distribution of major facies and associated rock unit assemblages in the Beypazari trona basin.

subrounded and are moderately- to well-sorted. Mudstones generally are light greenish, poorly bedded, and locally consist of siltstone, fine-grained sandstone, and plant detritus. These features of the mudstones indicate well-drained swamp conditions in a fluvial environment. Volcanic constituents are dominantly in the top part of the formation.

Sedimentary structures include planar and trough cross-bedding, parallel lamination, convoluted bedding, graded beds, and burrows. These sedimentary structures probably indicate a high- to mid-flow regime of meandering stream systems. Field measurements of internal sedimentary structures indicate that the dominant transport direction was to the southeast and southwest. The channel conglomerates are believed to have been formed by lateral and vertical migration of mobile stream channels on an alluvial plain, and were derived from the rocks of the West Pontids.

Hirka Formation

The Hirka Formation rests concordantly on the upper lignite bed of the Coraklar Formation and is composed mainly of mudstone, claystone, bituminous shale, trona, gray shale, calcareous shale, dolomitic limestone, siltstone, intraformational conglomerate, and tuff (**Figures 4** and **5**). The Hirka Formation was apparently deposited in a playa-lake environment. Trona was deposited in the central part of a playa-lake environment (**Figure 6**). Claystone and mudstone were deposited in the playa or mud-flat environment around the lake margins. The bituminous shales were deposited during periodic expansions of the lake.

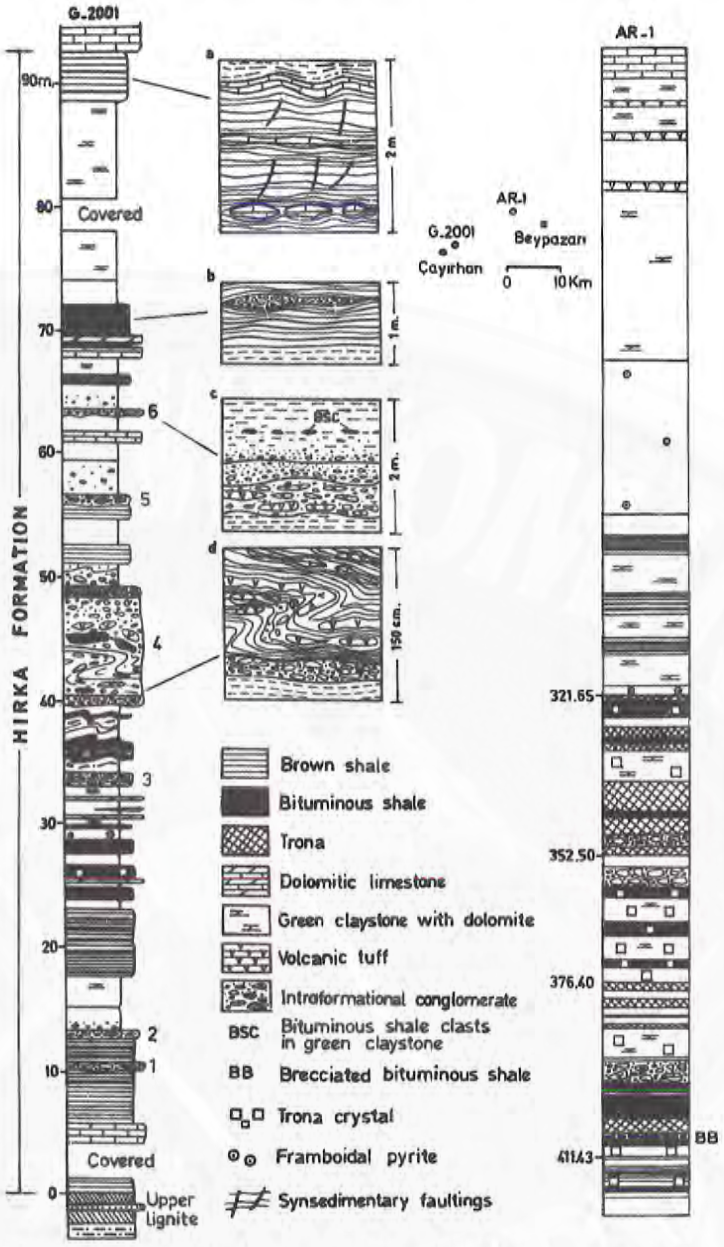


Figure 5. Type and reference sections of the dolomitic claystone, bituminous shale, trona, and intraformational conglomerate lithofacies of the Hirka Formation. AR-1, drill hole, depths in meters from surface; G-2001, underground lignite mine tunnel.

The Hirka Formation is gradational vertically and laterally with the underlying Coraklar Formation. The total thickness of the Hirka Formation increases eastward and exceeds 300 m where the trona deposit occurs. The formation interfingers with the Teke Volcanics along the Inozu Dere northwest of Beypazari (**Figures 6, 7,** and **8**).

Mudstone and claystone of the Hirka Formation are greenish and grayish, thick bedded, moderately consolidated, and include partially framboidal pyrite crystals (**Figure 9**). These rocks grade locally into argillaceous siltstone, calcareous shale, or gray shale. Bituminous shales are typically dark grayish- to brownish-black, thin-bedded, and finely laminated (**Figure 10**). The content of organic carbon is about 13% and the upper calorific values range between 600 and 1140 kcal/kg (Biron and others, 1979). Dolomitic limestones are usually thin (1 to 3 m), gray to whitish, micritic, and partially silicified. The intraformational conglomerate is whitish, micritic, partially silicified, thick bedded, well consolidated, clay and mud supported, and composed mainly of angular tuff and bituminous shale, gravels, cobbles, and minor boulders. The conglomerate interfingers with the other rock types of the Hirka Formation. The tuffs are generally whitish, thin and thick bedded, locally fragmented, and alternate with the other rock components of the unit. A tuff sample (SJ35-4) interbedded in the Hirka Formation gave a K-Ar age of 21.5+0.9 Ma.

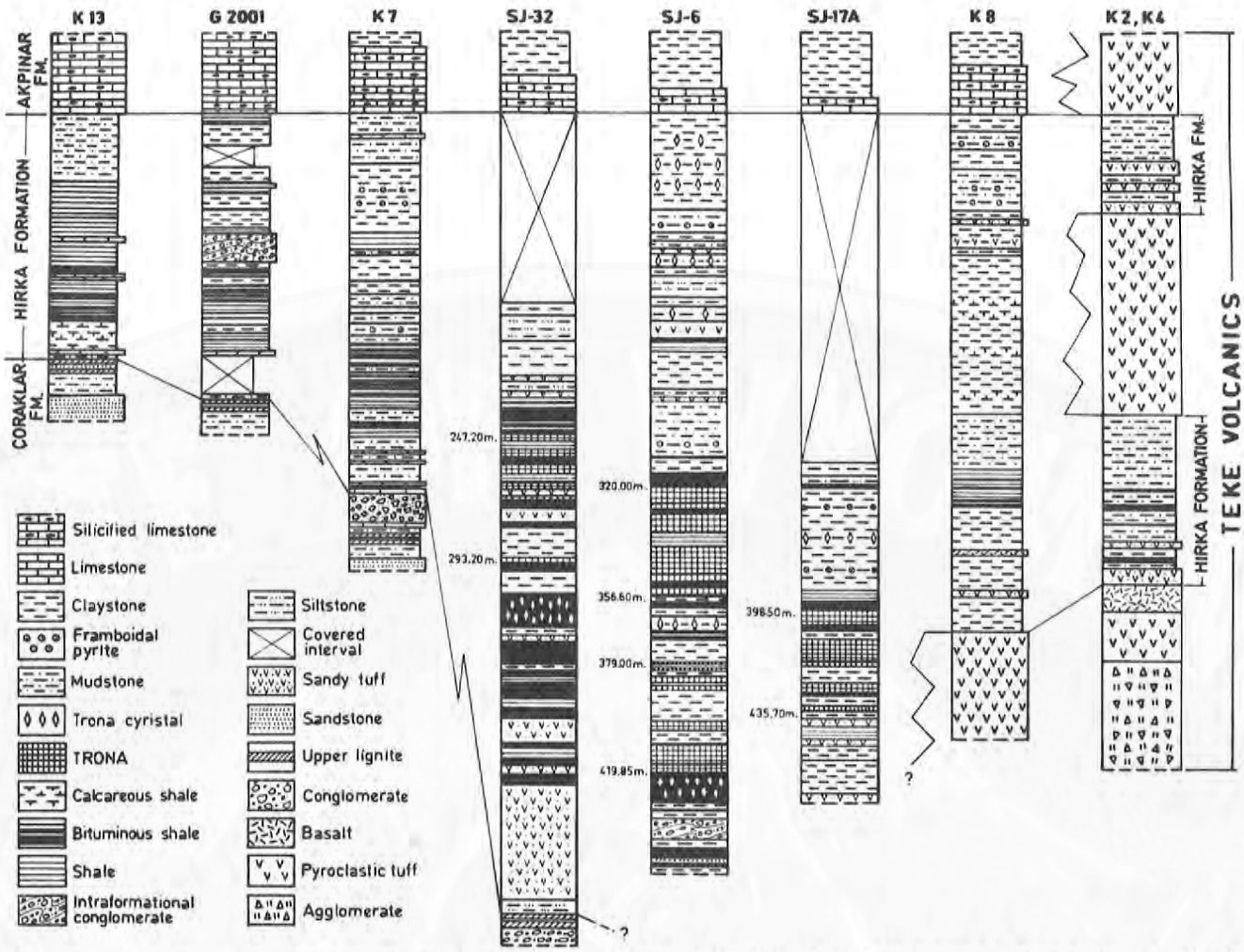


Figure 6. Type section, reference sections, and stratigraphic relations of the Hirka Formation. Section is from southwest (left) to northeast (right).

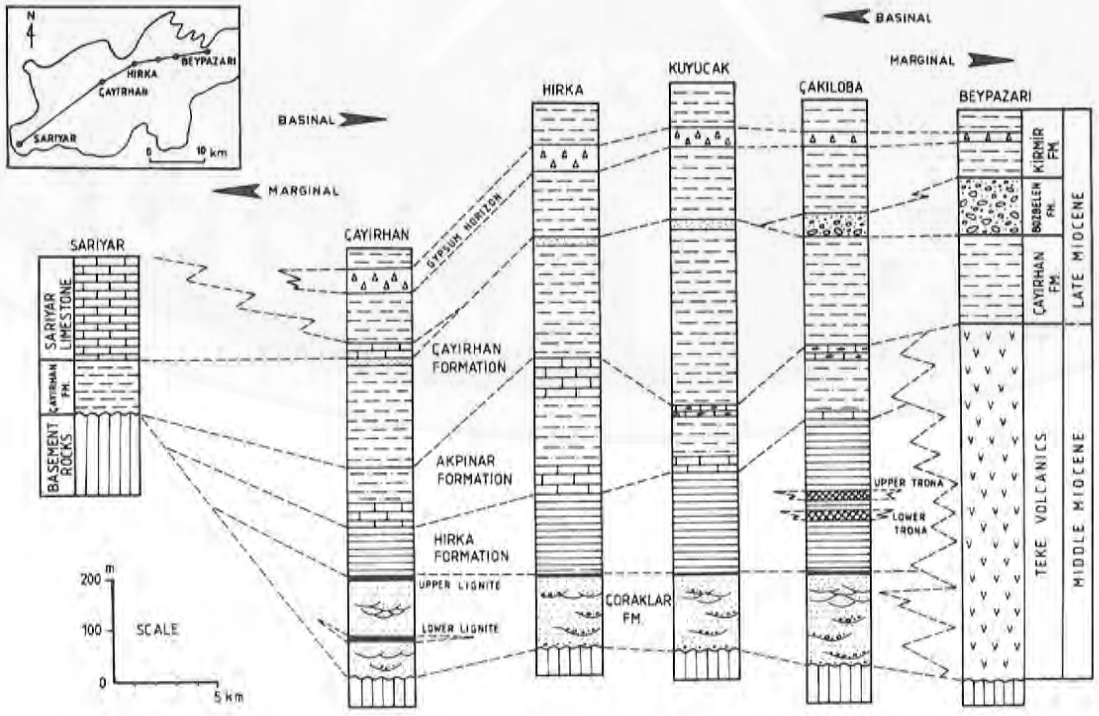


Figure 7. Correlation of the rock succession in different parts of the Miocene Beypazari basin.



Figure 8. Photograph showing the intercalations of the Teke Volcanics within the Hirka Formation in the northeastern part of the Beypazari basin.

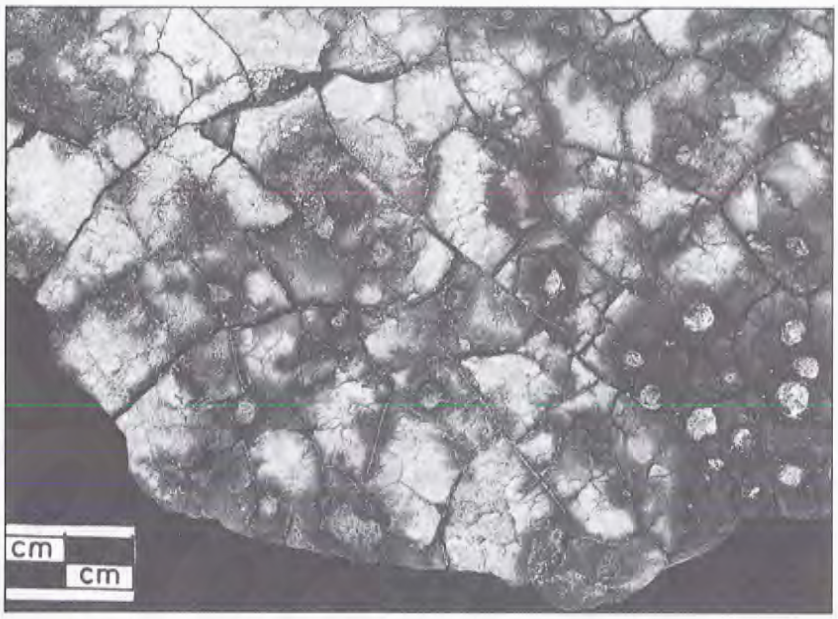


Figure 9. Framboidal pyrite crystals within claystone-mudstone of the Hirka Formation.

Some sections of the formation north of Beypazari include thin (1 to 2 m) basaltic sills and silicified wood fragments (**Figure 6,** sections K8 and K2, K4).

The trona deposit is within the lower part of the Hirka Formation and alternates with bituminous shale and claystones (**Figures 5, 6,** and **7**). The trona deposit covers approximately 8 km^2 around Cakiloba village, according to MTA drill data. The trona beds were deposited within a 70- to 100-meter-thick zone as lenticular bodies and grade laterally into and interfinger with mudstone, claystone, and bituminous shales at the edges of the trona deposit.

Akpinar Formation

The Akpinar Formation consists of silicified limestone, chert, tuff, claystone, and mudstone. The lower and uppermost parts of the unit are represented by the lower and upper limestone members whereas the middle part is represented by alternating green claystone and bedded chert. At the type section, the Akpinar Formation is 150 m thick and rests with gradational contact on the Hirka Formation. The Akpinar Formation grades into the Cayirhan Formation from east to west (**Figures 4** and **7**).



Figure 10a. The Coraklar Formation at the bottom of the photograph is overlain by the Hirka Formation at Hirka village, Beypazari basin.



Figure 10b. Photograph of the Coraklar Formation (lower part of exposure) and the overlying Hirka Formation south of Karakoy, Beypazari basin.

Cayirhan Formation

The Cayirhan Formation consists mainly of greenish claystone, mudstone, marl, and locally sandstone, Na-sulfates, and gypsum beds. Mudcracks, salt crystals, and burrows are dominant sedimentary structures of the Cayirhan Formation. This sequence contains playa-type lacustrine and mud-flat facies.

The Cayirhan Formation varies in total thickness from about 150 to 300 m, and rests conformably but with sharp contact on the Akpinar Formation (**Figures 4** and **7**).

Bozbelen Formation

The Bozbelen Formation consists mainly of reddish conglomerate, sandstone, and mudstone indicating an alluvial fan environment. The thickness of the formation increases from south to north and reaches 100 m near the marginal parts of basin. The Bozbelen Formation rests unconformably on all of the older rock units (**Figures 4** and **7**).

Kirmir Formation

The Kirmir Formation is mainly made up of gypsiferous green claystone, Na-sulfates, and bedded gypsum. This formation is widespread over the basin and occurs within the uppermost part of the Miocene sedimentary sequence. It contains numerous evaporite zones, which in ascending stratigraphic order are gypsiferous claystone facies, thenardite-glauberite facies, laminar gypsum facies, and crystalline gypsum facies (Yagmurlu and Helvaci, 1994). The unit is laterally and vertically gradational with the Sariyar Limestone and Bozbelen Formation (**Figures 4** and **7**).

Sariyar Limestone

The Sariyar Limestone is composed of mainly whitish, thick-bedded and micritic lacustrine limestone. The thickness of the unit increases from east to west reaching 150 m in the area around the Sariyar Dam (**Figures 4** and **7**).

Teke Volcanics

The Teke Volcanics are widespread in the area northeast of Beypazari and Kizilcahamam. These volcanics consist of alternating pyroclastic breccia, tuff, andesitic and basaltic lavas, and agglomerate and are of early Eocene to late Miocene age (**Figures 4** and **7**).

The lower and middle parts of the Miocene Beypazari sequence interfinger with the Teke Volcanics, which are composed of pyroclastic tuffs and basalts. The Beypazari trona deposit accumulated in a narrow area near this interfingering transition zone. The Inozu Tuff is composed of whitish, thick to massive alternating beds of crystal and lithic tuff, reworked tuff, and volcaniclastic conglomerate. Agglomerates are present below the tuffs in some localities. The Adaviran Basalt consists of black lava flows and minor amounts of tuff. The total thickness of the lava flows exceeds 300 m. The unit covers a wide area around Adaviran village.

The Miocene Beypazari sequence exposed in the eastern part of the basin and interfingered with the Teke Volcanics is thicker than the sequence in the western part of the basin. Tuff interlayers and grades of silicification increase toward the Teke Volcanics, which form the southwestern edge of the volcanics described by Ongur (1977) as an alternating sequence of pyroclastic breccia, tuff, and andesitic and basaltic lavas in the Kizilcahamam (Ankara) district. Chemical analyses of the Teke Volcanics is given in **Table 2**.

Table 2. Whole-rock analyses of major oxides and selected trace elements in the Teke Volcanics from the Beypazari basin. Oxide analyses in weight percent; elemental analyses in parts per million (ppm).

Oxide(%)	B6-2	B6-3A	B6-5	B6-6	B6-8	B6-10	B63	B67	B79	B82
SiO_2	66.30	65.73	65.92	65.21	66.79	67.00	44.68	66.75	58.54	62.10
Al_2O_3	16.05	16.76	16.04	16.14	15.41	15.20	15.46	16.13	16.27	16.60
$*Fe_2O^T_3$	3.18	2.59	3.18	3.47	3.37	3.22	8.11	2.95	5.91	5.26
MgO	1.34	1.26	1.82	1.97	1.56	1.83	5.55	1.55	3.70	1.83
CaO	4.36	4.86	4.82	5.28	4.38	4.67	10.20	4.35	5.63	4.98
Na_2O	3.55	4.02	3.27	3.48	3.49	3.31	5.09	3.38	4.42	4.28
K_2O	3.95	3.56	4.19	3.61	4.23	4.02	1.50	4.20	2.02	1.87
TiO_2	0.34	0.29	0.37	0.42	0.38	0.37	1.23	0.32	1.06	1.05
P_2O_5	0.29	0.32	0.31	0.34	0.29	0.30	0.74	0.28	0.44	0.35
MnO	0.09	0.06	0.09	0.08	0.09	0.09	0.09	0.08	0.07	0.06
H_2O	0.54	0.53	0.00	0.00	0.00	0.00	7.23	0.00	1.93	1.62
TOTAL	99.99	99.98	100.01	100.00	99.99	100.01	99.88	99.99	99.99	100.00
Elements (ppm)										
Rb	152	121	150	138	158	162	31.84	165	63	61
Sr	613	667	538	549	590	497	1007	585	592	552
Y	25	19	19	21	24	23	18	20	22	18
Zr	109	88	107	94	118	102	143	101	239	206
Nb	14	11	8	9	13	12	22	10	22	18

$*Fe_2O^T_2 : Fe_2O_3 + 1.111 \times FeO$

Structure

The Miocene Beypazari basin trends approximately east-west and is limited by growth faults to the north and south. The growth faults at the northern part of the basin have high displacements resulting from stepwise structural features, which occur dominantly at the contact between Miocene rocks and basement rocks. The growth faults at the southern margin of the basin have small displacements and developed during the first phase of tectonism. Fluvial and lacustrine sediments were deposited during Miocene time in asymmetric depressions controlled by the growth faults at the northern margin of the basin (**Figures 11** and **12**).

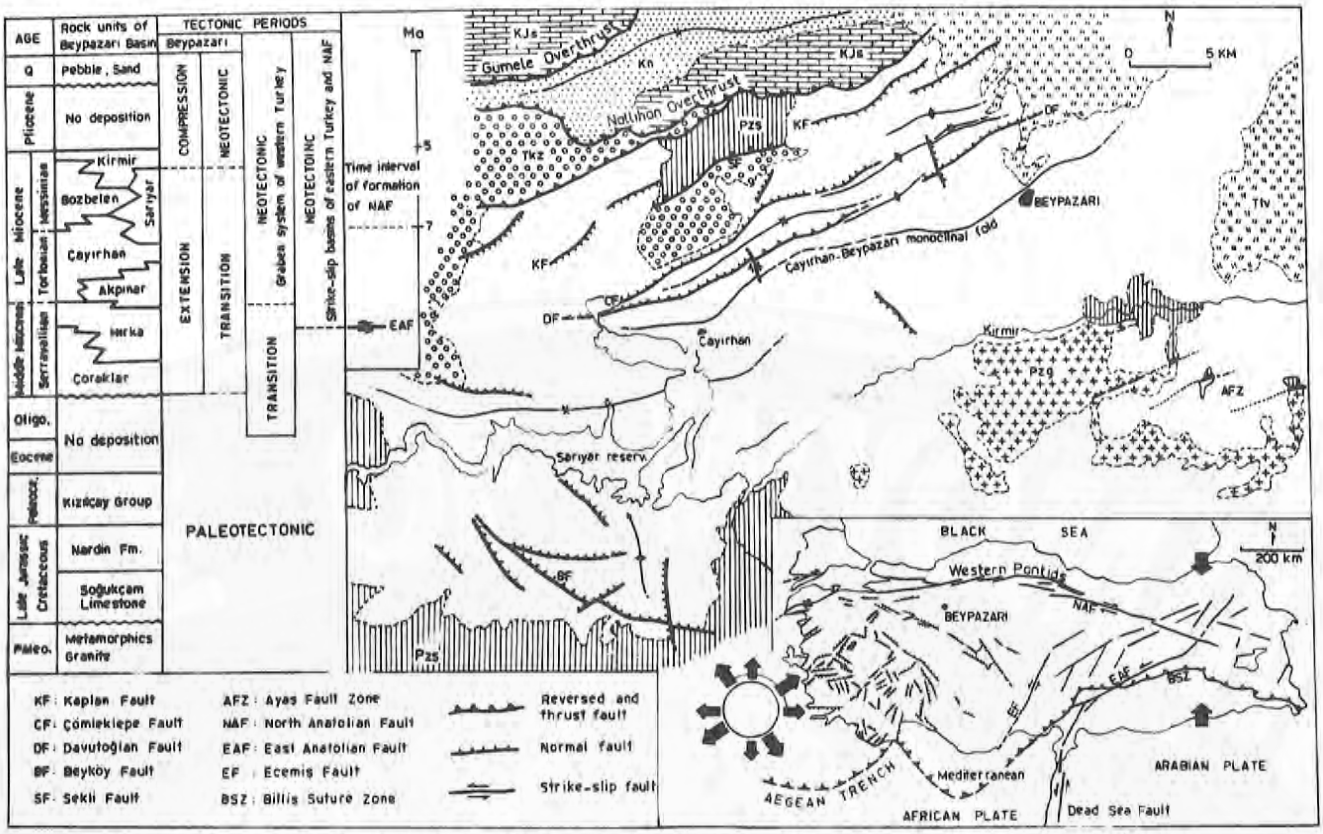


Figure 11. Tectonic structures in the Miocene Beypazari basin and major neotectonic features in Turkey.

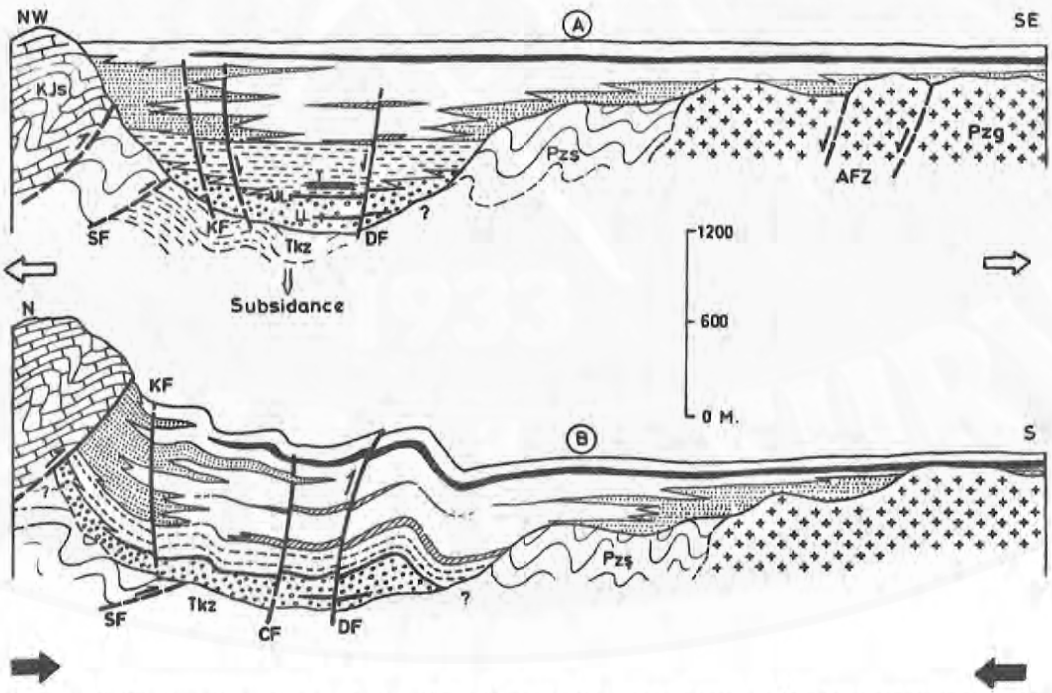


Figure 12. Tectosedimentary evolution of the Miocene Beypazari basin: A, Miocene extension phase; B, post-Miocene compressive phase. Pre-Miocene overthrusts, which developed between the Jurassic Sogukcam Limestone and Cretaceous-Paleocene units, probably occured during a late Eocene compressional phase, and resulted from the collision between the Torid-Anatolid platform and the Sakarya continent. Big dots= lower alluvial facies; small dots= upper alluvial facies; dashed lines= lithofacies of the Hirka Formation; LL= lower lignite; UL= upper lignite; T= trona; diagonal strips= carbonate rock; white= green claystone lithofacies; black= evaporite lithofacies (sulfates). See Figure 2 for other abbreviations.

The Beypazari basin was affected by an extensional tectonic regime during the middle and upper Miocene. Normal faults trending NE-SW developed and sedimentation in the basin was controlled by the faults throughout the Miocene. The stratigraphic and sedimentologic features of the sequence and the placement of the faults indicate a half-graben type of depressional basin. The extensional regime changed to a single-direction compressional regime during late Miocene and early Pliocene time. During this time, the Miocene rocks were folded, and the rocks of the northern margin of the basin were thrust over the basement rocks (**Figure 12**). The source of the compressional forces probably originated from movement of the strike-slip North Anatolian Fault against the passive block of the Eskisehir Fault and the Middle Sakarya massif (**Figure 13**) (Yagmurlu and others, 1988; Helvaci and Inci, 1989).

Extensional tectonics affected this region during middle Miocene time. A high degree of subsidence occurred under the influence of this extensional regime, and local growth faults developed in the southern margin of the basin during early and middle Miocene. In addition, intraformational breccias derived from the southern part of the basin, and synsedimentary small folds (overturned to the north) are observed in the Hirka Formation in the Cayirhan coal field. These occurrences are significant as they indicate the beginning of the synsedimentary tectonism penecontemporaneous with sedimentation in the southern part of basin during deposition of the Hirka Formation.

Growth faults, which were produced by gravity tectonics in the northern part of the Beypazari basin, probably originated during early Miocene and were active until the end of Miocene sedimentation. This tectonism is the result of N-S extension, which influenced west and central Anatolia during the Miocene.

Asymmetric anticlines, synclines, and monoclines are common in the Beypazari basin; their axes trend dominantly ENE. The fold axes trend E-W and NE-SW and the dips of their limbs range between 15° and 50°. These folds were generally developed near the northern part of the basin. High-angle limbs of the folds and monoclines usually face south, whereas the northern limbs are low angle and locally become near horizontal (**Figure 14**). The Beypazari-Cayirhan monoclinal fold is the largest fold of the region and extends 30 km in a NE-SW direction (**Figures 2** and **11**). The southern limb of this monoclinal fold dips at a high angle and locally reaches 70°.

The main structural elements of the study area include overthrusts, high-angle reverse faults, normal faults, and dominantly monoclinal and asymmetrical folds (**Figure 11**). The majority of the faults of the area are high-angle reverse faults. These faults change into overthrusts at some locations when traced laterally along their strikes. In the northern part of the area, north of Karakoy and Hirka, Jurassic and Cretaceous rock units are in tectonic contact with other rock units and are thrust southward over the Paleozoic metamorphic complex and the Paleocene clastic rocks (**Figures 1** and **11**). In the western part of Nallihan, this thrust fault is named "Tuzakli-Nallihan Overthrust" by Altinli (1976) (**Figure 1**). Several other high-angle reverse faults affecting Miocene and pre-Miocene rocks are also present within the Tuzakli-Nallihan overthrust zone. These faults roughly trend NE-SW and dip northward at angles ranging between 30° and 70°.

Normal faults trend E-W and NE-SW, dip both north and south between 50° and 70°, and have throws between 30 and 70 m. Their throw and dip decrease from the margins to the central part of the Neogene basin. One of these normal faults is called the Zaviye fault, which is observed in the southern part of the central basin. It trends roughly NE-SW. The trona deposit in the basin is bounded on the south by this fault (**Figure 15**). North-south-trending strike-slip faults in the area cut obliquely across the normal and reverse fault systems.

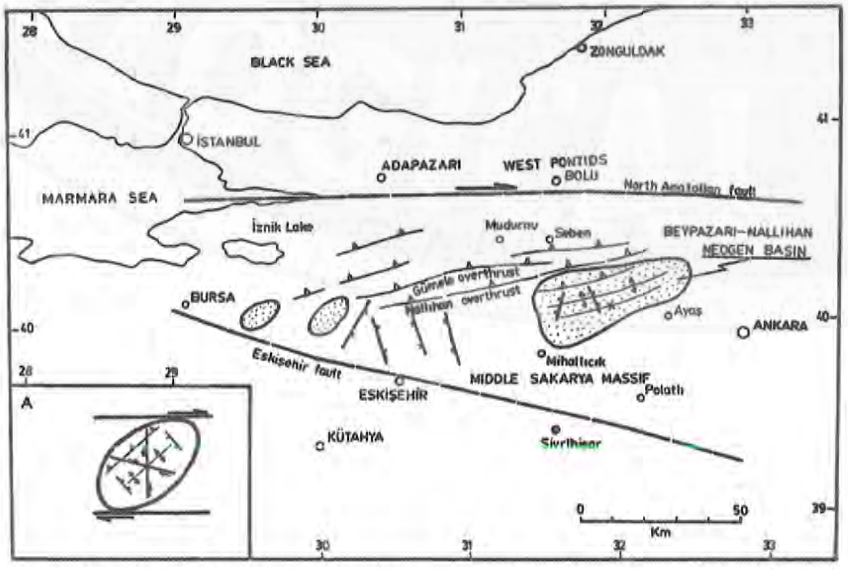


Figure 13. Geometric relationships between the tectonic features of the Neogene Beypazari basin and the North Anatolian and Eskisehir faults.

Rock units of the study area are affected by tensional and compressional tectonic forces. Some of the pre-Neogene normal faults probably changed into high-angle reverse faults and overthrusts under the effect of compressional forces which prevailed during the Neogene period. The strike-slip faults observed in the Neogene basin might also be produced by these compressional stresses. The reverse fault systems are most probably pre-Neogene to late Miocene in age (**Figure 12**).



Figure 14. Photograph showing monoclinal folds that affected the Miocene Beypazari basin. Photograph taken from the northeastern part of the basin.



Figure 15. Photograph showing the extension of the Zaviye normal fault, which forms the southern boundary of the trona deposit.

Facies analysis of the Miocene Beypazari sequence

Folded and faulted pre-Miocene basement rocks of the Beypazari region are associated with the western Pontide orogenic belt. The Miocene Beypazari basin was formed discordantly on this pre-Miocene geomorphic structure farther south of the western Pontide Mountains.

Three major facies, including different lithofacies, have been defined in the Beypazari basin: (1) lower alluvial facies, (2) upper alluvial facies, and (3) lacustrine. In general, gray and whitish volcanic conglomerate, sandstone, and greenish siltstone and mudstone beds characterize the lower alluvial facies; reddish conglomerate, fine-grained sandstone, and mudstone beds characterize the upper alluvial facies. Gray to brown shale, bituminous shale, green claystone, carbonate rocks, bedded chert, trona beds, and gypsum beds compose the lacustrine facies (Helvaci and Inci, 1989; Inci, 1991). **Figure 4** illustrates the distribution of the major facies and associated stratigraphic rock units as determined on the measured sections and drill holes; **Figure 16** is a schematic diagram of the facies relationships.

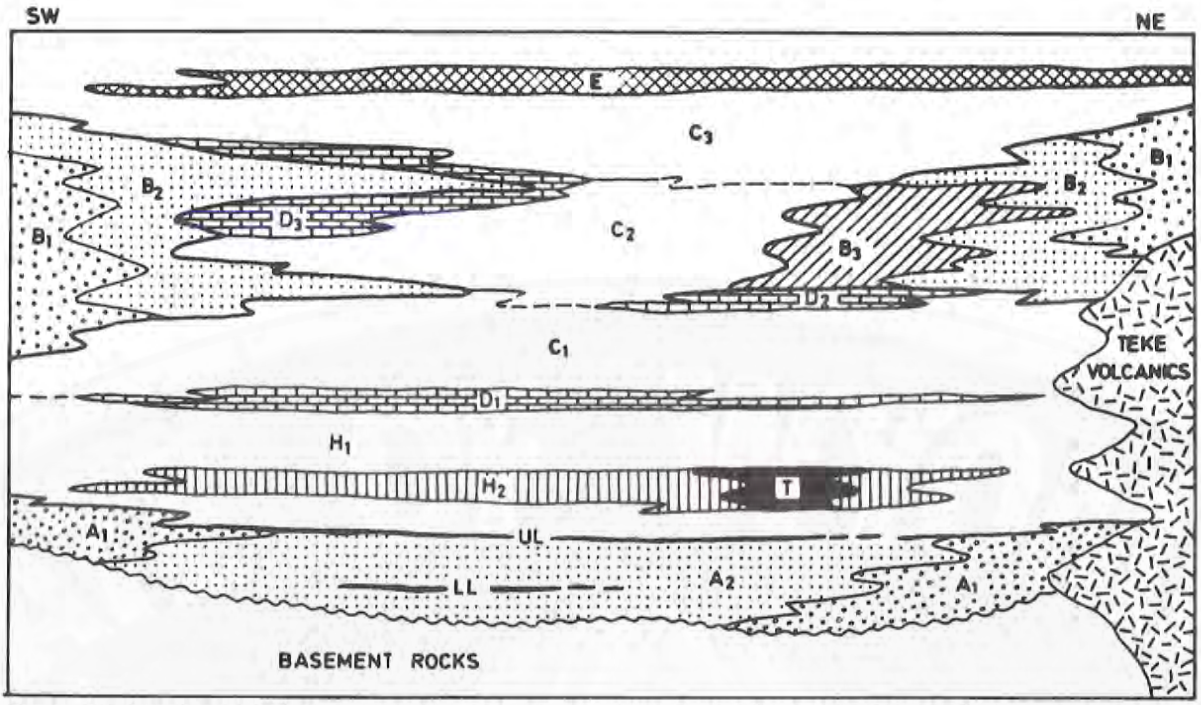


Figure 16. Simplified lithofacies associations and stratigraphic relationships in the Miocene Beypazari basin. Lower alluvial facies: volcaniclastic conglomerate lithofacies (A_1), sandstone-siltstone lithofacies (A_2), Lower Lignite (LL), Upper Lignite (UL). Lacustrine facies: dolomitic claystone lithofacies (H_1), bituminous shale and intraformational conglomerate lithofacies (H_2), trona (T), green claystone lithofacies (C_2, C_3), claystone-bedded chert-tuff alternation (C_1), olive-green evaporite (sulfates) lithofacies (E), and carbonate lithofacies (D_1, D_2, D_3). Upper alluvial facies: red conglomerate lithofacies (B_1), red sandstone lithofacies (B_2), and calcareous mudstone lithofacies (B_3).

The lower alluvial facies is characterized by volcanic sandstone and green siltstone beds (Coraklar Formation) exposed north of Cayirhan (**Figures 3** and **4**). The lignite deposits of Cayirhan district occur in the lower and upper parts of this facies. The northeastern edge of the facies is represented by volcaniclastics derived from the Teke Volcanics. The facies thickens in the subsurface to more than 200 m as found in exploratory drill holes for lignite. The thickness of the facies is about 80 m in the Koyunagili district of the basin (**Figure 2**).

Rocks of the lower alluvial facies were deposited in alluvial fans and subenvironments of a braided river system during the first sedimentation phase, which began in the late middle Miocene (**Figure 4**). The lower lignite beds formed in well-drained swamps; lignite distribution was controlled by braided channels. Following deposition of the lower lignite, the basin filled rapidly with volcaniclastics and flood sediments from adjacent basement rocks. At the end of this stage, the basin was occupied by a shallow lake surrounded by swamps and mud flats where the upper lignite beds were deposited. The lignites indicate a widespread forest-moor environment with a moist, subtropical climate.

Approximately 600 m of green claystone and carbonate rocks that crop out in the basin represent the most extensive suite of the lacustrine facies (**Figure 4**). The lower part of the lacustrine facies (Hirka Formation), including trona and bituminous shale deposits, accumulated along the depositional axis, which was situated in a southwest-northeast direction across the basin.

Red conglomerate and fine-grained sandstone beds represent the upper alluvial facies and reach maximum thickness at the southwestern and northeastern margins of the basin. The beds thin toward the basin center. The facies grades laterally into the green claystones of the lacustrine facies (**Figure 4**). The facies is represented by red, poorly consolidated conglomerate northeast of Beypazari, and channelform conglomerate and sandstone in the southwestern and northeastern parts of the basin.

The red-colored clastic rocks of the upper alluvial facies, and the green claystone, carbonate, and evaporite lithofacies of the lacustrine system present the most extensive rock suite in the Miocene Beypazari basin. These lithofacies were deposited both on the basin margins and in small, normal-fault-bounded inter-basins. During this sedimentation phase numerous rivers emptied into the subsiding basin creating a northeast-trending perennial lake. The green claystone-bedded chert-tuff succession was deposited in this lake environment. During the

initial and post-depositional phase of this rock succession, the lake twice changed into a siliceous carbonate lake environment. During deposition of the olive-green claystone, the lake water was hypersaline and dried up periodically. Ripple marks and desiccation cracks in these claystones indicate drying of the lake several times (**Figures 17** and **18**).

The upper part of the green claystone lithofacies is represented by lacustrine carbonates in the southwestern part of the basin. Preliminary investigations suggest that these carbonate rocks were deposited in a saline-alkaline lake environment. The salinity of the lake increased during the late Miocene and the lake became an extensive saline lake surrounded by saline mud flats (**Figure 4**). Thick gypsum and thin glauberite and tenardite layers were deposited in this environment.

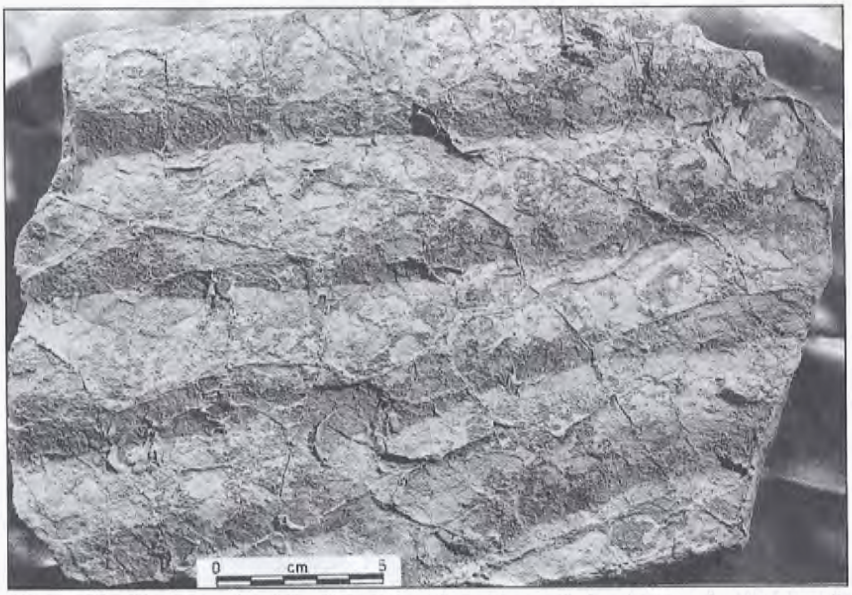


Figure 17. Photograph of the lower bedding plane of claystone indicating small-scale oscillation ripple mark cast of underlying claystone bed, Hirka Formation.



Figure 18. Polygonal mud-crack in claystone, Hirka Formation.

Trona deposit

Trona is associated with the Hirka Formation and alternates with bituminous shale, dolomitic claystones, and intraformational conglomerate (**Figure 5**). According to drill hole data, 33 trona beds with thicknesses generally between 40 cm and 2 m were deposited as two lensoid bodies within a 70- to 100-meter-thick zone of the Hirka Formation (**Figure 19**). The total cumulative thickness of trona beds is

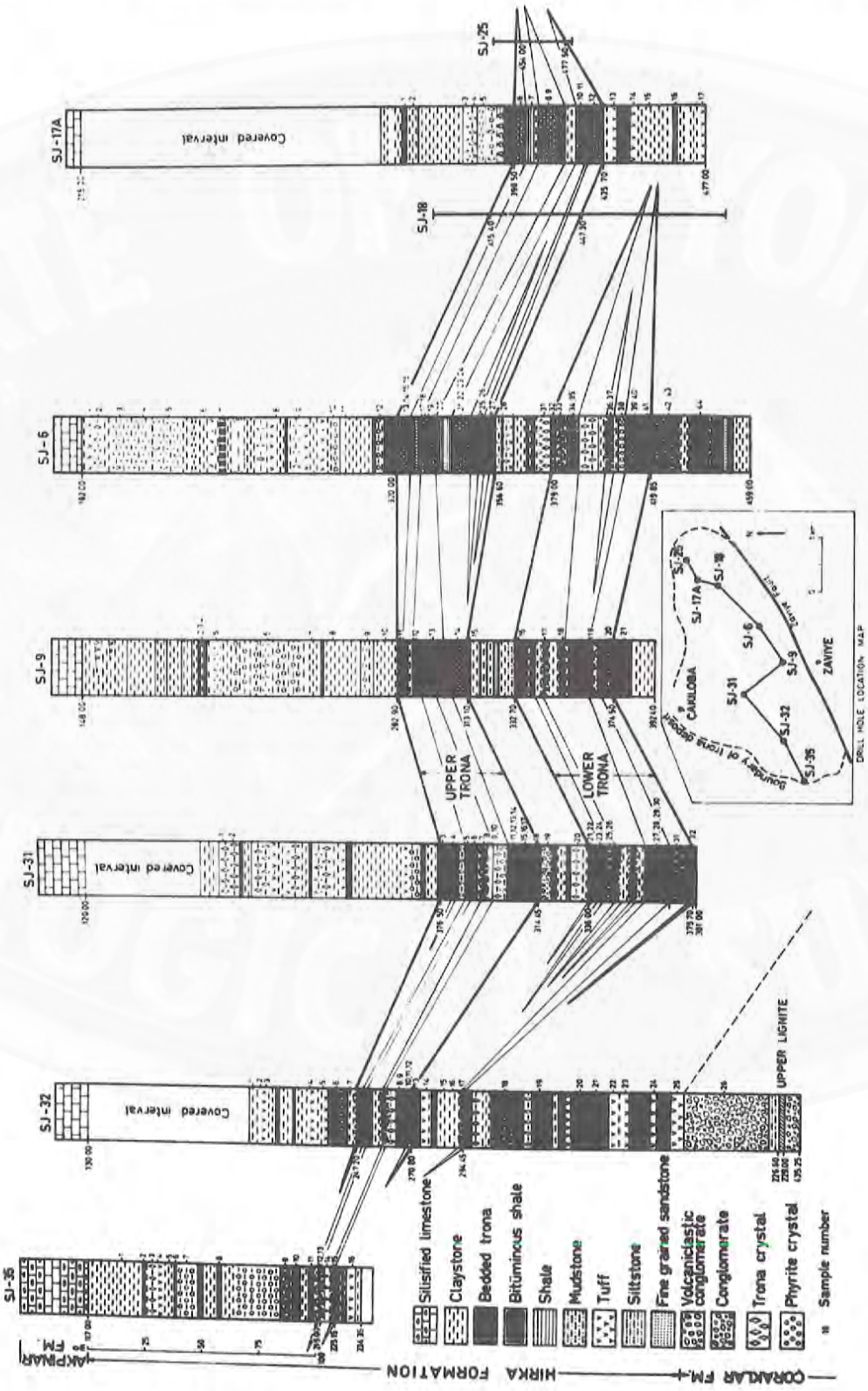


Figure 19. Northeast-southwest correlation diagram of lower and upper trona zones in drill holes, Beypazari trona deposit.

2.5 m in the marginal part and 34 m in the central part of the deposit. The dominant saline mineral is trona with minor amounts of nahcolite in the marginal parts of the deposit. Trace amounts of pirssonite and thermonatrite occur randomly within the deposit. The most common mineral associated with trona is dolomite. Clay minerals (mainly smectite and illite), zeolite, feldspar, opal-CT, quartz, and dolomite are dominant minerals of fine-grained rocks associated with the trona beds. The most likely sources of sodium for the trona are the tuffs interbedded with the fine-grained sediments, Neogene volcanics, and related springs.

Estimates based on borehole data indicate that the areal extent of the upper trona zone is approximately 8 km^2 whereas the areal extent of the lower trona zone is about 5.5 km^2 to the north of Zaviye village. Sixteen trona beds occur in the lower trona zone and 17 beds in the upper zone. The total thickness of the lower trona zone ranges from 40 to 60 m, and total thickness of the upper trona zone is about 40 m. Most of the trona beds contain brownish organic matter, pyrite, dolomite, and thin partings of normal sediment, all of which indicate that these beds are chemical deposits laid down on the lake floor during very low or ephemeral stages of the perennial saline lake. The interval between the lower and the upper trona zones varies from 30 to 35 m. The total cumulative thickness of all trona beds in both lenses ranges from 21 to 34 m in the central parts, and from 2.5 to 12 m in the marginal parts of the ore bodies. The thickness of individual trona beds in both trona zones usually ranges from 0.4 to 2 m, but varies between 2 to 3 cm and 11.5 m. Seventeen of these beds are considered to be significant because of their distinct thickness, as they are useful for correlations. Isopach maps of both trona zones are restricted by the Zaviye fault (**Figures 20** and **21**), which bounds the deposit on the south.

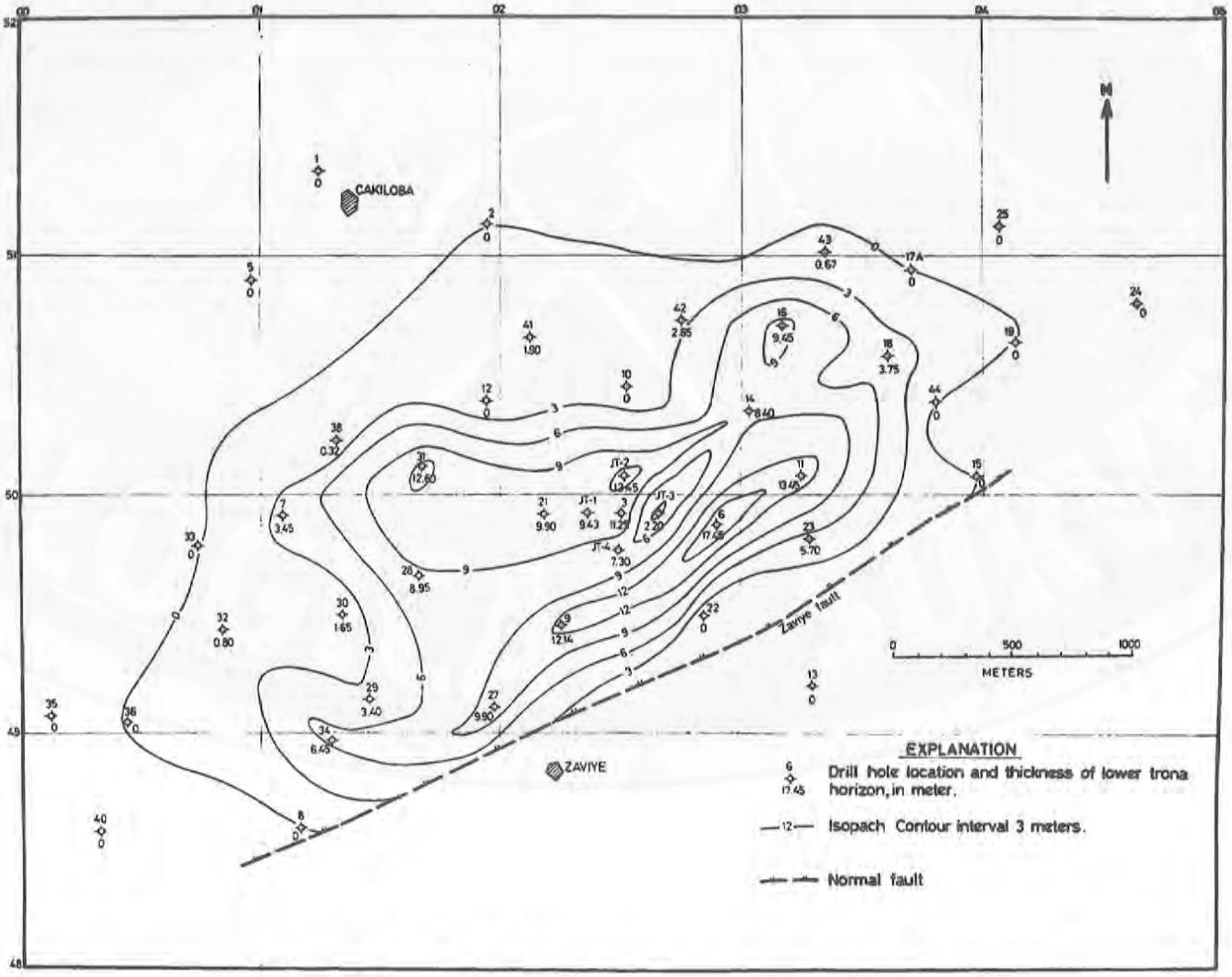


Figure 20. Isopach map of the lower trona zone, Beypazari trona deposit.

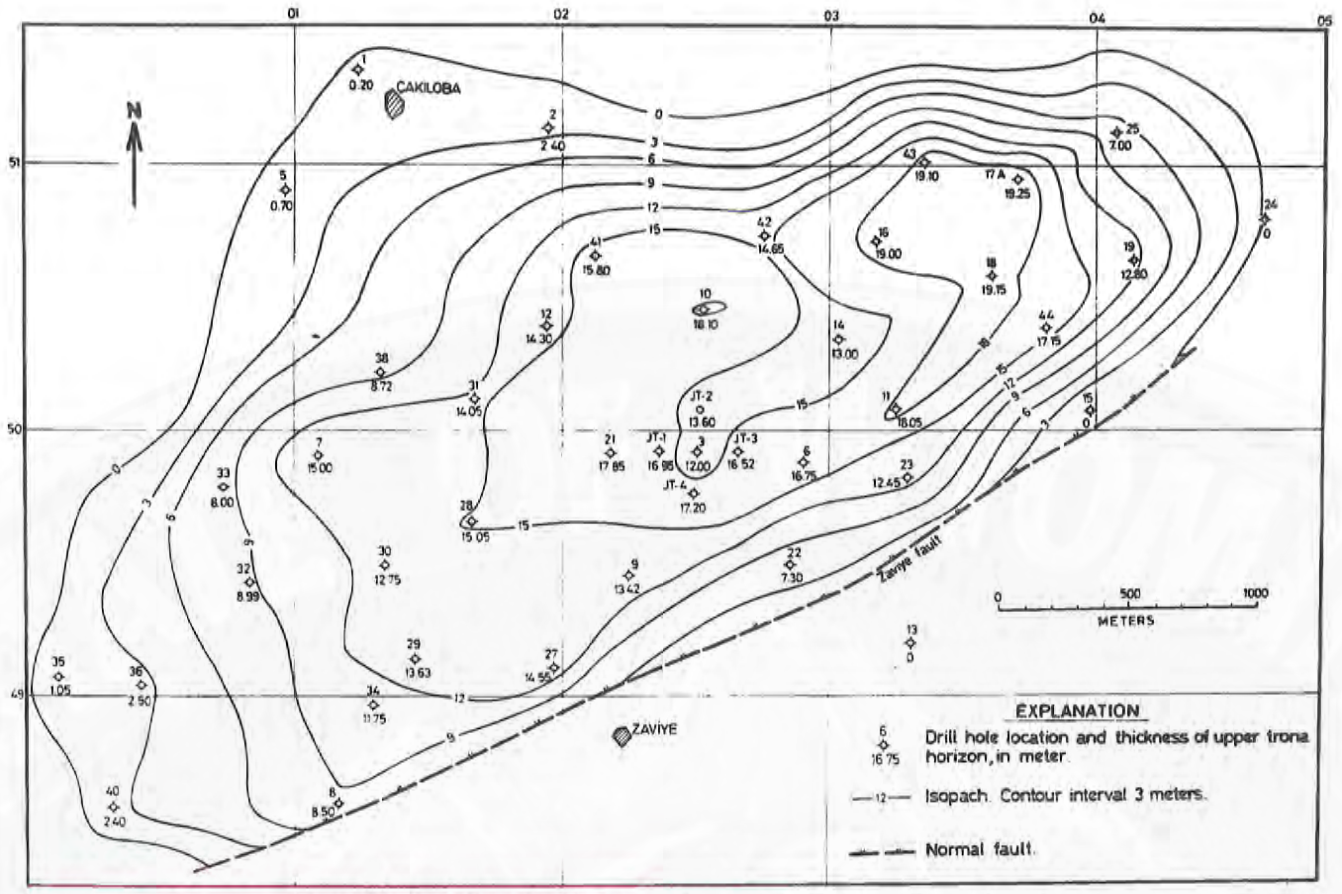


Figure 21. Isopach map of the upper trona zone, Beypazari trona deposit.

The lower trona zone occurs between the villages of Zaviye and Cakiloba and shows an elongated lensoidal shape in a NE-SW direction (**Figure 20**). The thickness of the lower trona zone varies in short distances as noted in the drill holes. Eight trona beds out of the 16 are significant in both thickness and areal extent. Lateral changes in thickness of the lower trona zone are very likely related to paleo-lake topography and geochemical conditions. This lower trona zone often contains brownish claystone on top of the trona and bituminous shale.

The upper trona zone has nine significant trona beds, three of which were formed when the basin was at its largest areal extent. These three beds are also the thickest and most uniform. The average thickness of the upper trona zone is 12 m. The upper trona zone shows a gradual lateral change of thickness between most of the drill holes. The upper trona zone was deposited under more stable conditions than those of the lower trona zone.

The trona beds grade laterally into dolomitic mudstones and claystones toward the edges of the basin. The subsurface position, lateral gradation, lateral thickness variations, the stratigraphic relationships between the lower and the upper trona zones, and the associated rock units are shown in **Figure 22**.

Structure

Structure contour maps of the lower and upper trona zones are shown in **Figures 23** and **24**. North of the Zaviye fault, a NE-SW trending syncline and anticline are noted (**Figure 22**). The Zaviye fault, which evidently acted as a growth fault during deposition of the trona and associated rocks, was formed as a result of the extensional tectonic regime which affected this region during early and middle Miocene. The synclinal and anticlinal structures in the trona field (**Figure 15**) developed from compression related to the movement of the North Anatolian fault during late Miocene and early Pliocene. On the structure contour map of the upper trona zone, a NW-SE trending monoclinal fold with a high-angle flank dipping south may be observed near Cakiloba (**Figure 24**).

The lower and upper trona zones were affected by the asymmetrical folding. The high angle flanks of these folds are generally inclined towards the south. In addition, this type of fold system suggests that com-

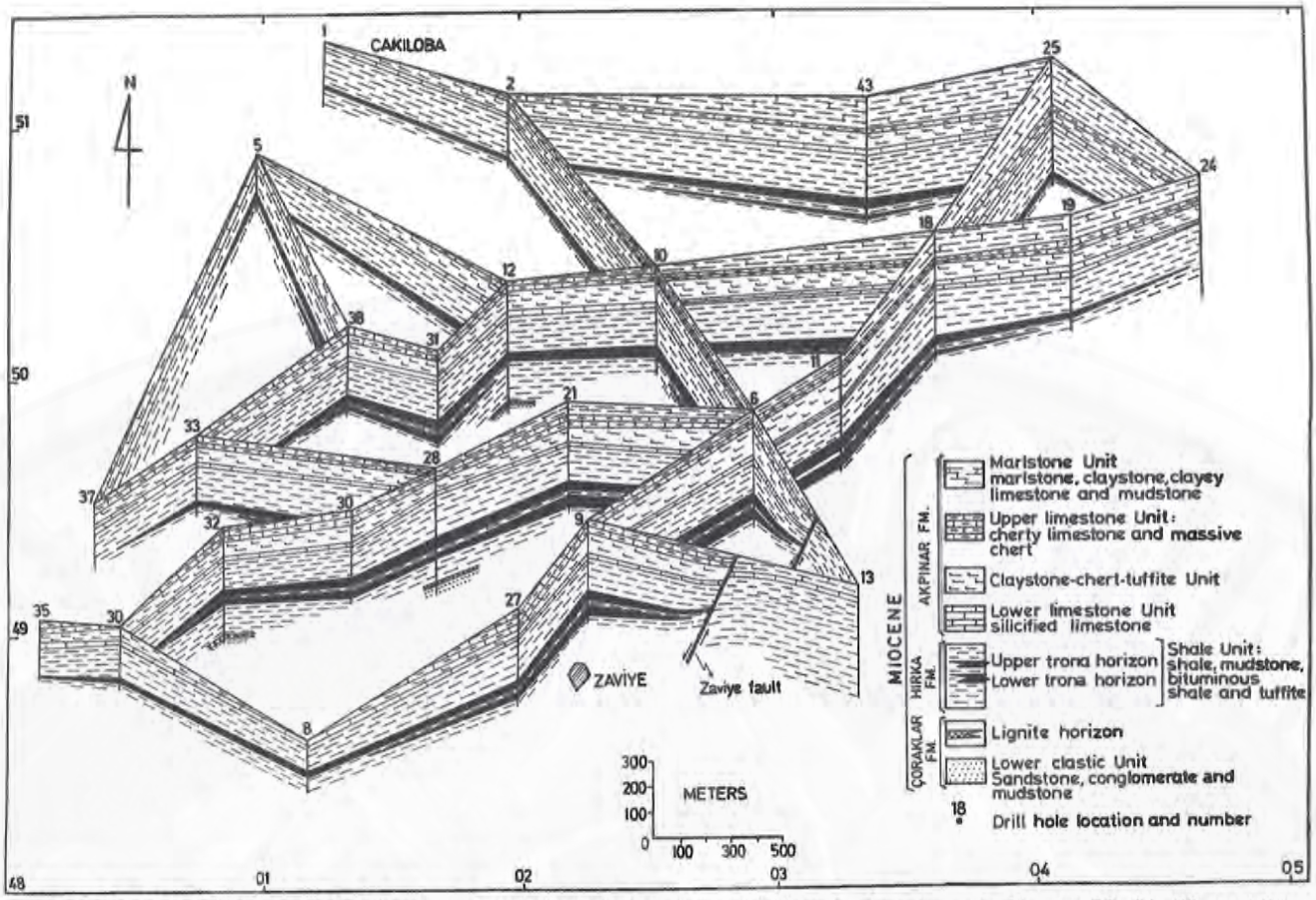


Figure 22. Panel diagram of the Beypazari trona deposit. Location of drill holes also shown in Figures 20, 21, 23, and 24.

pressional forces operated from north to south during and/or after trona deposition. These interpretations are confirmed by structural observations from other parts of the study area.

Mineralogy

The major mineral of the saline beds is trona. Minor amounts of nahcolite are found at the marginal parts of the deposit (**Figure 25**) and trace amounts of pirssonite and thermonatrite occur randomly within the deposit (**Table 3**). Neither shortite nor halite appears to be present. The trona crystals are generally white, massively bedded, and exhibit a clear crystalline columnar texture, but sometimes it seems grayish due to the presence of impurities. Trona occurs both as massive forms and as separate crystals in the claystones and shales (**Figures 25** and **26**). In the associated rocks, scattered euhedral trona crystals and crystal aggregates are present (**Figure 26**). Chemical analysis of trona and nahcolite samples are given in **Table 4**. Dolomite was estimated as the second major mineral of the trona core samples (**Figure 27**). In the transition zone between the Coraklar Formation and the Hirka Formation, epsomite, hexahydrite, and starkeyite are common. In the uppermost rock unit of the Miocene sequence, sulfates become abundant; dominantly gypsum, and less frequently, bloedite and rarely thenardite and glauberite, form thick sulfate deposits.

Zeolitization, dolomitization, and chloritization, which probably occurred shortly after deposition, or during diagenesis, are rather common within rocks associated with the trona deposit. The mineral components of the associated fine-grained sedimentary rocks of the trona beds consist of, in decreasing order of abundance, clay minerals, dolomite, calcite, analcime, K-feldspar, plagioclase, quartz, opal-CT, and α-quartz. The bituminous shales enclosing the upper and lower trona zones are composed of analcime, dolomite, calcite, opal-CT, and quartz, K-feldspar, and plagioclase (**Table 3** and **Figure 28**). Dolomite and K-feldspar are abundant in all units of the Hirka Formation. The bituminous shales of the Neogene sequence in Western Anatolia consist mainly of analcime, heulandite, clinoptilolite, illite, kaolinite, K-feldspar, opal-CT, and quartz, as shown by Inci (1983) and Helvaci and others (1993).

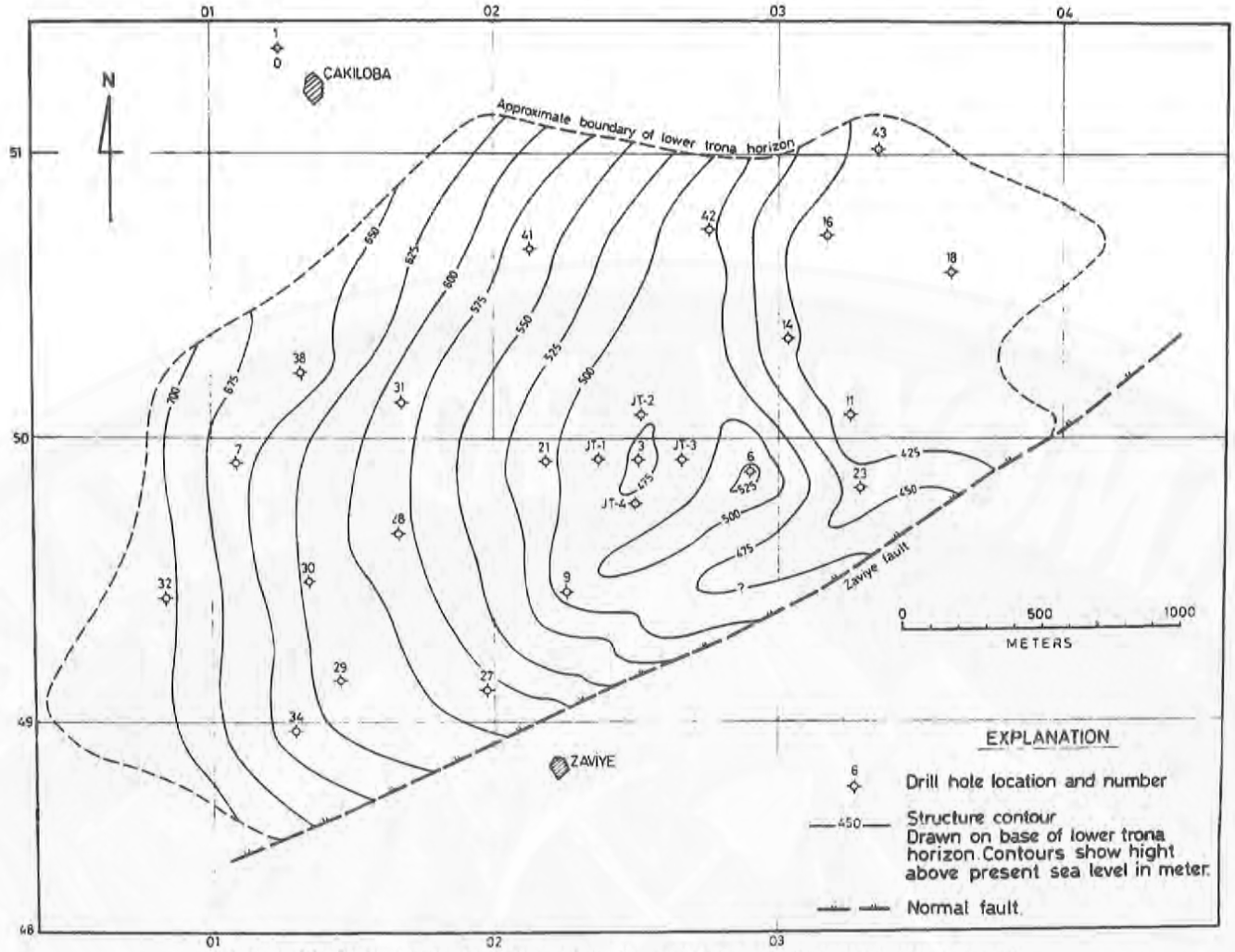


Figure 23. Structure contour map of the lower trona zone, Beypazari trona deposit.

The carbonate fractions of the rocks associated with the trona deposits are dominantly dolomite, frequently calcite, and less commonly magnesite, and collophane, the tuff fractions are dominantly zeolites (analcime, wairakite, natrolite, and clinoptilolite). K-feldspar (high-sanidine, microcline, and adularia), plagioclase (albite and anorthite), quartz, clays, frequently muscovite, biotite, and amphibole (mainly hornblende), and trace amounts of lepidolite, searlesite, apatite, tourmaline, and epidote are found (**Table 3**).

Mg, K, and K-montmorillonite, illite, saponite, and chlorite are the only clay minerals identified in all of the samples studied. Illite, only a minor component, is distributed randomly. Chlorite is continuously distributed within the deposits and is relatively abundant near or within the tuff zone (**Table 3**).

Associated clay minerals are trioctahedral smectite and dioctahedral illite. The exchangeable cation interlayer of the smectite is Ca^{2+} (Helvaci and others, 1988). According to these authors, clay minerals display a vertical zonation. For example: illite (dominant) + moderately crystallized smectite → well crystallized smectite (dominant) + illite → illite (dominant) + illite, which is indicative of changing geochemical conditions in the Miocene lake (i.e., more dilute or concentrated brine). Helvaci and others (1988) concluded that the smectite, as well as other authigenic minerals, formed by weathering of volcanic glass in an alkaline lacustrine environment.

Chemistry

Variations in the chemistry of trona and nahcolite from Beypazari are interpreted to reflect the different phases of concentration that occurred in the perennial saline lakes. The chemical composition of trona and nahcolite is listed in **Tables 4, 5, 6,** and **7**. The Na_2O content of the trona ranges from 37.2 to 41.78%, and that of the nahcolite from 29.73 to 35.76% (**Table 4**).

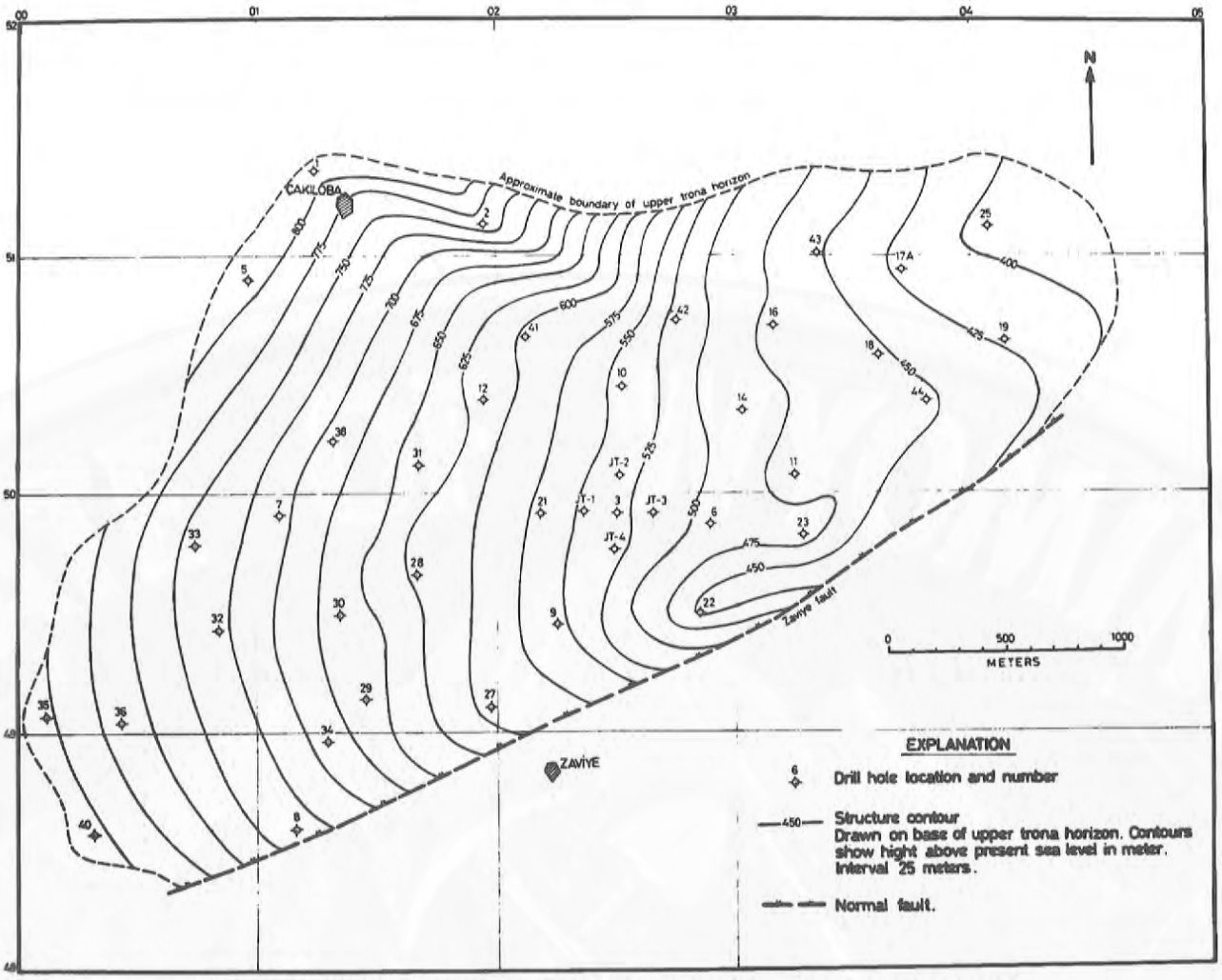


Figure 24. Structure contour map of the upper trona zone, Beypazari trona deposit.



Figure 25. Massive trona and nahcolite samples taken from drill hole 22 (SJ-22), 371 m below the surface, Beypazari trona deposit.

Table 3. Carbonates and other minerals occuring in the Beypazari trona deposit of the Hirka Formation. The predominant minerals are underlined.

SULFIDES

Pyrite FeS_2

OXIDES

Quartz SiO_2
α-Quartz SiO_2
Opal-C.T.
Hematite Fe_2O_3

CARBONATES

Nahkolite $NaHCO_3$
Trona $Na_2CO_3 \cdot NaHCO_3 \cdot H_2O$
Termonatrite $Na_2CO_3 \cdot H_2O$
Pirssonite $Na_2CO_3 \cdot CaCO_3 \cdot 2H_2O$
Brugnatelite $Mg_6FeCO_3(OH)_{13} \cdot 4H_2O$
Calcite $CaCO_3$
Dolomite $CaCO_3 \cdot MgCO_3$
Magnesite $MgCO_3$

SULFATES

Gypsum $CaSO_4 2H_2O$
Hexsahidrite $MgSO_4 \cdot 6H_2O$
Epsomite $MgSO_4 \cdot 7H_2O$
Bloedite $MgSO_4 \cdot Na_2SO_4 \cdot 4H_2O$

SILICATES

Clay minerals - Simectite(Saponite)
Illite
Chlorite
Loughlinite $Na_2Mg_3Si_6O_{15} \cdot 8H_2O$
Searlesite $NaBSi_2O_6 \cdot H_2O$
Hornblend $NaKCaMgFeAl_2SiAlO(OH)$
Tourmaline $NaMg_3Al_6B_3Si_6O_{27}(OH)_4$
Epidote $Ca_2(Al,Fe)_3Si_3O_{12}(OH)$
Biotite $K(Fe,Mg)_3AlSi_3O_{10}(OH)_2$
Muscovite $KAl_2Si_3AlO_{10}(OH)_2$
Lepidolite $K(LiAl)_3(Al,Si)_4O_{10}(OH,F)_2$
Phlogopite $KMg_3(Si_3AlO_{10})F_2$
Ortoclase $KAlSi_3O_8$
Microcline $KAlSi_3O_8$
High-sanidine $KAlSi_3O_8$
Albite $NaAlSi_3O_8$
Analsime $NaAl(SiO_3)_2 \cdot H_2O$
Natrolite $Na_2Al_2Si_3O_{10} \cdot 2H_2O$
Heulandite $CaAl_2Si_7O_{18} \cdot 6H_2O$
Clinoptilolite $NaCaKMgAlOSi \cdot 7H_2O$

PHOSPHATES

Apatite $Ca_5(PO_4)_3(OH,F,Cl)$
Collophane $Ca_5(PO_4)_3CO_3 \cdot H_2O$



Figure 26. Massive and disseminated trona minerals taken from drill hole 35 (SJ-35), 219.70 m below the surface, Beypazari trona deposit.

The soda minerals are high-grade ores reaching up to 99% in some beds (**Tables 6** and **7**). The Beypazari trona deposit contains trace amounts of S, Cl, Sr, As, and B.

Mg and Si are present in evaporitic and diagenetic minerals (e.g., as Mg in dolomites) and in the claystone, mudstone, bituminous shale, and tuff fractions, but mainly in the tuffs. Al and Fe oxides are present only in the clays, bituminous shales, and tuffs (e.g., Fe in pyrites). During diagenesis, chemical exchange between evaporites, clays, tuffs, and bituminous shales took place and led to the formation of diagenetic and authigenic minerals, such as pyrite, dolomite, K-feldspar, and analcite.

Sodium-carbonate minerals were chemically precipitated from brines, which may have been partly derived from thermal springs and partly from surface streams and underground waters. Major elemental compositions of the nearby volcanics and the granites were given in **Tables 1** and **2**. All the rocks are enriched in sodium relative to average values for these rock types. Surface streams and underground waters may have carried dissolved Na, Mg, HCO_3, and CO_3 into the basin from weathering of rocks exposed in the catchment area, but the major source of dissolved ions in the perennial saline lake is thought to be from leaching of the Neogene volcanics by thermal springs associated with the volcanic activity in the area, and by surface streams and underground waters.

In the system Na_2O-H_2O-CO_2, which contains the main chemical components of some saline lakes, water activity is a very important factor in determining the stability limits of mineral phases. In addition, partial pressure of CO_2 (Pco_2) is also one of the variables of the system. In ancient and present lakes, nahcolite, trona, natron, thermonatrite, wegscheiderite ($Na_2CO_3 \cdot 7H_2O$), and $Na_2CO_3 \cdot 10H_2O$ can be present as mineral phases. In order to determine the chemical conditions of ancient lakes (such as Na^+ activity, pH, and Pco_2 of the deposit), phase diagrams drawn with respect to different variables are very useful and descriptive.

Equilibrium activity diagrams and partial pressure diagrams were calculated for soda minerals of the Beypazari trona deposit in the Na_2O-H_2O-CO_2 system at 25°C and 1 atmosphere pressure, using available thermodynamic data (Wagnam and others, 1982). Phase diagrams indicate that all possible soda minerals except wegscheiderite are stable at given conditions (Birsoy, 1993).

For mineral phases in the Na_2O-H_2O-CO_2 system, 21 defining equations were derived for the activity diagram in **Figure 29**, and plotted with log $[Na^+]/[H^+]$ versus log $[H_2O]$ at 25°C and 1 bar pressure. All phases except wegscheiderite are stable. During deposition, the activity ratio $[Na^+]/[H^+]$ was lower at the marginal part of the deposit than at the central part of the deposit. Local increase of the activity ratio $[Na^+]/[H^+]$ allowed thermonatrite to coexist with trona, which means the central part of the lake had a

Table 4. Chemical analyses in weight percent, of 16 trona and three nahcolite samples collected from drill holes in the Beypazari trona deposit.

	Trona Samples																Nahcolite Samples		
Oxide (%)	SJ6 -13	SJ6 -16	SJ6 -18	SJ6 -23	SJ6 -26	SJ6 -28	SJ6 -35	SJ6 -40	SJ17A -6	SJ17A -8	SJ17A -9	SJ31 -5	SJ31 -16	SJ32 -8	SJ9 -14	SJ9 -17	S22 -14	S35 -13	S35 -15
SiO_2	0.11	0.43	0.66	0.26	0.53	1.65	1.92	1.04	2.43	1.64	0.70	1.25	1.49	0.39	0.79	1.30	3.91	5.53	2.08
Al_2O_3	0.09	0.00	0.06	0.00	0.02	0.40	1.13	0.06	0.28	0.09	0.09	0.06	0.73	0.04	0.13	0.17	0.77	0.61	0.03
$^*Fe_2O^T_3$	0.01	0.00	0.02	0.04	0.20	0.23	0.07	0.23	0.28	0.09	0.04	0.01	0.12	0.02	0.02	0.08	0.32	0.32	0.12
MgO	0.35	0.46	0.54	0.57	0.41	2.08	1.15	1.08	1.70	1.00	0.73	0.37	1.29	0.32	0.76	0.90	2.85	2.48	1.18
CaO	0.00	0.15	0.04	0.11	0.08	1.21	0.29	0.60	0.70	0.36	0.36	0.01	0.17	0.00	0.24	0.38	1.55	3.96	0.20
Na_2O	40.51	41.78	40.08	40.24	39.74	37.21	39.51	39.54	38.37	39.32	39.03	39.83	39.15	40.03	39.57	39.64	33.18	29.73	35.76
K_2O	0.01	0.01	0.02	0.03	0.04	0.12	0.06	0.06	0.17	0.06	0.02	0.03	0.43	0.01	0.04	0.06	0.16	0.33	0.08
SO_3	0.42	0.15	0.61	0.30	0.24	0.57	0.57	0.32	0.08	0.13	0.35	0.52	0.52	0.79	0.12	0.21	0.30	0.08	0.19
CO_2	28.39	29.67	28.46	29.28	28.22	29.63	28.05	28.07	27.25	27.92	29.01	28.28	29.26	28.25	28.98	29.01	24.01	27.00	25.53
H_2O	29.62	27.50	29.11	29.04	29.37	26.87	28.34	28.54	28.04	28.78	28.80	29.06	27.51	29.30	28.88	28.48	32.23	29.83	35.07
TOTAL	99.51	100.51	99.60	99.87	98.85	100.07	100.09	99.54	99.30	99.39	99.13	99.42	100.67	99.15	99.53	100.23	99.28	99.87	100.24

$^*Fe_2O^T_2 : Fe_2O_3 + 1.111 \times FeO$

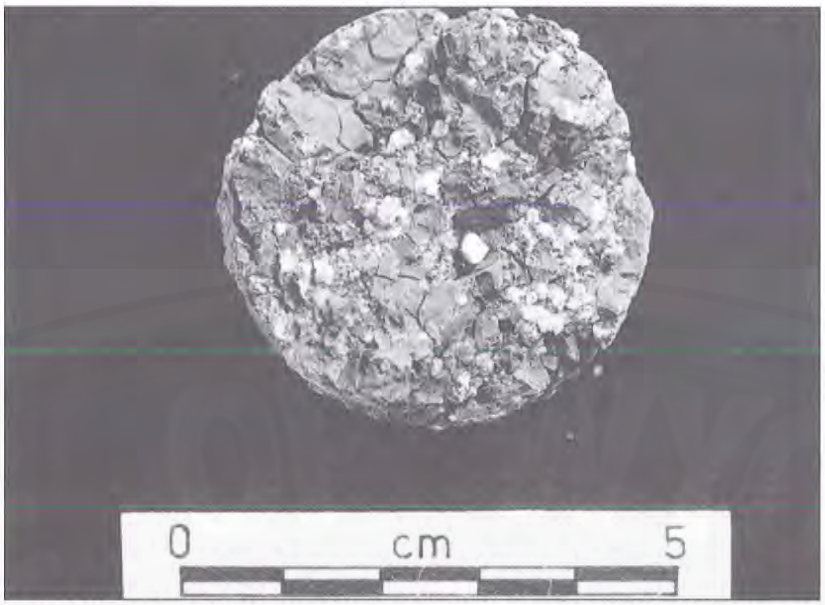


Figure 27. Authigenic dolomite crystals occurring in the claystone-mudstones of the Hirka Formation, Beypazari trona deposit.

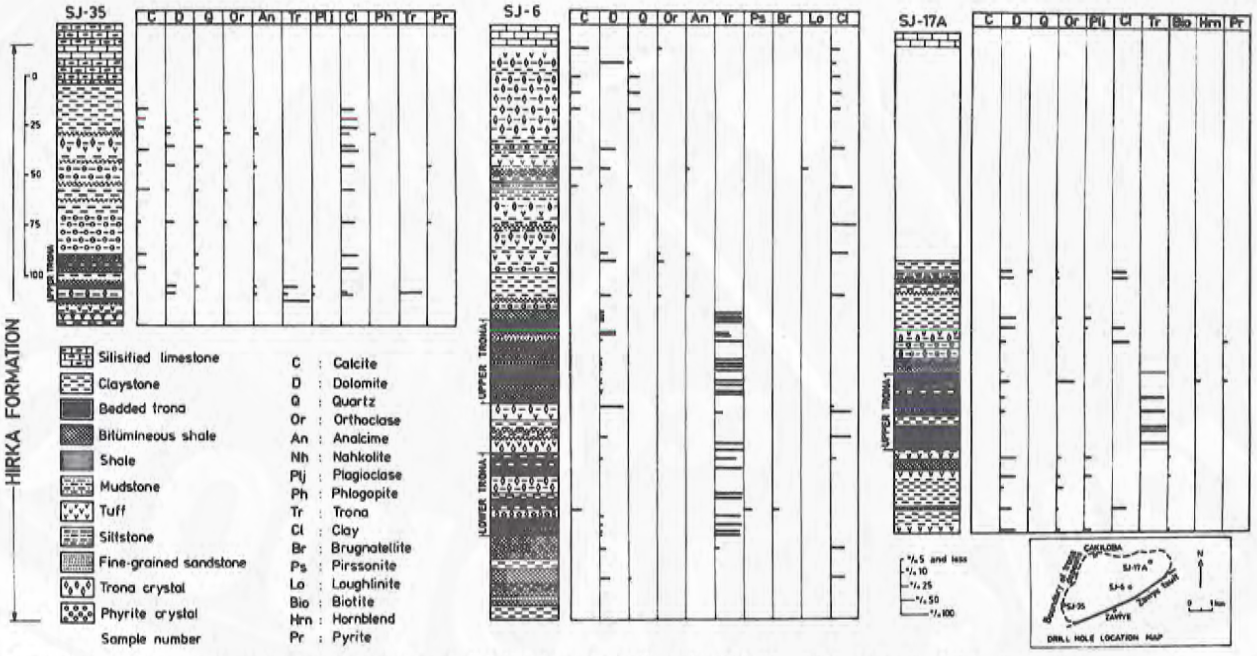


Figure 28. Mineral assemblages and mineral distributions in drill holes SJ-35, SJ-6, and SJ-17A, Beypazari trona deposit.

higher pH value than the marginal part of the lake during soda mineral deposition.

In the system Na_2O-H_2O-CO_2, six mineral phases out of seven are stable (**Figure 30**), and again, wegscheiderite is a metastable phase. Partial pressure of CO_2 in the atmosphere during the deposition of the lower trona horizon was approximately $10^{-2.5}$ at the marginal part of the lake and from 10^{-3} to 10^{-6} in the central part (when $P_{H_2O} = 10^{-2}$) (Birsoy, 1993). The middle Miocene atmosphere had higher partial pressure of CO_2 than the present day atmosphere. During deposition of the upper trona zone, however, the partial pressure of CO_2 was less than that during deposition of the lower trona zone, as nahcolite is not present in the lower trona beds.

Table 5a. Metal oxide concentrations in water leach core samples from the Beypazari trona deposit, Turkey. % = weight percent; ppm = parts per million.

Sample I.D	Depth of sample	Na_2O (%)	CaO (ppm)	Fe_2O_3 (ppm)	MgO (ppm)	K_2O (ppm)
SJ6-19	333.50 m	38.6	50	< 10	104	78
SJ6-27	355.00 m	36.2	200	< 10	116	44
SJ6-32	379.50 m	39.0	100	< 10	48	26
SJ6-33	383.00 m	35.2	90	44	102	22
SJ7-5	284.75 m	40.6	102	18	135	22
SJ9-19	366.70 m	41.4	78	< 10	146	19
SJ17A-6	398.50 m	39.2	100	18	280	66
SJ17A-10	425.00 m	40.2	68	< 10	90	41
SJ22-11	371.00 m	38.6	122	12	72	24
SJ22-13	380.00 m	40.2	60	16	170	38
SJ31-13	305.50 m	38.6	100	18	50	24
SJ31-18	314.90 m	41.4	72	< 10	110	14
SJ31-29	366.00 m	38.2	230	< 10	195	37
SJ32-10	267.55 m	37.8	88	16	184	27
SJ35-15	224.80 m	34.0	100	15	96	38

Table 5b. Metal oxide concentrations in solid core samples from the Beypazari trona deposit, Turkey. % = weight percent; ppm = parts per million.

Sample I.D	Depth of sample	As (ppm)	CaO (%)	Fe_2O_3 (%)	K_2O (ppm)	MgO (ppm)	Na_2O (%)
SJ6-19	333.50 m	1	1.3	0.087	290	2.6	37.1
SJ6-27	355.00 m	1	0.78	0.046	220	0.74	41.2
SJ6-32	379.50 m	1	0.24	0.018	92	0.34	44.6
SJ6-33	383.00 m	1	0.38	0.015	52	0.56	45.3
SJ7-5	284.75 m	1	0.33	0.020	68	0.43	45.8
SJ9-19	366.70 m	1	0.02	0.007	63	0.21	46.0
SJ17A-6	398.50 m	2	0.50	0.056	210	0.94	42.3
SJ17A-10	425.00 m	2	0.07	0.006	73	0.09	46.9
SJ22-11	371.00 m	2	0.14	0.016	87	0.18	47.3
SJ22-13	380.00 m	2	0.26	0.029	170	0.53	45.7
SJ31-13	305.50 m	1	0.56	0.019	170	0.54	40.9
SJ31-18	314.90 m	< 1	0.04	0.003	50	0.04	41.4
SJ31-29	366.00 m	< 1	0.32	0.021	140	0.55	40.6
SJ32-10	267.55 m	< 1	0.06	0.009	88	0.10	43.3
SJ35-15	224.80 m	3	0.25	0.064	290	0.84	35.3

Table 6. Concentration of ores and impurities (from titration) in selected Beypazari trona and nahcolite samples, Beypazari basin, Turkey. % = weight percent; ppm = parts per million.

Sample I.D	Depth of sample	Trona (%)	Nahcolite (%)	Insols (%)	NaCl (%)	Total (%)	Na_2SO_4 (ppm)	Ba (ppm)	B (ppm)	Li (ppm)	P (ppm)	Sr (ppm)	Mn (ppm)	Ti (ppm)
SJ6-19	333.50 m	86.0		11.7	0.07	97.8	< 25	21	436	46	35	78	45	55
SJ6-27	355.00 m	93.0		5.6	0.04	98.6	< 25	17	816	34	37	42	10	28
SJ6-32	379.50 m	98.0		1.1	0.03	99.1	< 25	< 10	379	13	< 10	< 10	19	< 10
SJ6-33	383.00 m	97.3		1.4	0.03	98.7	< 25	13	339	14	171	27	< 10	10
SJ7-5	284.75 m	98.0		1.0	0.03	99.0	< 25	< 10	315	15	124	22	14	< 10
SJ9-19	366.70 m	98.7		0.2	0.03	98.9	< 25	< 10	301	21	11	< 10	< 10	< 10
SJ17A-6	398.50 m	95.8		3.3	0.04	99.1	< 25	< 10	296	37	29	29	13	33
SJ17A-10	425.00 m	99.3		0.1	0.03	99.4	< 25	< 10	274	15	46	< 10	< 10	< 10
SJ22-11	371.00 m	99.2		0.4	0.03	99.6	< 25	< 10	239	16	65	< 10	< 10	< 10
SJ22-13	380.00 m	95.9		2.7	0.03	98.6	< 25	12	256	31	22	18	< 10	19
SJ31-13	305.50 m	95.9		3.0	0.03	98.9	< 25	< 10	231	20	26	30	21	< 10
SJ31-18	314.90 m	100.0		0.1	0.03	100.1	< 25	< 10	212	10	18	< 10	< 10	< 10
SJ31-29	366.00 m	97.1		2.0	0.03	99.1	< 25	< 10	239	28	20	11	< 10	20
SJ32-10	267.55 m	99.3		0.0	0.03	99.4	< 25	< 10	197	14	43	< 10	< 10	< 10
SJ35-15	224.80 m	14.6	78.2	4.4	0.03	97.2	< 25	< 10	157	42	52	14	< 10	31

Table 7. Analyses of trona ore concentrations and impurities in samples from trona beds 11 and 15 in different drill holes. Beypazari trona deposit. Surface elevations in meters above mean sea level; depths in meters below surface.

Drill hole	Surface elevation	Trona bed	Top depth	Bottom depth	Thickness	% Trona	% Other
SJ-32	998.66	11	261.20	265.06	4.40	93.66	6.34
SJ-10	890.84	11	344.15	348.95	4.80	94.00	6.00
		15	319.40	323.15	3.75	93.49	6.51
SJ-17A	854.71	11	425.10	427.90	2.80	94.27	5.73
		15	397.95	402.85	4.90	86.03	13.97
SJ-6	847.92	11	342.85	348.30	5.45	95.45	4.55
		15	320.75	325.55	4.80	94.73	5.27
SJ-9	868.67	11	299.35	304.65	5.30	87.75	12.25
		15	282.90	285.65	2.75	60.53	39.47

Lithofacies and depositional environments of the Hirka Formation and the trona deposit

Lithofacies

The Hirka Formation consists of dolomitic claystone, bituminous shale, trona, and intraformational conglomerate, which were deposited in a lacustrine depositional system (**Figures 5, 31,** and **32**).

Dolomitic claystone lithofacies

This lithofacies (H_1 in **Figure 16**) consists mainly of light green, thick-bedded, partially laminated claystone and minor amounts of mudstone (**Figure 5**). Dolomite is present as euhedral authigenic crystals and as microcrystalline matrix in the claystone and mudstone (**Figure 27**). X-ray diffraction patterns of these fine-grained rocks show the dolomite to be the second most abundant mineral constituent (Helvaci and others, 1988, 1989). Framboidal pyrite is common in the claystone beds (**Figure 9**). Analcitized thin volcanic tuff and green siltstone layers are minor constituents of this lithofacies. Remarkable sedimentary structures are thinly parallel and convolute laminations. Chemical analyses of the claystone and mudstone are given in **Table 8**.

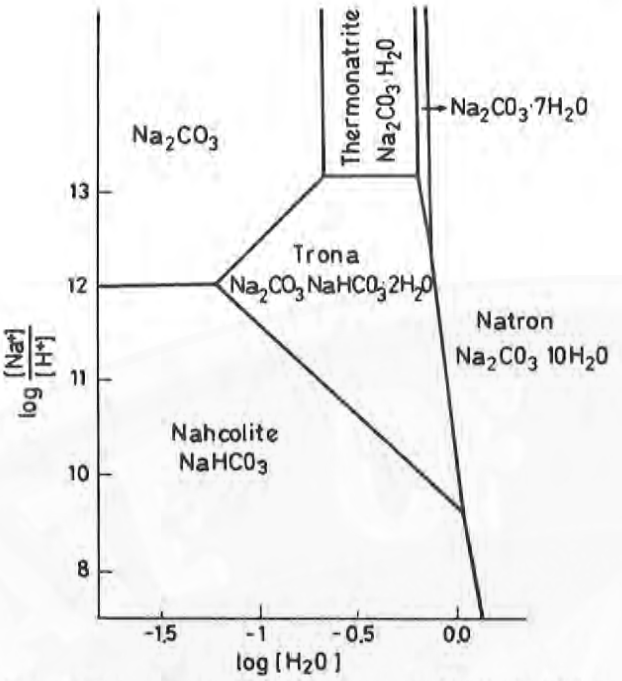


Figure 29. Activity diagram for the system Na_2O-H_2O-CO_2 at 25°C and 1 atmosphere expressed as functions of $[Na^+]/[H^+]$ and log $[H_2O]$ (after Birsoy, 1993).

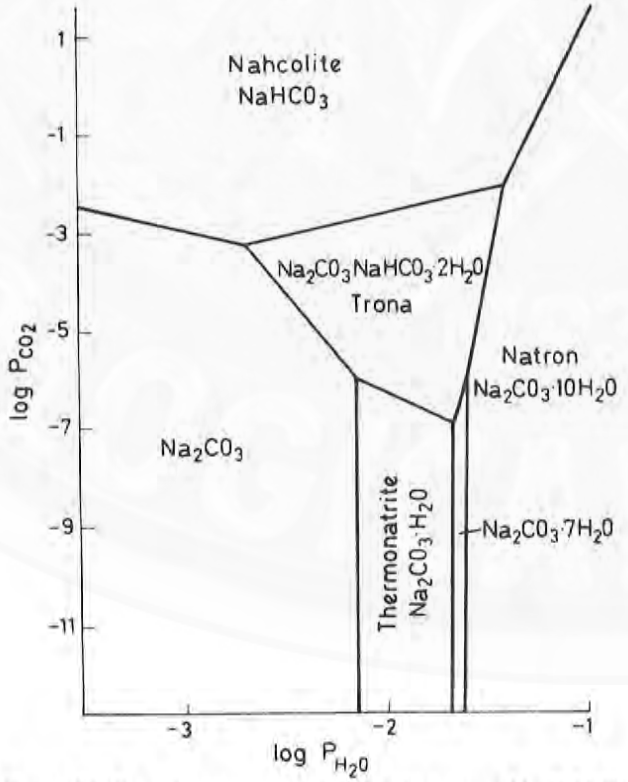


Figure 30. Partial pressure diagram for the system Na_2O-H_2O-CO_2 at 25°C and 1 atmosphere pressure as functions of P_{H_2O} and P_{CO_2} (after Birsoy, 1993).

Bituminous shale lithofacies

The bituminous shale lithofacies (H_2 in **Figure 16**) consists of two main rock types: thinly laminated, organic-rich, dark-gray and brown bituminous shale, and brecciated bituminous shale. The content of organic matter in the dark and brown bituminous shale is about 13%, and the upper calorific values range from 600 to 1140 kcal/kg (Biron and others, 1979).

Brecciated bituminous shale has been observed in trona exploration drill cores (**Figures 5** and **32**). A similar rock type has also been noted by Bradley (1931) and Eugster and Hardie (1975) in the Green River Formation in the western United States. The associated rocks of the bituminous shale lithofacies are thin interlayers of dolomitic limestone, shale, and volcanic tuff. Chemical analyses of the bituminous shale and volcanic tuffs are given in **Tables 9** and **10** respectively.

Intraformational conglomerate lithofacies

This lithofacies is represented by interclastic conglomerate composed of tuff, limestone, bituminous shale, and dolomite clasts derived from the underlying or associated rock units. The conglomerate exhibits six different layers ranging from about 80 cm to 10 m in thickness at the coal-mine tunnel section near Cayirhan (**Figure 5**, section G-2001). Large- and small-scale slumps, slides, and fining-upward graded bedding are common structures. The lower contact of the conglomerate beds is usually erosional and the upper contact is gradational with green claystone, including the small bituminous shale clasts (**Figure 5**, details c and d).

The intraformational conglomerate is also associated with trona in the northeastern part of the basin (**Figure 5**, section AR-1). The dominant clasts of the conglomerate are about 2 cm in size and composed of tuff and limestone and minor amounts of trona, dolomite, and bituminous shale, all supported by a tuffaceous matrix (**Figure 32**).

Environmental and depositional interpretation

The bituminous shale, trona, dolomitic claystone, and intraformational conglomerate of the Hirka Formation covers an area of about 500 km^2 in the Miocene Beypazari basin. The thickest sequence is present on the north side of the Davutoglan fault near Zaviye. An ephemeral salt lake or very small closed lake is visualized as a trona-brine body with a nor-

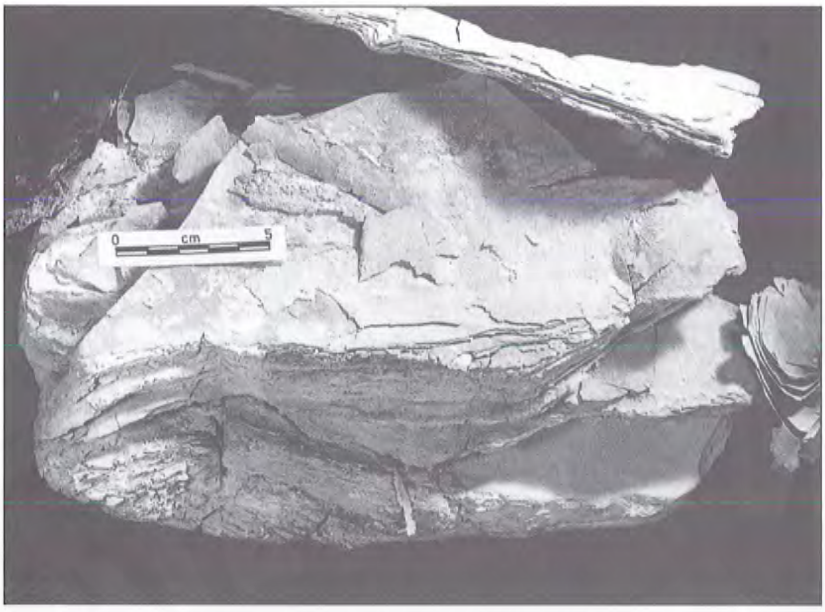


Figure 31. Photograph of bituminous shale from the Hirka Formation, Beypazari trona deposit.

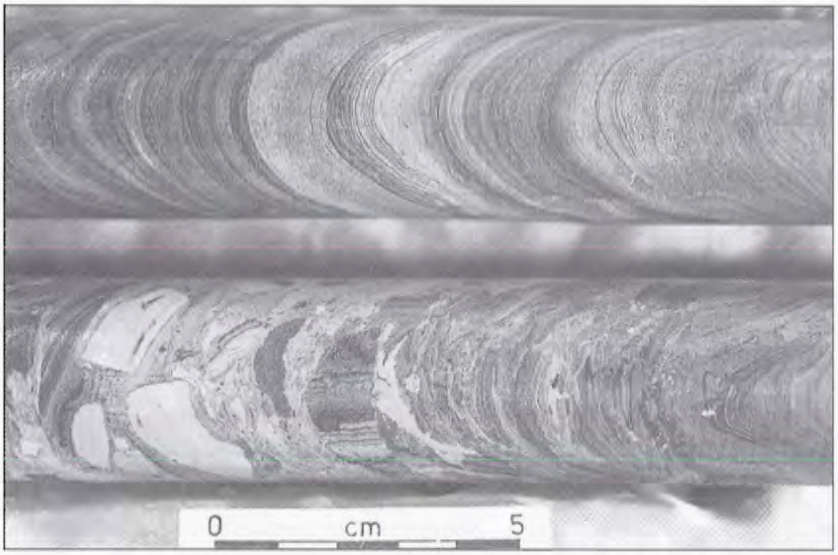


Figure 32. Photograph of normal (top) and brecciated (bottom) bituminous shale taken from a drill hole, Beypazari trona deposit.

Table 8. Major oxide composition (in weight percent) of mudstone and claystone samples collected along an east-west traverse of the Hirka Formation, Beypazari basin.

Oxide (%)	K4-3	K2-1	K2-3	SJ6-2	SJ6-6	SJ6-31	K7-24	K7-29
SiO_2	26.06	14.32	44.46	62.76	37.50	44.18	23.12	30.30
Al_2O_3	4.13	2.50	7.70	4.33	4.45	5.00	2.18	5.52
$*Fe_2O^T_3$	1.54	1.00	1.78	1.12	1.93	4.45	0.31	0.96
MgO	16.39	19.18	6.08	7.226	8.20	7.70	12.46	14.71
CaO	13.91	21.36	10.85	2.36	14.98	8.15	18.72	15.08
Na_2O	0.14	0.37	0.92	1.06	1.04	2.15	0.39	0.14
K_2O	0.80	0.92	2.06	2.76	1.93	3.34	1.87	1.93
TiO_2	0.25	0.35	0.75	0.35	0.75	1.00	0.40	0.15
P_2O_5	0.00	0.00	0.00	0.00	0.00	0.00	0.00	0.00
MnO	0.04	0.04	0.08	0.04	0.05	0.01	0.05	0.06
SO_3	0.57	0.60	0.64	0.52	0.55	0.52	0.59	0.53
CO_2	18.19	28.20	9.62	3.18	10.81	7.33	23.02	17.40
H_2O	17.16	11.01	15.09	13.63	17.02	15.38	16.42	13.20
TOTAL	99.72	99.85	100.03	99.37	99.21	15.38	99.53	99.98

$*Fe_2O^T_3$: Fe_2O_3 + 1.111 x FeO

Table 9. Major oxide composition (in weight percent) of bituminous shale samples collected along an east-west traverse of the Hirka Formation, Beypazari basin.

Oxide(%)	K4-1	SJ17A-1	SJ6-43	SJ32-13	SJ32-21	SJ32-22	K7-8	K7-16	K7-21	2001-3
SiO_2	23.32	18.22	28.12	30.00	34.36	46.10	27.68	27.50	31.86	37.56
Al_2O_3	5.41	4.06	4.37	6.56	7.23	10.09	6.87	3.43	7.03	6.98
$*Fe_2O^T_3$	1.98	1.43	0.81	2.30	3.25	4.79	2.39	1.12	3.09	2.88
MgO	15.81	15.49	6.74	9.81	5.24	3.43	8.07	10.51	6.96	6.46
CaO	12.55	19.91	14.31	12.47	10.97	3.91	12.27	16.38	19.98	12.97
Na_2O	0.24	1.20	2.16	1.23	4.80	3.98	0.14	0.85	0.37	0.88
K_2O	2.42	2.27	5.64	3.14	0.66	4.14	1.93	1.25	6.76	2.86
TiO_2	0.53	0.25	0.25	0.75	1.00	0.90	0.40	0.45	0.85	0.75
P_2O_5	0.00	0.00	0.00	0.00	0.00	0.00	0.00	0.00	0.13	0.00
MnO	0.04	0.70	0.03	0.02	0.04	0.03	0.04	0.07	0.12	0.04
SO_3	0.68	0.50	0.46	0.58	0.94	0.54	0.62	0.54	0.75	0.55
CO_2	11.58	18.98	4.94	3.75	8.12	5.17	9.78	20.85	11.24	13.11
H_2O	24.91	17.51	31.79	29.34	22.87	16.77	29.72	17.01	19.70	14.16
TOTAL	99.47	99.90	99.62	99.95	99.48	99.25	99.91	99.96	99.84	99.20

$*Fe_2O^T_3$: Fe_2O_3 + 1.111 x FeO

Table 10. Major oxide composition (in weight percent) of tuff samples from the Hirka Formation, Beypazari basin.

Oxide (%)	K2-5	K8-14	K8-15	K8-18	SJ17A-15	SJ32-15	SJ32-26
SiO_2	71.96	59.02	60.05	74.66	52.98	38.16	59.00
Al_2O_3	15.62	5.20	17.27	10.83	10.51	10.05	12.53
$*Fe_2O^T_3$	0.62	1.13	6.30	2.24	4.29	1.43	3.02
MgO	0.03	3.37	0.59	0.00	2.68	6.73	1.02
CaO	1.72	8.08	0.92	0.00	7.52	9.05	7.38
Na_2O	3.02	0.24	1.07	0.10	2.82	7.88	1.58
K_2O	2.11	2.50	7.8	8.56	5.00	1.47	2.39
TiO_2	0.45	0.75	1.00	0.65	0.55	0.25	1.05
P_2O_5	0.00	0.00	0.15	0.00	0.11	0.00	0.12
MnO	0.06	0.04	0.06	0.00	0.04	0.03	0.09
SO_3	0.60	0.57	0.83	0.77	0.53	0.55	0.53
CO_2	0.47	9.87	0.64	0.00	5.38	5.78	4.88
H_2O	3.36	8.96	2.75	2.05	6.68	18.09	5.74
TOTAL	100.02	99.73	99.43	99.86	99.09	99.47	99.33

$*Fe_2O^T_3$: Fe_2O_3 + 1.111 x FeO

mally dry surface, nearly in the transitional zone between the Hirka Formation and Teke Volcanics. Sodium-rich solutions were contributed to the lake primarily by thermal and alkaline springs originating from the Teke Volcanics and from pre-Miocene granitic rocks situated south of Beypazari (**Tables 11** and **12**).

The dolomitic claystones were probably formed on a playa flat similar to that described for the mudstone facies of the Green River Formation by Eugster and Surdam (1973) and Eugster and Hardie (1975). The playa flat in the Beypazari basin covered the westernmost part of the basin. In some localities of the Hirka Formation near Cayirhan, fibrous magnesium sulfate minerals including epsomite and starkayite fill desiccation cracks in the claystones. These mudcrack infillings are covered generally by bituminous shale (**Figure 18**). This kind of mineral enrichment can originate from biochemical contributions of algae forming the bituminous shale rocks, as explained in Desborough (1978), and they settled into the bituminous shale during post-depositional periods.

The intraformational conglomerate indicates six major synsedimentary deformation and transformation periods during the deposition of the Hirka Formation (**Figure 5**). This deformation was caused by

Table 11. Chemical analysis of Karakoca spring water, Beypazari area. mg/l = milligrams per liter.

Cations (mg/l)		Anions (mg/l)	
Na^+	455.676	SO_4^{--}	135.696
Ca^{++}	140.000	Cl^-	61.060
Mg^{++}	158.000	HCO_3^-	2244.800
$\frac{Na}{Ca+Mg}$	1.529	H_2SiO_3	156.006

Table 12. Chemical analyses, in parts per million, of thermal springs, mineral water, and artesian water from the Beypazari area. n.d. = not determined, short dashes = negligible value or undetected.

Elements	SJ-8 artesian well water	Ayas thermal springs	Dutlu-Tahtali thermal springs			Beypazari-Karakoca mineral water
	1	2	3	4	5	6
Na	6055.6	4609.0	1336.0	1453.0	1624.0	154.0
K	56.0	57.0	32.0	36.0	12.0	16.0
Ca	1.0	471.4	445.8	493.7	182.4	171.5
Mg	1.0	135.9	106.5	121.7	36.2	209.5
Sr	0.5	10.86	9.15	9.97	2.55	1.02
Ba	0.19	0.04	0.04	0.03	0.02	0.05
As	0.5	0.05	0.05	0.05	0.06	0.05
B	386.25	10.63	5.05	5.73	5.48	0.42
Li	0.31	1.65	0.91	1.00	0.48	0.46
Cl	2300	2200	1100	-	1200	16
F	7.3	n.d.	n.d.	-	n.d.	n.d.
SO_4	155	3050	2330	-	2360	115
CO_3	10.000	< 0.1	< 0.1	-	< 0.1	< 0.1
HCO_3	2500	810	480	-	200	1100
$\frac{Na}{Ca+Mg}$	3027.5	7.59	2.42	2.36	7.43	0.40

the northeast-southwest-trending Davutoglan fault. During deposition of the conglomerate, the rocks and semiconsolidated sediments in the mud-flat and very shallow lake environments were probably eroded by surface flushing and flows and redeposited in the depocenter located in the northeastern part of the basin (**Figure 33**).

The lithofacies of the Hirka Formation are interpreted to have been deposited in a playa-lake type environment similar to that of Eugster and Surdam (1973). Playa-lake deposition has been discussed and supported for the Green River Formation by various workers (Bradley, 1973; Wolfbauer and Surdam, 1974; Eugster and Hardie, 1975; Surdam and Wolfbauer, 1975; Lundell and Surdam, 1975; Surdam and Stanley, 1979). Dolomitic claystone was deposited in the lake-margin playa and/or mud flat. This lithofacies may be compared with saline mud flat lithofacies of the Cambrian Parakeelya Alkali Member of the Observatory Hill Formation in the Officer Basin, South Australia (White and Young, 1980; Southgate and others, 1989). One difference from the Parakeelya strata is that the dolomitic claystone lithofacies in the Beypazari area does not contain chert layers or nodules. The absence of gypsum and abundance of framboidal pyrite in the Beypazari area may be explained by bacterial sulfate reduction. Thick trona beds were deposited in a small, periodically drying, closed lake which settled in the east part of this playa flat. This lake was supplied from the alkaline-rich surface streams and underground waters originating from the adjacent rocks and playa flat. The bituminous shale lithofacies was deposited in a shallow, brackish-water lake environment which expanded by seasonal flooding. Characteristics of the intraformational conglomerate lithofacies indicate intrabasinal erosion, redeposition, and sediment selection toward the depositional center of the trona deposit (**Figure 33**).

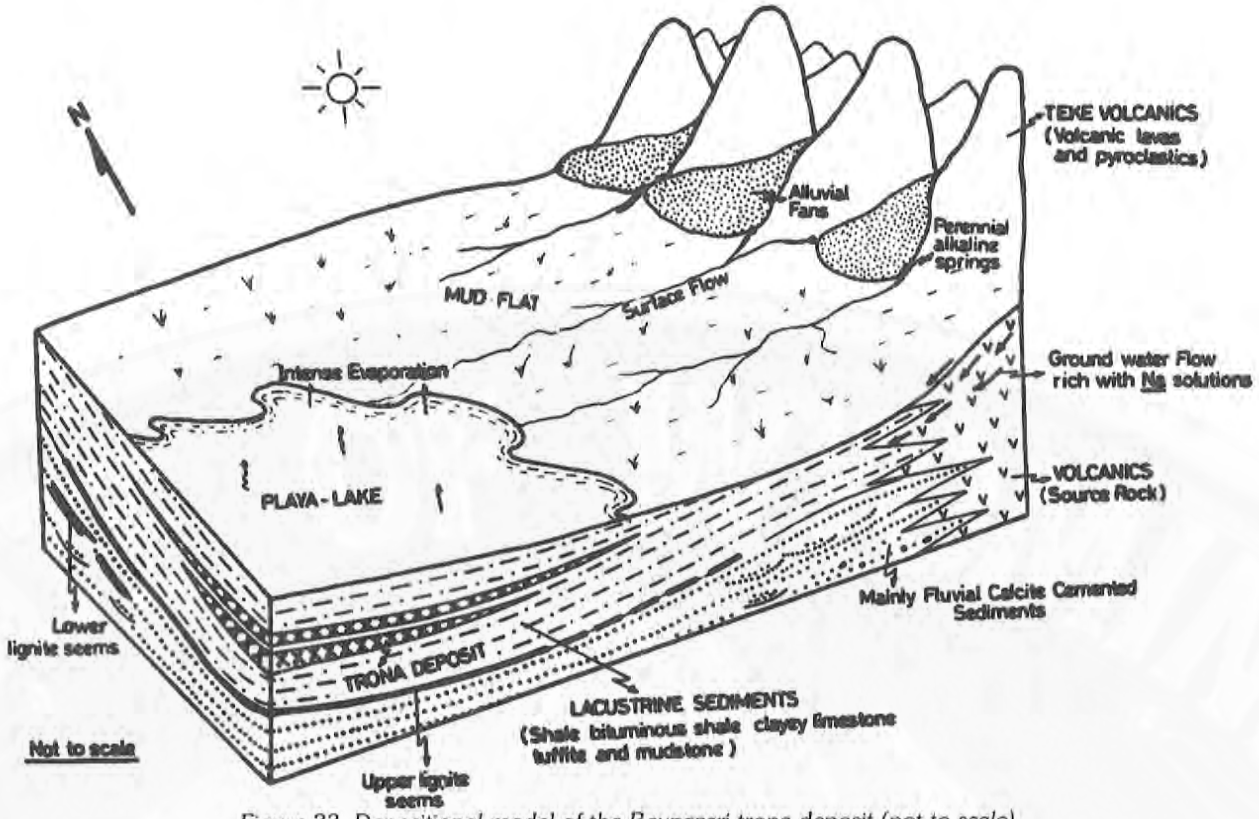


Figure 33. Depositional model of the Beypazari trona deposit (not to scale).

Conclusions

The Miocene sequence in Beypazari basin is composed of coarse- to fine-grained sedimentary rocks with trona, lignite and bituminous shale, carbonates, and volcanic rocks. The rocks were deposited within fluvial, lacustrine, and playa-lake environments. Laterally, the lacustrine and playa-lake deposits intertongue with fluvial deposits. The Beypazari basin represents a restricted, evaporite-rich cycle of deposition (**Figure 34**). The major sodium carbonate mineral is trona with minor amounts of nahcolite and trace amounts of pirssonite and thermonatrite. Trona and dolomite are found in association with each other throughout the deposit.

Dolomitic claystone, bituminous shale, trona, and intraformational conglomerate lithofacies of the Hirka Formation were deposited in a playa lake controlled by an extensional tectonic regime. The dolomitic claystone lithofacies was deposited in a lake-margin playa flat. The trona accumulated in an evaporitic lake depocenter east of the playa flat and parallel to the northeastern part of the Davutoglan fault; the lake was supplied with alkaline-rich surface and underground waters originating from the adjacent playa flat and volcanic and granitic terranes (**Figures 11** and **33**). When the lake water was freshened by seasonal floods, the lake expanded and bituminous shale was deposited in a wider area. The intraformational conglomerate and associated rocks are the result of synsedimentary tectonism, intrabasinal erosion, redeposition, and sediment selection toward the basin center.

The most likely source of sodium for the formation of the trona deposit is from the weathering of rocks in the source area (granites and Paleocene and Cretaceous volcanics); leaching of the tuffs interbedded with the sediments; and the extensive Teke Volcanics (from coeval volcanic activity) interfingered with the sediments in the northeastern part of the Beypazari basin (**Figures 33** and **34**). The Teke Volcanics were probably the major source of sodium for the trona and other sodium carbonate salts. The sodium entered the playa-lake system through surface and underground waters and thermal springs.

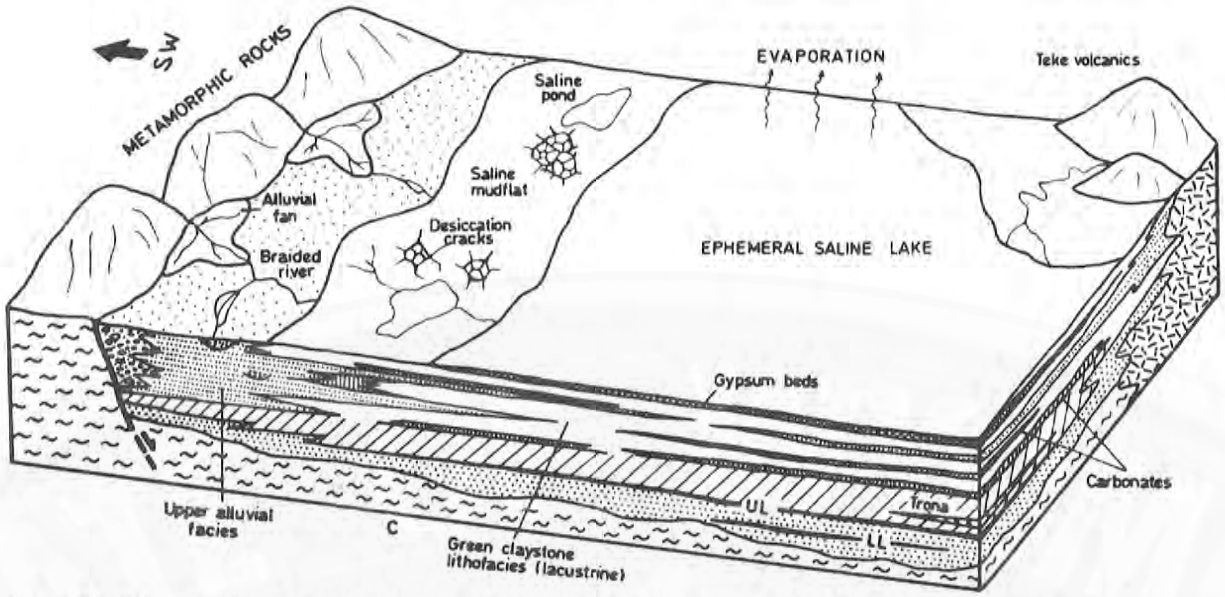


Figure 34. Schematic block diagram showing the depositional environments throughout Miocene time in the Beypazari basin (not to scale).

Acknowledgments

Field work was supported by the Turkish Council for Scientific and Technical Research (TUBITAK), the Turkish National Coal Board Branch (OAL), the Turkish Electrical Company (TEK), and the General Directorate of the Mineral Research and Exploration (MTA) in Ankara. The author wishes to thank to the management and technical staff for their assistance. He also thanks Mualla Gurle for drafting assistance, and N. Hulya Helvaci for typing assistance.

References cited

Altinli, I.E., 1973, Orta Sakarya'nin Jeolojisi: Cumhuriyetin 5. Yili Yerbilimleri Kongresi, Ankara, Bull. Mineral Research and Explor. Inst of Turkey, p. 159-191.

Altinli, I.E., 1976, Geology of the northern portion of the Middle Sakarya River: Ystanbul Univ. Fen. Fak. Mec. Section v. 41, no. 1-4, p. 35-36.

Altinli, I.E., 1977, Geology of the eastern territory of Nallihan (Ankara province): Istanbul Univ. Fen Fak. Mec. Seri B. v.42, no.1-2, p. 29-44.

Biron, C., Eskikaya, S., and Eskikaya, T., 1979, Turkiye Komur Isletmeleri Kurumu Beypazari bitumlu sistlerin kazilabilirlik ve yanabilirlik etudu. Tech. Univ., Istanbul, Rept., 4, 143 p.

Birsoy, R., 1993, Phase diagrams soda minerals: application to Beypazari soda deposit, Turkey: Tr. J. Earth Sciences, v. 2, p. 183-188.

Bradley, W.H., 1931, Origin and microfossils of the oil shale of the Green River Formation of Colorado and Utah, U.S. Geol. Surv. Prof. Pap., v. 168, 58 p.

Bradley, W.H., 1973, Oil shale formed in desert environment, Green River Formation, Wyoming: Geol. Soc. Am. Bull., v. 84, p. 1121-1123.

Breue, H., 1954, Nallihan-Beypazari linyit sahasina ait jeolojik rapor: M.T.A. Rept. Ankara, 2588 (unpublished).

Ciculic, M., 1969, Beypazari-Nallihan komur jeolojisi hakkynda rapor: T.K.I. Rept. Ankara (unpublished).

Cogulu, E., 1967, Etude petrographique de la region the Mihaliccik (Turque): B.S.M.P., 47, 683-803.

Damon, P.E., Shafigullah, M., and Clark, K.F., 1983, Geochronology of the porphyry copper deposits and related mineralization of Mexico: Canadian Journal of Earth Sciences, v. 20, p. 1052-1071.

Desborough, G.A., 1978, A biogenic-chemical stratified lake model for the origin of oil shale of the Green River Formation: an alternative to the playa-lake model: Geol. Soc. Am. Bull., v. 84, p. 1115-1120.

Eugster, H.P., and Hardie, L.A., 1975, Sedimentation in ancient playa-lake complex: The Wilkins Peak Member of the Green River Formation of Wyoming: Geol. Soc. Am. Bull., v.86, p.319-334.

Eugster, H.P., and Surdam, R.C., 1973, Depositional environment of the Green River Formation of Wyoming: a preliminary report: Geol. Soc. Am. Bull., v. 84, p. 115-1120.

Gokmen, V., 1965, Nallihan-Beypazari sahasinin jeolojisi: M.T.A. Rept. Ankara, 3802 (unpublished).

Goktunali, K., 1965, Beypazari linyitlerinin jeolojik et d : M.T.A. Rept. Ankara, 3391 (unpublished).

Gokisik, A., 1973, OAL Isletmesi sahasi jeolojik etudu, istihsal sondajli aramalarinin jeolojik etud neticeleri ile korelasyonu: T.K.I. Rept., Ankara (unpublished).

Helvaci, C., and Bozkurt, S., 1994, Geology, mineralogy and petrogenesis of Beypazari (Ankara) granite: Geological Bulletin of Turkey, v. 37, no. 2, p. 31-42.

Helvaci, C., and Inci, U., 1989, Beypazari trona yataginin jeolojisi, mineralojisi jeokimyasy ve yorenin trona potansiyeli: Turkiye Bilimsel ve Teknik Arastirma Kurumu. Temel Bilimleri Arastirma Grubu. Proje No: TBAG-685, 159 p.

Helvaci, C., Yilmaz, H., and Inci, U., 1988, Beypazari (Ankara) yoresi Neojen tortullarinin kil mineralleri ve bunlarin dikey ve yanal dagilimi: Jeoloji Muhendisligi, v. 32-33, p. 33-42.

Helvaci, C., Inci, U., Yilmaz, H., and Yagmurlu, F., 1989, Geology and Neogene trona deposit of the Beypazari region, Turkey: Turkish Journal of Engineering and Environmental Sciences. v. 13, no. 2, p. 245-256.

Helvaci, C., Stamatakis, M.G., Zagouroglu, C., and Kanaris, J., 1993, Borate minerals and related authigenic silicates in the northeastern Mediterranean late Miocene continental basins: Exploration and Mining Geology, v. 2, no. 2, p. 171-178.

Inci, U., 1983, Demirci (Manisa) ve Burhaniye (Balikesir) cevresinin jeolojisi ve bitumlu seyl olanaklari: Ph. D. Thesis, Dokuz Eylul Univ., Izmir, 184 p.

Inci, U., 1991, Miocene alluvial fan-alkaline playa lignite-trona bearing deposits from an inverted basin in Anatolia: sedimentology and tectonic controls on deposition: Sedimentary Geology, v. 71, p. 73-97.

Inci, U., Helvaci, C., and Yagmurlu, F., 1988, Stratigraphy of Beypazari Neogene basin, Central Anatolia, Turkey: Newsl. Stratigr. v. 18 (3), p. 165-182.

Kayakiran, S., Akinci, O., Celik, E., and Dundar, A., 1986, Beypazari trona yataginin jeolojisi: IVth Engineering Week, Isparta-Turkey, Abstracts, p. 75-76.

Ketin, I., 1966, Tectonic units of Anatolia (Asia Minor): Bull. Miner. Resour. Explor., Inst. Turkey, v. 66, p. 23-34.

Leake, B.E., Hendry, G.L., Kemp, A., Plant, A.G., Harrey, P.K., Wilson, J.R., Coats, J.S., Aucott, J.W., Lunel, T., and Howart, R.J., 1969 /1970, The chemical analysis of rock powders by automatic X-ray fluorescense: Chemical Geology, v. 5, p. 7-86.

Lundell, L.L., and Surdam, R.C., 1975, Playa-lake deposition, Green River Formation, Piceance Creek Basin, Colorado: Geology, v. 3, p. 493-497.

Narin, R., 1980, Beypazari and Beysehir lignite deposits in Central Anatolia, Turkey: Bull. Geol. Congr. Turkey, v. 2, p. 231-239.

Onal, M., Helvaci, C., Inci, U., Yagmurlu, F., Meric, E., and Izver, T., 1988, Stratigraphy, age, facies and depositional environments of the Sogukcam Limestone, Nardin Formation and Kizilcay Group in north of Cayirhan, northwest of Ankara: TAPG Bull., v. 1(2), p. 152-163.

Oz, D., 1976, IR-247, IR-248, IR-389, IR-400 No.lu ruhsat sahalarinin jeolojik ve jeofizik etudleri: T.K.I. Rept. Ankara (unpublished).

Oz, D., 1977, Nallihan-Cayirhan nahiyesi civarindaki Neojen'de bulunan bitumlu sistlerde acik isletme yapilmasi dusunulen saha hakkinda: T.K.I. Rept., Ankara (unpublished).

Saner, S., 1979, Explanation of the development of the Western Pontid Mountain and adjacent basins, based on plate-tectonic theory, northwestern Turkey: Min. Res. Exp. Ins. Bull., v. 93, p. 1-20.

Siyako, F., 1984, Beypazari (Ankara) komurlu Neojen havzasi ve cevresinin jeolojisi: M.T.A. Spec. Rept. 44 p.

Southgate, P.N., Lambert, I.B., Donnelly, T.H., Henry, R., Etminan, H., and Weste, G., 1989, Depositional environments and diagenessis in Lake Parakeelya: a Cambrian alkaline playa from the Officer Basin, South Australia: Sedimentology, v. 36, p. 1091-1112.

Stephenisky, V., 1941, Nallihan-Beypazari civarinin linyit sahasinin jeolojisi: M.T.A. Rept., 1363 (unpublished).

Surdam, R.C., and Stanley, K.O., 1979, Lacustrine sedimentation during the culminating phase of Eocene Lake Gosiute, Wyoming (Green River Formation): Geol. Soc. Am. Bull., v. 70, p. 93-110.

Surdam, R.C., and Wolfbauer, C.A., 1975, Green River Formation, Wyoming: A playa-lake complex: Geol. Soc. Am. Bull., v. 86, p. 335-345.

Wagnam, D.D., Evans, V.H., Parken, V.B., Schumm, R.H., Halow, I., Bailey, S.M., Chirney, K.L., and Nutthal, R.L., 1982, The NBS tables of chemical thermodynamic properties: J. Phys. Chem. Ref. Data, 11, supp. 2, 392 p.

Wedding, H., 1965, Nallihan-Cayirhan linyit sahasi hakkinda jeolojik rapor: M.T.A. Rept., 3924 (unpublished).

White, A.H., and Young, B.C., 1980, Cambrian alkali playa-lacustrine sequence in the northeastern Officer Basin. South Australia: J. Sediment. Petrol., v. 50, p. 1279-1286.

Wolfbauer, C.A. and Surdam, R.C., 1974, Origin of nonmarine dolomite in Eocene Lake Gosiute, Green River Basin, Wyoming: Geol. Soc. Am. Bull., v. 85, p. 1733-1740.

Yagmurlu, F., and Helvaci, C., 1994, Sedimentological characteristics and facies of the evaporite-bearing Kirmir Formation (Neogene), Beypazari basin, Central Anatolia, Turkey: Sedimentology, v. 41, p. 847-860.

Yagmurlu, F., Helvaci, C., Inci, U., and Onal, M., 1988, Tectonic characteristics and structural evolution of the Beypazari-Nallihan Neogene basin, Central Anatolia: Journal of Pure and Applied Sciences Series A "Geosciences" I, p. 127-143.

Ziegler, A., and Onen, H., 1936, Orta Anadolu linyit yataklari: M.T.A. Rept. Ankara, 119 (unpublished).

Additional references

Alkaya, F., 1987, Kimmeridgian-Berriasian ammonite fauna and stratigraphy of the Beypazari (Ankara) province (abstract): Melih Tokay Symposium 1987. Middle East Technical University, Ankara, p. 114.

Ataman, G., 1976, Occurrence of authigenic analcime in Turkey and probable relationship between genesis of zeolitic series and plate tectonic: Yerbilimleri, Pub. Hacettepe Univ., v. 1, p. 9-23.

Barka, A., 1984, Kuzey Anadolu fay zonundaki bazy Neojen-Kuvaterner havzalarynyn jeolojisi ve tektonik evrimi: Ketin Simpozyumu Kitabi, Spec. Publ. Geol. Soc. Turkey, Ankara, p. 209-227.

Bell, C.M., 1989, Saline lake carbonates within an Upper Jurassic-Lower Cretaceus continental red bed sequence in the Atacama region of northern Chile: Sedimentology, v. 36, p. 651-663.

Bergoughan, H., 1975, Relations entre les edifies pontique et taurique dans le Nord-Est de l'Anatolie. Bull. Soc. Geol. Fr., Ser. 7, v. 17, p. 1045-1057.

Bradley, W.H., and Eugster, H.P., 1969, Geochemistry and paleolimnology of the trona deposits and associated authigenic minerals of the Green River Formation of Wyoming: U.S. Geol. Survey Prof. Paper, 496-B, 71 p.

Brinkmann, R., 1976, Geology of Turkey: Enke, Stutgart, 158 p.

Dundar, A., 1988, Ankara-Beypazari trona deposit, geology and mineralogical characteristics: Industrial Minerals Supplement March, p. 41-43.

Gokcen, S.L., 1976, Haymana guneyinin sedimentolojik incelenmesi (SW Ankara): Ph.D. Thesis, Hacettepe Univ., Ankara, 191 p.

Gokcen, S.L., 1981, Zara-Hafik guneyindeki Paleojen istifinin sedimentolojisi ve paleocografik evrimi: Yerbilimleri Pub. Hacettepe Univ., v. 8, p. 1-21.

Gokcen, S.L., and Kelling, G., 1985, Oligocene deposits of the Zara-Hafik region (Sivas, Central Turkey): Evolution from strom-influenced shelf to evaporitic basin: Geol. Rundsch., v. 74, p. 139-153.

Gundogdu, M.N., Tenekeci, O., Oner, F., Dundar, A., and Kayakiran, S., 1985, Beypazari trona yataginin kil mineralojisi: on calisma sonuclari: Turkiye II. Ulusal Kil Sempozyumu Bildirileri, Hacettepe Universitesi, Ankara, p. 141-153.

Hardie, L.A., and Eugster, H.P., 1971, The depositional environment of marine evaporites: a case for shallow, clastic accumulation: Sedimentology, v. 16, p. 187-220.

Hardie, L.A., Smoot, J.P., and Eugster, H.P., 1978, Saline lakes and their deposits: a sedimentological approach, *in* Matter, A., and Tucker, M.E., editors, Modern and Ancient Lake Sediments: Int. Assoc. Sedimentol. Spec. Publ., v. 2, p. 7-41.

Hunt, C.B., Robinson, T.W, Bowles, W.A., and Washburn, A.L., 1966, Hydrologic basin, Death Valley, California: U.S. Geol. Surv. Prof. Pap., 494-B.

Kalafatcioglu, A., and Uysalli, H., 1964, Geology of the Beypazari-Nallihan-Seben area: Bull. Min. Res. Exp. Inst. Turkey, v. 62, p. 1-12.

Kocyigit, A., 1984, Intra-plate neotectonic development in southwestern Turkey and adjacent areas: Bull. Geol. Soc. Turkey, v. 27 (1), p. 1-16.

McBride, E.F., 1974, Significance of color in red, green, olive, brown and gray beds of Difunta Group, northwestern Mexico: J. Sediment, Petrol., v. 44, p. 760-773.

McKenzie, D.P., 1972, Active tectonics of the Mediterranean region: Geops. J.R. Astron. Soc., v. 30, p. 109-186.

Miall, A.D., 1978, Lithofacies types and vertical profile models in braided river deposits–a summary, *in* Miall, A., editor, Fluvial Sedimentology: Can. Soc. Pet. Geol. Mem., v. 5, p. 597-604.

Nasun-Saygili, G., Erdol, N., Okutan, H., Yuzer, H., Isbilir, F., and Ekinci, E., 1974, Turkish trona, integrated process development and cost estimation: Industrial Minerals, April, p. 91-93.

Ongur, T., 1977, Kizilcahamam GB'sinin volkanolojisi ve petrografi incelemesi: TJK Bulteni, v. 20, p. 1-12.

Scheriber, B.C., Roth, M.S., and Helman, M.L., 1982, Recognition of primary facies characteristics of evaporites and differentitation of these forms from diagenetic overprints, *in* Handford, C.R., Loucks, R.G., and Davies, G.R., editors, Depositional and diagenetic spectra of evaporites: Core Workshop No. 3, Soc. Econ. Paleontol. Mineral., Calgary, Alta, p.1-32.

Schreiber, B.C., Freidman, G.M., Decima, A., and Schreiber, E., 1976, Depositional environments of Upper Miocene (Messinian) evaporite deposits of the Silician Basin: Sedimentology, v. 23, p. 729-760.

Sengor, A.M.C., 1980, Fundamentals of the neotectonics of Turkey: Spec. Publ. Geol. Soc. Turkey, v. 2, 40 p.

Sengor, A.M.C., and Yilmaz, Y., 1981, Tethyan evolution of Turkey: A plate tectonic approach: Tectonophysics, v. 75, p. 181-241.

Sengor, A.M.C., Gorur, N., and Saroglu, F., 1985, Strike-slip faulting and related basin formation in zones of tectonic escape: Turkey as a case study: Soc. Econ. Paleontol. Mineral., Spec. Publ., v. 37, p. 228-264.

Thomson, A.M., 1970, Geochemistry of color genesis in red-bed sequence, Juniata and Bald Eagle Formation, Pennyslvania: J. Sediment. Petrol. v. 40, p. 599-615.

Tunc, M., 1980, Davutoglan (Beypazari)-Seben (Bolu) arasinda kalan ve Aladag Cayi boyunca olan bolgenin stratigrafisi: Ankara Univ. Fen. Fak. Ph. D. Thesis, 74 p.

Tunc, M., 1984, Biostratigraphy of the Upper Cretaceous rocks in Seben (NW Ankara): Bull. Faculty of Engineering, Cumhuriyet Univ. v. 1, p. 19-30.

Varol, B., and Kazanci, N., 1981, The litho-and biofacies properties of the Upper Jurassic-Lower Cretaceous carbonate sequence, in Nallihan-Seben (Bolu) region. Bull. Geol. Soc. Turkey, v. 24, p. 31-38.

Walker, T.R., 1967, Formation of red beds in modern and ancient deserts: Geol. Soc. Am. Bull., v. 83, p. 2761-2772.

Yilmaz, Y., Gurpinar, O., and Yigitbas, E., 1988, Tectonic evolution of the Miocene basins of the Amanos mountains and Maras region: TAPG Bull., v. 1 (1), p. 52-72.

Youxun, Z., 1983, Geology of the Wucheng trona deposit in Henan, China: Sixth International Symposium on Salt, The Salt Institute, v. 1, p. 67-73.



Frontispiece: Aerial view of General Chemical Corporation's trona mine and processing plant west of Green River, Wyoming. According to the Wyoming State Inspector of Mines (Annual Report) for 1997 about 4.1 million net short tons of trona were mined underground in 1997. An estimated 2.3 million short tons of soda ash were refined in 1997 (data derived by dividing trona production by 1.8, the accepted ratio of mined trona to refined soda ash). Photograph by John R. Dyni, July, 1998.

Acquiring trona leases on Wyoming state lands

Harold D. Kemp
Wyoming Office of State Lands and Investments
Cheyenne, Wyoming 82001
and
Ray E. Harris
Wyoming State Geological Survey
Laramie, Wyoming 82071-3008

Abstract

The State of Wyoming administers the leasing of surface and mineral rights for the production of minerals from State Trust Lands. The Office of State Lands and Investments is the agency responsible for mineral leasing. In the Known Sodium Leasing Area in the Green River Basin west of Green River, Wyoming, this office administers leases for trona. A small annual rental is charged prior to production, and a royalty is charged on production from state lands.

Introduction

Like many western states, Wyoming was granted surface and mineral ownership of two school sections per township upon statehood. Approximately $^{1}/_{18}$ of the surface and mineral rights in the state of Wyoming are held by the state, and administered by the Office of State Lands and Investments (State Lands). Originally, these lands were sections 16 and 36 in each township. Due to state-federal and state-private trades and sales, not every township (36 mi^2) contains two state sections. **Figure 1** shows the location of state lands west of Green River, Wyoming within the Known Sodium Lease Area (KSLA) established by the U.S. Bureau of Land Management. In some cases, the state owns the minerals while the surface is held by a non-state landowner. Although state leases are issued for sodium/trona (meaning sodium minerals other than trona as well as trona), only trona is being leased in the KSLA at present. For purposes of discussion, this paper uses trona in place of sodium/trona. Mineral rights are leased to individuals and corporations on an annual basis, with royalty payments made to the state during production.

Over the last three fiscal years (July 1 through June 30), just under one million short tons of trona have been produced per year from Wyoming state lands and an average yearly gross royalty of just under $3.5 million paid to the state by the producers.

Leasing Wyoming state lands for trona

State leases for trona are issued over the counter, but the Wyoming State Board of Land Commissioners, as the lessor, may auction such mineral leases where it deems this more beneficial to the state. The locations of unleased state lands within the KSLA and in adjacent lands has generally not made this option worthwhile.

State of Wyoming trona leases are issued for a ten-year term upon approval of the Board of Land Commissioners. The application fee is $25.00 (March, 1998). The lease form is not specific just to trona, but is titled "Metallic and Non-metallic Rocks and Minerals Lease." It may be used to lease a number of solid minerals other than trona.

The standard lease does not contain a clause extending or holding it for production, but the lessee is granted by statutory provision [Wyoming Statutes WS-36-6-101(m) and (n)] an exclusive right to renew the lease for successive terms of ten years each, if at the time of the application for renewal, trona is being

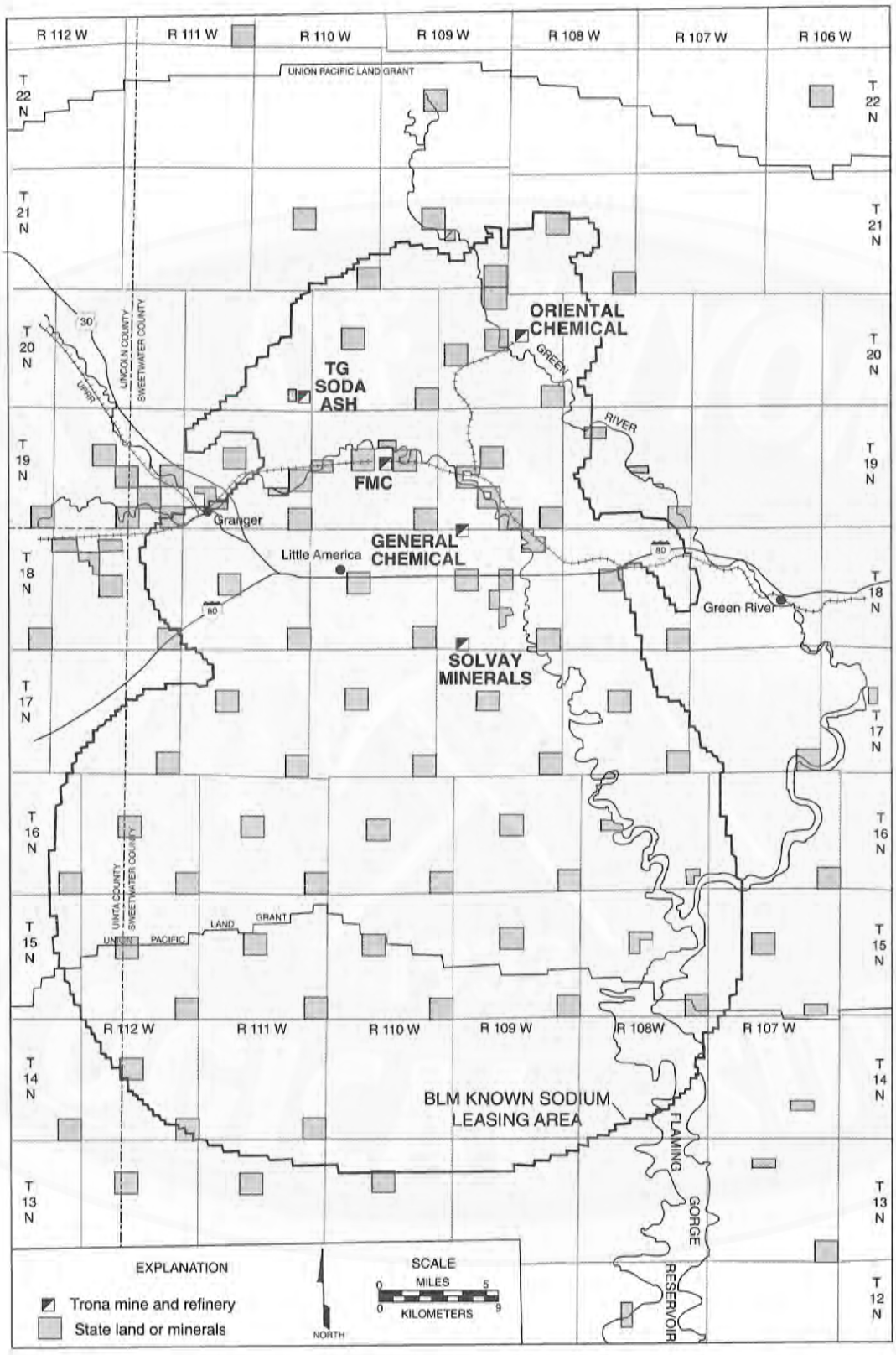


Figure 1. Map of the Known Sodium Leasing Area, Green River Basin, Wyoming, showing Wyoming state lands and related trona mining and refining activities.

produced. The lease is included with a cooperative mining development plan. The lessee must show good faith to develop the leased lands unless the lessee can show delay in development directly tied to compliance with governmental requirements or permitting, licensing, and the like. As provided by the statute, substantial expenditures or commitments to exploration, engineering, environmental studies, hydrological studies, or research and development necessary to develop the lease are taken into account as good faith development. The lease requires conformance with all state statutory requirements and regulations. Leases are assignable in all or in part. The person signing the lease agreement must be a citizen of the United States.

The annual rental fee for a lease is $1 per acre for the first through fifth years and $2 per acre for the sixth through the tenth years, and any renewals thereafter. If a commercial discovery of trona is made, the lease rental rate beginning with the next lease anniversary date and thereafter is $2 per acre. The State Board of Land Commissioners (the Board) also retains the right to raise the lease rental rate an unspecified amount after the second year of the lease if it does not then appear that commercial production is being diligently pursued.

Annual rentals can be credited against the royalty paid once the lease is in production and such rental then serves as a minimum annual royalty. Currently, the Board does not require an annual rental payment at each anniversary date as is stipulated in the lease. Instead, the first rental paid after the first year of production suffices as a minimum royalty roll-forward for the next producing year. This eliminates the necessity for yearly rental payments and credits or refunds. This system works well and cuts down significantly on paperwork for the involved parties.

Currently, the trona lease royalty rate is 5%. However, that rate is being compared with federal and private trona lease rates in the KSLA. Future changes to the current rate would be for the purpose of equalizing the state trona royalty rate with the average trona lease rates for non-state leases in the KSLA to optimize of trust values for these minerals.

The state royalty rate is based on the gross value of merchantable trona. Royalty rates are typically paid on bulk soda ash equivalents since this is usually the first merchantable product. A conversion rate of about 1.8 to 1 is used for trona to soda ash calculations.

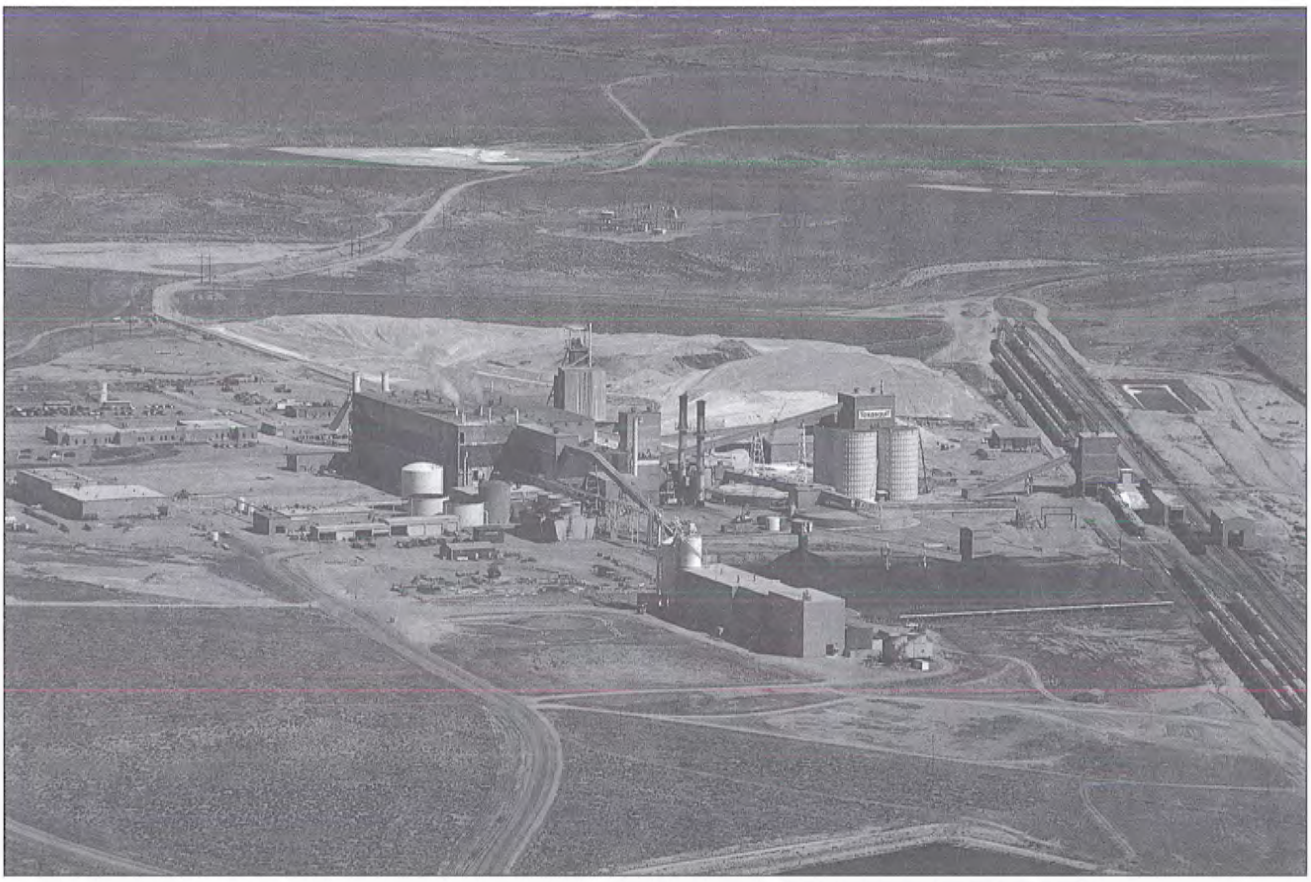
The state lease does provide for a Board-approved royalty rate reduction from the standard lease rate. This may be enacted if it is determined that such a reduction will allow a lessee to undertake additional new operations and/or continue to operate with the expectation of a reasonable profit. According to the terms of state leases, the production royalty may be taken in kind, although this option has never been exercised in the history of the leasing program.

Wyoming state leases allow as much of the use of the surface as is necessary for the mining operation. As with federal leases, this use must compensate the surface estate for damages. This includes both state and non-state landowners.

A bond is also required for a lease. The amount of the bond and the enforcement of the requirements is at the discretion of the Director of State Lands. In most cases, the bond provided by the lessee to the Wyoming Department of Environmental Quality for mining permits is accepted *in lieu* of a bond held by State Lands.

Summary

Trona leases of state-owned minerals may be obtained from State Lands. The application fee is $25 per lease. The annual rental is $1 per acre for the first five years and $2 per acre thereafter. Good faith development must be proven to hold a lease. Upon entering production, a 5% royalty rate based on the value of soda ash (as converted from trona) is charged the producer. This royalty rate is constantly under review and being compared with state and federal royalties for trona. This royalty also covers the annual lease rental. Leases are renewed to the producer as long as production is continuing or good faith development continues. A bond is also charged, but State Lands accepts the bond posted to the Wyoming Department of Environmental Quality without requiring a separate bond.



Aerial view of Tg Soda Ash, Incorporated's trona mine and refinery in the Green River Basin, Wyoming.

Leasing federal sodium lands

Ted Murphy
U.S. Bureau of Land Management
Rock Springs, Wyoming 82902-1869

Abstract

Competitive leasing is the procedure for offering mineral deposits to the public which are not under an outstanding permit or application for preference-right lease. The Bureau of Land Management advertises and conducts competitive mineral sales of certain federal lands. Lands which are classified as known to be valuable for leasable minerals are subject to competitive leasing. Competitive leases containing sodium mineral deposits are offered to the highest bidder(s) at a sale, provided that the amount of the bid(s) equals or exceeds the fair market value.

Authority and procedures for leasing federal sodium deposits

Federal sodium deposits are leased under the authority of The Mineral Leasing Act (MLA), 30 U.S.C. 262. The purpose of the MLA is to promote the development of the mineral resources on federally administered lands and to obtain for the public a reasonable financial return on its assets, of which the Secretary of the Department of Interior is the guardian. The Federal Land Policy and Management Act of 1976 requires that the United States "receive fair market value of the use of the public lands and their resources" [43 U.S.C.§ 1702(A)(9)].

Leasing

Within Wyoming, the public lands subject to competitive leasing are those within the Known Sodium Leasing Area (KSLA). The KSLA was established on March 4, 1954 and now comprises about 700,000 acres, or 1100 square miles, wherein trona deposits exceeding four feet in thickness are known to exist (**Figure 1**). The Green River Basin (GRB) KSLA was officially designated after a number of leases were issued as a result of the preference right lease application (PRLA) process. The original GRB KSLA has been modified five times owing to new information provided by exploratory drilling for trona.

Development of an underground trona mine in southwestern Wyoming requires that a lessee/producer acquire federal, Union Pacific Resources, state, and private leases [in order to assemble a large enough tract of land and resources to conduct a mining operation or extraction process]. The existing trona mines are within a portion of the area covered by the Land Grant Acts of 1862 and 1864. These acts provided the Union Pacific Railroad with every alternate section of "public land" for 20 miles on each side of the railroad right-of-way, for each mile of track laid. Both surface and subsurface mineral rights were granted. The even-numbered sections remained in the public domain, with two sections from the public domain deeded to the state as school lands. The ownership of sodium lands within the KSLA is the Federal Government (57.2%), private (37.9%), and the State of Wyoming (4.9%).

Federal sodium leases in the Green River Basin may be obtained two ways–competitively and noncompetitively. Competitive leases are offered for those lands within the KSLA and require a bonus payment. A sale may be initiated by either a Bureau of Land Management motion or upon request by the public. Noncompetitive preference right leases are issued for lands outside the KSLA where prospecting is required to determine the existence of the sodium resource, and do not require a bonus payment. Noncompetitive leasing of lands is also allowed in instances where the lands adjoin an active mining unit and there is no competitive interest.

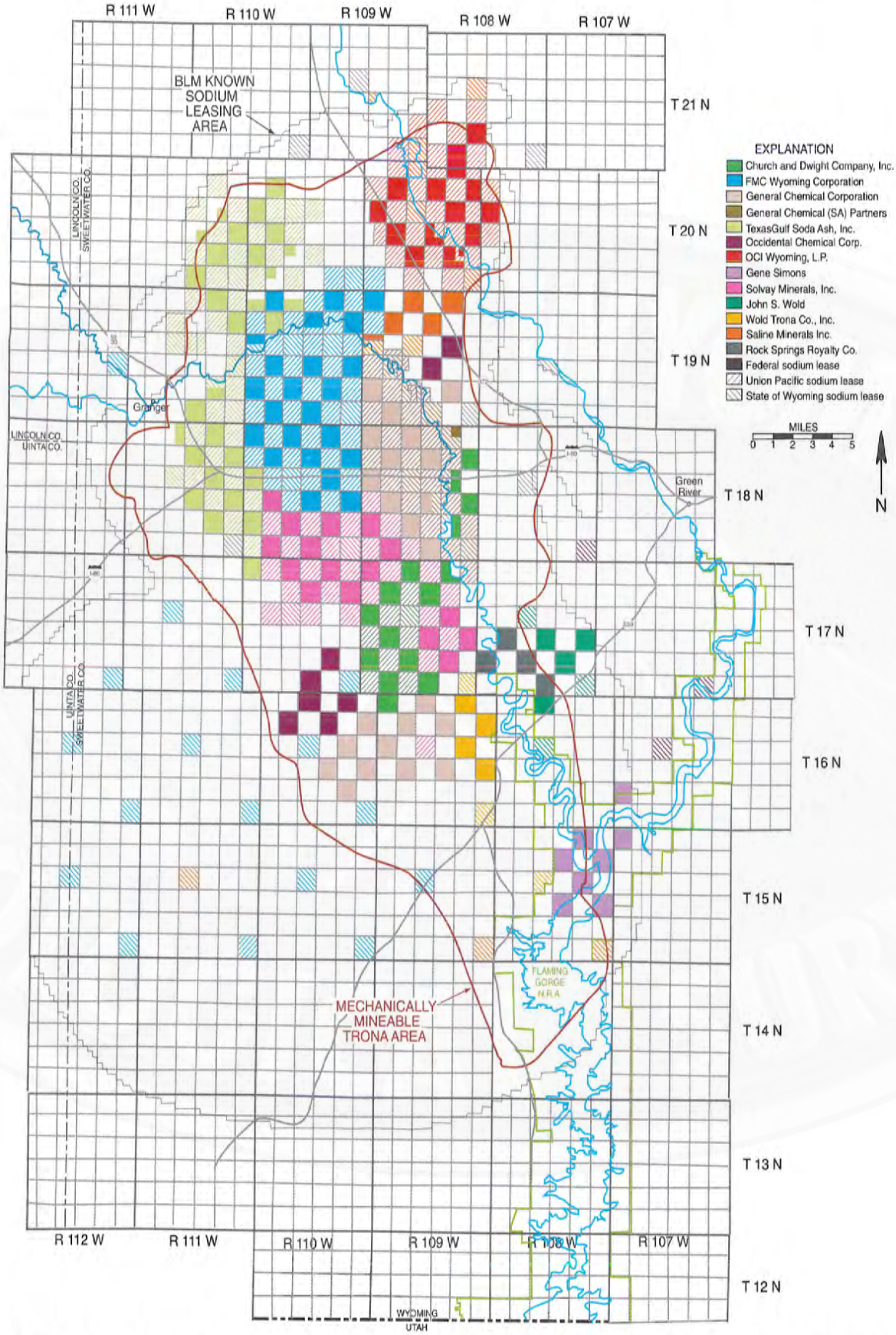


Figure 1. Federal, state, and private (Union Pacific Resources) sodium leases in the Green River Basin, Wyoming.

The Bureau of Land Management (BLM) issued the first federal sodium lease to FMC Corporation in 1947. The majority of the sodium leases were issued in the late 1950s to mid-1960s. Presently, there are 64 active Federal sodium leases containing a total of 89,201 acres (139.3 square miles) within the Green River Basin.

Leases and permits may only be held by citizens of the United States, associations (including partnerships and trusts) of such citizens, and corporations organized under the laws of the United States or of any state or territory thereof. Citizens of a foreign country may only hold interest in leases or permits through stock ownership, stock holdings, or stock control.

Citizens of a foreign country may only hold interests in leases and permits for leasable minerals if the laws, customs, or regulations of their country do not deny similar or like privileges to citizens or corporations of the United States. Further explanation of these requirements can be found in 43 CFR, subpart 3502.

General leasing regulations

To qualify as a lessee or permittee, no person, company, association, or corporation may hold at any particular time, directly or indirectly, more than 5120 acres under prospecting permit and lease in any one state, unless the Secretary of the Interior determines, pursuant to 30 U.S.C. 184(B)(2), that if it is necessary to secure the economic mining of sodium compounds, holdings may equal 15,360 acres.

The BLM conducted two sodium lease sales in 1996 (**Table 1**). These two sales held in response to expressions of interest filed by the public, represented the last leasing activity since 1986. The first lease sale was held on May 1, 1996. The two leases sold totaled 1280 acres and contained 37.7 million tons of minable trona. Minable trona is defined as a bed or beds which are 8 feet or greater in thickness, contain 85% or greater total trona and 2% or less halite, and are 2000 feet or less below the surface. The bonus bid for these tracts was $3.7 million or $2870.00 per acre. General Chemical Soda Ash Partners was the successful bidder for both leases.

In September, 1996, six sodium leases were sold. These six leases totaled 7592 acres and contained approximately 340 million tons of minable trona. The bonus bid for all six leases totaled about $10 million or $1426.43 per acre. The successful bidders included Church and Dwight (1 lease), Solvay Minerals (3 leases), and Rock Springs Royalty Company, a unit of Union Pacific Resources (2 leases).

Table 1. Summary of federal sodium lease sales in Wyoming, 1996.

Competitive leasing results	Sale of May 1, 1996	Sale of Sept. 26, 1996	Total
Leases Issued	2	6	8
Acres	1280	7592	8872
Minable tons of trona (x1,000,000)	37.7	340.0	377.7
Average bonus bid per acre	$2870.00	$1426.43	$1634.70
Total bonus bid	**$3,673,600**	**$10,829,460**	**$14,503,060**

According to the leasing regulations, the granting of a permit or lease for prospecting, development, or production of sodium: 1) shall not preclude the issuance of other permits or leases for the same lands for deposits of other minerals with suitable stipulations for simultaneous operation; 2) shall be issued in conformance with the decisions, terms, and conditions of a comprehensive land use plan; and 3) the authorized officer or the appropriate surface management agency shall comply with the requirements of the National Environmental Policy Act of 1969.

Rents and royalties

The annual lease rental is 25 cents per acre for the first year, 50 cents for the second through fifth calendar years and $1 per acre for each year thereafter. Rentals paid are credited against royalties. Federal sodium leases also require the payment of minimum royalty in lieu of production beginning the 6th lease year in the amount of $3 per acre.

All new sodium leases issued after February 19, 1996, for public lands within the Green River Basin in the state of Wyoming, require the payment of a production royalty of 8% of the quantity or gross value of the output of sodium compounds and other related products at the point of shipment to market.

All sodium leases initially issued on or before February 19, 1996, for public lands within the Green River Basin in the state of Wyoming, when renewed, require the payment of a production royalty of 6% of the quantity or gross value of the output of sodium compounds and other related products at the point of shipment to market, during the 10-year term of that renewal.

Diligence

All sodium leases issued or renewed after February 19, 1996, include a provision requiring rejection of an application for renewal of a sodium lease if, at the end of its term, sodium is not being produced in paying quantities from the lease or the BLM-approved contiguous mining block in which the lease is included.

Lease duration

Federal sodium leases have a determinate 20-year primary term with discretionary 10-year renewal periods thereafter. A sodium lease is not automatically extended or renewed. The Secretary of Interior may renew the lease upon the lessee's timely application for renewal. During the adjudication process, the lease terms and conditions and special stipulations are reviewed, changed, or modified for conformance with existing policy and regulations.

Summary

Federal sodium leasing plays an important role in the soda ash industry in southwestern Wyoming. Development of mining and other extractive operations for trona here is dependent on the management and success of the federal leasing program. For those interested in obtaining federal sodium leases, permits, or licenses in the Green River Basin, or for those that want further information about federal lands in southwestern Wyoming, please contact:

Rock Springs District Office
U.S. Bureau of Land Management
P.O. Box 1869
Rock Springs, WY 82902-1869

The offices are located north of Rock Springs on State Highway 191 and can be reached at (307) 352-0256.

The history of leasing sodium minerals on the Union Pacific land grant

Bob See
and
Neil Brown
Union Pacific Resources Group, Incorporated
Fort Worth, Texas 76101

Abstract

This paper will describe the history of the Union Pacific land grant and the leasing of Union Pacific trona resources in Wyoming. It will begin with the discovery of pure massive trona in the John Hay, Jr. #1 well by Mountain Fuel Supply Company and will outline the role of Union Pacific in the promotion, development, and production of soda ash. The subsequent leasing and development activities of the five current soda ash producers is also described.

Introduction

This year, 1998, Union Pacific Resources (UPR) and Food Machinery Corporation (FMC) will celebrate the 50th anniversary of the first sodium minerals mining lease covering UPR's lands in the Green River Basin, Wyoming. Union Pacific Railroad (**Figure 1**) was instrumental in the early development of sodium minerals in the Green River Basin and worked with a predecessor company of FMC (Westvaco) to bring about the first commercial soda ash development.

Union Pacific Resources owns the minerals, and in some cases both minerals and surface, within the odd numbered sections of land within a 40-mile-wide strip centered on the Union Pacific Railroad right-of-way. Acquisition of these sections dates back to the late 1860s when the Union Pacific Railway Company (UPRR) received a land grant from the Federal Government to build a transcontinental railroad (**Figure 2**). The UPRR would sell parcels of these lands to settlers as a way to pay for the construction of the rail line and to establish base industries that it could serve. By 1869, when the Central Pacific and Union Pacific railroad companies met at Promontory, Utah, the UPRR was mining coal in Carbon, Rock Springs, and Almy, Wyoming to meet the needs of its steam en-



Figure 1. Location of Union Pacific Railroad right-of-way in 1869 (left) and construction of the railroad (right).

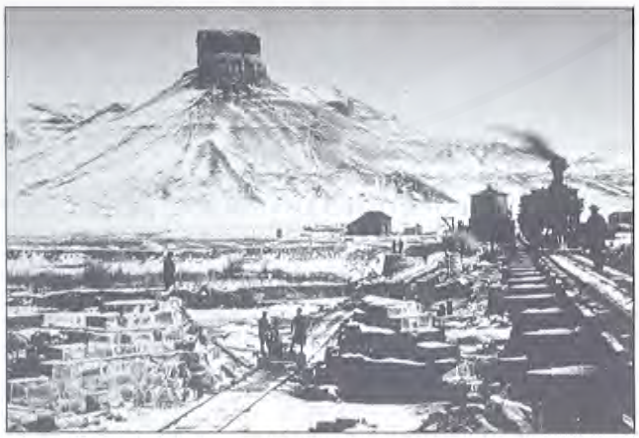


Figure 2. Early photograph of the Union Pacific Railroad near Green River, Wyoming.

gines and the local communities that had sprung up along its path. Union Pacific coal mines provided the fuel to settle the West from Omaha, Nebraska to Sacramento, California.

Today, UPR is a stand-alone company, no longer affiliated with UPRR, that owns and manages approximately 7.9 million acres of mineral rights within the land grant corridor in Colorado, Wyoming, and Utah (**Figure 3**). Something less than one million acres of these rights include surface ownership.

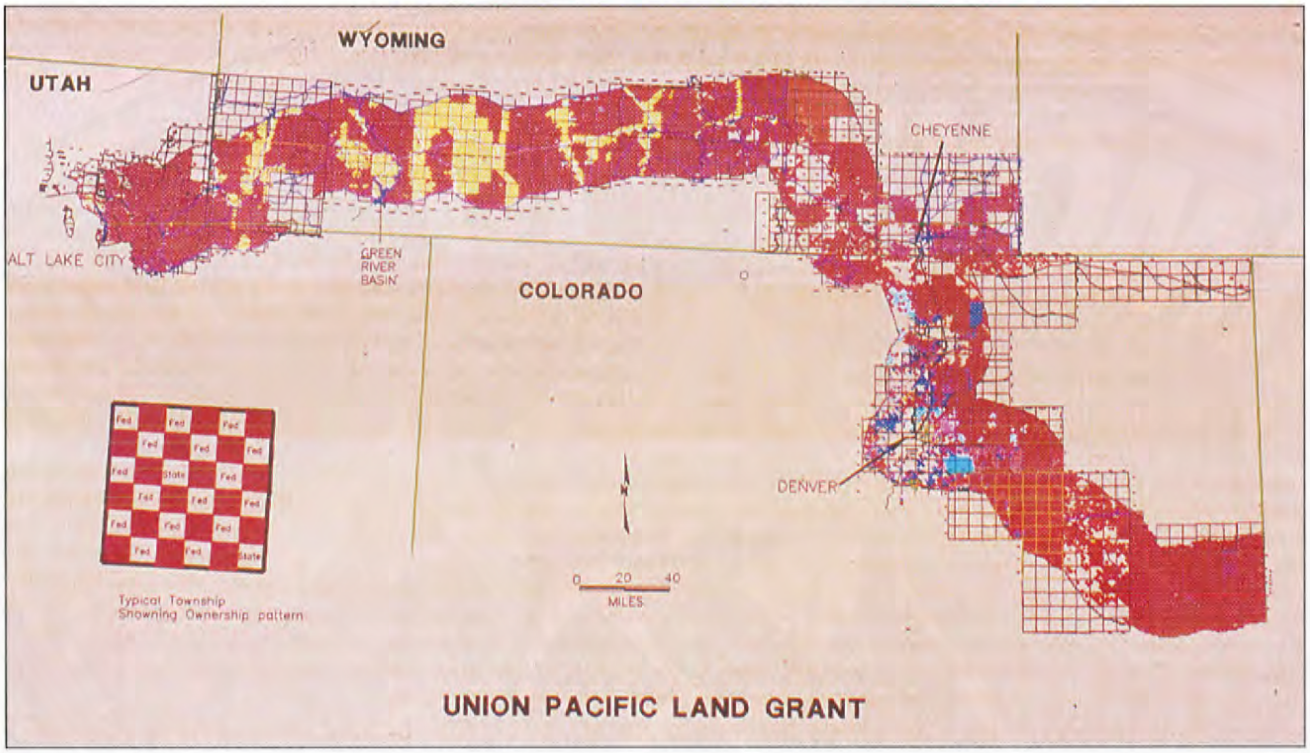


Figure 3. Location of the Union Pacific land grant in northern Colorado, southern Wyoming, and Utah.

History of sodium minerals leasing

Early soda extraction

The route taken by the early railroad engineers cut through a desolate patch of badlands known as the Green River Basin in southwestern Wyoming. Little value could be seen for this region since trona was an unknown mineral at the time the railroad was constructed. In the early 1870s, sodium alkali lakes were discovered west of Laramie and Union Pacific Railroad became interested in producing soda from the land grant. Due to delays in obtaining surveys and subsequent title, Union Pacific Railroad did not complete development and production activities at the lakes until about 1885. However, the life of the Union Pacific Alkali Works, as the project was called, was short lived and succumbed to the production of sodium mineral products produced by the cheaper Solvay synthetic plants in the eastern U.S.

In the late 1890s Green River Fuel & Oil Company drilled a test well in Green River and encountered alkali water at a depth of 125 feet. Western Alkali Corporation then drilled several wells to supply caustic and washing soda until around 1920 when the operation was closed, also due to competitive pressures from the Solvay plants.

Leasing developments in the 1930s and 40s

The real beginning of the Green River Basin soda ash story, however, resulted from the drilling of the John Hay #1 oil and gas well in 1938 by Mountain Fuel Supply Company (**Figure 4**). While the well failed as a hydrocarbon test, a drill core sample taken from a depth of 1590 to 1600 feet revealed a 10-foot-

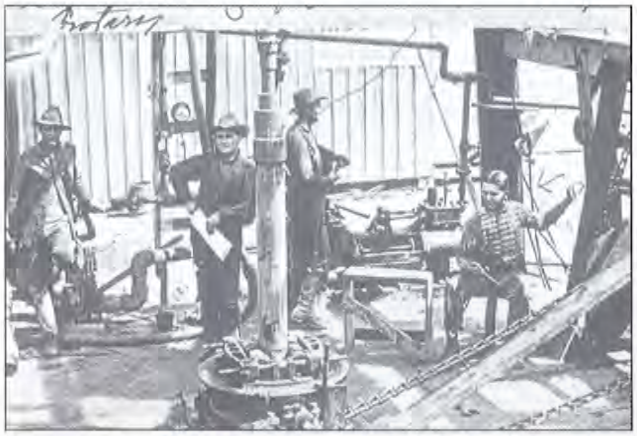


Figure 4. Early rotary drilling rig.

thick bed of a sodium carbonate mineral. The core was analyzed and found to consist largely of the mineral called trona.

Robert Pike, a chemical engineer (**Figure 5**), was retained by Union Pacific to promote this newly discovered mineral and in 1940, under Pike's direction, Union Pacific drilled two test holes spaced about 5 miles apart and located around the Mountain Fuel discovery well to further test the occurrence of trona. Cores from both holes confirmed the presence of a 10-foot-thick bed of trona at a depth of approximately 1500 feet. Pike was now confident that a huge deposit of trona ore had been discovered and, during 1941, he attempted to interest virtually all of the U.S. soda ash producers in forming a development company to exploit the deposit. Unfortunately, his efforts did not meet with much enthusiasm. Union Pacific drilled three more holes in 1942 and the deposit was determined to range in thickness from 7 to 11.7 feet at depths from 1477 to 1671 feet. In May of 1942, Pike reported to Union Pacific that an outstanding result of the exploratory drilling was the proving up of an immense deposit of trona which was almost completely free of sodium chloride and sodium sulfate. No such body of almost pure trona has since been discovered. While Union Pacific continued with attempts to promote trona development, the war effort delayed further work until 1944.



Figure 5. Robert Pike, early trona promoter.

In 1944 UPRR concluded negotiations with Westvaco Chlorine Products Corporation and a two-year non-exclusive prospecting permit covering a nine-township area was granted to Westvaco (**Figure 6**). Westvaco was one of the companies that had been contacted earlier by Pike. This permit contemplated the completion of a pilot solar evaporation unit to test the flow of brine from wells drilled into the main trona bed. It was anticipated that sodium salts would be obtained in sufficient quantities for commercial purposes by the production of brine from these wells. The results obtained from the drilling of three test wells indicated that brines could not be produced and that the extraction of trona would need to be pursued by sinking a shaft for underground mining.

Due to the greater costs associated with underground mining, Westvaco requested and was granted an exclusive revised prospecting permit. The revised permit was actually an exploration agreement that carried with it certain lease or license rights. Under the permit arrangement, Westvaco was to complete a test shaft and mine workings capable of removing 54,000 short tons per year of trona and construct a plant capable of producing 30,000 short tons per year of soda ash (**Figure 7**). Westvaco prepared a feasibility study and, on August 1, 1946, commenced work on sinking a 12-foot-diameter circular shaft (called the Marston Shaft) which was completed on September 12, 1947. By this time, Westvaco had merged into Food Machinery Corporation and was known as the Westvaco Chemical Division. Upon completion of the mine and processing facility, Westvaco was granted a mining license covering about 12 sections of Union Pacific lands (**Figure 8**). Westvaco also obtained state and federal leases and controlled several federal prospecting permits.

Leasing developments in the 1950s and 60s

By mid-1951, Westvaco began sinking a second shaft for ore removal and was producing 350 short tons of ore per day through room and pillar mining

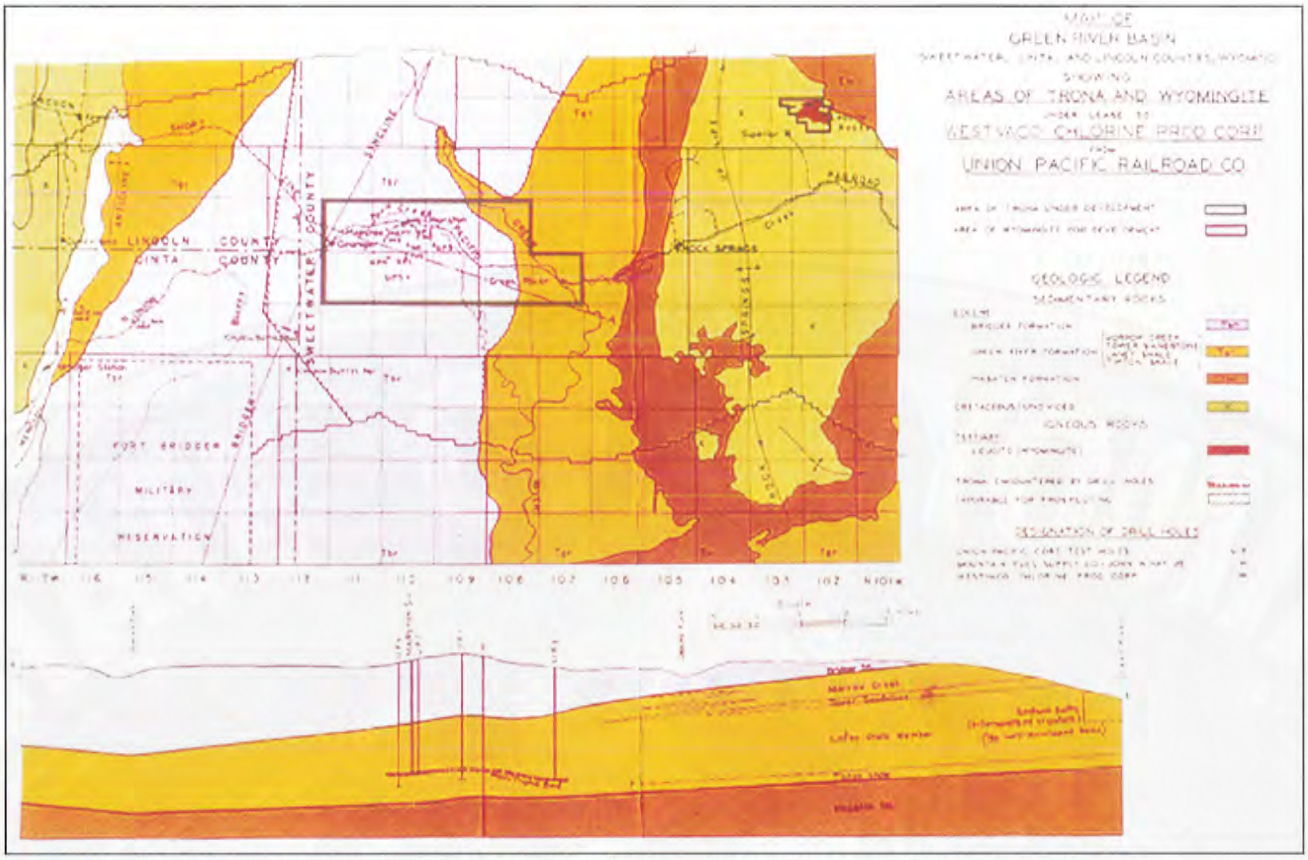


Figure 6. The original 1944 geologic map and cross section of Westvaco's trona prospecting permit.



Figure 7. Headframe of the Marston Shaft (center) and part of Westvaco's trona refinery.

methods. In December 1951, Food Machinery Corporation sold the mine to Intermountain Chemical Corporation (ICC) which was subsequently merged into Food Machinery Corporation in October of 1952. During 1952 ICC installed a solution plant that used the sodium sesquicarbonate refining process to produce soda ash. Up to 1957, the 1947 trona mining license was expanded on three different occasions resulting in a total of 20 sections of Union Pacific lands held under lease (**Figure 8**).

The second trona mining and processing operation began when Union Pacific granted a sodium license to Stauffer Chemical Company of Wyoming in March, 1961. Stauffer Chemical Company of Wyoming was a corporation jointly formed by Stauffer Chemical Company, who acted as operator, and Union Pacific Railroad Company. Stauffer held 51% of the interests in the newly formed corporation and Union Pacific held 49%. The original Stauffer license covered a total of 12,400 acres under 19 sections of Union Pacific land (**Figure 8**). Production at the Stauffer complex commenced in 1962 at an initial capacity of 200,000 short tons per year of soda ash.

Leasing developments in the 1970s and 80s

A third sodium mining lease was entered into with Allied Chemical Corporation in April of 1972 and covered 10,800 acres under 13 sections of Union Pacific lands (**Figure 8**). The lease terms were finally concluded following a number of years of negotiations. The Allied mining and processing facility was constructed and placed into operation in 1968, well in advance of the granting of the lease by Union Pacific.

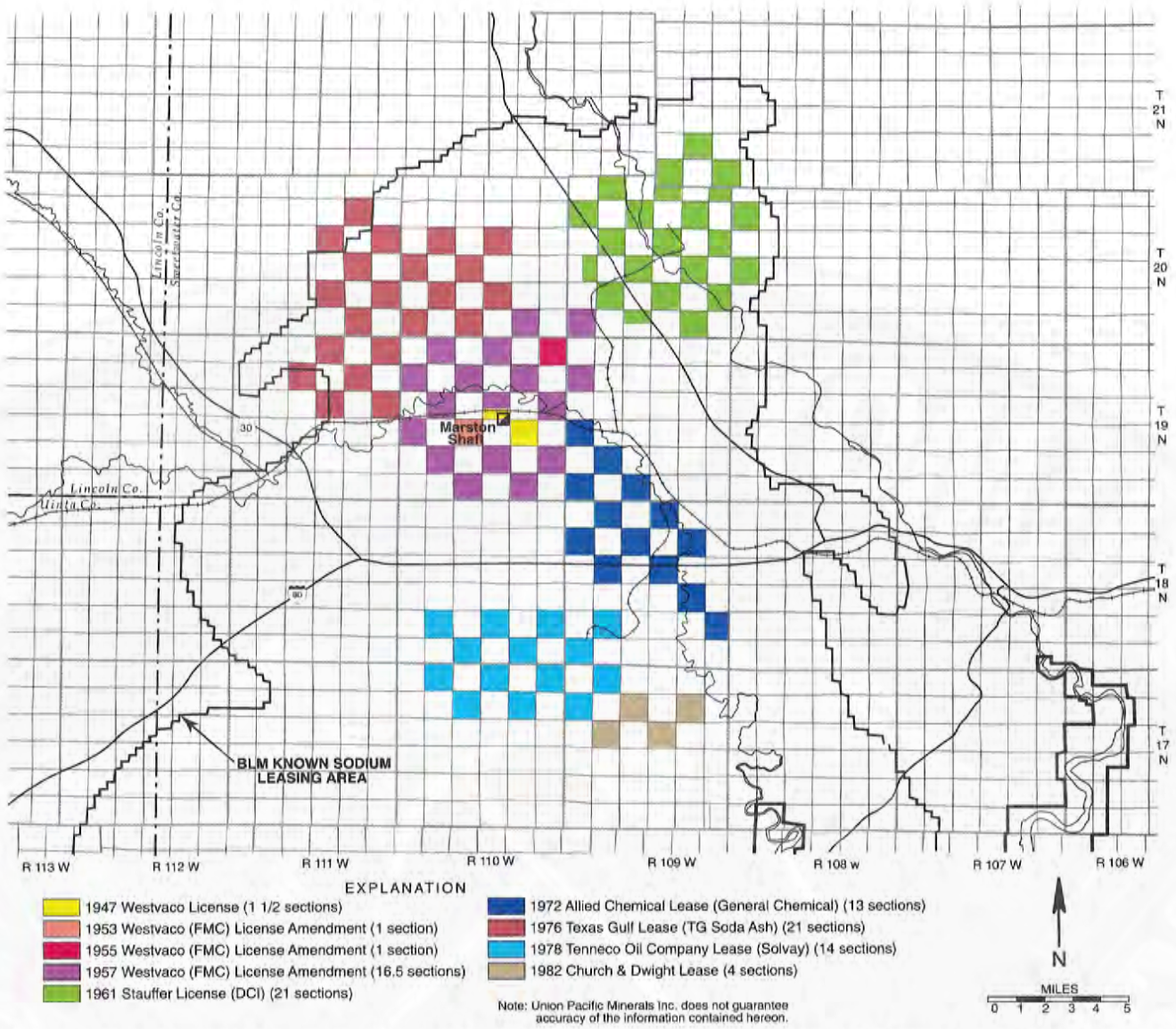


Figure 8. Map showing history of trona leasing (1947-1982) by Union Pacific Resources in the Green River Basin, Wyoming.

Union Pacific granted a sodium mining lease to Texas-Gulf Incorporated (the fourth producer) in March, 1976 covering 13,400 acres under 21 sections (**Figure 8**). The start-up of the mining and processing complex also took place in 1976.

The fifth producer, Tenneco Oil Company, acquired its original sodium mining lease covering 8900 acres under 14 Union Pacific sections in December of 1978 with the production facility becoming operational in 1982 (**Figure 8**).

While not currently operating a mining complex, Church and Dwight acquired a sodium mining lease covering 2560 acres under 4 sections of Union Pacific lands in January, 1982 (**Figure 8**). Church and Dwight does not mine and process trona but uses soda ash purchased from others to produce sodium bicarbonate and other products marketed under the Arm & Hammer name.

Summary

We have briefly covered the history of Union Pacific's leasing up to the current sodium mineral operators within the Known Sodium Lease Area of the Green River Basin. Since the granting of the original licenses and leases, there have been numerous amendments, consolidations, and supplements granted to the operators that have resulted, today, in the lease blocks (including federal and state holdings) as shown on **Figure 9**.

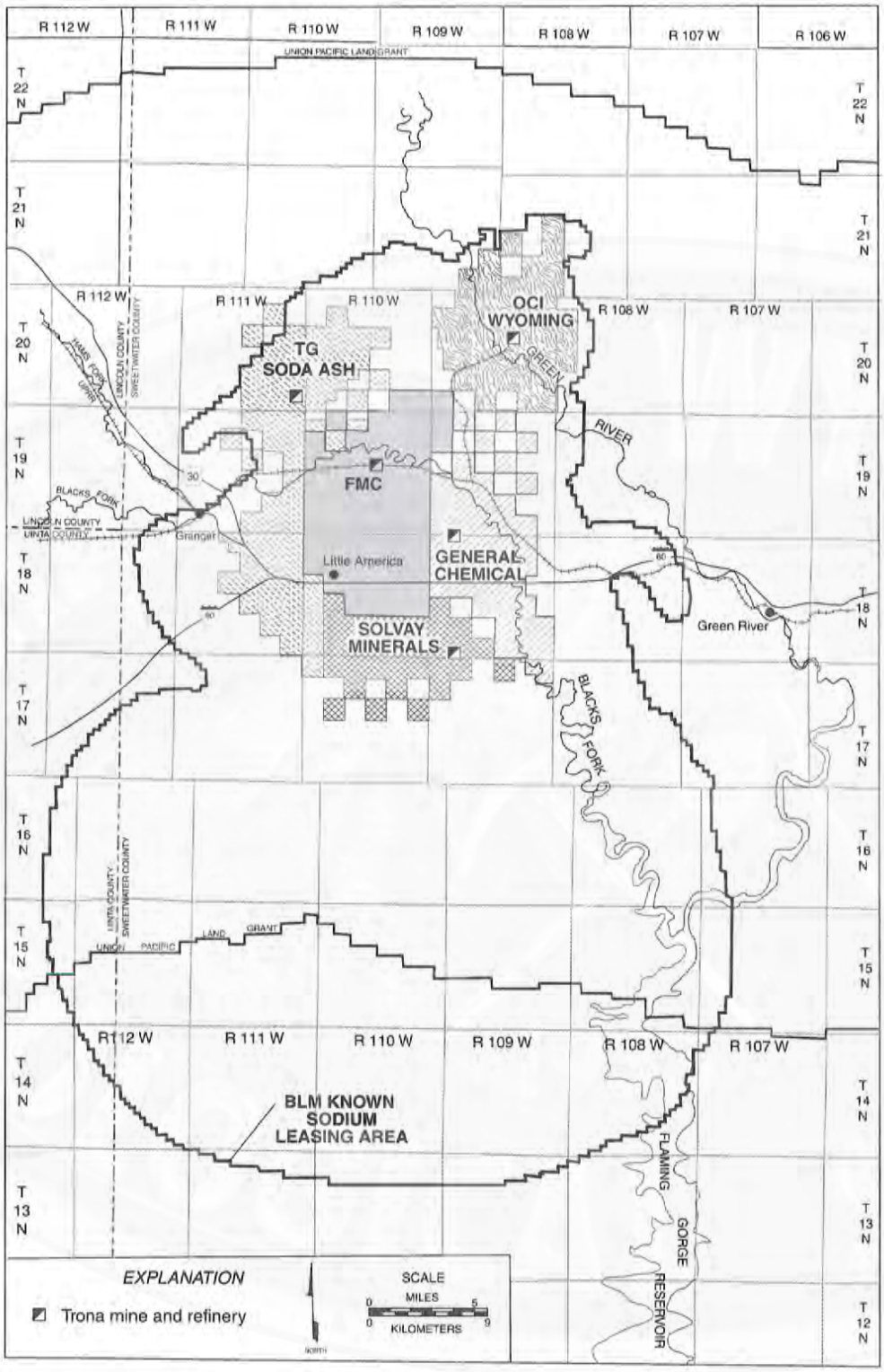


Figure 9. Major trona lease blocks in the Green River Basin, Wyoming. Includes federal, state, and private holdings controlled by the five companies currently mining trona.

UPR presently acts as lessor of a total of approximately 84,000 acres covered by active sodium mineral leases and licenses. Of the 84,000 acres, FMC (formerly Westvaco) holds 19,700 acres under two lease arrangements; OCI (formerly Stauffer) holds 15,300 acres under two lease arrangements and the OCI complex continues to be operated as a 51%-49% venture with UPR; General Chemical (formerly Allied) holds 11,000 acres under one consolidated lease; Tg Soda Ash (formerly Texas Gulf) holds 20,400 acres under two leases; Solvay (formerly Tenneco) holds 12,900 acres under three leases, and Church and Dwight holds 4500 acres under one lease. In total, about 225,000 acres are currently held under state, federal, and private leases within the Known Sodium Lease Area by the current producers and others.

While the terms and provisions of UPR's existing contracts are confidential and have evolved over time, UPR's current lease expectations with respect to a new entrant in the industry are first tied to insuring that the prospective lessee possesses the technical and financial capabilities to operate profitably. A competitive bonus and, currently, an 8% royalty on soda ash are expected. Other components of the lease arrangement include an advance royalty provision keyed to the lessee's entire mining operation (this being intended as a mechanism for equalizing production between the Union Pacific holdings and other lands), and comprehensive mining and production reporting requirements. Each

lease is unique and lease terms applicable to a particular transaction are not shared with other lessees or outside of UPR.

As mentioned earlier, Union Pacific Resources is a stand-alone company no longer affiliated with Union Pacific Railroad. This was accomplished through an Initial Public Offering in October, 1995 and was concluded with a spin-off from Union Pacific Corporation in October, 1996. As a part of this transaction, Union Pacific Resources acquired title to the Union Pacific land grant. UPR has become proactive since going out on its own and, late last year, was the successful bidder on two sodium lease tracts offered in the federal sodium lease sale. UPR's objectives for the future of trona are centered around the concept of expanding the Wyoming natural soda ash industry through working with their existing lessees and forming alliances with potential new entrants into the industry.

The author thanks Neil Brown, UPR's Principal Geologist, for providing much of the background material that has been presented in this paper.



Frontispiece: Aerial view of White River Nahcolite Company's mine and processing plant in the Piceance Creek Basin, Colorado about 48 miles northwest of the town of Rifle. Sodium bicarbonate is recovered by solution mining a 26-foot-thick nahcolite bed in the Green River Formation at a depth of about 2000 feet below the surface. July, 1998 photograph courtesy of Marie Mozden, Nederland, Colorado; pilot, Joseph Fox.

Solution mining of Colorado nahcolite

Roger L. Day
White River Nahcolite Minerals L.L.C.
Rifle, Colorado 81650

Abstract

The Green River Formation of the Piceance Creek Basin in northwestern Colorado is estimated to contain 30 billion tons of nahcolite ($NaHCO_3$). In 1991, White River Nahcolite Minerals (WRNM) started commercial nahcolite mining in the basin using a combination of horizontal drilling and hot water solution mining technology. Hot aqueous solution is pumped from the cavity to the surface facility where it is cooled, causing dissolved nahcolite to recrystallize as high purity sodium bicarbonate. Dewatering, drying, and sizing prepares this product for the U.S. Pharmacopeia (USP), food grade, industrial, and animal feed markets. WRNM's nahcolite solution mine has become an efficient, dependable, high-quality sodium bicarbonate source that has seen an increase in sales each year since start-up in 1991.

The primary mining interval is a 24- to 30-foot-thick, 80% nahcolite bed located 2000 feet below the surface. Two widely spaced production wells are connected by a horizontal borehole drilled near the base of the mining interval. A mining chamber or cavity is produced by the dissolution of nahcolite as hot solution passes along the horizontal borehole between the wells. Proper positioning of the chambers results in a chamber and pillar mining arrangement. Mining has produced 85 short tons per foot of chamber without signs of exhaustion. The anticipated chamber production is 220 short tons per foot. Chamber length has ranged from 1000 to 2000 feet.

Setting

White River Nahcolite Minerals (WRNM) solution mines nahcolite, a naturally occurring sodium bicarbonate mineral, on a 8222-acre Federal sodium lease located approximately 48 miles northwest of the town of Rifle in northwestern Colorado (**Figure 1**). The lease is located in the north central Piceance Creek Basin near the center of the saline mineral deposits within the Eocene Green River Formation. The lease is contained within the boundaries of T1S, R98W, 6th Principal Meridian in Rio Blanco County. Surface elevation ranges from 6200 to 6800 feet. The topography of the lease area is characterized by shallow alluvial valleys, broad soil-covered ridges, and mesas. Pinyon, juniper, and sagebrush are the dominant plants.

Geology

The uppermost stratigraphic unit in the lease area is the Uinta Formation. This formation consists of deltaic and fluvial sandstones and siltstones deposited during Eocene age. It contains no economic mineral resources. Also of Eocene age, and immediately below the Uinta, is the Green River Formation. It consists of a thick sequence of alternating lean and rich oil shales interbedded in certain areas with saline minerals, principally nahcolite, dawsonite, and halite. The thick sedimentary rocks beneath the Green River Formation are prospectively valuable for oil, gas, and coal.

The Parachute Creek Member of the Green River Formation is the principal resource interval in the basin. It averages about 1750 feet in thickness (**Figure 2**). The saline zone, approximately the lower 1000 feet of this member, contains the saline minerals nahcolite ($NaHCO_3$), dawsonite ($NaAlCO_3(OH)_2$), and halite (NaCl) along with oil shale. The top of the

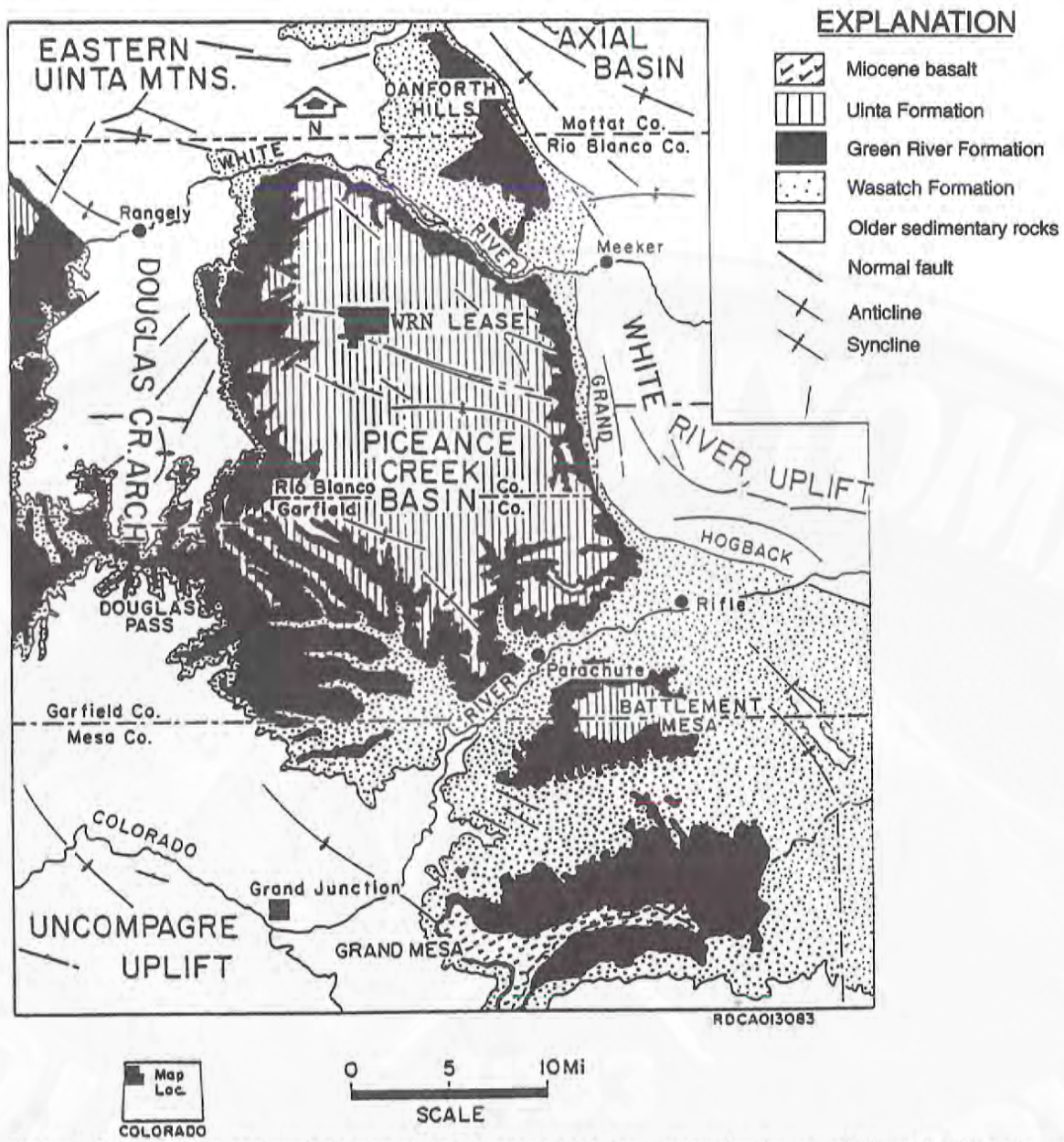


Figure 1. General index and geologic map of the Piceance Creek Basin area (after Tweto, 1979). WRN, White River Nahcolite Minerals L.L.C.

saline zone is referred to as the dissolution surface. In the leached zone above the dissolution surface all water soluble minerals were dissolved and removed as the aquifer system moved downward. Within the leached zone, the most economically promising oil shale interval is the Mahogany Zone. The Mahogany Zone is about 175 feet of rich oil shale averaging 29 gallons of shale oil per ton of oil shale. Beneath the Mahogany Zone down to the dissolution surface the generally leaner oil shales have fracture and collapse breccia, rubble zones, and cavities (voids) created by the dissolution of the soluble minerals.

Within the saline zone, nahcolite occurs in two major forms: a "disseminated" type, where the nahcolite consists of single or compound crystal bodies supported in a matrix of oil shale, and a "stratiform" type, where the nahcolite forms discrete mappable beds (Cole, 1983, unpublished report). Subdivision of these two types was proposed by Dyni (1974, 1981) and Cole (1982, unpublished report). Subtypes of stratiform nahcolite are distinguished by texture as granular or microcrystalline. Granular nahcolite occurs primarily in the upper and lower salts

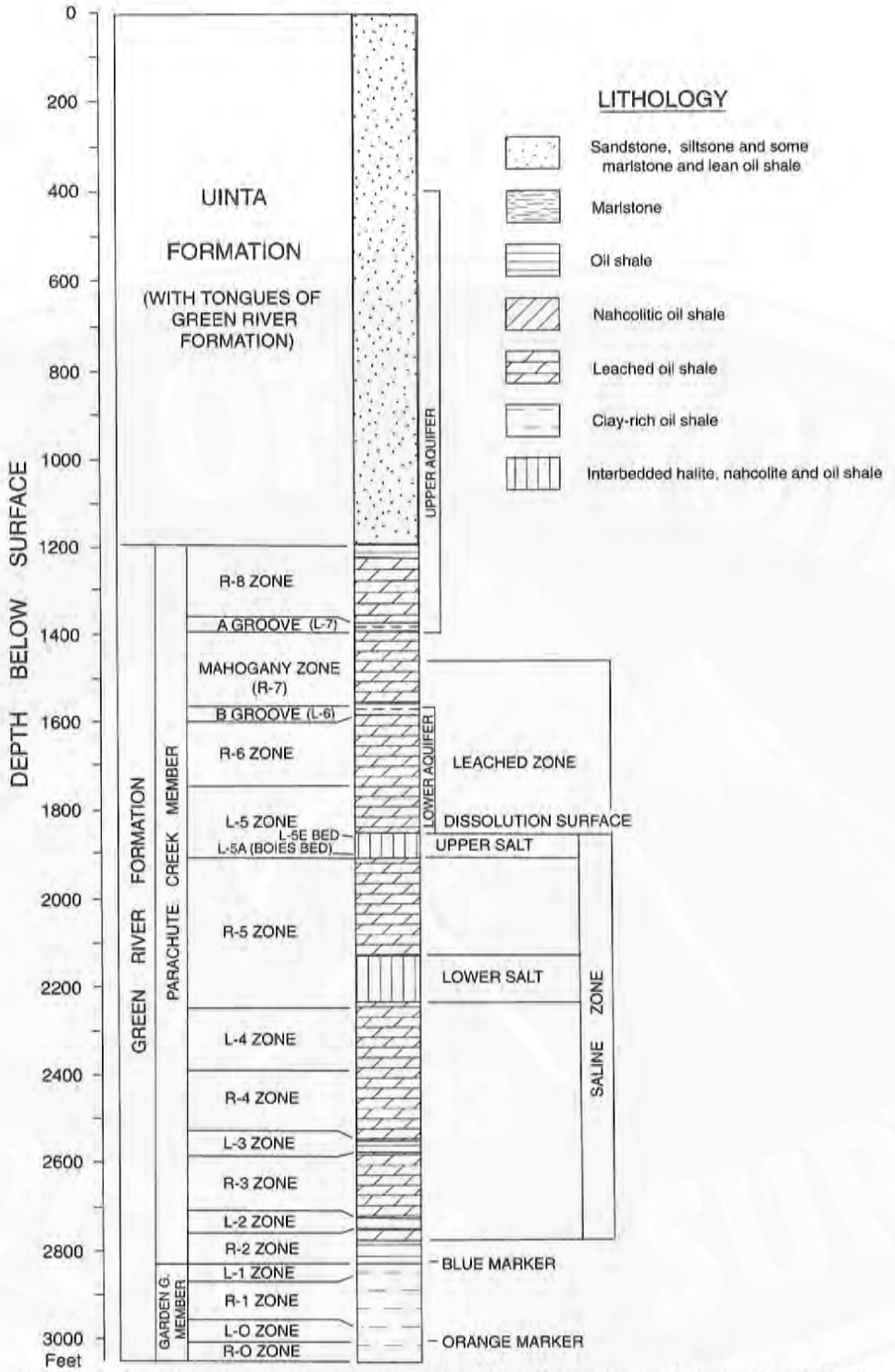


Figure 2. General stratigraphic column of the Uinta Formation and upper Green River Formation in the area of White River Nahcolite's lease in the Piceance Creek Basin.

where it is associated with or replaced by halite. White granular nahcolite often has porosity and contains stringers of oil shale. The thickest and richest stratiform nahcolite horizon in the saline zone is the Boies bed (**Figure 3**). In WRNM's well field area, this bed can be more than 30 feet thick and contain about 80% nahcolite.

Microcrystalline nahcolite is generally a dense, tan, nonporous variety found in beds 0.5 to 10 feet thick. In the upper and lower salts it is often found interbedded with white crystalline nahcolite and salt. The best example of tan microcrystalline nahcolite is the Love bed which is about 7 feet thick and contains about 65% nahcolite.

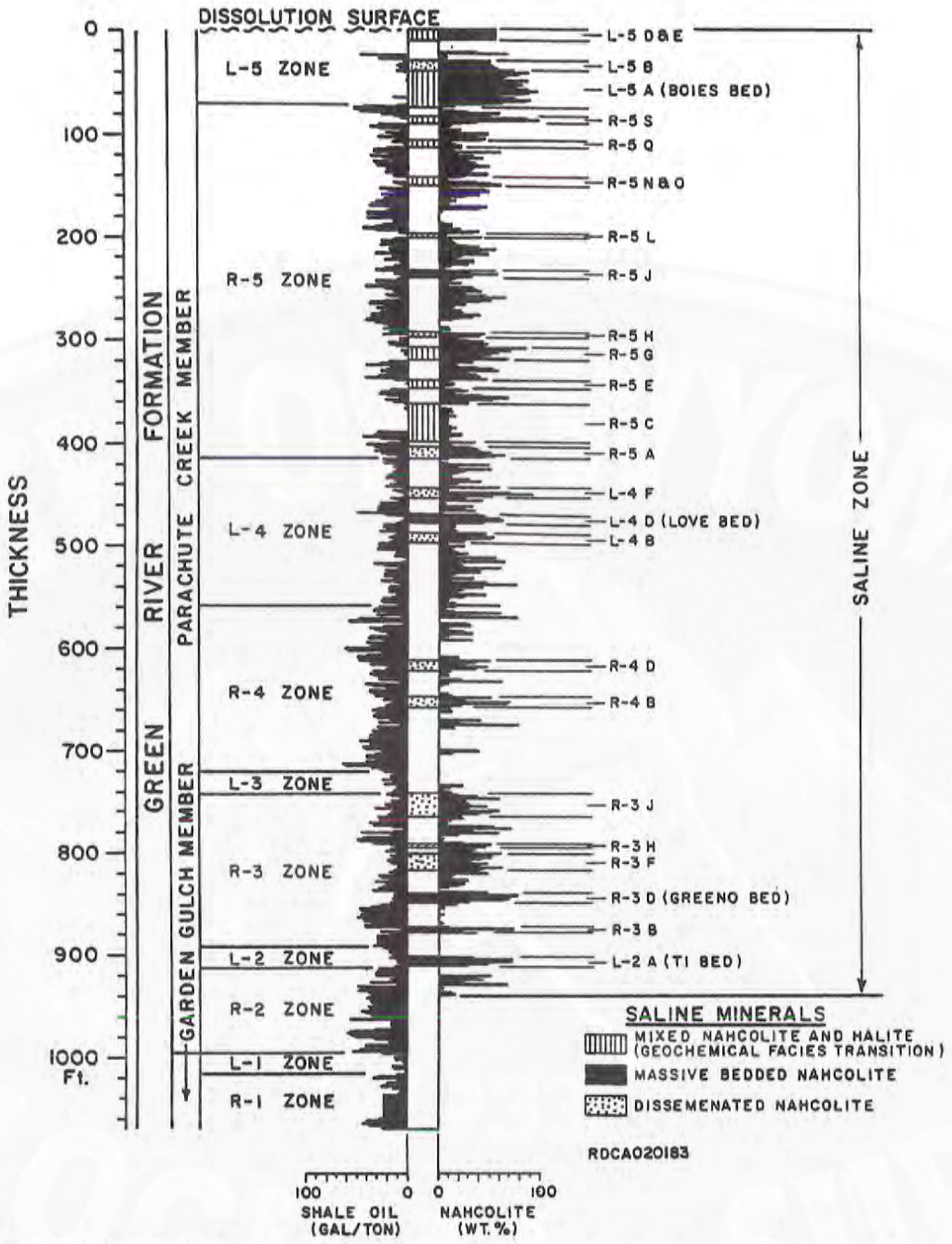


Figure 3. Stratigraphy of mappable saline mineral horizons in the saline zone of the Parachute Creek Member of the Green River Formation, based on Shell Oil Company core hole 22X-1 (modified from Dyni, 1974, 1981).

Nahcolite which occurs as scattered bodies in an oil shale matrix and does not form continuous beds has been called disseminated. Disseminated nahcolite is subdivided into two major groups: crystal aggregates and individual crystals. In both types, individual nahcolite bodies are isolated from each other by the enclosing oil shale matrix. Bodies may be separated by as little as 0.04 inch or by 3 feet or more. Concentration of nahcolite bodies within a given oil shale interval is often high enough for stratigraphic mapping.

Aggregates are a solid mass of two or more nahcolite crystals. They commonly occur in oil shale and often have a rind (up to 0.4 inch thick) of nonmetallic "sooty" pyrite or marcasite. Some aggregates may be totally replaced by iron sulfide (Cole, 1983, unpublished report). Aggregate bodies normally range in size from 0.4 inch to 3 feet, but have been reported in the Horse Draw mine up to 10 feet long and 3 feet high. These large aggregates may appear as beds when penetrated by drill core. Close examination of

the crystals in an aggregate often shows they are separated from each other by less than 0.2-inch-thick septae of kerogen-like material.

The second type of disseminated nahcolite is individual crystals scattered throughout oil shale. These crystals are often rectangular or bladed and less than 0.2 inch in length. These are classified by crystal abundance as 1) sparsely disseminated, up to 20% by volume; 2) normally disseminated, 20 to 40%; 3) semi-honeycomb, 40 to 60%; and 4) honeycomb, above 60%. Honeycomb refers to the drill core appearance after drilling mud leaching has exposed the oil shale matrix. This oil shale matrix often has unusually high kerogen content, imparting the feeling and resiliency of a sponge. Honeycomb nahcolite crystals also have a high kerogen content, a characteristic which gives the nahcolite a black to very dark brown color. The two major honeycomb intervals are the Greeno bed and TI bed near the base of the saline zone. They are each 6 to 7 feet thick and have a 60 to 70% nahcolite content.

Dyni's (1981) study of 10 core holes in the area shows that aggregate bodies represent about 62% of all nahcolite in the saline zone while crystals comprise 24%. Stratiform (microcrystalline and granular combined) nahcolite makes up about 14% of the nahcolite resource in the Piceance Creek Basin.

Hydrology

The Piceance Creek Basin hydrology has been extensively explored as part of energy industry and government oil shale development activity. This gives a solid regional hydrologic foundation for nahcolite development.

Regionally there are two major bedrock aquifers, the upper and the lower (**Figure 2**). The aquifers are separated by the 175-foot-thick Mahogany Zone. The top section of the upper aquifer is located in low porosity Uinta sandstone. The remaining portion of the upper aquifer and all of the lower aquifer is found in very low primary porosity oil shale. In oil shale formations, water storage is almost entirely within secondary porosity fractures and voids created as the groundwater leached the soluble salt nodules and layers within the oil shale. The highest groundwater yield of such a zone is the A Groove which produced as much as 1100 gallons per minute during mist drilling. Regionally, both the upper and lower aquifers have generally poor water quality but, nevertheless, are protected as future sources of potable water.

Hydrology testing and evaluation in WRNM's nahcolite well field area determined the baseline and site specific hydrologic knowledge needed to develop the drinking water aquifer protection and monitoring aspects of the mine plan. This site specific knowledge differed from the regional in two major ways. The confining Mahogany Zone is leaky in the well field area, and the bottom portion of the lower aquifer is isolated. The isolated aquifer section is under less pressure and is saline (up to 80,000 ppm total dissolved solids recorded). The water in the isolated aquifer section has been found to have no drinking water potential and has been exempted by the Environmental Protection Agency (EPA).

Mining interval

WRNM solution mines the Boies bed. In the well field area, the Boies bed is located about 2000 feet below surface and 30 to 40 feet below the dissolution surface. The Boies bed is unusually thick–two to three times the thickness of any other known nahcolite bed (**Figure 3**). The white, granular nahcolite is low in organic content and ranges in purity from 80 to 85% $NaHCO_3$. In the mining section the impurities consist primarily of oil shale interbeds; the nahcolite itself is quite pure in most locations.

Within the WRNM lease area, the exceptional thickness and nahcolite purity of the Boies bed, and even the thin horizontal oil shale interbedding, combine to give an exceptional solution mining opportunity. PB-KBB's core lab in Germany found the leach rate of Boies bed nahcolite was as high as simulated core made of pure sodium bicarbonate. Hazen and Cliffs Engineering laboratories showed that these interbeds act as a barrier to solution mining. The natural sandwiching of highly leachable nahcolite with horizontal barriers to vertical leaching is likely what causes good horizontal development of the mining chambers. The interbeds are thin and will fail, but only after wide undercutting. Then, on failing, the nahcolite above is dissolved across a wide exposed surface from below. Without the horizontal leach barriers, leaching would advance rapidly upward and undercut only at the roof, leaving much of the nahcolite unmined.

Originally, cavity size was limited to 40,000 short tons per 1000 feet because it was assumed that preferential vertical leaching would leave the walls sloping upward and that only the roof would be undercut. In such a case, insoluble debris buries the upwardly sloping walls and floor and nahcolite below the debris would be lost. The high cavity recovery and confirming sonar surveys demonstrate that good horizontal cavity development is being naturally achieved without the use of the gas caps typically used in vertical well solution mining.

Protection of oil shale minability, while mining nahcolite, is another critical issue. Restrictions placed on Federal sodium mineral leases in the Piceance Creek Basin have roots dating back to World War I when domestic oil resources were a national security issue. The Bureau of Land Management (BLM) used this lease restriction to reject alternate nahcolite solution mining plans proposed by WRNM. These rejections were to protect the oil shale deeper in the saline zone where the distance from the aquifer increased the potential for oil shale mining in the future.

The Boies bed generally dips from 1.5 to 2 degrees to the northeast but is subject to local undulations. The bed consists of two distinct facies, nahcolite and nahcolitic halite. Halite limits nahcolite solution mining. Solution mining is further limited to nahcolite facies where the bed has not been invaded by groundwater. The third limiting factor determining minability is a 100-foot mining restriction along the lease boundary. Although the minable Boies bed is limited by these factors, the gross resource in the high grade (80+%), 24-foot-thick section of the Boies bed is 80 to 100 million short tons of nahcolite. In addition to the prime Boies bed resource, the mining interval also includes a lower 8-foot section of the Boies bed and the resource in the roof to the dissolution surface. In much of the well field area, this doubles the gross nahcolite resource contained in the mining interval. The current mine plan calls for recovery of 48,000 short tons of nahcolite per acre. The recovery may come from the Boies bed and/or the roof section.

The 48,000-short-ton-per acre nahcolite recovery mine plan results from WRNM's experience, improved technology, and subsidence impact evaluations by Aggapito and Associates. Potential impacts to oil shale minability, sources of underground drinking water, and surface land uses were found acceptable. These potential subsidence impacts were more than offset by reduced impacts from drilling, roads, and well pads. Mining at 48,000 short tons per acre with today's chamber spacing requires recovery of 220,000 short tons per 1000 feet of length. Should this potential be fully realized, a single 3000-foot cavity would provide over 650,000 tons, displacing the environmental and cost impact of 16 original mine plan cavities. One aspect of the subsidence impact evaluation was that, in this case, horizontal solution mined cavity shape was unimportant. Tall slender cavities or short wide cavities have similar subsidence impact potential. The subsidence monitoring program in the well field has been expanded to confirm these subsidence impact predictions.

The two currently operating cavities have been mined to about 85,000 short tons per 1000 feet. These cavities have shown no sign of approaching excessive size. The mining rate per cavity has been high enough that a single cavity can support full plant production. But WRNM prefers the production stability of multiple (two or three) cavities, each at a different stage of production.

Nahcolite solution mining

In 1982, Ed Rosar, president of Industrial Resources Inc. (now WRNM) teamed with Cliffs Engineering and Hazen Research to develop a hot water nahcolite solution mining plan. The use of individual vertical solution mining wells to mine the Boies bed was examined. In a similar mining situation, a 1949 solution mining test by US Borax in California failed. This attempt failed because insoluble materials released during leaching covered the walls, preventing solution contact with the ore.

A potential solution to the problem experienced by US Borax existed in the 1929 undercut solution mining patent by Allied Chemical. PB-KBB laboratories examined Boies bed nahcolite core and proposed a vertical well solution mine plan using a gas cap undercutting method. This was technically less challenging but failed to offer the potential for drilling costs under $5 per ton like the horizontal drilling alternative now developed by WRNM.

In the early 1980s, the oil and gas industry was developing the ability to accurately drill long horizontal holes. This evolving drilling technology appeared to have solution mining potential. Its mining potential was first demonstrated in 1983 when WRNM successfully connected two vertical wells in the Boies bed with a horizontal drill hole. Following the horizontal drilling, a hot water leaching and cooling crystallization process was developed and demonstrated during

pilot scale nahcolite production. From this work, U.S. Patent 4,815,790, "Nahcolite Solution Mining Process" was issued to Edward C. Rosar and Roger Day on March 28, 1989 (**Figure 4**). The patent contains 46 claims for nahcolite mining which cover single and multiple well solution mining, horizontal hole development, undercutting in the cavity using an air cap, wellhead pressures below 150 psi and cavity tem-

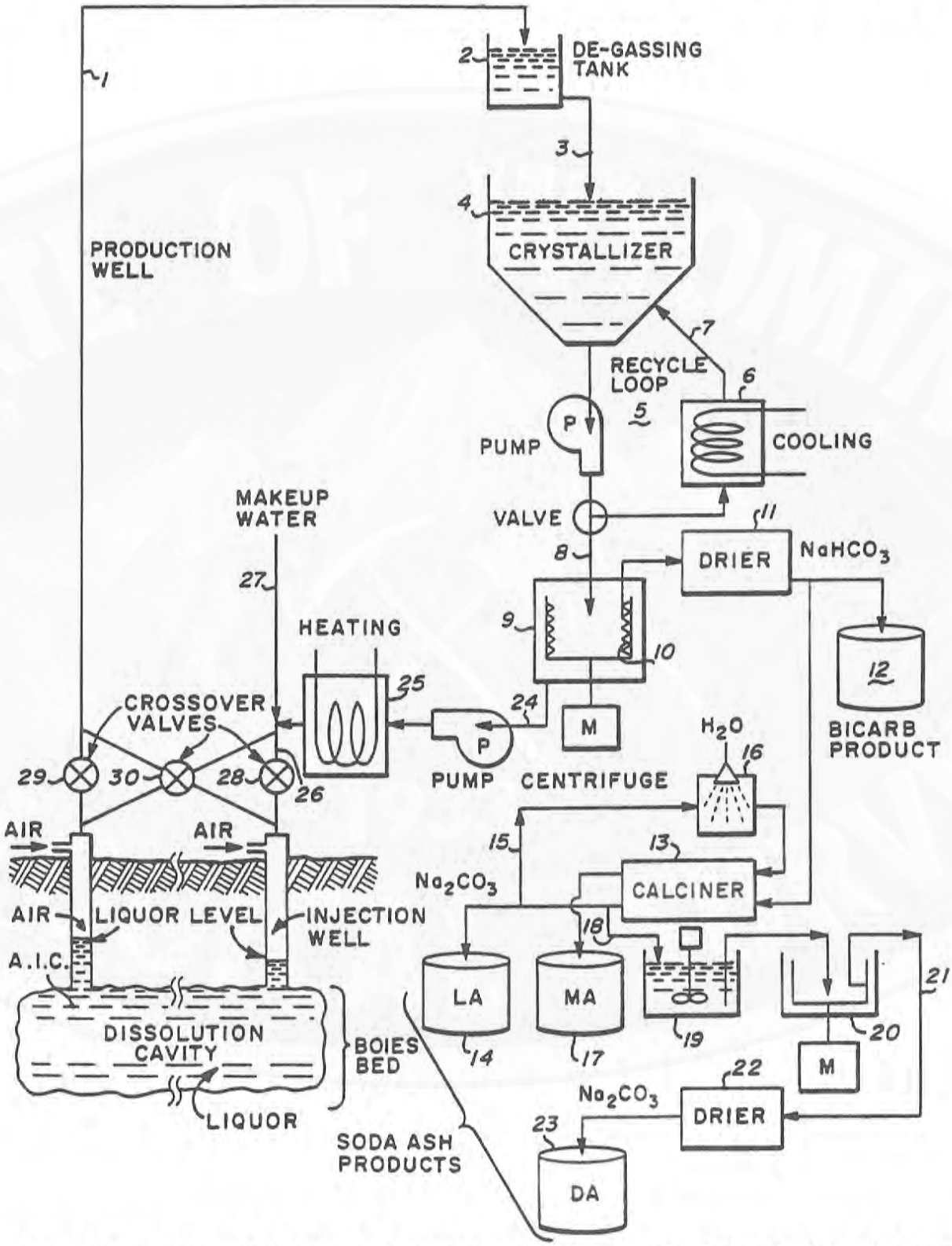


Figure 4. Schematic drawing of U.S. Patent 4,815,790 issued to E.C. Rosar and R.L. Day on March 28, 1989 for the mining and processing of nahcolite to produce soda ash.

peratures below 250°F, cooling crystallization to recover the sodium bicarbonate, washing of the crystals to produce a purified sodium bicarbonate, and calcining the sodium bicarbonate to produce soda ash.

A 125,000 stpy (short tons per year) commercial plant to recover industrial grade sodium bicarbonate from Boies bed nahcolite began operating in 1991. Plant changes in 1993 upgraded product quality to a food grade that exceeds the purity standards set by the USP. The current Environmental Impact Statement (EIS) includes expanding capacity to 500,000 stpy.

The typical drilling program for developing long horizontal cavities adopted by WRNM is summarized as follows. A vertical production well is completed by cementing a casing to the Boies bed roof and leaving an open hole across the primary mining interval. The directional well is then drilled to approach the Boies bed roof at a predetermined angle. Casing is slid around the curve of the directional well and cemented to the Boies bed roof. The directional drilling advances out of the casing, running parallel to and just above the mining interval floor, and is directed to intersect the vertical production well.

During production, the mining solution is pumped through the tubing strings suspended in the cemented casings. Thermal insulation is provided by high pressure air in the annulus gap between the tubing string and the cemented casing. This also better insures the mining solution will not enter the aquifer system should the cemented casing develop a leak. Downhole submersible centrifugal pumps lift the solution from the cavity.

The drilling and mining program has advanced substantially since 1990. Advancements include:

1) Horizontal drilling started at 1000 feet for cavity 1. The longest chamber to date is 2000 feet long. The mine plan includes chambers 3000 feet and longer in the future.

2) Recovery per 1000 feet of cavity started at 40,000 short tons in the original mine plan. The two currently operating cavities are in the 85,000 short tons per 1000 foot range and show no sign of being overextended. Recovery of 220,000 short tons per 1000 feet is planned.

3) Submersible pumps are used to eliminate pressurized cavities. No longer does a roof fall or a fracture to the aquifer threaten production or shipments to our customers.

4) WRNM is now better able to identify and isolate cavity sections which have excessive salt (NaCl).

5) Numerous exploration holes and mining experience since 1991 have better identified the location of salt problems in the well field area. Starting with cavity 4, the field was successfully rearranged to avoid salt.

6) Improved directional drilling control and logging data improves horizontal hole position in the resource. This has improved nahcolite solution mining performance while avoiding the halite producing strata.

The 1000-foot cavity 4 is the first to be drilled and mined under the 1996 revised mine plan. The new mine plan is initially focused on short 1000-foot cavities, avoiding salt underground and increasing the nahcolite recovery per foot of cavity. Longer cavities will follow since they will double and triple production at minor additional drilling cost or risk. The major drilling expense and difficulty is drilling the leached zone, due to the aquifer leaching impacts. The fast and predictable horizontal drilling in the Boies bed presents low additional cost per mining chamber footage.

Sodium bicarbonate production

The pregnant liquor from the cavity is crystal clear, containing no detectable sludge or oily substances. It has the appearance of 7 UP® soda pop including the carbonation bubbles. Food grade sodium bicarbonate crystals are produced by simply cooling the hot pregnant liquor from the cavity to about room temperature. Controls must be used to crystallize the preferred crystal size and shape required for good processing efficiency and to meet customer expectations related to particle size distribution, dusting, caking, etc. The crystallizer product is thickened, washed, and dewatered in a centrifuge and flash dried. The dried product is differentiated by particle size distribution into all major commercial sodium bicarbonate grades. WRNM expects production to continue growing to the 125,000 stpy plant capacity and is currently in the design stage of a project doubling the plant capacity.

Perspective and conclusion

Solution mining of the Boies bed by circulating hot water through horizontal bore holes was conceived and field tested in 1983. This produced a few hundred tons of sodium bicarbonate which was used in a demonstration of dry flue gas desulfurization. Although this first mining test was successful, it left many unanswered questions. It was recognized that true piloting of this solution mining concept would require mining three commercial-sized cavities, each at least 1000 feet long with 42 short tons of nahcolite per foot removed. Only at this scale could mining performance be measured and the impacts on rock mechanics determined.

Product disposal costs for even one commercial-sized cavity were found to be unacceptably high. Therefore, a 125,000 stpy production facility was constructed in 1990 (**Figure 5**) to produce a salable product from the large-scale pilot test of solution mining. Although the product was initially to be sold for flue gas desulfurization, this market never developed to a commercial size. This required moving first into the animal feed market and eventually into the food grade markets. These markets forced WRNM to achieve active control over the crystallization and screening to recover multiple products based on particle size.

Test solution mining encountered just two problems of significance. The first was occasional concurrent mining of halite with the nahcolite. This problem has been addressed by better learning the locations of halite in the Boies bed so that cavities can be developed where halite constitutes an acceptably low fraction of the soluble reserves.

The other problem was failure of the pressurized cavities. Cavities were sufficiently pressurized by the injection fluid to force the product brine to the surface at the recovery well. This concept works well where the cavity is leakproof, since a production pump is not required. WRNM found that when the Boies bed is solution mined, leaks to the aquifer often develop. Once this was recognized, the solution to the problem was simple–install a pump to maintain cavity pressure equal to the pressure in the aquifer above. Actually, once a pump was installed, the issue of maintaining cavity integrity (necessary to have a leakproof cavity) was no longer relevant. This has allowed much more nahcolite per foot to be mined from a cavity: for example, the mining goal of 42 short tons per foot, when cavity integrity had to be maintained, increased to 220 short tons per foot when subsidence impact potential and resource recovery became the primary issues.

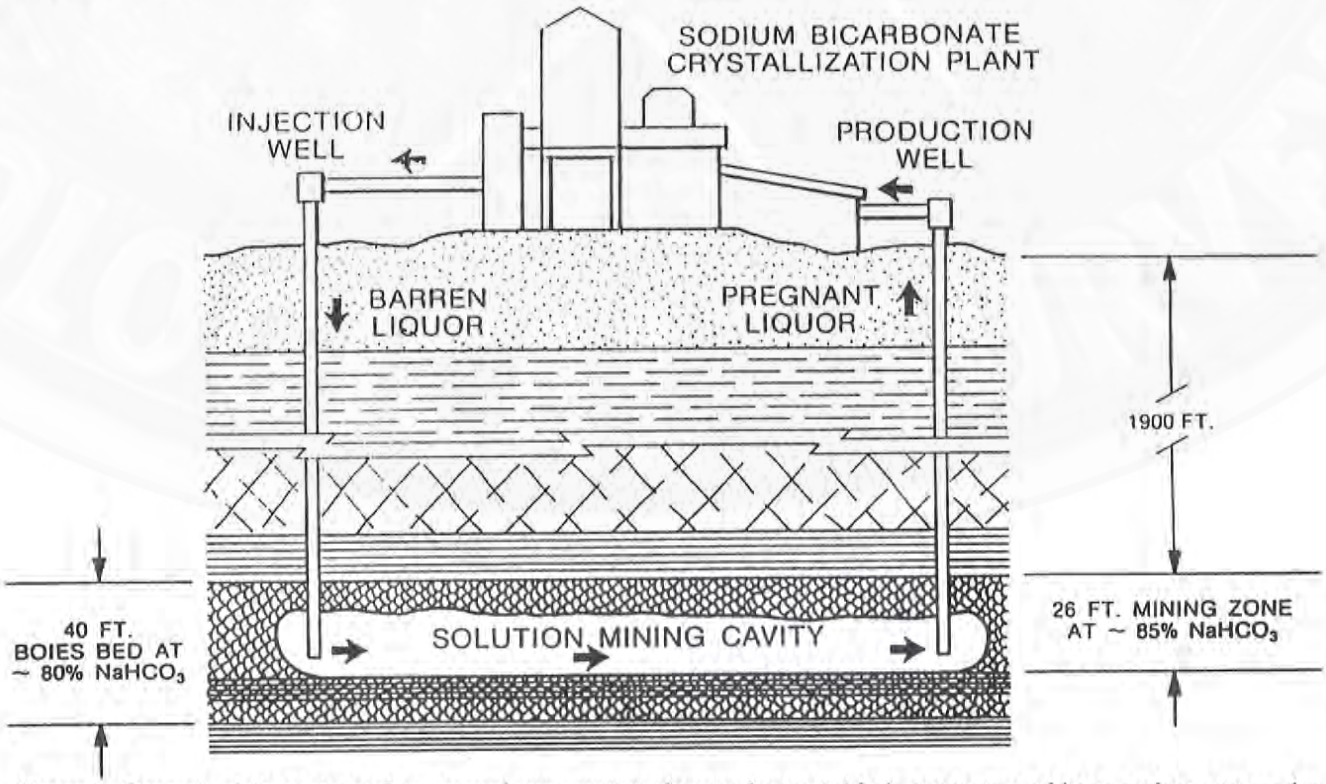


Figure 5. General solution mining diagram and cross section showing horizontal hole geometry and basic surface process for solution mining of the Boies bed at cavity 1, WRNM's nahcolite mine, Colorado.

There are two ways that the drilling costs for solution mining can be reduced. One is to recover more tons per foot of drilled cavity as discussed above. The other is to drill longer cavities–WRNM has also made progress on this front. Of the four existing cavities, two are 1000 feet long, one is 1500 feet long and one is 2000 feet long. WRNM has plans to drill even longer cavities where the length would be limited primarily by drilling technology and by the geologic properties of the Boies bed.

As described earlier, problems were encountered developing this project. These have been addressed and successfully circumvented by WRNM. We are looking forward to expanding our operations, secure in the knowledge that the technology necessary to be successful is available.

References cited

Dyni, J.R., 1974, Stratigraphy and nahcolite resources of the saline facies of the Green River Formation in northwest Colorado, *in* Murray, D.K., editor, Energy resources of the Piceance Creek Basin, Colorado: Rocky Mountain Association of Geologists, Twenty-fifth Field Conference Guidebook, Denver, Colorado, p. 111-122.

Dyni, J.R., 1981, Geology of the nahcolite deposits and associated oil shales of the Green River Formation in the Piceance Creek Basin, Colorado: Ph.D. Dissertation, University of Colorado, Boulder, 144 p.

Tweto, O., compiler, 1979, Geologic map of Colorado: U.S. Geological Survey, scale 1:500,000 (color).

Feasibility of trona solution mining

Edward C. Rosar
ECR Consulting
Lakewood, Colorado 80228
and
Wolfram H. Kube
Kube Consulting
Denver, Colorado 80237

Abstract

This paper discusses the present status of solution mining cavities which are developed by directionally controlled drilling techniques to produce elongated cavities as opposed to hydrofractured cavities. Drilling accuracy, effecting communication, and projected costs of drilling and completion are covered. Also, estimated operating costs for proprietary technologies as developed by the authors are included for the congruent dissolution of trona. Based on conservative cost estimates used for this presentation, the solution mining of thick trona beds in Wyoming appears to be economically viable.

Introduction

A number of primary factors affect the commercial feasibility of a trona solution mining operation: design of stable solution mining cavities; development and cost of solution mining cavities; trona bed thickness and quality; selection of the appropriate solvent in view of trona's incongruent solubility; dissolving rate of trona; method and cost of treating the recovered solution prior to the final refining step in conventional crystallizers; and recovery of the sodium carbonate values from the solution remaining after solution mining has been terminated in a cavity.

In our opinion, solution mining of soluble evaporite beds, such as trona deposits, should be performed in horizontally confined elongated cavities, comparable to a chamber and pillar mining method. These cavities would be initially developed by employing directional drilling techniques. This method of solution mining is viable at depths where solution mining utilizing hydrofracturing is impractical because of the likelihood of producing vertical rather than horizontal fractures.

At shallower depths, less than about 1500 feet (457 m) to 1800 feet (549 m), hydrofracturing can produce a horizontal fracture from a vertical well and communicate to one or more other vertical wells. However, it would be difficult to develop the cavities in a manner that provides a stable configuration and prevents roof failure. The stratigraphic sequence of the saline section in the Green River Basin consists of alternating beds of oil shale, trona, and marlstone (Garrett, 1992), with the trona beds being the more competent structural members. Under these conditions only a limited roof span can be maintained in a tabular cavity before roof control is lost. Horizontal drilling permits the development of elongated cavities to design specifications, and assures their structural stability during the solution mining operation.

Demonstrated viability of technology

The first successful commercial operation using modern directional drilling techniques to produce horizontal cavities occurred in the Piceance Creek Basin of northwestern Colorado. The mineral nahcolite, a naturally occurring sodium bicarbonate, was extracted from a 25-foot (7.6 m)-thick bed by solution mining at a depth of 2000 feet (610 m) using the methods of Rosar and Day (1989). The first horizon-

tal commercial cavity was developed in 1990 with a length of 1000 feet (305 m). The second cavity was drilled in 1993 and allowed a developed length of 1500 feet (457 m). In 1994 a third horizontal hole was drilled for solution mining of a 2000-foot (610 m)-long cavity. A fourth horizontal hole was planned to be drilled for a length of 3000 feet. All horizontal holes were drilled to communicate with a vertical target production well which is drilled for each cavity. In the second and third cavities the horizontal hole was drilled 500 feet (152 m) past the vertical well; thereby allowing a portion of the cavity to retreat back to the vertical well.

Directional drilling and completion

Rock mechanics evaluation

Prior to the cavity drilling operations, oriented drill core should be taken of the floor rock, evaporite bed, and roof rock, and analyzed in a rock mechanics facility in order to determine the rock properties and the direction of the major and minor lateral force fields. With this information the long axes of the cavities would be oriented perpendicular to the direction of the major lateral force field which in turn aids in the support of the cavity roof. The other determined physical rock properties, such as tensile and compressive strengths, elastic modulus, shear modulus, angle of internal friction, and Poisson's ratio, are used for pillar and roof design.

The injection directional well from which the horizontal hole will be drilled is located at a point where the alignment between this well and the vertical target production well is perpendicular to the major lateral stress field as determined by the oriented drill core.

Initial drilling procedures

After the 15-inch (381 mm) OD (outside diameter) surface casing is installed and cemented, a typical cavity development procedure is to drill a 12¼-inch (311 mm)-diameter vertical target production hole with or without directional control. The hole is stopped at the top of the target evaporite bed. The entire hole is surveyed during the drilling operations. The open hole is logged using sonic, gamma, neutron, and caliper tools. A 9⅝-inch (245 mm) OD steel casing is installed in the hole and cemented in, preferably to surface. After the cement has set for about 48 hours, a cement bond log is run. The well is reentered and drilled as an open hole to the floor of the evaporite bed. This open hole can vary from 8¼ inches (210 mm) to 6½ inches (165 mm) in diameter.

Initially the drilling procedure for the directional hole is the same as for the vertical hole. After the surface casing is installed and cemented, a 12¼-inch (311 mm)-diameter vertical hole is drilled, surveyed, and stopped at the KOP (Kick Off Point). Starting at the KOP, the drill hole will be curved at predetermined angles to tangentially intercept the bottom of the evaporite bed. The chosen initial angle is 20°per 100 feet (30.5 m) of arc. This translates to a 286.6-foot (87.4 m) radius. In order to drill at this angle, the hole size diameter must be reduced to 8¾ inches (222 mm) to accommodate the positive displacement motor (PDM), which is also known as a mud motor, in a 6½-inch (165 mm) OD housing. The PDM rotor is a screw that is rotated by a fluid forced through the drill pipe. The PDM in turn rotates the drill bit. The drill pipe does not rotate. The housing is bent to drill at the predetermined angle around the curve. Azimuth of the drill hole can be controlled with a slight rotation of the drill string on the surface.

GeoSteering® tool system

To measure the location of the drill hole, one of the available directional technologies uses the GeoSteering® tool of Anadrill, a subsidiary of Schlumberger. The GeoSteering® tool can be installed behind the 8¾-inch (222 mm) bit for real-time control of bit orientation. It also measures lithologic changes through focused gamma ray and/or resistivity, and may be used to determine the distance of the bit above the floor of a trona bed (**Figure 1**). These measurements are transmitted to a MWD (Measurements-while-drilling) unit behind the PDM by wireless telemetry. The data measurements from the MWD unit are recoded and transmitted by a Mud Pulse Siren® (**Figure 2**) through the pipe's internal mud column to the surface at rates up to 10 bits per second in real time. The IDEAL® system of Schlumberger (**Figure 3**) is an integrated well site information system which permits the driller to respond rapidly to changing downhole conditions. From the information received by pulse telemetry, the driller can change the drillhole direction by rotating from surface or by varying the weight on the bit.

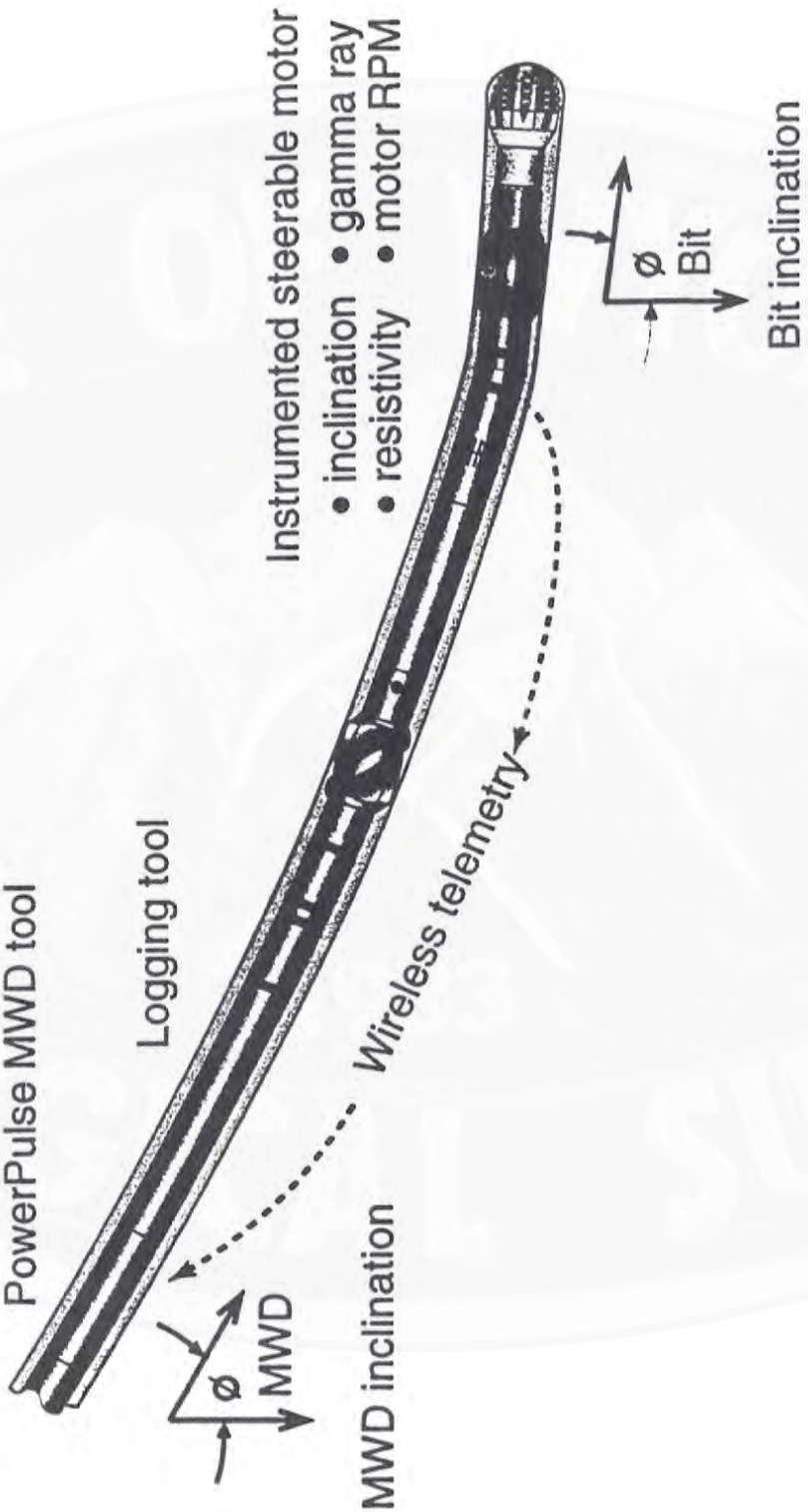


Figure 1. The GeoSteering® tool of Anadrill (Schlumberger) using wireless telemetry for measurements (at the bit) while drilling (MWD).

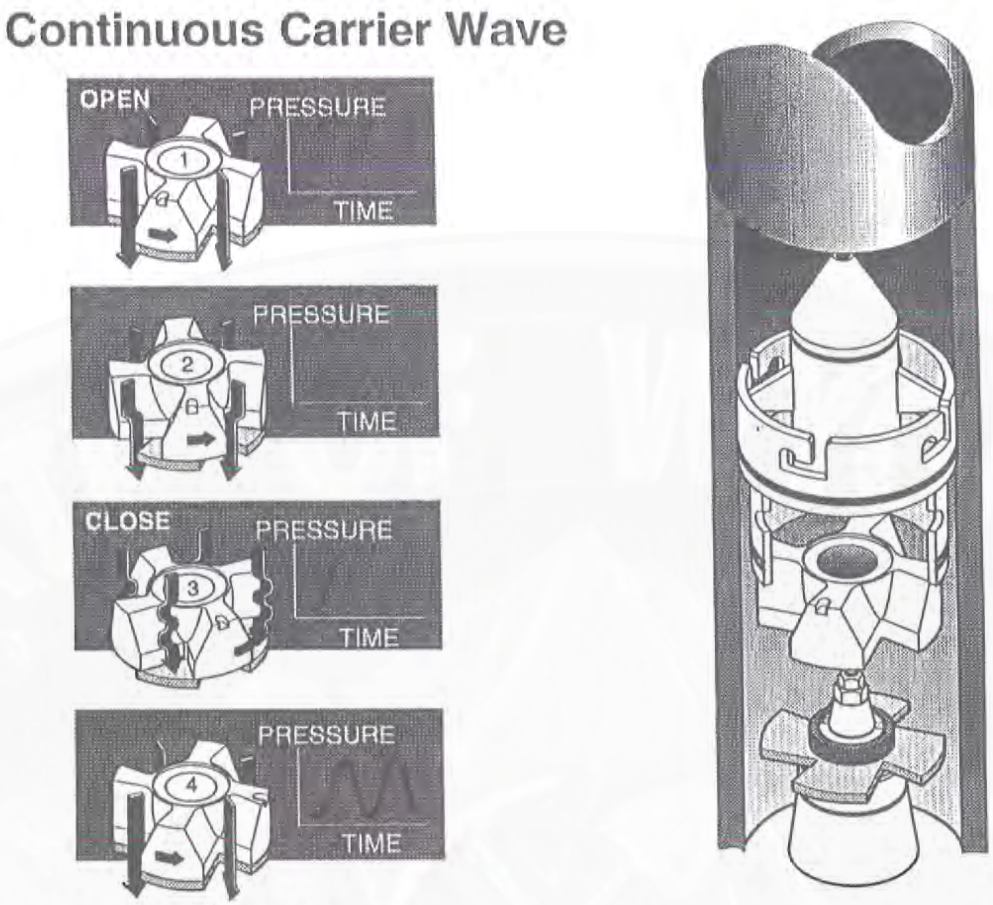


Figure 2. The Mud Pulse Siren® of Anadrill, used to transmit data to surface through the drilling mud system.

Wet Connect Steering Tool System®

Another directional technology is the Wet Connect Steering Tool System® of Bighorn Directional Incorporated of Westminster, Colorado, which appears to be a simple and reliable system. The steering tool is located in a monel collar that is located about 40 feet (12.2 m) behind the drill bit. Normally, measurements are taken at least every 30 feet (9.1 m) around the curve which give the directional driller the planar coordinates, azimuth, length of the drill hole (closure), true depth, gamma ray log, and temperature. Since the data collection by the steering tool takes place at a greater distance from the drill bit, drilling decisions cannot be made as promptly as in the case where measurements are obtained right at the bit. The wet connect system allows a wireline connection that can be "plugged in" or "unplugged" (when adding a drill pipe) safely inside the drill string from the steering tool to the surface monitoring equipment. The directional crew consists of a driller and two surveyors.

Directional and horizontal drilling procedures

Once the directional hole has formed a 75° to 80° arc from the KOP, the drilling angle is changed to allow better drilling control to intercept the bottom of the evaporite bed. The drill system is removed from the hole and the PDM housing re-set (re-bent) to allow a drilling angle of 3° to 9° per 100 feet (30.5 m) or equivalent radii of 1910.7 feet (582.4 m) to 636.9 feet (194.1 m). The hole is re-entered and the $8^{3}/_{4}$-inch (222 mm)-diameter hole is drilled into the evaporite bed and stopped. The gamma ray log identifies the boundary between the roof and the evaporite bed.

The drill string is pulled from the hole and the $8^{3}/_{4}$-inch (222 mm)-diameter hole is then reamed to a diameter of $12^{1}/_{4}$ inches (311 mm). The reamed hole will penetrate the evaporite bed. The $9^{5}/_{8}$-inch (245 mm) casing can bottom out at the roof of the evapor-

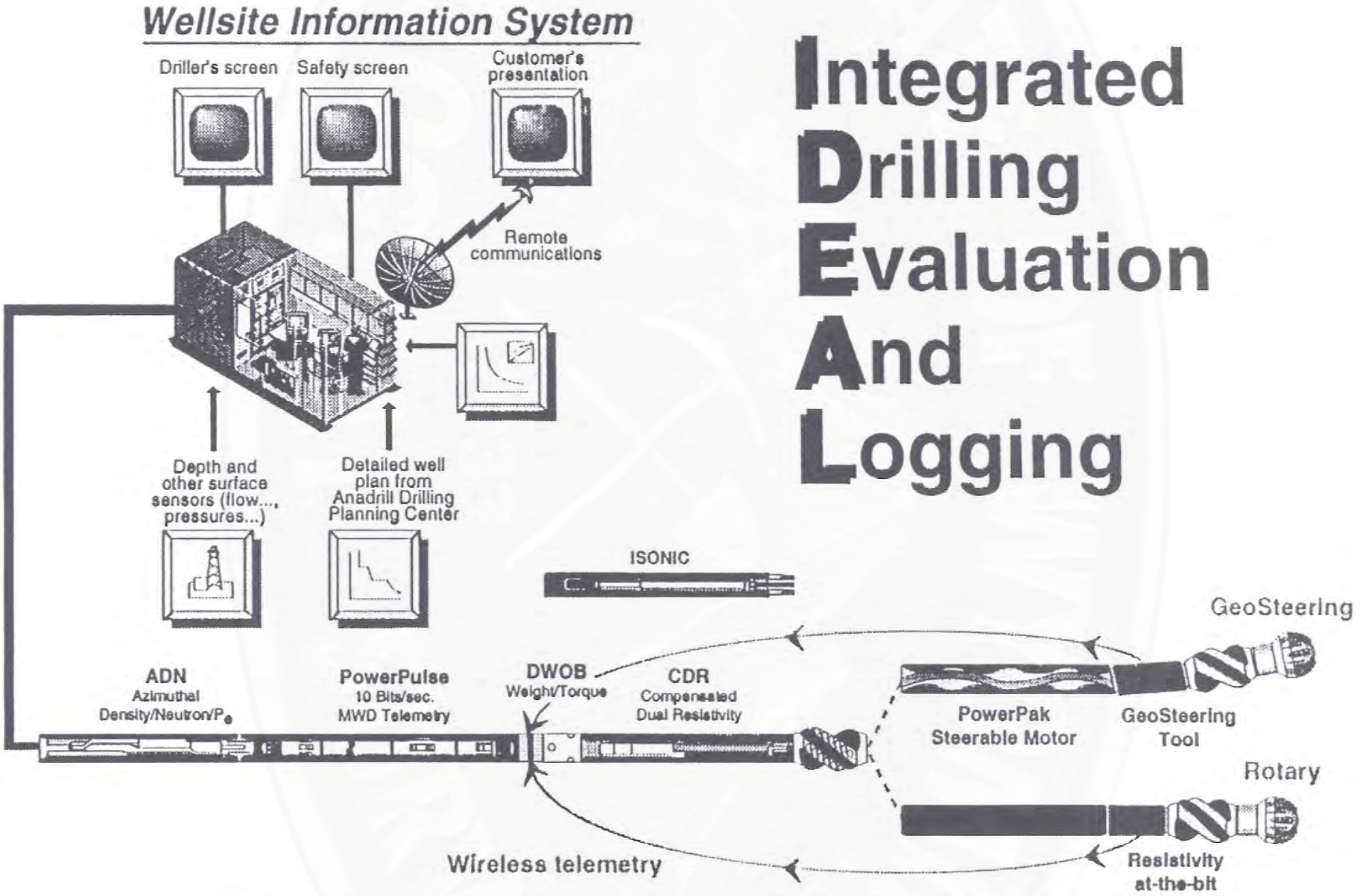


Figure 3. Schlumberger's IDEAL® (Integrated Drilling Evaluation And Logging) system for horizontal drilling.

ite bed or in the bed itself. Typically, hinged centralizers are spaced on the outside of the curved section of the casing in order to allow peripheral and upward flow of cement that surrounds the casing. Forty-eight hours after the cement is installed, a cement bond log is run.

The cased well is re-entered with either the Wet Connect Steering Tool System® or the Geo-Steering® tool system and drilling commences in the evaporite bed with a 8¾-inch (222 mm)-diameter bit. The horizontal hole is drilled along the floor of the evaporite bed. Drilling penetration rates, drill hole cuttings, tool inclination, focused gamma and/or resistivity logging act as aids in keeping the drill hole close to the bed floor.

The drilling penetration in an evaporite bed is normally quite rapid. When drilling in nahcolite, the penetration rate can vary from 120 feet per hour (ft/hr) (36.6 m/hr) to 180 ft/hr (55.2 m/hr). However, it is expected that the penetration rates for trona will be reduced due to trona's dense crystalline structure.

Drilling accuracy and well communication

When drilling a horizontal hole in the nahcolite bed, the drilling contractors maintain that they came from a few inches to a few feet of hitting the vertical production target well. In any event, communication between the target well and the horizontal well was always made within less than 24 hours after jetting with water from the vertical target well. One directional drilling contractor maintains that with the present advanced drilling technology, a 2- to 3-foot (0.6 to 0.9 m) radius from the target is consistently hit.

In the unlikely event that the directional well fails to communicate with the vertical well, the target area can be enlarged. Hi Tech Natural Resources, Inc. of Midland, Texas has a high energy gas fracturing system to provide fluid communication between the horizontal and vertical holes. A propellant-based downhole gas generating tool is packed in the 6½-inch (165 mm)-diameter vertical open hole that transects the evaporite bed. The cased well above the open hole is filled with water and acts as a tamping agent. The propellant charge is designed to emit radial fractures upon ignition. The detonation provides a controlled pressure pulse of about one order of magnitude above the *in situ* stresses but below the flow stresses of the rock. The fractures can be 35 feet (10.7 m) in length and, if desired, as high as the evaporite bed. Therefore, the outline of the maximum target area for interception by the horizontal hole would be about 70 feet (21.3 m) wide by the height of the evaporite bed.

Well completion

Once all drilling operations are completed and the wells have established fluid communication, 7-inch (178 mm) OD tubing strings are suspended in the cement-cased wells. This tubing is actually formed from regular pipe casing. However, 2⅜-inch (60 mm) OD actual tubing is used to flush out the production tubing string whenever a substantial accumulation of evaporite crystals occurs on the interior of the production tubing.

The 7-inch (178 mm) tubing is initially suspended in the vertical production well so it bottoms out a few feet above the evaporite bed floor. In the injection well, the tubing is suspended in the vertical section but it is shoved to near the end of the horizontal hole section. The tops of the wells are sealed and high pressure air is introduced in the annuli, i.e., between the outside of the tubing and the inside of the cemented casing. Any fluid in the annuli is forced down towards the roof of the evaporite bed. In both wells the fluid level is maintained about 50 feet (15.6 m) to 75 feet (22.9 m) above the evaporite bed roof. The air cushion in the annulus acts as insulation between the tubing and casing, and provides for leak detection of the tubing and casing strings.

Solution mining parameters

Primary targets for solution mining consideration in the Green River Basin are trona beds 1 and 2, which attain maximum thickness of 32 feet (9.8 m) and 24 feet (7.3 m), respectively, and are the thickest beds in the basin. The NaCl content of these beds is less than 2%. The areas where each of these beds are greater than 16 feet thick are shown in **Figure 4**. Since the trona bed thickness and viable roof span directly affect drilling and associated costs, the solution mining cavities would be developed in one of these beds.

Evaporite minerals, such as nahcolite, halite, or borax dissolve congruently–that is, they dissolve entirely in water up to the saturation point. However, many double salts including trona dissolve incongruently, i.e., they dissolve in part but also yield a solid phase residue. In the case of trona, due to the better

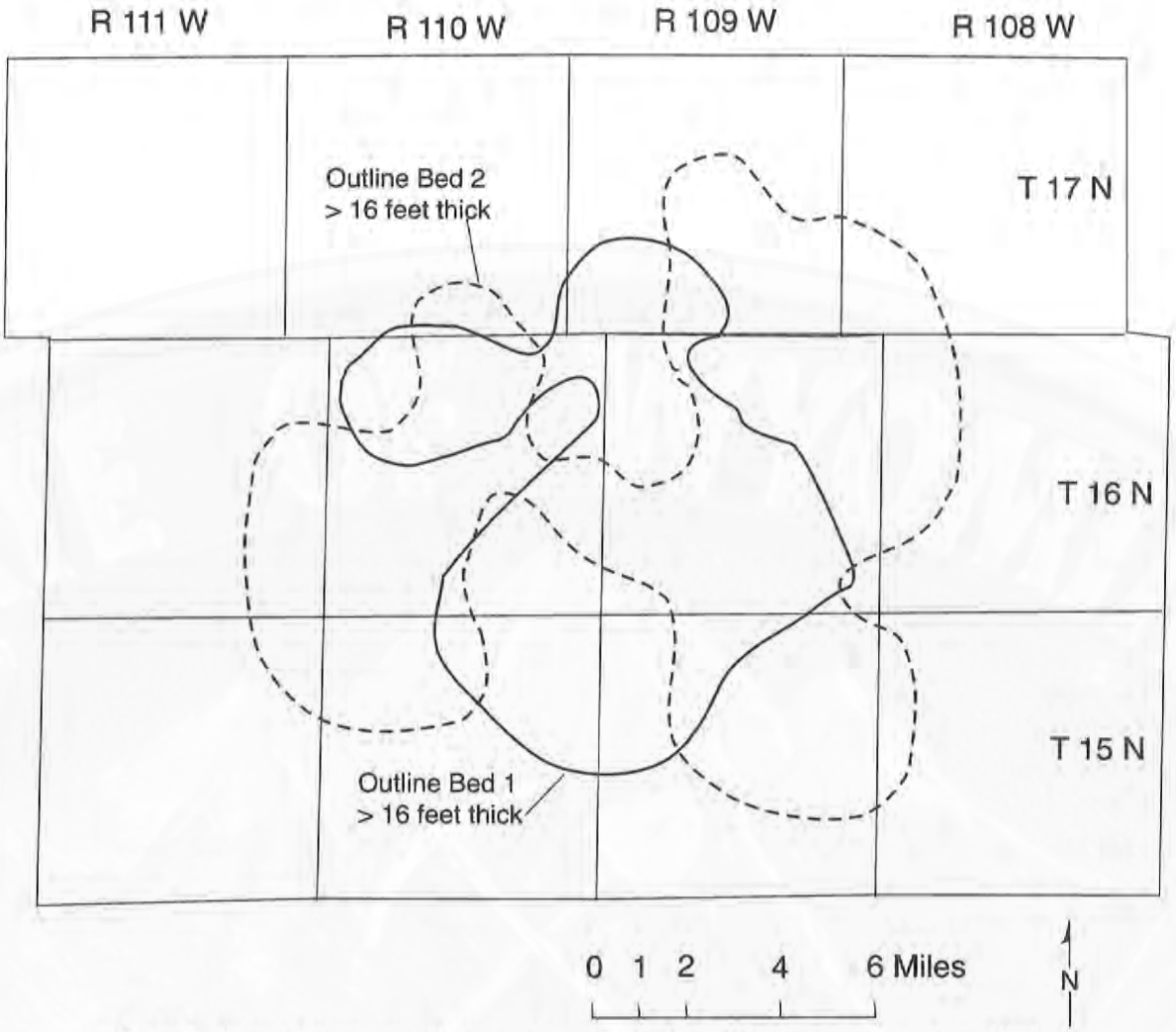


Figure 4. Areas of maximum thickness of trona beds 1 and 2 (from Wiig and others, 1995).

solubility of the sodium carbonate fraction, some of the less soluble sodium bicarbonate is left behind and blinds the dissolving face. This dissolution preference causes the deterioration of the sodium yield per unit of solution as the sodium bicarbonate layer thickens. Eventually the solution contains only sodium bicarbonate. **Figure 5** shows various dissolving paths at a temperature of 50° C for dissolving trona in water and sodium hydroxide solutions. The incongruent dissolution of trona in pure water produces solution composition changes from point A to point B and then reaches the nahcolite/trona equilibrium point E, yielding saturated solution and a nahcolite residue. An aqueous solution containing 2.2% NaOH dissolves trona congruently as the dissolution path moves from point A to point C and then to the equilibrium point E. Another congruent dissolution path starts at point A and reaches point D when over 9% NaOH is present in the solvent. The solvent proposed by the authors would ensure the congruent dissolution of trona.

The dissolving rate of trona in water at 23°C has been determined by Nigbor (1983) to be in the range of 2.9 to 3.9 g x 10^{-4}/cm^2/sec. The authors have not conducted dissolving rate tests on trona from bed 1 or bed 2 with the solvent of their choice. The cost calculations for a given plant output are based on a conservative dissolving rate value of 1 g x 10^{-4}/cm^2/sec. This low dissolution rate is used for all temperature regimes even though the dissolution rate would increase with higher temperatures.

The solvent is pumped into the injection string via a centrifugal pump. The solution flows out of the end section of the horizontal injection string and starts dissolving the evaporite mineral. In turn the saturated solution enters the vertical production tubing and flows to the surface processing facility.

The solution mining operation is a pressurized system that is nearly in hydrostatic balance. The power required for pumping is due primarily to differ-

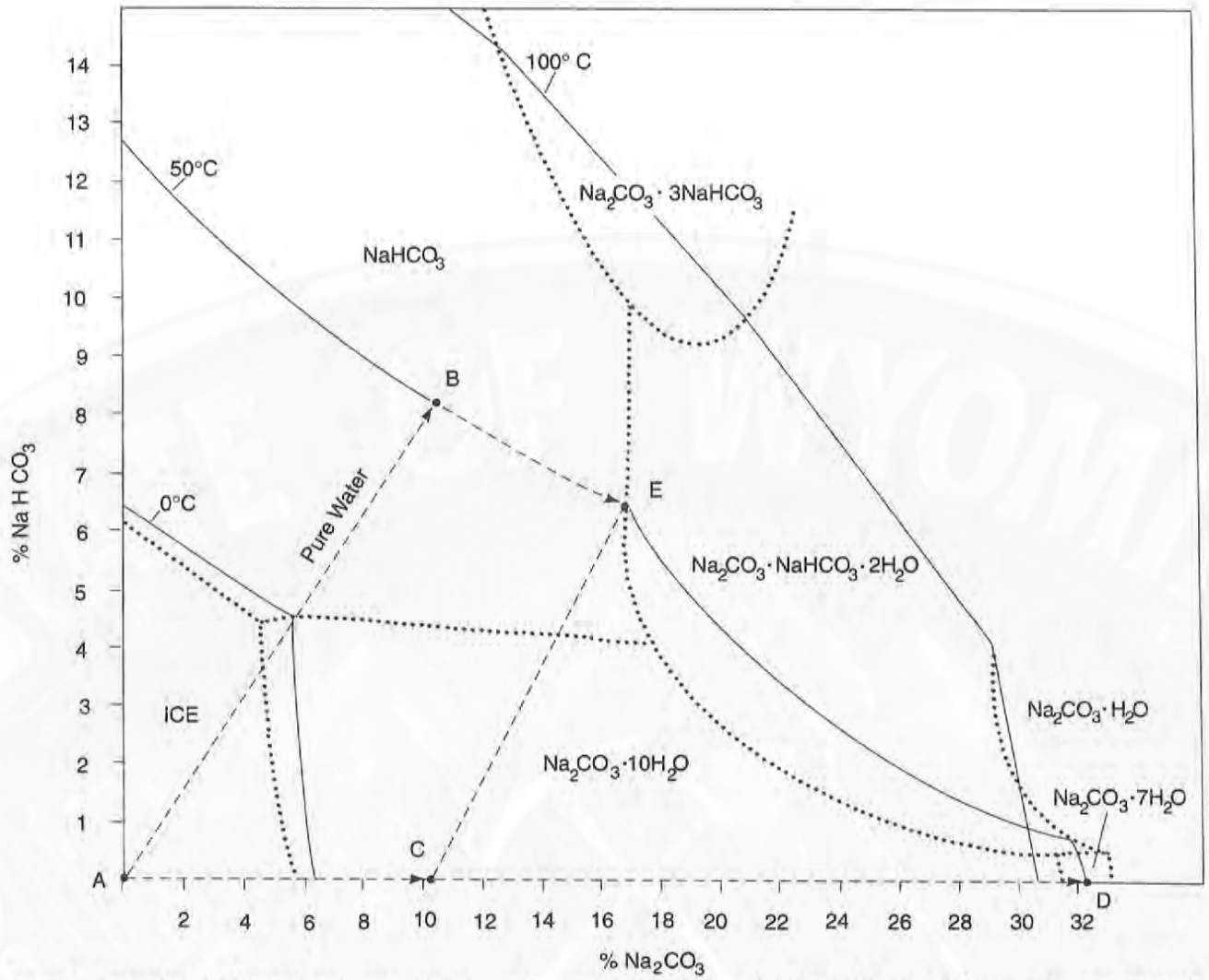


Figure 5. Examples of different dissolving paths for trona. Dotted lines are stability field boundaries for different sodium compounds (modified from Wegscheider and Mehl, 1928).

ences in specific gravities of solutions in the tubing strings, solution viscosities, and pipe friction. As a result the pumping power requirements are relatively small.

For the structural stability of the solution-filled cavities, it is important to note that the major stress field will aid in the roof support. In addition, the hydrostatic pressure of about 900 psi [6300 kilopascals (kPa)], transmitted by the solution, will enhance the support for the roof and pillars.

Since the solution mining environment is conducive to crystal precipitation, the horizontal injection tubing string periodically has to be moved laterally and partially rotated to avoid being immobilized by crystal encasement. In addition, periodic flushing with fresh water or barren solution should be performed around the annulus of the injection string.

To control the cross sectional area of the solution mining cavity, the method and apparatus in U.S. Patent 5,246,273 issued to Edward C. Rosar (1993) may be used. In this patent, the PDM and bit are removed from the drill string and a jetting tool is installed in its place. The drill string, steering, and jetting tools re-enter the injection well and are shoved downdip to the vertical production well. The floor rock is underreamed at the production well in order to provide a sump for collection/pumping. The evaporite bed is undercut by the water jetting laterally in open air through cutting and dissolving the evaporite (**Figures 6a**, **6b,** and **6c**). In the event solution and solids are entrained to form blockages on low lying or flat floors, a programmed pneumatic pressurization system forces an opening through the obstructions.

An electromagnetic radiation (EMR) device is part of the jetting tool in order to measure the width of the

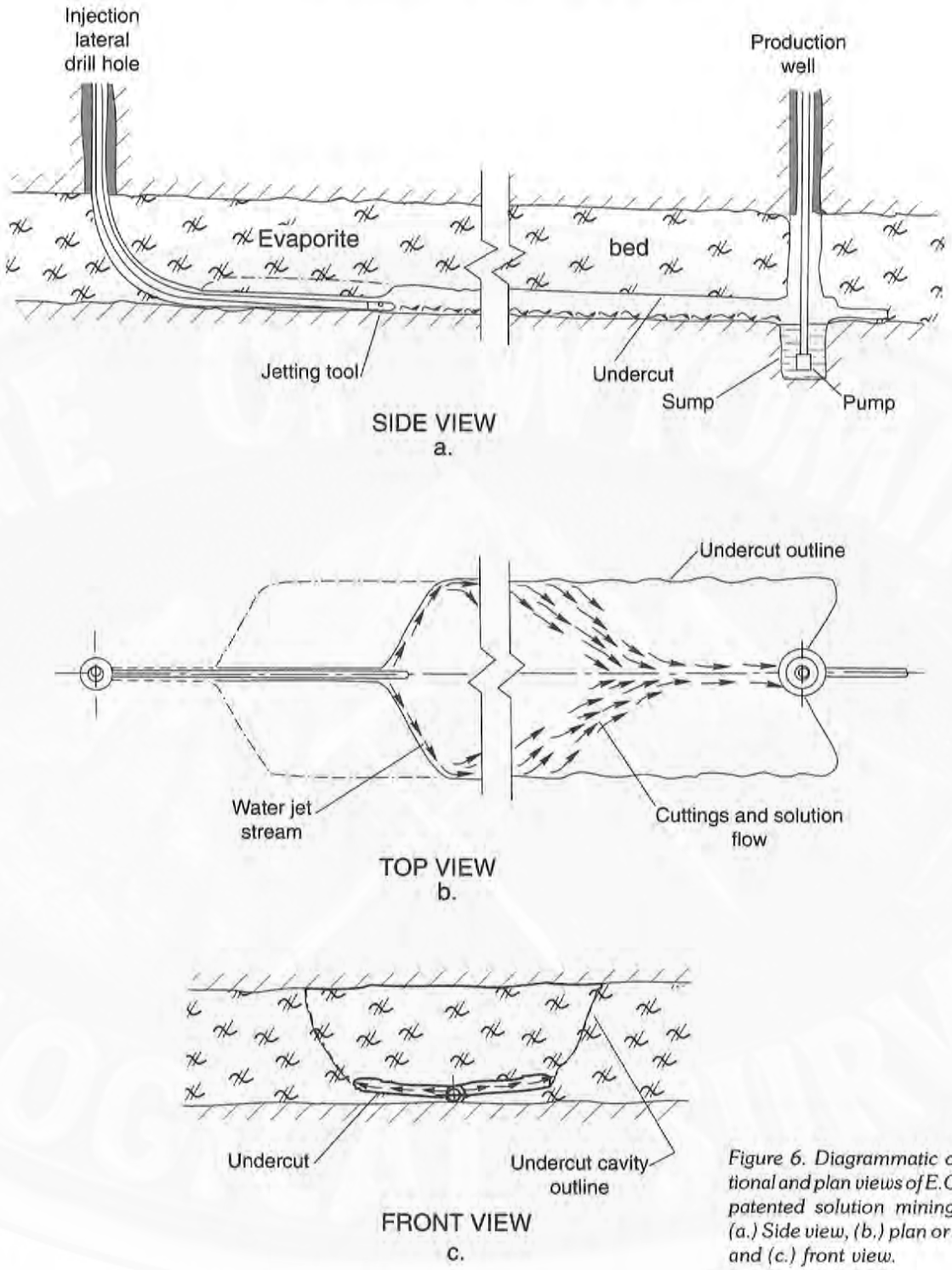


Figure 6. Diagrammatic cross sectional and plan views of E.C. Rosar's patented solution mining system. (a.) Side view, (b.) plan or top view, and (c.) front view.

undercut and to transmit information to the steering tool and then to the surface monitoring station. This allows the jetting tool to be retreated at the proper rate.

When solution mining proceeds from a single horizontal hole, the cavity cross section forms a morning glory configuration as shown in **Figure 7a**. The accumulation of saturated solution at the cavity bottom and the undissolved solids that settle on the cavity walls prevent normal lateral dissolution. This type of cavity can also result in producing roof widths that can be unstable and result in roof failures. The undercut cavity using the methods developed by Rosar (1993) produces a stable cavity configuration whereby evaporite extraction can be increased from 50% to 70% (**Figure 7b**). Because of the horizontal undercut, the dissolution rate can be about doubled as compared to the morning glory-type cavity.

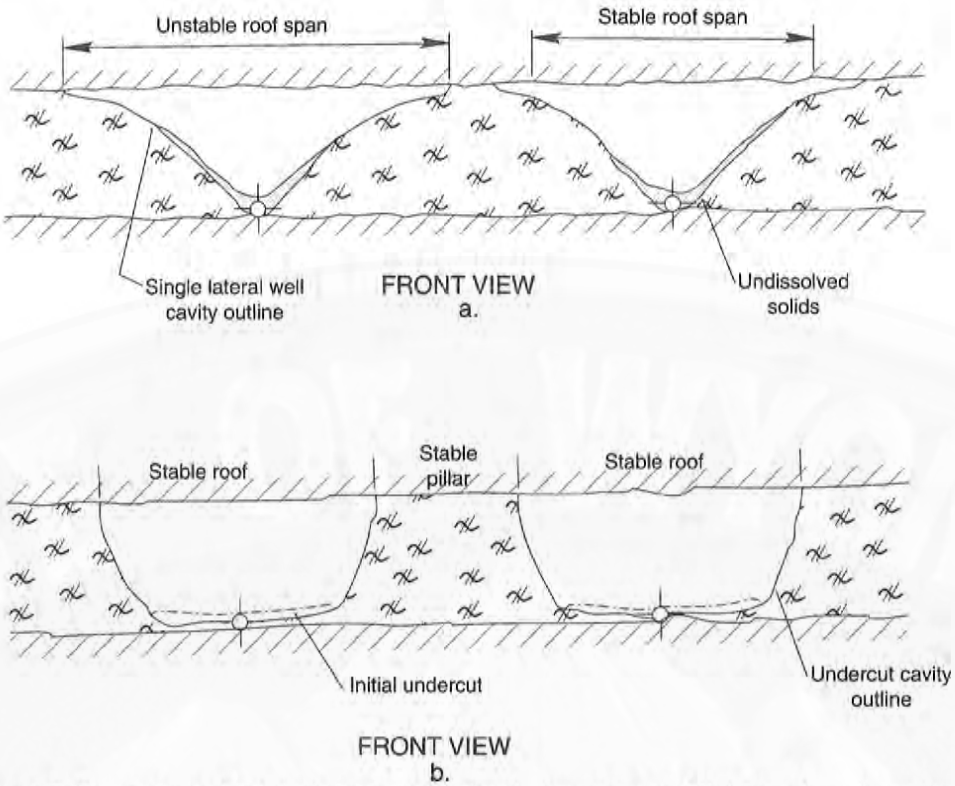


Figure 7. Comparison of (a.) single horizontal hole solution mining and (b.) Rosar's undercutting solution mining methods. Both cross sections are front views, as in Figure 6c.

Drilling, well field, and monitoring well costs

The drilling, well, well field, and monitoring well costs on a soda ash per ton basis are estimated in **Table 1** for a 2500-foot (762 m)-long trona cavity that varies in height from 20 feet (6.1 m) to 25 feet (7.6 m) with a roof span varying from 20 feet (6.1 m) to 30 feet (9.1 m). These costs are based on conservative drilling rates from 20 to 25 ft/hr (6.1 to 7.6 m/hr) to drill the curved hole and 14 to 17 ft/hr (4.3 to 5.2 m/hr) to drill the horizontal hole. As of 1997 these costs, which range from $8.60/short ton to $16.10/short ton, would represent a conservative scenario to develop a 2500-foot (762 m)-long trona cavity in bed 1 or bed 2.

Technology developments

The authors have devised additional solution mining technologies that address the problems of trona's incongruent dissolution, total extraction of trona from a cavity, and pirssonite scale deposition. Thus far these technologies have been submitted to the U.S. Patent and Trademark Office (PTO) as two Provisional Patent Applications. A third technology is forthcoming and will also be submitted to the PTO. One of our technologies results in delivering a feed solution to the monohydrate crystallizers at a temperature of 212°F (100°C) containing 30% Na_2CO_3 by weight.

Estimated cost to produce mono feed solution

The largest cost items are the drilling and associated items, already discussed (refer to **Table 1**), and the thermal requirements.

For one operating scenario, the estimated cost of producing 500,000 short tons per year (453,900 metric tons per year) of soda ash that is contained in a 30% Na_2CO_3 solution at 212°F (100°C) is listed in **Table 2**. Under this scenario the cavity lengths are 2500 feet (762 m) and the cross section is 25 feet (7.6 m) high and 20 feet (6.1 m) wide. Note that the cost of $32.01/short ton does not include taxes and insurance, G&A, royalty, capital and interest expense for

Table 1. Cost summary for drilling, well field, and monitoring wells for varying sizes of trona cavities. Based on 2500-foot-long cavities and a production rate of 500,000 short tons per year Na_2CO_3.

Cost items	Basis	$/Short ton Na_2CO_3			
	Cross section size Short tons per cavity	20'hx20'w 44,382	25'hx20'w 55,477	20'hx30'w 66,573	25'hx30'w 82,216
(1) Directional wells		$8.63	$6.90	$5.75	$4.60
(2) Vertical wells		$3.72	$2.97	$2.48	$1.98
(3) Well equipment		$1.91	$1.52	$1.28	$1.03
(4) Well field equipment		$1.15	$0.93	$0.77	$0.62
(5) Monitoring wells		$0.69	$0.55	$0.46	$0.30
	TOTAL*	**$16.10**	**$12.87**	**$10.74**	**$8.60**

*Includes all costs for capital and current year's expense for drilling injection and production wells, monitoring wells, and wellhead and well field equipment. Does **not** include cost of permitting.

Table 2. Summary of direct operating and maintenance costs, including all drilling and well field costs, for producing 500,000 short tons per year Na_2CO_3. Based on 2500-foot-long trona cavities and delivering a 30% Na_2CO_3 solution at 212°F to monohydrate crystallizers.

Cost items	Basis	$/Short ton Na_2CO_3
	Cross section size Short tons per cavity	25'Hx20'W 55,477
A) Direct costs		
(1) Labor		
(a) Salaried		$1.21
(b) Hourly		2.56
(2) Operating and maintenance supplies		1.39
(3) Utilities		
(a) Electric power		2.06
(b) Heat		8.09
(4) Other operating materials		3.83
	Sub-Total[1]	19.14
B) Drilling, well field, monitoring costs[2]	(from **Table 1**)	12.87
	TOTAL	**$32.01**

[1]Does **not** include taxes and insurance, royalty and G & A, **nor** does this include capital cost or interest expense for the surface processing facilities.
[2]Includes all costs for capital and current year's expense for drilling injection and production wells, and wellhead and well field equipment. Does **not** include cost of permitting.

the proprietary surface processing facility, or environmental studies and permitting. However, the cost does include all costs for capital and current year's expense for the injection and production wells, monitoring wells, wellhead and well field equipment; all labor, operating, and maintenance supplies; heat; electrical; and other materials expenses for both the solution mining and processing operations.

A solution mining operation is equivalent to a conventional soda ash production operation that comprises all underground mining activities, hoisting, storage, feeding, crushing, screening, calcining, mixing, dissolving, thickening, filtering, heating, pumping, slip stream rejection, and tailings disposal. Not included are monohydrate crystallization, centrifuging, drying, product handling, and product shipping.

Cost reduction opportunities

A cost reduction would be realized if the cavity lengths were increased from 2500 feet (762 m) to 3000 feet (914 m) or 3500 feet (1067 m).

The drilling, well field, and monitoring costs would decrease by 33% if the roof span in a 20-foot (6.1 m)-high cavity can be increased by 5 feet (1.5 m), i.e., from 20 feet (6.1 m) to 25 feet (7.6 m).

For this paper it was assumed that the directional drilling will take more than three times longer than in the Piceance Creek Basin. Future performance data in the trona area might exceed the assumed penetration rates.

In addition, the actual dissolution rate in trona beds 1 and 2 may exceed the value of 1.0 g x 10^{-4}/ cm^2/sec. which was used for the calculations. The figure used is about 25 to 33% of the published rate at 23°C (73°F). For the presented cost scenario at a production rate of 500,000 short tons per year, eight operating cavities are required when dissolution occurs in 500-foot (152 m) increments in each cavity. If future tests show the dissolution rate is doubled, the cavity requirements are halved.

The ideal situation for a grass roots solution mining operation is to have an attendant cogeneration electric power plant on the property. The waste heat from the cogeneration plant would be used in solution mining and surface processing. In addition, the solution mining operator and developer would share in the gross profits from the sale of electricity.

Conclusions

Trona beds 1 and 2 are considered attractive targets for solution mining consideration. Each of these beds exceeds 20 feet (6.1 m) in thickness in the deeper part of the trona area.

Rock mechanics analyses are an important prerequisite for determining the configuration of a cavity, which in turn effects trona recovery, and especially the drilling and well field costs. Directional and horizontal drilling are essential components for the development of long and structurally stable solution mining cavities. There is a definite need to obtain actual drilling data for the Green River Basin.

The solution mining of thick trona beds in Wyoming appears to be economically viable based on conservative cost projections used here. There is potential for reducing the projected solution mining costs.

References cited

Garrett, D.E., 1992, Natural soda ash: Van Nostrand Reinhold, New York, New York, 633 p.

Nigbor, M.T., 1983, Dissolution rate experiments on Wyoming trona ore: In Situ, v. 7, no. 4, p. 370; AIChE Metals and Minerals Processing Symposium, August 28-31, 1983, Denver, Colorado, 27 p.

Rosar, E.C., and Day, R.L., 1989, Nahcolite solution mining process: U.S. Patent 4,815,790, NaTec (March 28, 1989), 12 p.

Rosar, E.C., 1993, Method and apparatus for solution mining: U.S. Patent 5,246,273 (September 21, 1993), 17 p.

Wegscheider, R., and Mehl, J., 1928, Uber Systeme Na_2CO_3-$NaHCO_3$-H_2O und das Existenzgebiet der Trona: Monatsh. Chemie, v. 49, p. 283-315.

Wiig, S.V., Grundy, W.D., and Dyni, J.R., 1995, Trona resources in the Green River Basin, southwest Wyoming: U.S. Geological Survey Open File Report 95-476, 88 p.

A new technology for the soda ash deposits near Trona, California

James L. Fairchild
Michael E. Lovejoy
and Gail F. Moulton, Jr.
North American Chemical Company
Trona, California 93592-0367

Abstract

Mineral extraction in Searles Valley, California began in 1873 with borax and raw trona scraped from the surface. Brine processing started in 1914 with potassium chloride and borax recovery. Expansions over the years added sodium sulfate and soda ash to the product mix. The deposit characteristics and limited availability of water resulted in the need for a different application of technology to remain competitive. Today, Searles Lake is one of the largest saline mineral producers in the United States.

A new understanding of lake geology has allowed the development of new, more productive solution mining technology. Minerals currently solution mined include trona, borax, and thenardite. Products are recovered from the resulting brines using carbonation for soda ash, refrigeration for borax and sodium sulfate, and solvent extraction for boric acid. Trona is also dredged as a crude product from extensive surface deposits.

Introduction

Searles Valley is 125 miles (200 km) northeast of Los Angeles. The basin is 10 miles (16 km) wide and 20 miles (32 km) long. The lowest part of the depression is an area 6 miles (10 km) wide and 10 miles (16 km) long called Searles Dry Lake Playa. This playa is 1614 to 1624 feet (492 to 495 m) above sea level with an exposed halite center that covers 6.5 square miles (17 km^2) (**Figure 1**). The periphery of the playa, covered by mud and clay, overlies an additional 28 square miles (73 km^2) of the salt body. The valley is surrounded by various mountain ranges that rise to a maximum of 6560 feet (2000 m) above sea level. Well developed alluvial fans extend into the valley from the east while those in the west are considerably less developed. Rainfall in the valley ranges from 3/4 to 8 inches (20 to 200 mm) per year with an average of 3 1/2 inches (100 mm) per year. Air temperature ranges from 8 to 120°F (-13 to 50°C). Wind speeds reach 84 miles per hour (135 km/h) or more and are predominately from the southwest.

The lake brine aquifer has been the principal plant (refinery) feed for over 80 years. This aquifer is recharged primarily by winter runoff and plant effluent. The plant effluent is either directly injected or ponded on the lake where it percolates into the salts. The recharge dissolves additional minerals, undergoes some evaporation and is then captured by production wells in a saturated state and returned to the plant for extraction of dissolved minerals.

The principal product of the valley is soda ash followed by sodium sulfate and boron products. Earlier operations recovered potash but this is no longer the case. As the years have passed, the dissolved potassium declined by depletion of glaserite and also from dissipation as a result of non-potash extraction by some of the processing plants. Because the potassium resource was specific to certain areas of the lake (similar to the presently known borax distribution), as the lake was mined these areas were mixed with other brine such that potassium quality in the brine became uncompetitive to recover as a product.

The model used for new development was constructed as that fraction of the formation which would

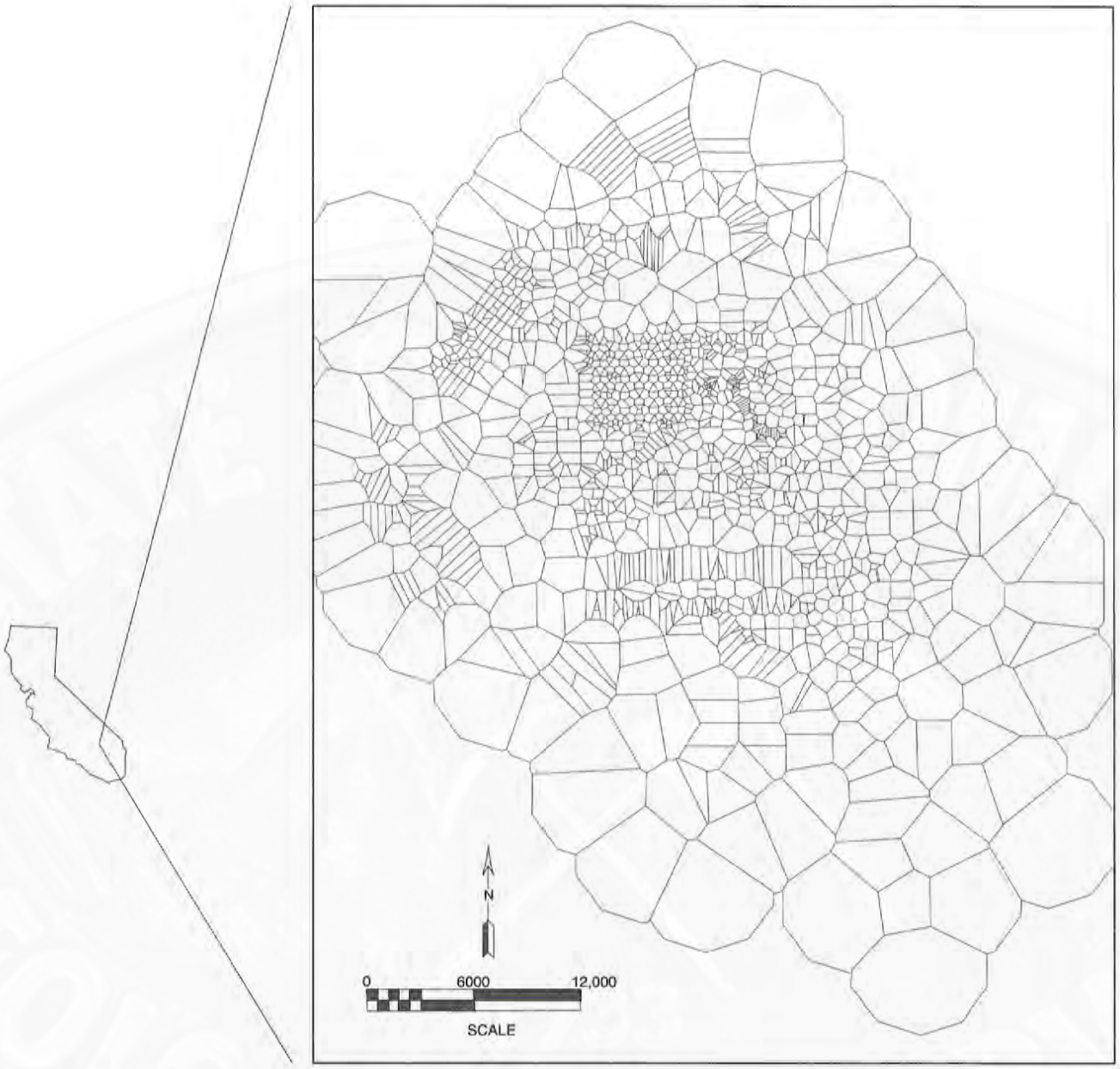


Figure 1. Location and data polygons outlining the major extent of the Searles Lake salt body and some of the mud-covered periphery.

be accessible by solution mining fluids. The total model contains an area of 90 square miles (233 km^2) to 700 feet (213 m) in depth. This represents some 90 billion short tons [82 Giga tonnes (billion metric tons)] and includes all or part of at least two distinct aquifers. The brackish aquifer at the boundaries of the model is used as the primary makeup water for plant feed and is separated from the lake brine aquifer by an aquitard.

Geology of Searles Lake

Searles Valley is a closed structural basin filled with alluvium and non-marine evaporites. The thickness of the fill is over 6560 feet (2000 m) in the deepest portions of the basin. Basement rock under the playa was found at 3050 feet (930 m) in a deep test drilled in 1968. The rock was quartz monzonite, which is also the major rock type of the Argus Range to the west and the Northern Slate Range to the east. Seismic work done by the Naval Weapons Center in the southern part of the valley near the Garlock fault

indicated a basement depth in excess of 6560 feet (2000 m) (Monastero, 1995, unpublished seismic data).

In Searles Lake, evaporite deposits alternate with mud beds. Evaporite beds were formed during periods of high evaporation and low rainfall. The resulting beds are generally thicker in the lake center and thin to pinch out where the base formation slopes upward from the lowest area. Mud beds were formed during full lake conditions and thus cover virtually the entire lake basin. These become thicker toward the edge of the lake basin and grade into coarse, clastic sediments at the base of the mountains where the surface rises above the lake level.

The salt beds are generally brine saturated, white to pink in color, hard, and very porous. The important chemical ions are Na^+ (sodium), K^+ (potassium), $CO_3^=$ (carbonate), HCO_3^- (bicarbonate), $SO_4^=$ (sulfate), Cl^- (chloride), and $B_4O_7^=$ (borate). These ions are present in the brines in various concentrations and have combined to form the major evaporite minerals of halite, trona, hanksite, nahcolite, burkeite, borax, thenardite, sulfohalite, and glaserite.

The mud beds are generally dark green to brown, soft, porous, and may have a distinct odor. The important chemical ions in the mud are Ca^{++} (calcium), Na^+ (sodium), Mg^{++} (magnesium), and $CO_3^=$ (carbonate). These have precipitated as fine-grained aragonite and dolomite, and as fine and coarse-grained gaylussite and pirssonite. The surface mud bed also contains clay-sized halite, coarse borax, and hanksite.

Mixed layer

The mixed layer is a sequence of mud and evaporite beds overlying up to 985 feet (300 m) of arkosic basement sands. The lowermost lake muds are estimated to be three million years old (Smith, 1979). The lateral and vertical extent of these beds has not been fully explored although it is thought they may cover less area than the younger, near-surface evaporites. The mixed layer also has a complicated structure including sharp folds and faults, which are rare in the younger (overlying) bottom mud and in beds above.

The upper mixed layer is divided into several units based on differences in electrical conductivity and mineral composition while the lower mixed layer is divided on the basis of mineral composition alone. The upper mixed layer salt beds are predominantly permeable trona beds which can be solution mined for soda ash. The deeper mixed layer beds contain not only trona, but also halite and thenardite. When these latter minerals dissolve during solution mining they reduce sodium carbonate solubility. This limits sodium carbonate grade in the resulting brine and also limits the suitability of these deeper mixed layer beds for solution mining to feed the present soda ash plant. However, even trona resources most heavily contaminated by sulfate and chloride are potentially recoverable through solution mining, provided the soda ash plant is designed to handle larger volumes of weaker brines.

Bottom mud

The bottom mud is underlain by the mixed layer and overlain by the lower salt. This mud bed covers a much wider area than the saline beds above. The bottom mud is 100 feet (30 m) or more in thickness and forms a bowl-shaped structure with the lowest and thickest part near the lake center. The unit is composed of clay layers with abundant gaylussite and minor dolomite, calcite, halite, thenardite, mirabilite, trona, and borax.

Lower salt

The lower salt is underlain by the bottom mud and overlain by the parting mud. The thickness ranges from zero at the edge to approximately 40 feet (12 m) in the lake center. It covers 35 square miles (90 km^2) in the lowest part of Searles Valley. The unit is composed of seven evaporite beds separated by thin mud beds. These evaporite layers are predominately trona and halite, but limited amounts of borax, burkeite, nahcolite, and northupite are also found.

The lower salt evaporite beds change laterally from the edge to the center. Lying almost symmetrically around the lake's edge is a rich trona zone about 1.5 miles (2.4 km) wide. Thicker mud layers also occur near the edge of the lake. The evaporite beds thicken toward the lake center and trona is partially replaced by halite. The mud layers are composed of dark, clay-sized saline and clastic minerals with megascopic crystals of gaylussite, pirssonite, halite, and borax.

Parting mud

The parting mud is underlain by the lower salt and overlain by the upper salt where these evaporites exist. It is in contact with the bottom mud and overburden mud around the edges of the lake. The bed is 10 feet (3 m) thick in the lake center and thickens to

26 feet (8 m) or more toward the edges. This mud occurs far beyond the saline beds and may, in places, be in contact with bedrock at the basin's edge. Away from the evaporites, the bed is difficult to distinguish from the bottom and overburden muds. Parting mud is composed of saline and clay-sized clastic minerals, as well as abundant megascopic pirssonite and gaylussite with minor amounts of borax, northupite, trona, and hanksite. The content of soluble minerals may exceed 50% in some areas.

Upper salt

The upper salt is underlain by the parting mud and overlain by the overburden mud everywhere except in the playa center where it crops out. It ranges in thickness from 75 feet (23 m) at the lake center to zero along the edges.

The upper salt demonstrates the depositional sequence of minerals postulated by Matsuo and others (1972) as a result of studies at Owens Lake, California. The lowest mineral bed, and the first to be deposited, extends to the outer edge of the body and is composed mostly of beds of trona and halite with only minor amounts of borax and sulfate minerals (hanksite, burkeite, and thenardite). Similar to the lower salt, the halite content of this bed decreases toward the lake edge. This bed is generally thinner in the lake center and thickens toward the edge before it pinches out, although on the east side of the lake the bed thins abruptly without thickening.

On top of the trona/halite bed are extensive beds of sulfate minerals containing substantial amounts of halite and lesser amounts of trona, borax, and sulfohalite. Above the sulfate bed and extending either to the playa surface or to the bottom of the overburden mud is a bed of nearly pure halite. This is about 23 feet (7 m) thick in the lake center and thins to 0 near the contact with the overburden mud.

Overburden mud

The overburden mud is underlain by the upper salt. Its thickness ranges from 0 in the lake center to 20 feet (6 m) where the upper salt pinches out. The clay-sized material and salines of the overburden mud grade laterally toward the basin edge into silt, sand, and gravel. The bed extends over the upper salt up to 1.9 miles (3 km) on the south but only 0.93 miles (1.5 km) on the east.

In areas where mud covers the upper salt, it is composed of dark brown and black clay-sized saline minerals and clastics that interfinger with silt and sand at the lake edge. Isolated beds of hanksite and trona occur in many areas; rich pockets of euhedral borax crystals occur occasionally above the upper salt contact. Pirssonite and thenardite are also found in the overburden mud.

Lake sediment deposition

Although the geologic history of Searles Lake is not fully understood, a great deal has been learned in the past several years using new theoretical models of post-depositional changes, new exploratory drilling, geophysical studies, and computer analyses of the vast amount of available information.

Searles Valley contained a large lake for much of the past million years. The last lake filling, some 3500 years ago (Smith, 1979), produced a lake 25 miles (40 km) long, 10 miles (16 km) or more wide and some 148 feet (45 m) deep. Searles Lake was part of a chain of lakes chiefly nourished by runoff from the east side of the Sierra Nevada Range. Owens Lake, the first of these, overflowed southward into China Lake which overflowed eastward into Searles Valley forming Searles Lake. At the highest stages, Searles and China Lakes coalesced into one lake that drained southeast into a stream that led to Panamint Valley. However, Searles Lake was usually the last in the chain and, as a result, underwent extreme fluctuations in water level. With the large combined drainage area of the connected lakes, small changes in regional precipitation drastically changed the quantity of water flowing into Searles Lake. When the lake was cut off from upstream water sources, inflow was greatly reduced and evaporation quickly converted Searles to a small saline lake or salt playa. When precipitation increased enough to restore the inflow from upstream, the basin would fill, occasionally reaching the overflow at approximately 460 feet (140 m) above the present surface.

The fine clastics in the lake muds were transported into Searles Valley by inflow waters. These sediments were mixed with showering chemical precipitates formed when calcium and magnesium ions in predominately fresh runoff water reacted with carbonate-rich brackish water and brines trapped in Searles basin.

Post-depositional changes

In 1982, Friedman and others suggested that during periods of high lake levels, water left Searles Valley not only through Randsburg Wash as overflow, but also through the Slate Range itself as underflow. This hypothesis is supported by data they published as well as by recent investigations and correlations of mineralogy and structure done by North American Chemical Company (NACC). This post-depositional leaching produced nearly pure trona beds, contaminated only with nahcolite. These conditions are required for solution mining to produce brines rich in soda ash.

Data published by Friedman and others (1982) demonstrated that the sodium calcium carbonate minerals such as pirssonite and gaylussite, which are found only to a depth of 950 feet (290 m), were crystallized long after bed deposition occurred. In their view, surface water during the full lake periods, when the bottom mud was being deposited, seeped downward through the mud and salt beds. This caused saline bed leaching and secondary recrystallization. Validation of the hypothesis would require the occurrence of pirssonite and gaylussite in the uppermost beds where evaporites have been removed by groundwater. The gaylussite and pirssonite would have been formed by water rich in sodium carbonate which converted some of the calcium carbonate beds to the sodium calcium carbonate minerals. Below this there should be pure nahcolite beds where leaching had removed all other saline minerals (the sodium carbonate fraction of trona, thenardite, and halite). The beds below the nahcolite beds should be nearly pure trona where only enough water would have passed to remove the thenardite and halite but not the carbonate fraction. In the beds below the pure trona, the fractions of sulfate and chloride minerals would increase with depth. All of the above mineralogical consequences of leaching have been confirmed by recent exploration and correlation of the mixed layer beds.

Yet another consequence of leaching and removal of large quantities of evaporate minerals would be subsidence of the overlying mud beds. In some areas vertical displacements of 65 feet (20 m) have occurred over such short distances that faulting could exist. To determine if faulting caused the displacement, two seismic surveys were run across a displacement area. This seismic work showed only deep folding, not faulting. But it did confirm that considerable vertical displacement occurs within the mixed layer. The seismic data also demonstrated that the early model of the mixed layer, where the beds were assumed to be relatively planer, could not be reliably used to interpret the geology.

Present interpretation of mixed layer geology

The present geologic correlations of the mixed layer beds are guided by two concepts: (1) because the mud beds were deposited while the lake was full (or nearly so), the mud beds should be continuous across the entire lake, and therefore, (2) the mud beds should be the best markers for identification of the intervening saline mineral beds.

Seismic reflectors from the surface down were designated "A" to "M"; electric log correlation of the reflectors E through M proved that these were mud beds in the upper part of the mixed layer. Cuttings obtained from the E, F, G, and H muds all have pronounced bedding and a light gray tan to gray-green color. The H bed always contains an abundance of the mineral northupite and was previously identified as "Am1." Several of the mud beds also have distinctive geophysical characteristics which are used for structural correlation. Subsequent correlations were made for the remaining mixed layer at each drill hole.

Using the forgoing concepts, a knowledge of the deposition and subsequent alteration of the mixed layer, seismic data and its correlation with geophysical logs, geophysical and core (or cuttings) data from many additional wells, and a powerful computer to handle the vast amounts of data, all mixed layer beds that have potential for soda ash solution mining have now been mapped in great detail. Correlations extend from the bottom mud through a small area of the old 'C' zone, a total of 11 beds. From this it was found that several of the saline mineral units are not described in the literature (Smith and others, 1983). **Figure 2** compares Smith and others' (1983) work with the present designations.

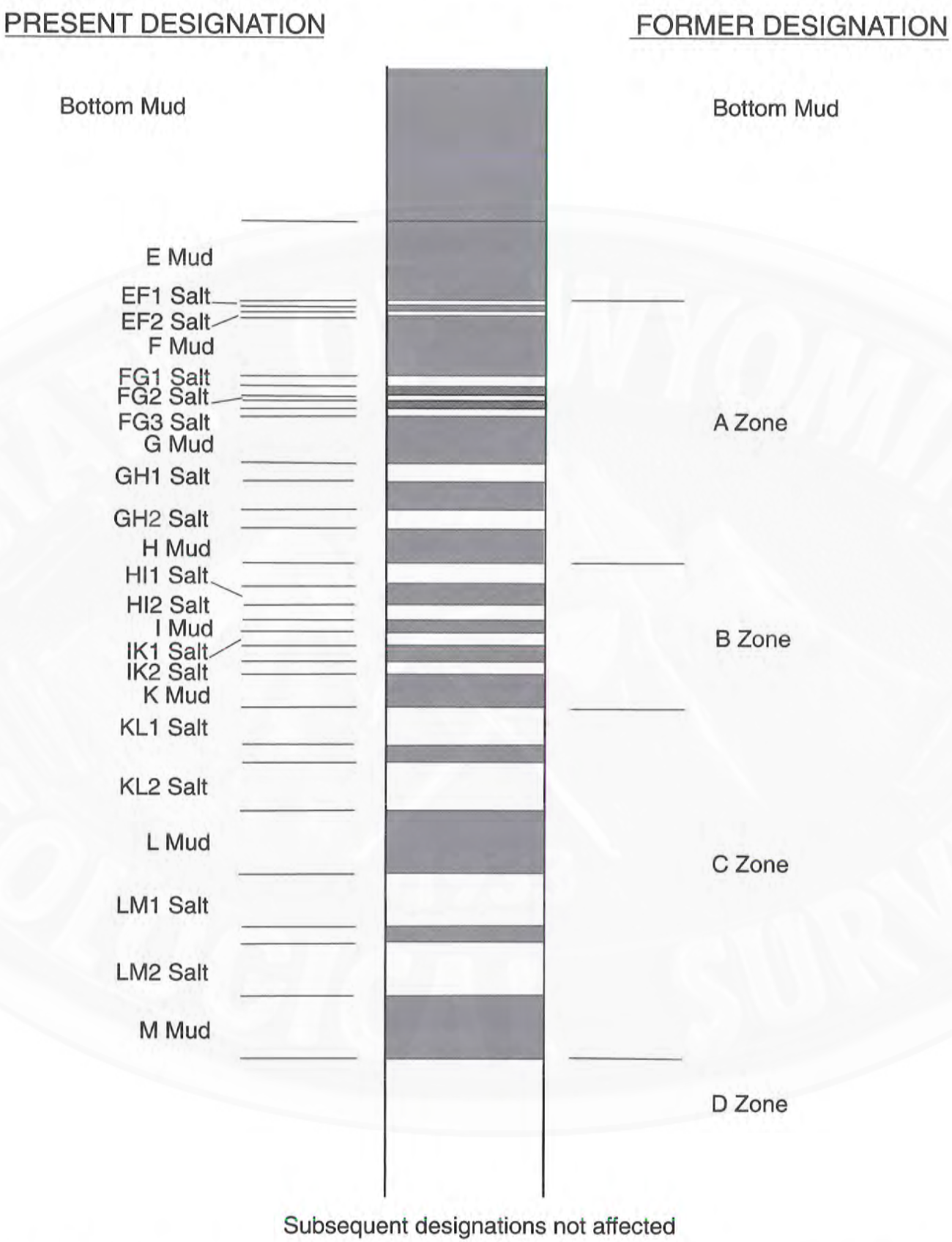


Figure 2. Stratigraphic column of the mixed layer showing present designations of salt and mud beds as compared to earlier designations. All zones and beds are not formal lithostratigraphic units.

Present Searles Lake resources

Figure 3 is a typical north-south cross section through the mixed layer. This shows not only bed thickness, but mineral content through color shading. NACC modeled the deposit's reserves and resources from which the mining plan was developed and is presently operating (**Table 1**).

Mixed layer solution mining

John Searles drilled the first well into the mixed layer in the 1880s, but no use was made of the brine found. In 1955 American Potash and the U.S. Geological Survey cored several holes into the mixed layer. G.I. Smith used this limited data to make the first interpretation of mixed layer geology. In the late 1960s Kerr-McGee drilled several additional core holes including (KM-3) to bedrock, to better define the resource.

Stauffer Chemical was the first to produce mixed layer brine in the early 1970s. Production was all connate brine; Stauffer did not attempt to solution mine trona. In the early 1970s, Kerr-McGee drilled more mixed layer exploration wells and conducted hydrologic tests to determine fluid flow properties and natural recharge rates. They also pilot-tested solution mining of the trona beds and piloted the extraction of soda ash from these brines. Following the completion of these programs, construction of the Argus soda ash plant and mixed layer solution mining facilities for plant feed were completed. Production from these facilities began in 1978 and continued with little change, other than injection well replacements, into the early 1990s.

In the late 1980s the need to replace the original solution mining facilities within three to five years was apparent. A program to develop better solution mining procedures was undertaken because the original facilities had many deficiencies. The key to developing these procedures was a better understanding of the geology previously described.

The most important improvements to solution mining procedures are:

1) Tailor mining systems and operations to the geology of the trona bed being mined. This includes: separating the injection and production wells by sufficient distance to achieve saturation in the recovered brine; locating injection wells in thinner sections of the bed to minimize the cavity size beneath the injection wells; optimizing injection flows to each well to minimize transport of material away from beneath the injection well (again to minimize cavity size beneath the well); optimizing flow rate from each production well to minimize the risk of channels forming from the injection wells; and maintaining fluid balance in each bed by balancing total injection into each bed with production from each bed.

2) Mine the trona beds in a way which minimizes interactions with other beds being mined. This requires mining the trona beds starting from the top down and mining no more than two beds in a given area at the same time.

3) Condition the injection fluid prior to injection into the trona beds. This includes: controlling the blend of plant waste waters and process effluent so that the resulting fluid can be reconstituted to high-grade brine, cooling to the natural temperature of the mixed layer before injecting so that temperature sensitive muds will not be altered, and operating with minimum variation in temperature to avoid expansion and contraction of the injection well casings to minimize physical damage.

The application of these rules has produced a brine which is 20% richer, increased the volume of brine available to the plant, and more than doubled injection well life. These improvements are being translated directly into higher soda ash production and lower production costs at North American Chemical Company.



Figure 3. North-south stratigraphic cross section through the mixed layer, Searles Valley evaporite beds. North is on the left, depth (in feet) from the surface on left side of section.

Table 1. Reserves of saline minerals at Searles Lake. M=million or mega; B=billion; G=giga.

Mineral	Short tons		Metric tons (tonnes)	
Na_2CO_3	1.168	B	1.06	G
$Na_2B_4O_7$	95.95	M	86.68	M
Na_2SO_4	407.0	M	369.2	M
K_2SO_4 + KCL	71.07	M	64.5	M
NaCl	1.085	B	984	M
$NaHCO_3$ as trona	693.4	M	629	M
$NaHCO_3$ as nahcolite	155.4	M	140.9	M
Insoluble fraction	798.5	M	724.4	M

References cited

Friedman, I., Smith, G.I., and Matsuo, S., 1982, Economic implications of the deuterium anomaly in the brine and salts in Searles Lake, California: Economic Geology, v. 77, no. 3, p. 694-702.

Smith, G.I., 1979, Surface stratigraphy and geochemistry of Late Quaternary evaporites, Searles Lake, California: U.S. Geological Survey Professional Paper 1043, 130 p.

Smith, G.I., Barczak, V.J., Moulton, G.F., and Liddicoat, J.C., 1983, Core KM-3, a surface-to-bedrock record of Late Cenozoic sedimentation in Searles Valley, California: U.S. Geological Survey Professional Paper 1256, 24 p.

Matsuo, S., Friedman, I., and Smith, G.I., 1972, Studies of Quaternary saline lakes—I. Hydrogen isotope fractionation in saline minerals: Geochimica et Cosmochimica Acta, v. 36, p. 427-435.

Additional references

Lovejoy, M.E., and Fairchild, J., 1994, 4-D Modeling in time of a heated injection fluid: Proceedings of the First International Conference on Tailings and Mine Waste, Fort Collins, Colorado, A.A. Balkema, Rotterdam, p. 249-258.

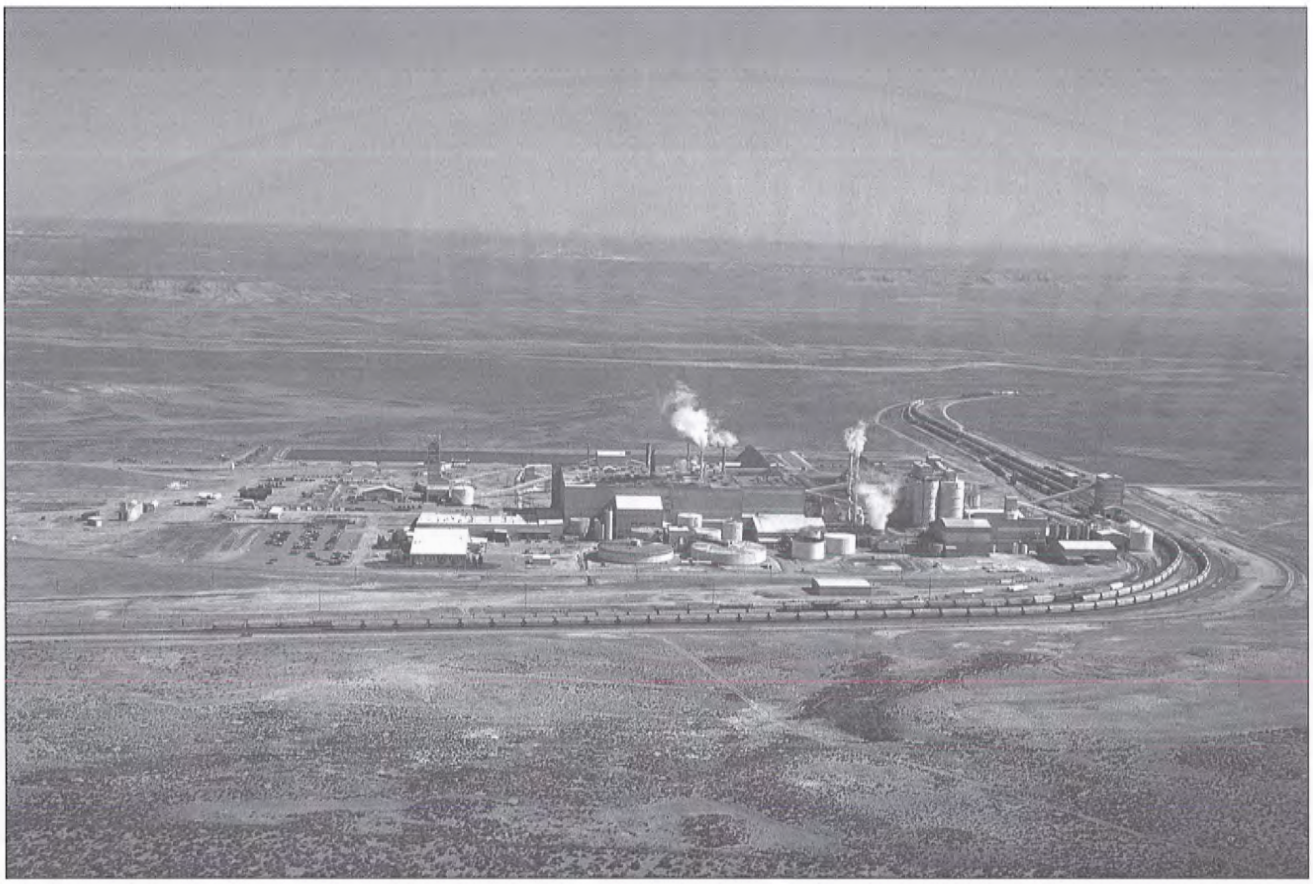
Lovejoy, M.E., 1995, Modeling a soda ash deposit with Techbase: Mining Magazine, Mining Journal Limited, United Kingdom, May 1995, p. 293-295.

Lovejoy, M.E., 1997, Operation and monitoring a geologic heat sink in solution mining: Proceedings of the Fourth International Conference on Tailings and Mine Waste, Fort Collins, Colorado, A.A. Balkema, Rotterdam, p. 417-423.

Moulton, G.F., 1980, Compendium of Searles Lake operations: Society of Mining Engineers of AIME, Transactions, v. 270, p. 1918-1922.

Moulton, G.F., and Santini, K., 1995, The geology and economic development of Searles Lake, *in* Proceedings of the 29th Forum on the Geology of Industrial Minerals: California Department of Conservation, Division of Mines and Geology Special Publication 110, p. 161-168.

Sonia, J.A., Fairchild, J.L., and Moulton, G.F., 1978, Exploration and mining of the mixed layer resources of Searles Lake, California: Kerr-McGee Chemical Corporation, Trona, California.



Aerial view of trona refinery, mine, and loadout facilities operated by Solvay Minerals, Incorporated in the Green River Basin, Wyoming.

A model for solution mining trona

Henry W. Haynes, Jr.
and
Animesh Ukidwe
Department of Chemical and Petroleum Engineering
University of Wyoming
Laramie, Wyoming 82071

Abstract

A mathematical model has been developed for a trona solution mine of the type that results when solvent is pumped between two wells drilled into a horizontal trona bed. Dissolution rates are assumed to be mass-transfer controlled. Literature correlations are combined to describe mass transfer from the initial production stage where forced convection dominates to later operations where mass transfer is primarily via density-driven free convection. Computations on two examples are discussed, one employing fresh water as solvent at near ambient temperature (30°C), and one using a 7 wt.% Na_2CO_3 solvent at 80°C. These computations indicate that conditions can be selected to produce a brine that can be economically processed into soda ash.

The model is entirely predictive; however, certain assumptions need further investigation. Suggestions for model improvements are also discussed.

Introduction

Solution mining of trona has long been touted as an attractive alternative to underground mechanical mining, with the first U.S. patent issued to Pike (1945). However, early experience with solution mining did not produce a viable process, and mechanical mining took the forefront where it still is today. A form of solution mining is currently being practiced by several Green River operators whereby a previously mined area is flooded creating an underground lake. Dissolution of trona from the pillars, floor, and roof takes place and the brine is pumped to the surface for processing. Pike and Seaton (1953) described such an operation in their patent, and a more recent version is described in a patent issued to Frint and others (1991).

In the mining operation of this study, two or more wells are drilled into a virgin trona bed, and a low-pressure connection is established by some means (hydraulic fracturing or directional drilling). Solution is injected into one well and product brine is collected from one or more production wells (**Figure 1**). This method of operation provides the only practical means of production from thin and/or deep trona seams. Field tests were conducted by the FMC Corporation beginning in the early 1980s and extending into the 1990s (see Jackson, 1981; Frint, 1985). Despite the extensive field work (with apparent successes suggested by the duration of these tests), little

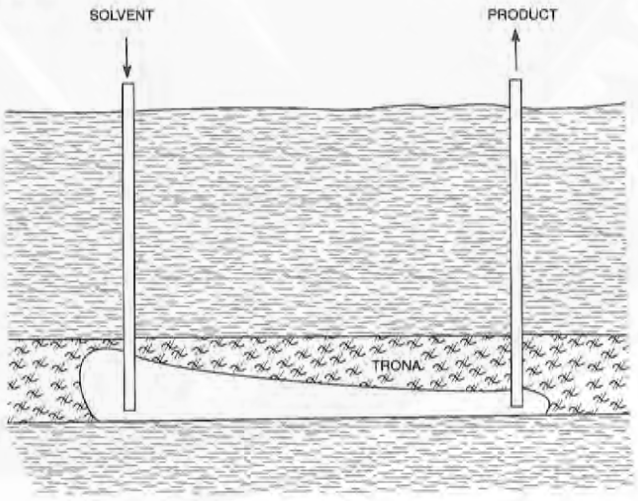


Figure 1. Illustration of a "Type I" solution mine.

has been published on the process and no modeling effort has surfaced.

This report describes a first attempt at modelling the type of solution mine illustrated in **Figure 1**. In order to obtain predictive results based on information at hand, it has been necessary to make some crude assumptions and to extrapolate correlations far beyond the range for which they were intended. The absolute reliability of these predictions is therefore very much suspect. Still, the trends predicted by the model appear reasonable when viewed qualitatively. More importantly, the model forms the foundation upon which improved versions can be constructed in the future. This study has also identified a critical need for certain laboratory information that should improve the model.

Physical property correlations

Physical properties data were collected from a number of sources and regressed with empirical expressions to obtain the desired property correlations. For density, data compiled by Garrett (1992) for sodium carbonate (components 1, 2, and 3 correspond to Na_2CO_3, $NaHCO_3$, and H_20, respectively) and by Lobo and Quaresma (1989) for sodium bicarbonate are represented by:

$$\rho = 1014.4 - 0.5704T + 1060\omega_1 + 805.4\omega_2 \quad (1)$$

where ρ is the solution density, T is the temperature (°C), and ω_1 and ω_2 are the weight percentages of sodium carbonate and sodium bicarbonate, respectively. A regression on sodium carbonate viscosity data from Garrett (1992) and sodium bicarbonate data from Roshkovskaya and Bratash (1973) provided:

$$\mu \times 10^8 = (6.4782 - 43.108\omega_1 + 493.67\omega_1^2 - 55.932 \times \omega_2 + 0.44088T\omega_1 + 1.7722T\omega_2) \times \exp\left(\frac{2934}{T + 273.16}\right). \quad (2)$$

Diffusivity data from Leaist and Noulty (1985) at 25°C were adjusted for temperature using the Stokes-Einstein equation. The diffusivity of sodium carbonate is then estimated from:

$$D_1 = 1.158E\text{-}9 \times \frac{(T + 273.16)\mu_{25}}{298.16\mu_T}. \quad (3)$$

The ternary Na_2CO_3-$NaHCO_3$-H_2O phase diagram is shown in **Figure 2**. The model requires values

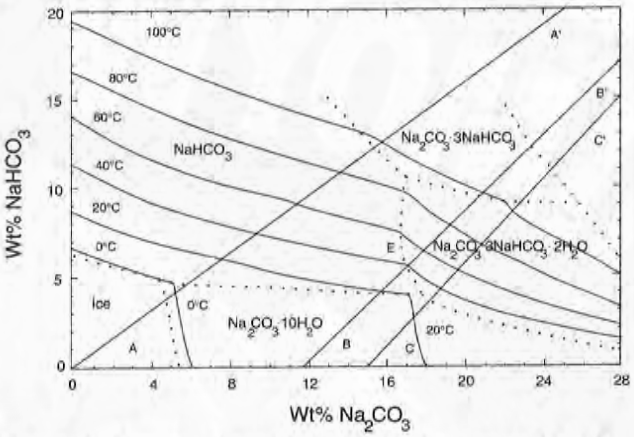


Figure 2. Ternary phase diagram for the system Na_2CO_3-$NaHCO_3$-H_2O.

along the Na_2CO_3-$NaHCO_3$ saturation line which are adequately represented by:

$$\omega_1 = 19.514 - 0.0861T + 0.000696T^2 \quad (4)$$

and:

$$\omega_2 = 3.0176 + 0.0156T + 0.000892T^2. \quad (5)$$

Solubility relationships in the trona region are in approximate accord with:

$$\omega_1 = 28.482 + 0.086916T + 0.0011331T^2 - 0.012464T\omega_2 - 4.9586\omega_2 + 0.54551\omega_2^2 - 0.021145\omega_2^3. \quad (6)$$

For the appropriate units to employ with these equations, see the nomenclature (**Table 1**) at the end of this paper.

Mass transfer correlations

Initially the two wells are connected by a small diameter channel, and mass transfer is predominantly by forced convection. If we assume that the channel is of circular cross section, the Dittus-Boelter correlation (see Bennett and Myers, 1982) can be applied. The Dittus-Boelter equation was originally developed for

forced convective heat transfer in cylindrical tubes. The mass transfer analogy is:

$$Sh = 0.023Re^{0.8}Sc^{0.33}. \quad (7)$$

All dimensionless groups (Gr, Re, Sc, and Sh) are defined in **Table 1**. As the channel enlarges, forced convection becomes of lesser importance, and free convection assumes dominance. Density driven free convection does not appear to have been studied in large diameter cavities. The only correlation that might be applicable is one due to Oliver (1962) who investigated the effect of natural convection on viscous-flow heat transfer in horizontal tubes. Under zero flow conditions, the mass transfer analogy to Oliver's correlation is:

$$Sh = 0.35\,(GrSc)^{0.25}. \quad (8)$$

As a crude approximation, a mass transfer correlation for the entire region spanning forced flow to free convection can now be constructed by simply adding these two correlations. Thus:

$$Sh = 0.35\,(GrSc)^{0.25} + 0.023Re^{0.8}Sc^{0.33}. \quad (9)$$

This equation will be used to calculate point values of the mass transfer coefficient (contained in *Sh*) at local values of velocity, cavity diameter, compositions, etc.

Dissolution model

The dissolution of trona in water proceeds along the dissolution line A-A' (**Figure 2**) which connects points corresponding to pure water (0% Na_2CO_3, 0% $NaHCO_3$) and trona (46.89% Na_2CO_3, 37.17% $NaHCO_3$). The trona point lies off the figure. Suppose the system is maintained at 40°C. The dissolution line encounters the 40°C isotherm in the sodium bicarbonate or nahcolite region. At this point the solution is saturated with respect to the bicarbonate, but not with respect to the carbonate. With further trona dissolution, bicarbonate precipitates and the solution is enriched in carbonate until point E is reached. At point E, nahcolite, trona, and a solution of composition 17.0% Na_2CO_3, and 5.6 % $NaHCO_3$ are all in equilibrium.

The critical question is, "Where does the bicarbonate form?" Does it deposit on and adhere to the trona surface, thereby slowing or preventing further contact with solution? Or does it precipitate loosely in the cavity in regions removed from the surface allowing the trona surface to remain exposed? The literature contains frequent reference to "bicarbonate blinding" as a possible explanation for unexpectedly slow dissolution rates mostly associated with large scale field tests. On the other hand, no systematic study of the blinding effect has appeared in the literature, and the only published investigations of trona dissolution rates were performed at low concentrations where blinding would not be expected to occur (see Nigbor, 1983; Nasün-Saygili and Okutan, 1996).

Referring again to **Figure 2**, consider dissolution along the line C-C' corresponding to the dissolution of trona in a 15% sodium carbonate solution. The 40°C isotherm is now intersected in the trona region, hence no solid bicarbonate can form. The line B-B' drawn through point E separates these two regions, i.e., the regions where solid bicarbonate can and cannot form.

The dissolution of a crystal and the reverse process of crystallization generally involve two resistances in series: surface reaction and mass transport. Our model assumes that the dissolution of trona is controlled by mass transport. This is supported by Nigbor's (1983) study and the near carbon-copy investigation of Nasün-Saygili and Okutan (1996). These researchers measured the rates of dissolution of trona in quiescent solutions and found that a simple convective mass transport model predicted results similar to experiment. It is important to keep in mind that mass transfer control represents the maximum attainable dissolution rate, and hence our model may be expected to predict optimistic results. Consistent with this expectation, the possible bicarbonate blinding effect has been ignored.

When trona ($Na_2CO_3 \cdot NaHCO_3 \cdot 2H_20$) dissolves in the absence of chemical reaction, stoichiometry dictates that the relation among molar fluxes be in accord with:

$$N_1 = N_2 = \frac{1}{2}N_3 = \text{Constant}. \quad (10)$$

In terms of the mass fluxes, n_i, this equation is written:

$$\frac{n_1}{M_1} = \frac{n_2}{M_2} = \frac{1}{2}\,\frac{n_3}{M_3}. \quad (11)$$

where M_i is the molecular weight of species i. The diffusion of sodium carbonate across the boundary layer is described by Fick's Law:

$$n_1 = -\rho D_1 \frac{d\omega_1}{dx} + \omega_1 \Sigma_j n_j \quad . \qquad (12)$$

Strictly speaking, one should consider the diffusion of ionic species when dealing with electrolyte solutions. However, provided that highly mobile H^+ and OH^- species are not involved, no great error is introduced by the use of "molecular" diffusion coefficients.

For constant component fluxes, this equation is readily integrated across the film of thickness δ to obtain:

$$n_{w,1} = \frac{k_{m,1}\bar{\rho}}{\alpha} Ln \left(\frac{1-\alpha\omega_1}{1-\alpha\omega_{s,1}} \right) \qquad (13)$$

where $k_{m,1} = D_1/\delta$ is the convective mass transfer coefficient and:

$$\alpha = \frac{1}{M_1}(M_1 + M_2 + M_3). \qquad (14)$$

The density, ρ, is the average of the surface and bulk fluid densities.

System equations

Consider a fluid flowing through a channel in a horizontal trona seam of infinite thickness (**Figure 3**). The channel is assumed to be cylindrical, but the diameter is allowed to vary. The channel grows via dissolution of trona at the walls according to the mass transfer controlled process described above. It is further assumed that the channel is isothermal at the feed temperature.

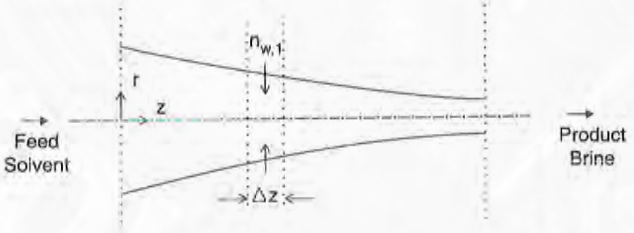


Figure 3. Idealized cylindrical channel connecting the injection and production wells.

Assuming plug flow, an overall mass balance across the increment, Δz, in the time interval, Δt, provides in the limit:

$$\frac{\partial(r^2\rho v)}{\partial z} = 2r(1-\rho/\rho_s)\Sigma_j n_{w,j} - r^2\frac{\partial\rho}{\partial t} \quad . \qquad (15)$$

Similarly, the component mass balances for i = 1 (Na_2CO_3), 2 ($NaHCO_3$), and 3 (H_2O) may be written:

$$\frac{\partial\omega_i}{\partial z} = \frac{2}{r\rho v}(n_{w,i} - \omega_i \Sigma_j n_{w,j}) - \frac{1}{v}\frac{\partial\omega_i}{\partial t} \qquad (16)$$

The solid phase mass balance is:

$$\frac{\partial r}{\partial t} = \frac{1}{\rho_s}\Sigma_j n_{w,j} \quad . \qquad (17)$$

Considerable simplification can be realized by ignoring the time dependent terms on the right hand side of equations (15) and (16). This "pseudosteady-state" approximation is acceptable if the channel grows slowly by comparison to the time required to establish the composition gradients, a reasonable assumption in our case.

With this simplification, the overall mass balance can be written as:

$$\frac{\partial(r^2\rho v)}{\partial z} = \frac{\partial u}{\partial z} = 2r(1-\rho/\rho_s)\alpha n_{w,1} \qquad (18)$$

and the component mass balances become:

$$\frac{\partial\omega_1}{\partial z} = \frac{2n_{w,1}}{r\rho v}(1-\alpha\omega_1) \qquad (19)$$

$$\omega_2 = \frac{1}{\alpha}\left[\frac{M_2}{M_1} - \left(\frac{M_2}{M_1} - \alpha\omega_{2,0}\right)\left(\frac{1-\alpha\omega_1}{1-\alpha\omega_{1,0}}\right)\right] \qquad (20)$$

$$\omega_3 = 1 - \omega_1 - \omega_2 \quad . \qquad (21)$$

For the solid phase mass balance, we have:

$$\frac{\partial r}{\partial t} = \alpha n_{w,1}/\rho_s \qquad (22)$$

The composition of the feed solvent, the solvent flow rate, and the initial channel radius are all assumed to be known and to remain constant. The appropriate initial conditions are therefore:

$$\omega_1(0, t) = \omega_{1,0} \qquad (23)$$

$$u(0, t) = u_0 = r_0^2 \rho_0 v_0 \qquad (24)$$

and:

$$r(z, 0) = r_0 \; . \qquad (25)$$

Computational algorithm

The system equations were solved numerically using the finite difference scheme illustrated in **Figure 4**. The derivatives were approximated by centered differences about the midpoints (x) in the figure, and values of the dependent variables were obtained at the points (o). The computational algorithm involves successive iterations for the (i+1, j+1) values between two sets of equations [equations (26), (27), and (28) in one set and equations (29), (30), and (31) in the other set:

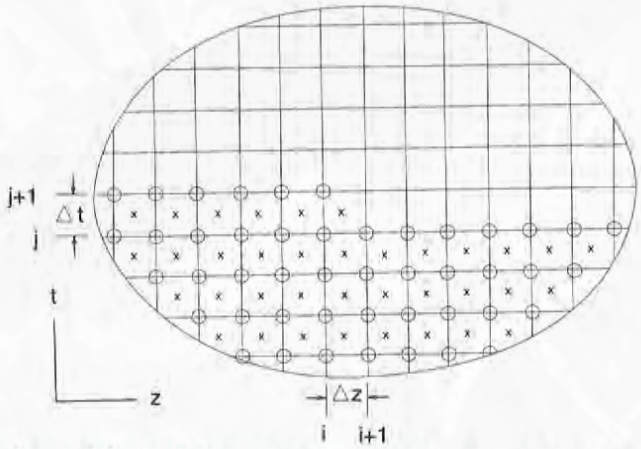


Figure 4. Finite difference approximation to system equations.

$$u_{i+1,j+1} = u_{i,j+1} - u_{i+1,j} + u_{i,j} + 2\Delta z[2r(1-\rho/\rho_s)\alpha n_{w,1}]_m \qquad (26)$$

$$\omega_{1,i+1,j+1} = \omega_{1,i,j+1} - \omega_{1,i+1,j} + \omega_{1,i,j} + 2\Delta z \left[\frac{2n_{w,1}}{r\rho v}(1-\alpha\omega_1)\right]_m \qquad (27)$$

$$r_{i+1,j+1} = -r_{i,j+1} + r_{i+1,j} + r_{i,j} + 2\Delta t[\alpha n_{w,1}/\rho_s]_m \qquad (28)$$

and:

$$u_m = \frac{1}{4}(u_{i,j} + u_{i+1,j} + u_{i,j+1} + u_{i+1,j+1}) \qquad (29)$$

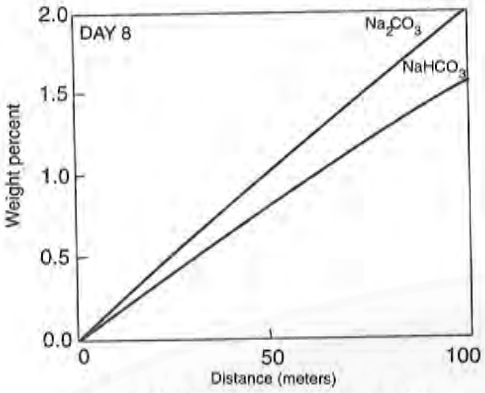
$$\omega_{1,m} = \frac{1}{4}(\omega_{1,i,j} + \omega_{1,i+1,j} + \omega_{1,i,j+1} + \omega_{1,i+1,j+1}) \qquad (30)$$

$$r_m = \frac{1}{4}(r_{i,j} + r_{i+1,j} + r_{i,j+1} + r_{i+1,j+1}) \qquad (31)$$

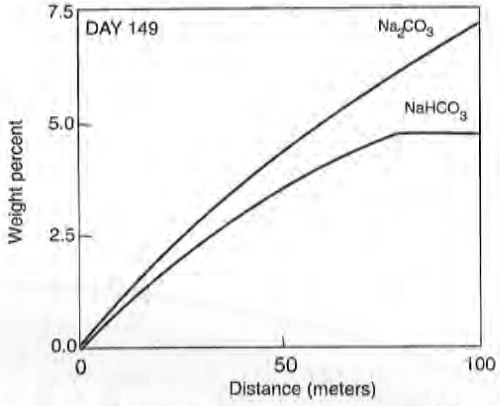
until a convergence criterion is satisfied.

Results

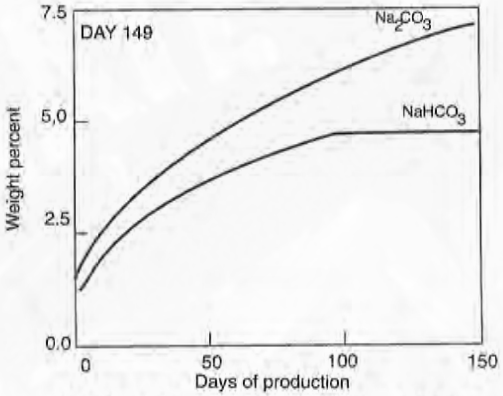
Computational results for an example employing fresh water solvent at 30° C are presented in **Figure 5**. The well spacing is 100 m, the initial channel diameter is 0.15 m and the inlet flowrate is 50 m^3/hr. The initial composition profiles are plotted in **Figure 5a**. The product brine is unsaturated in both Na_2CO_3 and $NaHCO_3$. However, after 149 days of operation, the brine becomes saturated in bicarbonate at a position approximately 80 m from the inlet, **Figure 5b**. The critical length corresponding to bicarbonate saturation moves towards the inlet with time as shown in **Figure 5d**. The exit brine composition is plotted versus days of operation in **Figure 5c**. Except for a brief early period when brine composition decreases, the product brine compositions generally increase with time. This improvement is due primarily to the increase in surface area as the cavity grows. The curious early dip in brine composition is due to the decrease in mass transfer coefficient while forced convection is dominant. As the cavity enlarges, free convection effects assume dominance and the mass transfer coefficient actually increases with cavity diameter. The cavity size and shape after 149 days of operation at these conditions is shown in **Figure 5e**.



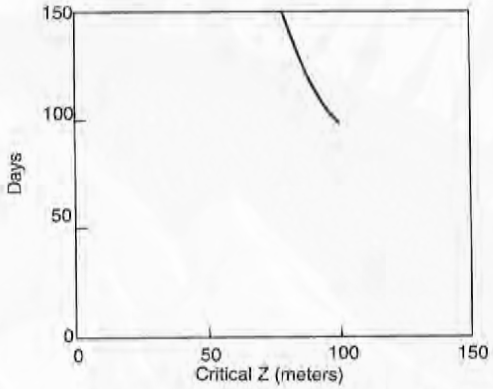
(a) Initial composition profiles.



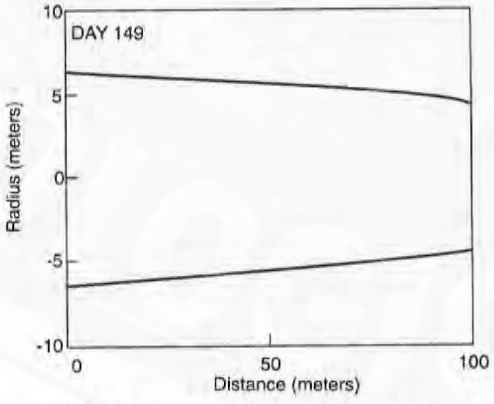
(b) Composition profiles after day 149.



(c) Product composition vs. days of production.



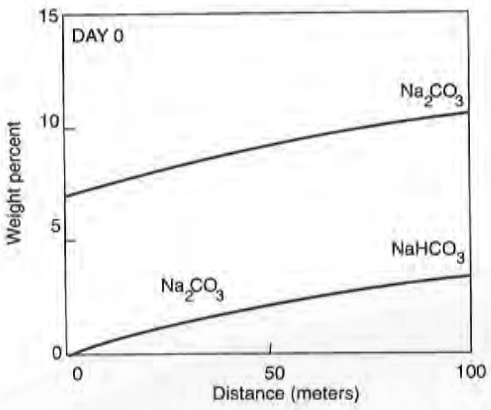
(d) Critical length corresponding to bicarbonate formation.



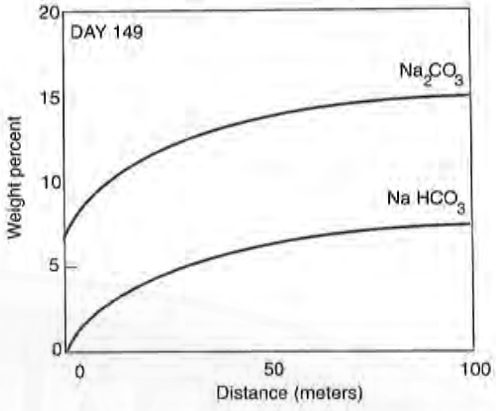
(e) Cavity after 149 days of production.

Figure 5. Solution mining results for composition of brines and cavity size using fresh water solvent at 30 °C. Computations for L = 100 m, d_c = 0.15 m, T = 30 °C, Q_v = 50 m^3/hr, solvent: fresh water.

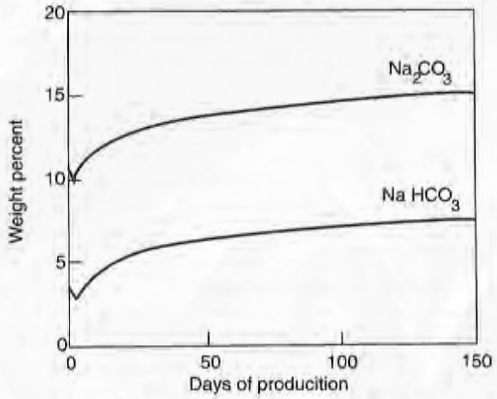
Results computed for a second illustrative example are plotted in **Figure 6**. Well spacing, initial channel diameter, and inlet flow rate are the same as in the first example. However, the current calculations are for a 7 wt.% Na_2CO_3 solvent, and the temperature is assumed to be constant at 80°C. The first thing to note is that no bicarbonate precipitates at these conditions. As a matter of fact it is evident from the phase diagram, **Figure 2**, that no solid bicarbonate can form. (A trona dissolution line analogous to B-B', but passing through the 80°C isotherm will intersect the abscissa at just over 6 wt.% Na_2CO_3. Thus the 7 wt.% excess carbonate line intersects the 80°C isotherm in the trona region.) It is also evident that product brine compositions are much higher than in the first example. This happy situation is of course tempered by the fact that the feed solvent contains a considerable alkali value and it has been necessary to provide heat



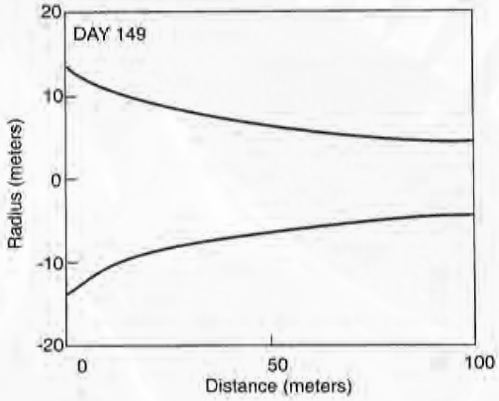
(a) Initial composition profiles.



(b) Composition profiles after day 149.



(c) Product composition vs. days of production.



(d) Cavity after 149 days of production.

Figure 6. Solution mining results for composition of brines and cavity size using a 7 wt.% Na_2CO_3 solvent at 80°C. Computations for L = 100 m, d_o = 0.15 m, T = 80°C, Q_o = 50 m^3/hr, solvent: 7 wt.% Na_2CO_3.

to the system. Other trends noted in the first example, most notably the increased brine composition with production time, are also observed in the current example.

To provide some perspective, it is claimed that brines containing bicarbonate can be economically processed into soda ash provided that the:

$$\text{Total Alkalinity} = (\text{wt.\% } Na_2CO_3) + 0.631 \times (\text{wt.\% } NaHCO_3)$$

is on the order of 8 wt.% or higher (Frint and Copenhafer, 1993; Copenhafer and others, 1994). It is clear from **Figure 6c** that all the brines produced by the second example would meet this requirement. However, the brines produced early in the first example would probably be too dilute to process economically (**Figure 5c**). Optimum operating conditions could be sought by an analysis of the combined solution mining operation and processing scheme. The availability of a reliable solution mining model would be indispensable in such an endeavor.

Critique

The University of Wyoming Trona Solution Mine Model, Ver. 01, (UWTSM01) which has been presented here is entirely predictive. No unknown parameters are contained in the model. However, the model in its current state contains considerable uncertainties that are in need of further investigation. Most notable is usage of Oliver's correlation for describing mass transfer in the free convection regime. This cor-

relation was developed from heat transfer experiments on water flowing through half-inch-diameter horizontal tubes. Application to large diameter cavities of the type encountered in trona solution mining involves extrapolation of the correlation over several orders of magnitude in Grashof Number. An investigation is sorely needed to develop mass transfer correlations for density-driven free convection in large cavities.

Dissolution rate measurements are also badly needed, particularly in concentrated brines where bicarbonate blinding might occur. The carbonate/bicarbonate ratio should be varied. The most useful experiments would be designed to separate intrinsic kinetics from mass transport effects. Refinements in the dissolution model would account for the double salt, and the possible additional mass transfer resistance imposed by a bicarbonate layer.

The circular geometry assumption is certainly subject to criticism. With the anticipation that highly concentrated, highly dense fluid will tend to reside near the bottom of the cavity, dissolution should take place preferentially near the upper zones of the chamber. A "morning glory" cavity cross section might therefore be more appropriate. For the same reason, a more realistic model would take into account stratified flows.

It is expected that an energy balance could be added to the model without great difficulty. With this addition it would be possible to account for numerous phenomena such as heat loss to the surroundings, and localized dissolution and reaction heat effects. The model should also be modified for application to trona seams of finite thickness.

Finally, allowance should be made for chemical reactions. The reaction of bicarbonate with caustic has been proposed as a means of circumventing the blinding problem (Gancy, 1965; Rube, 1976). Certain advantages are also claimed for solution mining solvents containing ammonia (Frint and others, 1981), sodium sulfide (Sadlick and Cohen, 1981), and mineral acids (Ilardi and Goldstein, 1985; Mani and Chlanda, 1987). For very rapid reactions, the assumption of mass transfer control will be reasonable.

Conclusions

A mathematical model has been developed which allows the user to explore the effects of flow rate, temperature, well spacing, and solvent composition (feed Na_2CO_3 and/or $NaHCO_3$) on the operation of a trona solution mine. From the examples investigated, it appears that product brines can be produced which are amenable to economical processing into soda ash.

While the model in its current state contains numerous uncertainties, and quantitative results should not be expected, we believe that the "essence" of trona solution mining is described.

References cited

Bennett, C.O., and Myers, J.E., 1982, Momentum, heat, and mass transfer, 3rd ed.: McGraw-Hill, New York, New York.

Copenhafer, W.C., Smith, D.E., and Niedringhaus, G.F., 1994, Process for producing sodium salts from brines of sodium ores: U.S. Patent No. 5,283,054 (February 1, 1994).

Frint, R., 1985, FMC's newest goal: Commercial solution mining of trona: Engineering and Mining Journal, p. 26-35.

Frint, W.R., and Copenhafer, W.C., 1993, Process for producing sodium salts from brines of sodium ores: U.S. Patent No. 5,262,134 (November 16, 1993).

Frint, W.R., Rithell, M.M., and Fischer, W.G., 1991, Soda ash production: U.S. Patent No. 5,043,149 (August 27, 1991).

Frint, W.R., Copenhafer, W.C., and Pinsky, M.L., 1981, Recovery of alkali values from sodium bicarbonate-containing ore with ammonia: U.S. Patent No. 4,283,372 (August 11, 1981).

Gancy, A.B., 1965, Process for the production of soda ash from underground trona deposits: U.S. Patent No. 3,184,287 (May 18, 1965).

Garrett, D.E., 1992, Natural soda ash–occurrences, processing, and use: Van Nostrand Reinhold, New York, New York.

Ilardi, J.M., and Goldstein, D., 1985, Solution mining of trona or nahcolite ore with aqueous NaOH and HCl solvents: U.S. Patent No. 4,498,706 (February 12, 1985).

Jackson, D., 1981, Trona solution mining–FMC goes after deep Wyoming deposits: Engineering and Mining Journal, p. 68-69.

Kube, W.H., 1976, Process for the solution mining of subterranean sodium bicarbonate bearing ore bodies: U.S. Patent No. 3,953,073 (April 27, 1976).

Leaist, D.G., and Noulty, R.A., 1985, Multicomponent diffusion of aqueous sodium carbonate and aqueous sodium bicarbonate: Canadian Journal of Chemistry, v. 63, p. 2319.

Lobo, V.M.M., and Quaresma, J.L., 1989, Handbook of electrolyte solutions, Pt. B: Elsevier, New York, New York.

Mani, K.N., and Chlanda, F.P., 1987, Solution mining of sodium minerals with acids generated by electrodialytic water splitting: U.S. Patent No. 4,636,289 (January 13, 1987).

Nasün-Saygili, G. and Okuntan, H., 1996, Mechanism of the dissolution of Turkish trona: Hydrometallurgy, v. 43, p. 317.

Nigbor, M.T., 1983, Dissolution rate experiments for Wyoming trona: National Meeting of American Institute of Chemical Engineers, Paper 50c, (August, 1983).

Oliver, D.R., 1962, The effect of natural convection on viscous-flow heat transfer in horizontal tubes: Chemical Engineering Science, v. 17, p. 335.

Pike, R.D., 1945, Solution mining of trona: U.S. Patent No. 2,388,009 (October 30, 1945).

Pike, R.D., and Seaton, M.Y., 1953, Mining operation: U.S. Patent No. 2,625,384 (January 13, 1953).

Roshkovskaya, E.A., and Bratash, E.G., 1973, Viscosity of solutions of ammonium bicarbonate, sodium bicarbonate and ammonium chloride in the range 20 - 100°C: Zhurnal. Prikla. Khimi, v. 46, no. 2, p. 273.

Saldick, J., and Cohen, B., 1981, Recovery of alkali values from trona ore: U.S. Patent No. 4,285,915 (August 25, 1981).

Table 1. Nomenclature for equations used in this paper. m = meters, s = seconds, kg = kilograms.

d	=	Diameter, m
D_i	=	Component i diffusivity, m^2/s
g	=	Gravitational constant = 9.8 m/s^2
$k_{m,i}$	=	Convective mass transfer coefficient, m/s
M_i	=	Component i molecular weight, kg/kmol
n_i	=	Component i mass flux, $kg/m^2 \cdot s$
N_i	=	Component i molar flux, $kmol/m^3 \cdot s$
r	=	Channel radius, m
t	=	Time, s
T	=	Temperature, °C
u	=	$r^2\rho v$
v	=	Velocity, m/s
x	=	Length coordinate measured from wall, m
z	=	Length coordinate measured from channel entrance, m

Greek letters:

α	=	Constant defined by equation (14)
δ	=	Film thickness, m
ζ	=	$\frac{1}{\rho}\left[\frac{\partial \rho}{\partial \omega_i}\right]$ = Reduced density gradient
μ	=	Viscosity, centipoise
ρ	=	Density, kg/m^3
ω_i	=	Weight percent or weight fraction of component i in solution

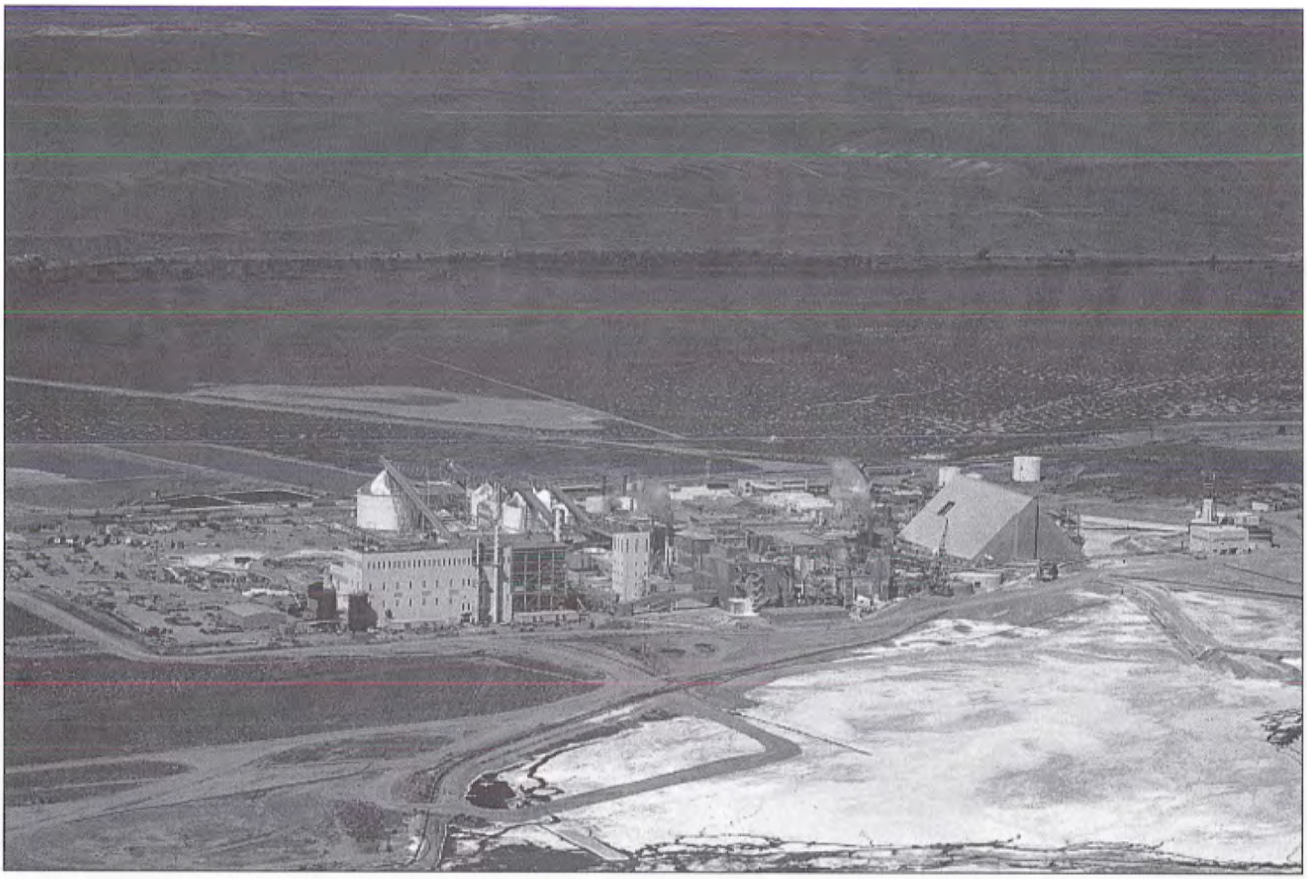
Dimensionless groups:

$Gr = \frac{d^3\rho^2 g\zeta\Delta\omega_i}{\mu^2}$ = Grashof Number

$Re = \frac{dv\rho}{\mu}$ = Reynolds Number

$Sc = \frac{\mu}{\rho D_i}$ = Schmidt Number

$Sh = \frac{k_{m,i}d}{D_i}$ = Sherwood Number



Aerial view of the trona mine, refinery, and tailings disposal ponds of OCI Wyoming, L.P., in the Green River Basin, Wyoming.

Process selection criteria for refining trona to commercial products

Roger Aitala
and
Mark Aitala
Isonex, Incorporated
Briarcliff (Austin), Texas 78669

Abstract

Trona deposits vary in geological and chemical characteristics. Location and site characteristics such as environmental matters, specific energy resources, distribution methods, and trade barriers are key elements in a trona-refining project. A commercially successful trona-refining project, capable of surviving the inevitable competition in this global business, rests on the rational integration of the major project parameters.

There should be no inconsistencies or discontinuities between the ore from the mine, the feed to the refinery, and the market requirements. These factors must match or economic disaster is possible, even after investing the several hundred million dollars required to build a world-class trona refinery. The major parameters in process selection are: the characteristics of the trona deposit; whether the project involves an expansion or a "dry desert;" available forms of energy and its costs; and the geographical market under consideration for soda ash and suitable derivatives.

This paper outlines a logical methodology for process and selection of a slate of products. Existing commercial technologies and mining and refining technologies currently under development are briefly reviewed.

Introduction: the project

There are three main types of trona-refining ventures possible: 1) expansion of an existing trona-refining complex; 2) development of a new complex in a known deposit; and 3) development of a new complex in a new deposit.

The objective in all cases is to structure a trona-refining operation which will maximize economic returns for the long term that is consistent with safety and environmental safeguards.

The trona deposit

Location

The location of a trona deposit is paramount for project development, especially as affecting product distribution. Not only is the distance from major consumers and the transportation/distribution systems in place or required to reach target markets a factor, but logistics for people and materials during construction must also be considered.

Surface or deep

Owens Lake, California; Lake Natron, Tanzania; and Magadi, Kenya are examples of surface deposits. The Green River Basin of Wyoming, and Beypazari, Turkey are examples of massive, bedded deep trona deposits. The hydrology of the area should be known for both surface or deep trona deposits. The presence of aquifers and their relationship to trona beds, arte-

sian flows, and water infiltration rates should be determined. Groundwaters may be a source of water in desert areas with scarce surface water.

Geology and reserves

The collection of geological information and the delineation and sizing of reserves should include seismic data and geological descriptions, including extent of faulting. Trona-refining complexes are capital-intensive; therefore, reserves need to be adequate to support a project, preferably for more than 20 years.

Ore sample analysis

A complete ore analysis based on extensive sampling is required to evaluate a trona deposit. Certainly, a high trona assay is desirable, but other considerations like low salt, low organic matter (kerogens), and a high degree of homogeneity in the ore in all directions also have economic impacts. Dry and wet analyses are necessary to determine, among other characteristics: a break down of water-insolubles and at what temperature(s), calcium carbonate ($CaCO_3$); shortite ($Na_2CO_3 \cdot 2CaCO_3$); pirssonite ($Na_2CO_3 \cdot CaCO_3 \cdot 2H_2O$); gaylussite ($Na_2CO_3 \cdot CaCO_3 \cdot 5H_2O$); burkeite ($Na_2CO_3 \cdot 2Na_2SO_4$); nahcolite ($NaHCO_3$); silicates, which form sodium silicates and can show up in products; wegscheiderite ($Na_2CO_3 \cdot 3NaHCO_3$, with extra carbon dioxide as bicarbonate); sodium chloride; thenardite (Na_2SO_4, especially in California's soda lakes); organics that cause color, foaming, and increase costs; and other values, such as borates, potassium and magnesium salts, double salts, and other compounds available in a complete chemical analysis.

Products

The probable main products considered in a trona-refining project are various forms of sodium carbonate, especially dense soda ash; caustic soda; and sodium bicarbonate. Downstream derivatives may also be of interest in certain geographical markets.

Market requirements

The physical characteristics of the product, such as granulation, flowability, and particle and bulk density must be included in the specifications for soda ash, sodium bicarbonate [Technical or USP (U.S. Pharmacopeia) Grade], and caustic soda (50% or solid).

Product samples from pilot operations are highly desirable. Potential customers will consider a project more seriously and can confirm its suitability for their applications.

Distribution considerations

Trona-refining complexes usually require only fuel from other locations. Therefore, the distribution plan mostly concerns the product(s).

Wyoming trona refiners distribute most soda ash via fleets of owned or leased closed railroad hopper cars. Trucking of soda ash directly to the consumer has declined dramatically. Most of the product destined for overseas markets is handled by the American Natural Soda Ash Corporation (ANSAC). Most of the railroad cars and shipping and receiving terminals are dedicated to soda ash to prevent cross-contamination. ANSAC ships most of the soda ash via unit trains and eight ocean-going vessels.

Mining alternatives and plans

These are interdependent with process selection. The mining plan must establish early in the project whether the deposit will be mined exclusively by mechanical means or will be followed by solution mining. The long-term mining plan may in some cases include mining beds at different depths. In Wyoming, mining technologies have evolved and improved considerably. For example, **Figure 1** shows that the trona miners' productivity has almost doubled over the past twelve years.

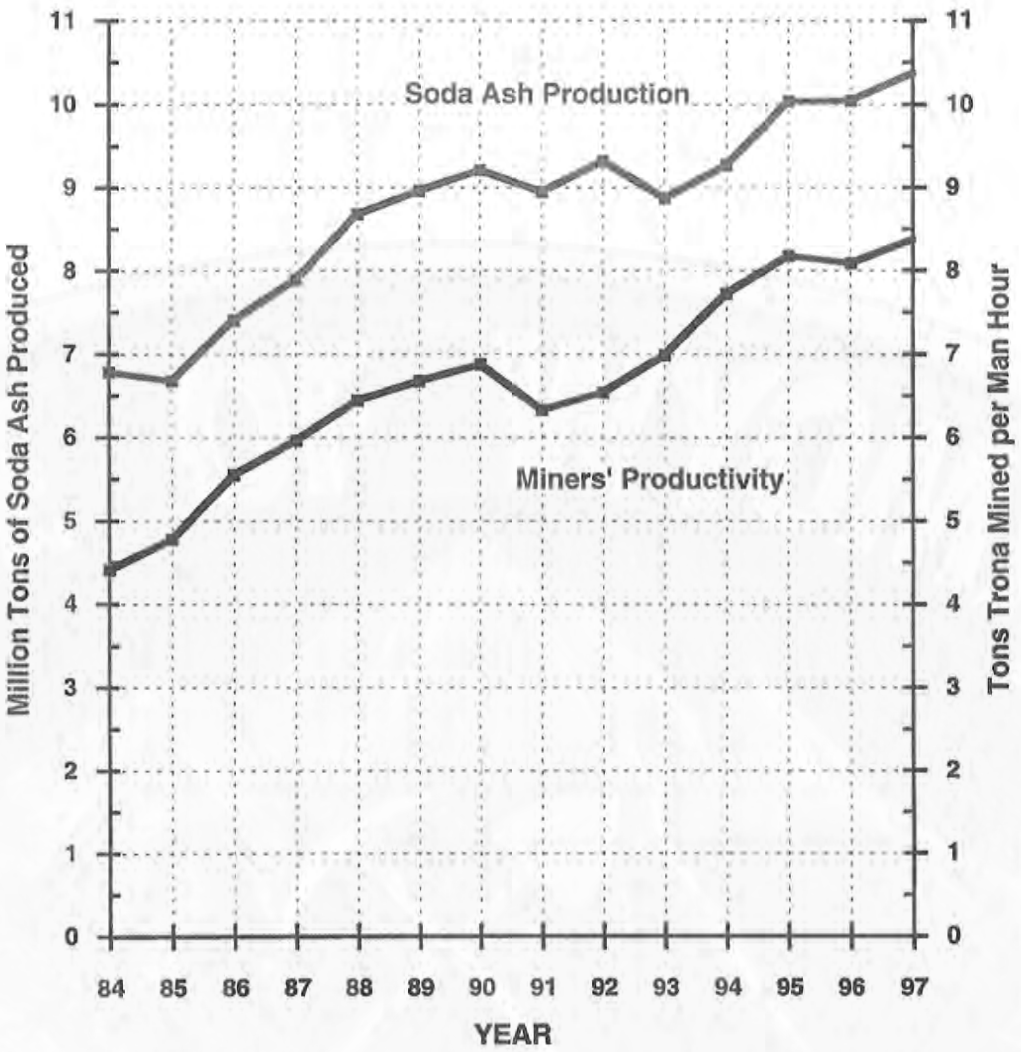


Figure 1. Soda ash production and miners' productivity in Wyoming, 1984 to 1997.

Mechanical versus solution mining

FMC has been practicing solution mining following post-mechanical mining commercially since November 1995.

Tg Soda Ash has been operating a caustic soda plant based on "mine waters" since 1994 and may have been recycling some liquids to the mine. Tg Soda Ash recently obtained a patent for carbon dioxide stripping of mine waters containing sodium carbonate and sodium bicarbonate. Tg has also applied for a process patent, presumably involving solution mining of trona, refining to soda ash and caustic soda, and recycling to the mine.

These new solution-mining technologies hold promise for further improving miners' productivity and in reducing mining costs.

Solution mining–new complex

The advantages of solution mining for a new complex are several. Most of the insolubles are left in the mine, capital costs both underground and in the refining system are lower, and labor costs, especially in the mine, are lower. Energy consumption is lower and post-mechanical solution mining increases resource recovery and project life.

Projected mine effluent

Mine effluents from both underground mining and solution mining (or a combination) should be characterized. For solid trona, the size of the ore rocks from the mining process will determine how the trona reacts with the underground solutions. For trona solutions, one should know the degree of saturation, and

how it is affected by return solutions. Expected temperatures, expected consistency of the effluents, and finally, a complete analysis of the effluents should be made.

Process selection

As already mentioned, the process selected must be considered in conjunction with the mining alternatives. To produce the probable main product, dense soda ash, from trona requires the following stoichiometry for the main reaction:

$$2Na_2CO_3 \cdot NaHCO_3 \cdot 2H_2O \xrightarrow{90°\text{-}150°C} 3Na_2CO_3 + CO_2 + 5H_20.$$

The overall stoichiometry yields water, which is an important observation for projects located in desert regions.

The above reaction can be carried out on solid trona at about 150°C or by steam stripping the carbon dioxide from a water solution at lower temperatures. Some of Solvay's operations called this steam stripping equipment decarbonators or DCBs. Wet calcination has many advantages over dry calcination, except that the degree of decomposition is not as complete. This can be remedied by adding small amounts of lime, which will convert the bicarbonate to sodium carbonate.

The separation of the sodium carbonate from all other ore components can be carried out via many processes. The dry calcination process (**Figure 2**) is used by all Wyoming refiners. A solution mining/wet calcination process (**Figure 3**), as taken from a recent Tg Soda Ash patent, is one of several possible configurations for this process.

In both dry and wet calcination processes, the final product is obtained by precipitating sodium carbonate monohydrate crystals in evaporators, centrifuging the crystals, and dehydrating to the anhydrous dense soda ash in steam tube dryers or fluid bed dryers, as shown by the reaction:

$$Na_2CO_3 \cdot H_2O \longleftrightarrow Na_2CO_3 + H_20\uparrow.$$

As is the case in all reactions in this field, they are reversible and are driven in one direction or the other by concentrations, temperatures, and by removing components from the reaction medium.

The monohydrate evaporator-crystallizers systems are complex. Among other considerations, they must be designed and operated to control the size distribution of the crystals to match the granulation specifications for the final product. Even crystal shape

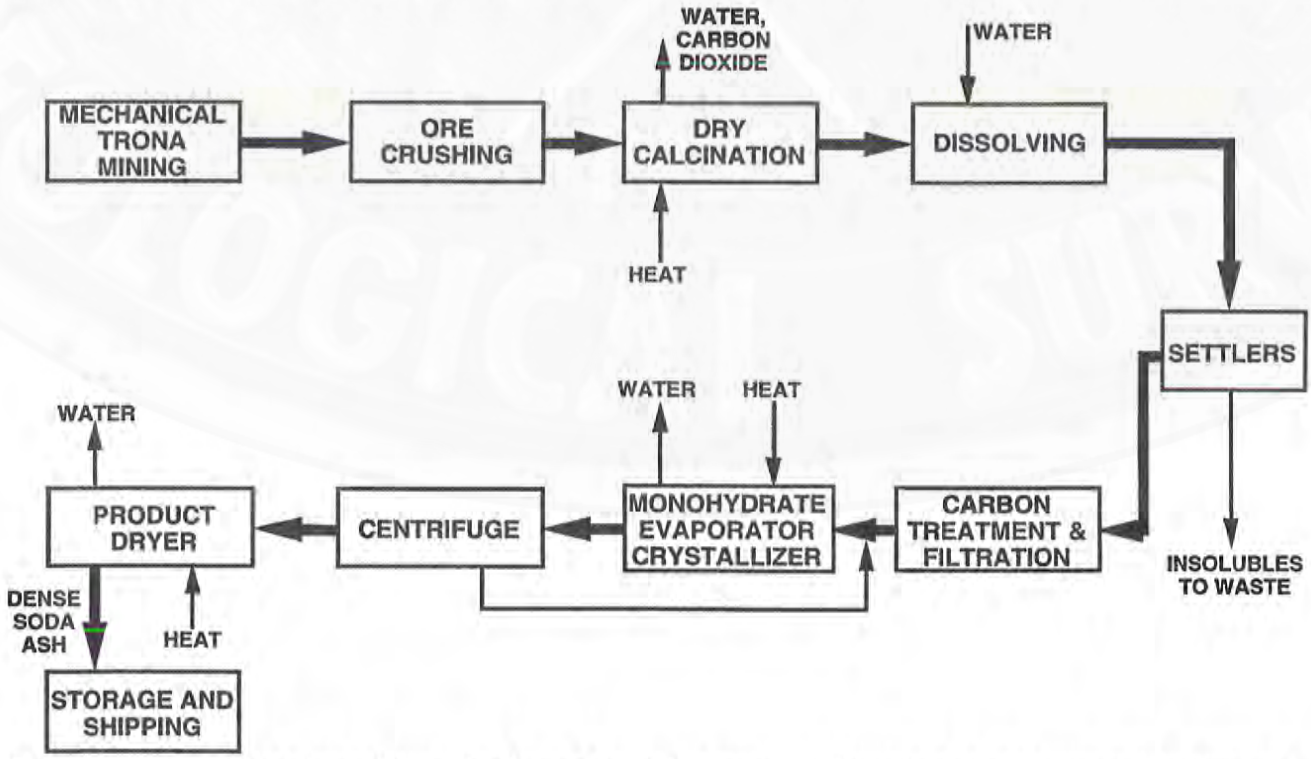


Figure 2. Flow diagram for refining dense soda ash using a monohydrate process based on dry trona mining and dry calcination.

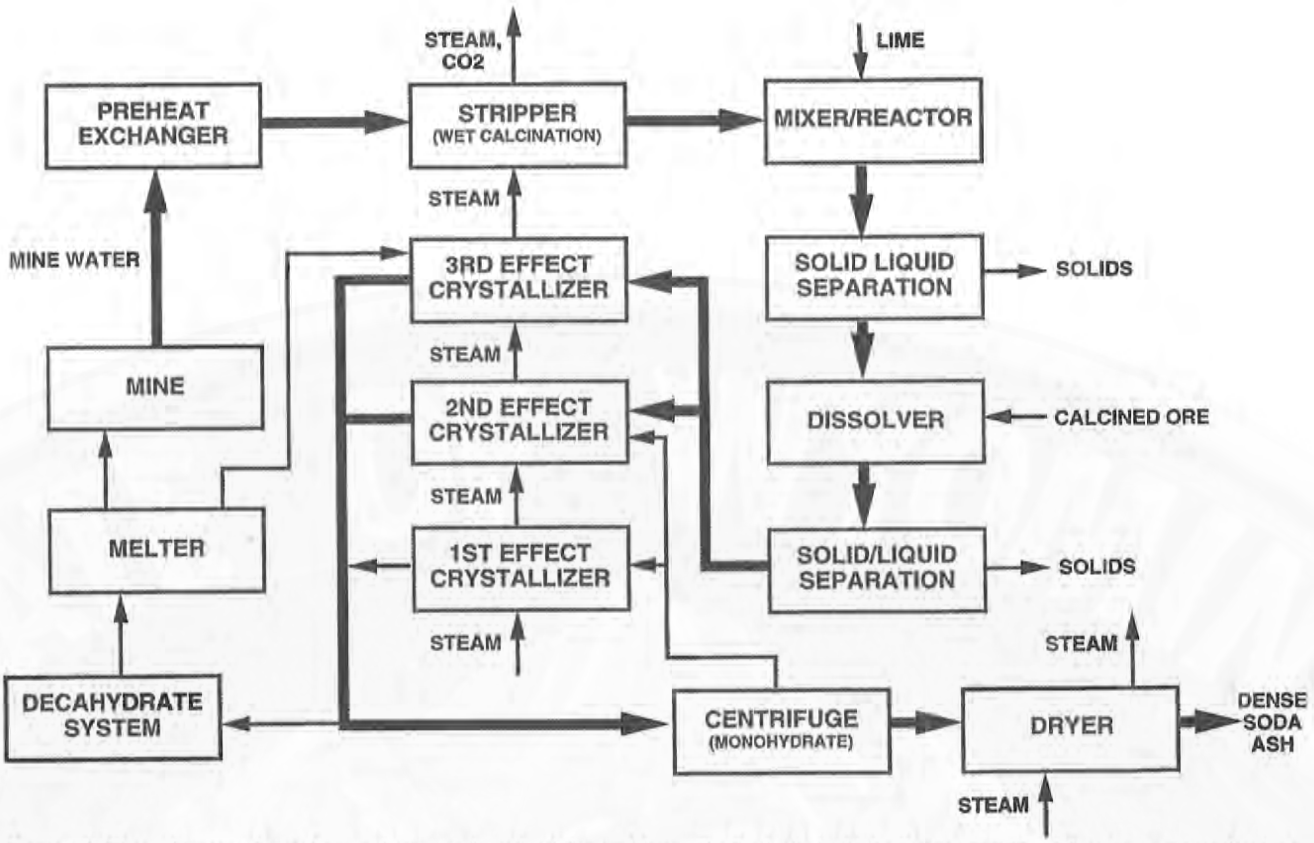


Figure 3. Flow diagram for refining dense soda ash. Adapted from Tg Soda Ash, U.S. Patent 5,609,838 using a monohydrate process based on solution mining and wet calcination.

and single crystal diameter to length ratio may be important and require additives and/or shape modifiers. Formation of complex crystal clusters ("stars") must be avoided as they tend to break down and generate fines. Some dry classification of the final product can also be done, but at extra cost.

In Wyoming, about 1.8 short tons of trona yields 1 short ton of dense soda ash. The specific yields at each producer depend on the assay of the mined trona, which can vary from 79 to 96%, and on the details of the operation.

Phase diagrams (**Figure 4**) are the main road maps guiding the process design. As for all road maps and ventures, it is crucial that they be for the right system with the relevant components. They show which solid sodium carbonate hydrates are in equilibrium with the liquid phase as a function of temperature and concentration of sodium carbonate. They can be difficult to interpret, especially when sodium chloride, calcium carbonate, sodium silicates, and other compounds, such as gaylussite or pirssonite, are included. These diagrams can be important in order to avoid regions conducive to scaling of internal equipment surfaces. Equipment can be descaled by washing, but frequent washing reduces effective plant capacity and increases energy costs to remove the excess water.

Many other issues must be addressed in the process design. These include (along with some possible processes or options for remediation):

1. How is salt removed? (Purge and decahydrate crystallizers can be used to remove salt(s).)
2. How are insolubles removed? (The insolubles can be left in the mine, filtered, or sent to a tailings pond.)
3. How is organic matter removed? (Carbon treatment, high-temperature calcination, or oxidizing agents can be applied.)
4. Overall water balance. (The use of a decahydrate system or condensate recovery can control water balance.)
5. Sulfur content of fuels.
6. Overall energy consumption versus capital cost. (Systems used to attain better energy efficiencies

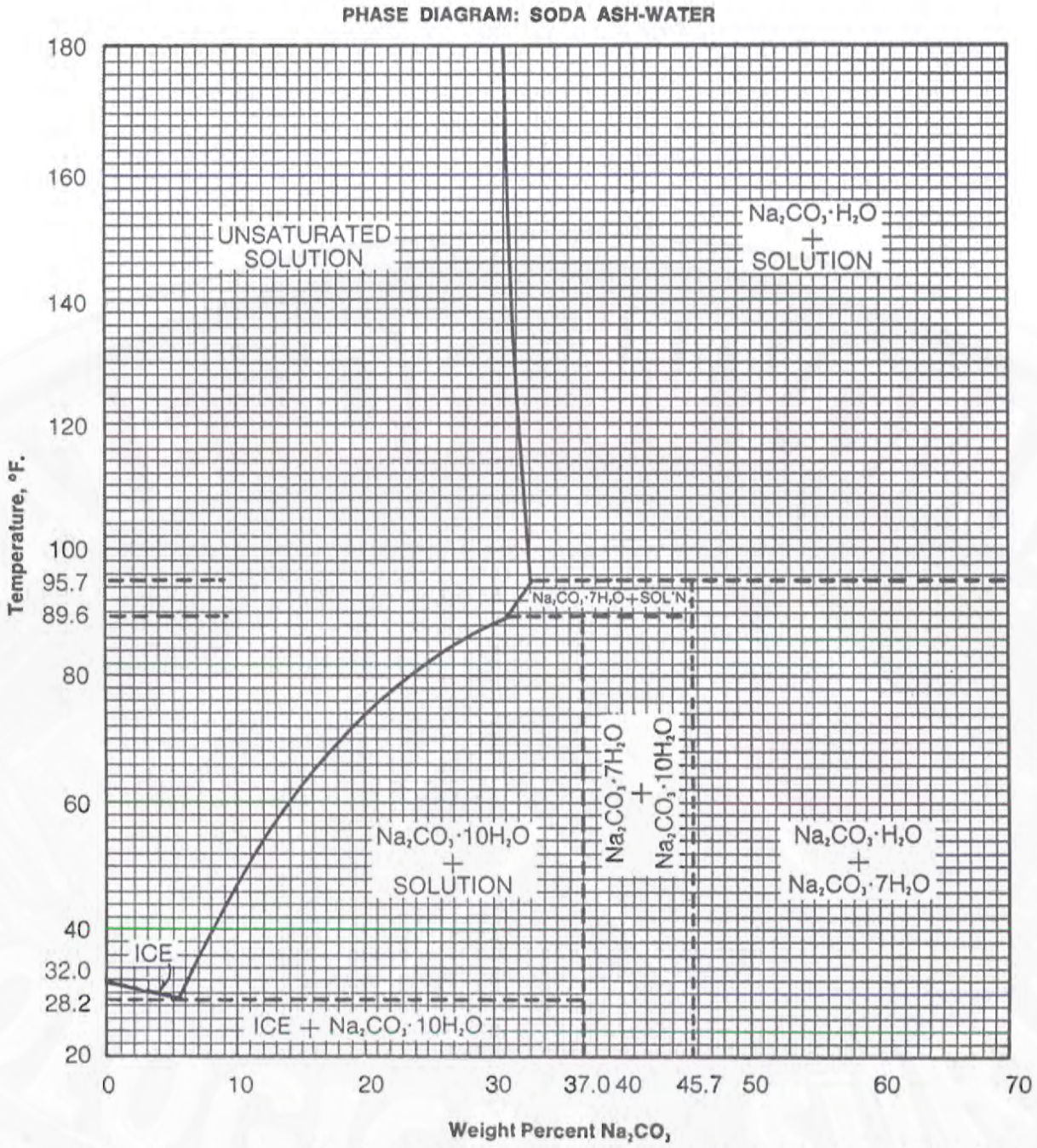


Figure 4. Phase diagram for a water-sodium carbonate system. Source: "Natural Soda Ash," Rhône-Poulenc Basic Chemicals Company.

include multi-effect evaporation, mechanical vapor recompression, and various heat recovery systems.)

7. Formation and control of return solutions for steady operation above and below ground. (The temperature, composition, and flow rate of return solutions must be monitored and controlled.)

8. Disposal of insolubles to tailing ponds or mine.

9. Environmental issues.

A decahydrate system is an effective way to accomplish several objectives such as recovering sodium carbonate values from dilute solutions (while) also recovering relatively pure water, concentrating purge streams, and providing an economic feed for downstream products.

The challenge is to design a process which optimizes the overall economics for an integrated, multi-product complex. This requires that all major process streams and economic elements be analyzed as an integrated system. Optimization of processes for each product may not be ideal for the same solutions.

Innovative refining processes under development

Papers in this volume include those on separation of insolubles via electrostatic precipitation of calcined trona and wet calcination of trona in microwave ovens. Other technologies have been attempted or can be visualized which would separate the insolubles or other components via physical means such as classification or flotation.

Innovation has always been a characteristic of the soda ash industry both in synthetic and natural-based processes. Many of these novel processes have attractive features, but the definitive main test is whether they can yield the product purity and physical quality obtainable via processes based on traditional crystallization methods.

Sodium carbonate not meeting the specifications of the generally accepted commercial product may instead target specific market niches. One disadvantage is that a different grade product may require an independent distribution system. Another concern should be that all American producers can degrade their present processes to compete with a lower grade product. The net effect on a new producer could be an increase in distribution costs and a decrease in profit margins.

Caustic soda from trona

The overall stoichiometric equation for the main reaction to produce caustic soda (NaOH) from trona is given below.

$$Na_2CO_3 + H_2O + CaO \longleftrightarrow 2NaOH + CaCO_3 .$$

A typical flow chart detailing the process is given in **Figure 5**. The sodium carbonate feed can be obtained by dissolving trona in a dilute caustic soda recycle stream (as done by Solvay Minerals), by taking a slip stream from a weak soda ash solution–possibly from a decahydrate system (as done by FMC), or by using mine waters (as done by Tg Soda Ash-Elf Atochem).

The lime used in this process can be purchased or obtained by calcining the precipitated calcium carbonate. Theoretically, makeup calcium carbonate could be obtained from shortite, which is often present in trona deposits. However, economic considerations may lean toward the purchasing alternative.

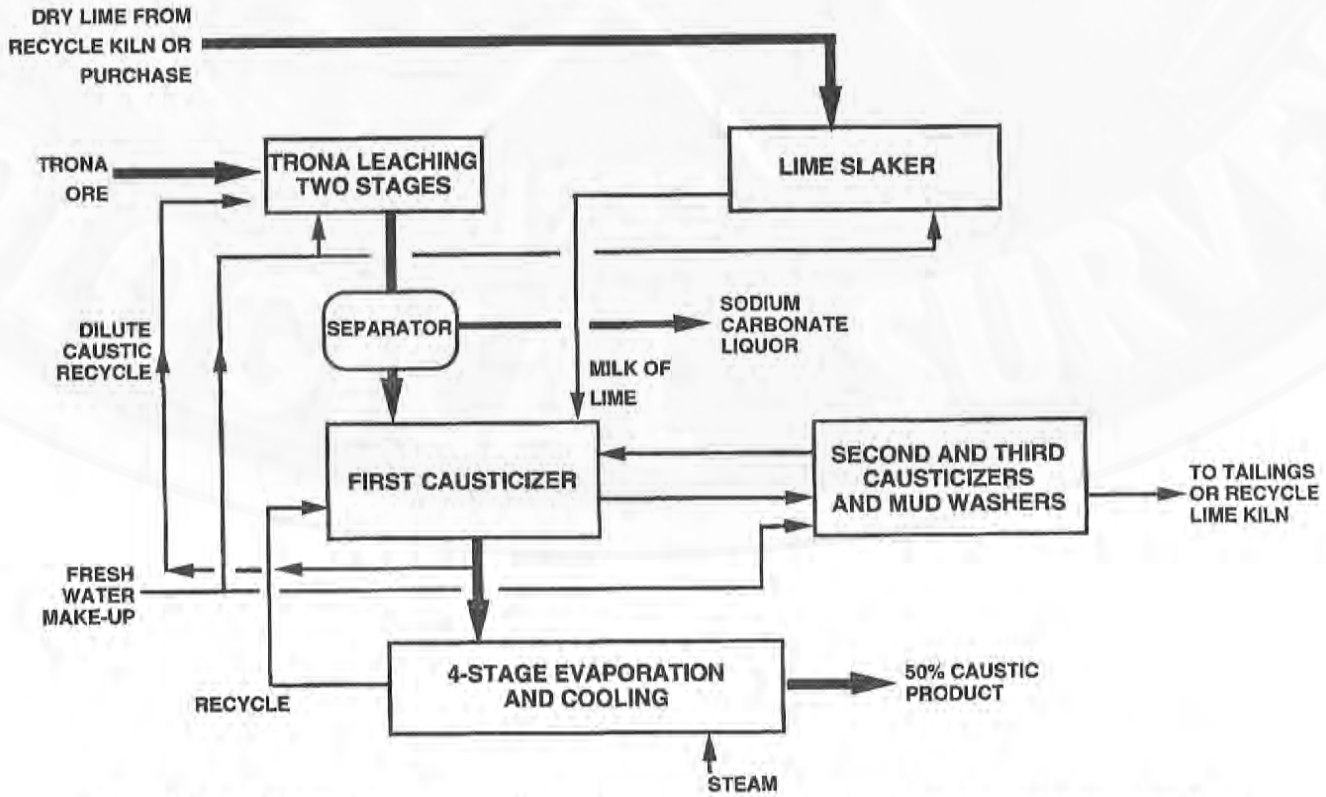


Figure 5. Flow diagram showing process for producing caustic soda from trona ore from the Green River Basin.

Important details for this process must deal with side reactions involving silicates, burkeite, and saponification of organic matter, which may cause foaming in the evaporators.

Sodium bicarbonate from trona

Most sodium bicarbonate is used in baking soda, dentifrice, deodorants, and pharmaceuticals. All these end uses must meet stringent, high-purity specifications. Usually, they can be met most economically by starting with high purity raw materials.

The overall stoichiometry for the main reaction is:

$$Na_2CO_3+H_2O+CO_2 \longleftrightarrow 2NaHCO_3.$$

As detailed in **Figure 6**, sodium bicarbonate crystals are formed in an absorption (carbonating) tower. The crystals are recovered by centrifugation, dried, and classified to meet granulation specifications. The process selection is mostly governed by product specifications, but the relative amounts of soda ash and coproducts or derivatives in the slate of products also play a role. Most likely, the demand for sodium bicarbonate is much lower than for soda ash and a liquid feed containing sodium carbonate in solution is adequate for the process.

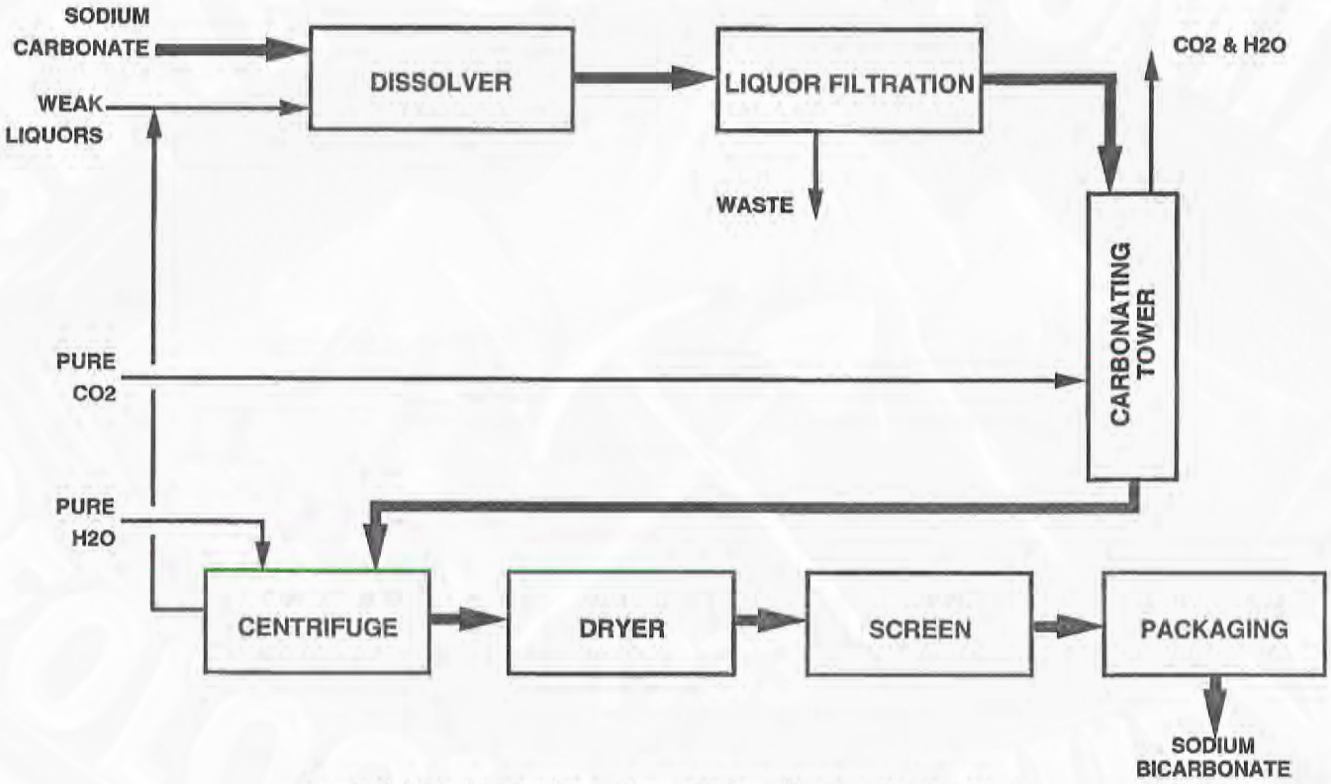


Figure 6. Flow diagram for producing sodium bicarbonate from trona.

Developing and selecting the best project alternative

The project's viability is evaluated mainly by comparing the project's cost structure to existing and potential firms (in the market) under consideration for comparable product quality. The project must also meet the firm's financial objectives and risk limits. The major elements affecting process selection during the project development phase of the venture are: slate of product(s) and their specifications; new or old mine; new or existing operation; products; capital cost; operating cost, especially energy and labor components; and the project must be competitive with existing and planned projects.

All these elements must be considered almost simultaneously, which is possible with computers. Compromises are not possible in environmental and safety matters, but many compromises are required among different disciplines, and technical and economic factors along with risk/reward ratios must be balanced. It is the essence of "design."

Project design should be done early and thoroughly before the project generates a life of its own and revisions to incorporate the best overall mining/refining technologies are discouraged by project ex-

ecutives responsible for meeting budgets and schedules. A company does not want to build a brand new, but technically obsolete complex at start-up. It might require considerable expensive retrofitting later to remain competitive.

Each trona-refining project is unique. Most projects are expansions of existing operations. Some benchmarks for an economically viable new project in Wyoming are: minimum economically minable trona reserves of 75 million short tons; a minimum trona assay of 80%; the major product is dense soda ash meeting ANSAC's specifications; a planned capacity of 2 million short tons per year, probably built in two phases; a mining plan that starts with mechanical mining and follows with solution mining; and a project life of 20 years minimum. In addition, the new project should use a process in which the final product should be derived from dehydration of sodium monohydrate. The front end of the project should be able to process solid trona and/or solutions. Finally, preliminary cost targets for a dry-desert project should require order-of-magnitude capital investment of $360 million in Phase 1 for production of 1 million short tons per year. Totally loaded operating costs before corporate charges and royalties should be about $61 per short ton in Phase 1.



Frontispiece: Aerial view of the trona mine and processing plant operated by FMC Wyoming Corporation west of Green River, Wyoming. In 1997, about 4.4 million net short tons of trona were produced from underground mining (data from Wyoming State Inspector of Mines, Annual Report for 1997). This production translates to an estimated 2.4 million short tons of refined soda ash and other products (data derived by dividing trona production by 1.8, the accepted ratio of mined trona to refined soda ash). Photograph by John R. Dyni, July, 1998.

Evolution of Wyoming soda ash processes

William Ramon (Ray) Frint
Consultant
Green River, Wyoming 82935

Abstract

This paper reviews the historical choices and aspects that have occurred in the development of Wyoming trona processing. The definition of processing for this purpose includes mining as well as the basic implementation of surface operations to produce marketable products. The approach used is to follow the time line as it occurred, from the discovery of the deposit up to the present.

Discovery to first production

The Wyoming trona "discovery well" was drilled in 1937-38, by the Mountain Fuel Supply Company as an exploratory oil and gas well. W.H. Bradley was a geologist for the U.S. Geological Survey at that time, and he had a special interest in the Green River Formation. He therefore requested that Mountain Fuel core a portion of the Green River Formation. Sections of this core were eventually sent to the U.S. Geological Survey laboratories in Washington, D.C. for examination in 1939. As a result of this examination, Dr. J. Fahey reported that two new and several other rare minerals had been discovered in the John Hay #1 well. In 1940, it was reported that there could be a 10-foot (3.05 m) bed of trona at a depth of 1590 feet (484.6 m). Some of the trona had dissolved and several sections of the core were missing. The Union Pacific Railroad confirmed the discovery with two wells drilled in late 1940 and two more wells drilled in 1941.

By the time discovery was confirmed, World War II was underway. The war created a shortage of almost everything, including soda ash, so interest developed in the trona deposit as a source of soda ash. One particular individual who pursued the development of the deposit was Robert Pike, a chemical engineer who believed that southwestern Wyoming, with its abundance of nearby mineral resources, had the possibility for creation of a major chemical industry. Mr. Pike, with the cooperation of the Union Pacific Railroad, made visits to most, if not all, of the then-existing soda ash producers in an attempt to interest them in the development of the trona deposit. They were not successful in their efforts. The primary objections put forth by those existing soda ash producers were: 1) the nature of the ancient lake bed deposit (with overlying weak shale formations) would not enable safe, economical mining; and 2) the location in Wyoming was too far from soda ash markets to compete with existing plants, i.e., freight costs would make the deposit non-competitive.

Mr. Pike lived in the San Francisco Bay area, and the Westvaco Chemical Company had several chemical operations in California and the Bay area. Westvaco was interested in detergent chemicals and needed soda ash for their rapidly growing sodium tripolyphosphate sales. By chance the two parties came together, and the prospects of a trona project became a reality. Mr. Pike proposed using solution mining for trona, which would negate any objections to the presumed drawbacks of mechanical mining. Westvaco was planning on new phosphate plants in the west, which required soda ash, and would thereby furnish a marketing base for the mined trona.

Agreements were then reached between Westvaco and Union Pacific in 1944, and further exploration of the deposit and testing of trona solution mining began. The 1945-46 solution mining tests were a failure. Because the phosphate plants were well underway, a decision was made to sink a shaft and try mechanical mining. In conjunction with the 1947 shaft, a trona processing plant was also approved.

Exploration had indicated that the deposit was of high quality. This, coupled with lack of capital, resulted in a low-cost plant, centered around a used kiln, with the process consisting of hand sorting, calcination of the ore, and physical separation into different products. These products consisted of: a 0.5- to 1-

inch (1.27 to 3.81 cm)-size fraction of raw trona in burlap bags; a smaller sized calcined-trona product containing about 94 wt.% soda values and 6 wt.% insoluble material with a bulk density of 51 pounds per cubic foot (0.817 g/cc), which was called Natural Soda Ash, Dense; and the smaller screen fractions plus dust, which was of higher quality–about 96 wt.% soda ash. This product had a bulk density of 44 pounds per cubic foot (0.705 g/cc) and was designated as Natural Soda Ash, Light. There was really no resemblance of these three products to the higher quality light and dense soda ash being offered by the producers of synthetic (ammonia-soda process) products marketed in the east, or the natural-type soda ash marketed in the west which was produced from brines pumped from Searles and Owens Lakes. The crude product was not acceptable for making sodium tripolyphosphate, so the market for the crude natural Wyoming products was small, but so was the production capability.

The second process

In 1948, the Food Machinery Corporation (FMC) purchased Westvaco Chemical Company as a major acquisition in their move toward diversification. With new management and improved access to capital, the Green River Trona Project continued to solve the mechanical mining problems, and the need for a refined soda ash process and plant became more evident. Several different refining processes were proposed. The final selection of what is now referred to as the "sesquicarbonate process" or "sesqui process soda ash plant," was made primarily on the ability of that process to produce light soda ash as well as dense soda ash products. At that time the market demand for soda ash was about one-third dense ash, and a significant selling price differential existed. Glass producers used the dense ash which had a 10% premium in price; other users purchased light ash at the lesser price. The ability to supply both markets was considered to be essential to the success of the proposed Wyoming Refined Ash Project.

The sesquicarbonate process involves crushing the mechanically mined ore to small particles, dissolving these in a hot, recirculating solvent (containing excess sodium carbonate), removing the undissolved material from the solution, and cooling the solution in multiple-effect crystallizers to produce pure sodium sesquicarbonate crystals. The crystals are then calcined to remove water and excess carbon dioxide, resulting in a low-density light soda ash. To make dense ash, water was added in a hydrator to the hot light ash to form sodium carbonate monohydrate crystals, which were then heated to form dense ash. These were basically the same processing steps used by the ammonia-soda process to convert light ash into dense ash, and the additional manufacturing cost justified the premium in selling price. The hydrating process to produce dense ash in the sesquicarbonate process was replaced in the late 1960s by a heat-densification process. By subjecting the 49-pounds-per-cubic-foot (0.785 g/cc) product to temperatures in excess of the calcination temperature required to convert the sesquicarbonate crystals into sodium carbonate, the soda ash crystal pseudomorphs shrink in size, thus increasing the bulk density to above 70 pounds per cubic foot (1.121 g/cc), when the time-temperature parameters are near the maximum. This heat densification process is less costly and results in a superior product when compared with the hydrating process.

Although the sesquicarbonate process had been piloted at the company's caustic-chlorine plant in West Virginia, the Wyoming plant had a long, difficult start-up. The major problems were: corrosion, foaming, sesquicarbonate crystals too small to process in the centrifuging and calcining equipment which had been installed, and product quality problems. Actual output was way below the 300,000 TPY (tons per year [272,155 mt (metric tons or tonnes) per year] design capacity of the plant.

The plant start-up commenced in late 1952, and by 1955 rumors still persisted that the plant might be shut down. Fortunately, the problems were solved without major plant modifications, and the design capacity of the plant was able to be doubled at nominal cost. Solving the processing problems also significantly improved product quality. The production of large sesquicarbonate crystals changed the physical characteristics of the light ash. The bulk density increased from 35 pounds up to about 50 pounds per cubic foot (0.561 to 0.801 g/cc), which was substantially more than the density of ammonia-soda light ash, but still below the 60-pounds-per-cubic-foot (0.961 g/cc) plus weight of dense ash. This is because sesquicarbonate crystals contain only 70% soda ash equivalent, compared to 85% for monohydrate crystals. Some glass producers were willing to try this coarse, medium-density soda ash in their furnaces, and found it worked very well. More importantly, it sold for light ash prices. The increased demand for this less expensive soda ash product insured the viability

of Wyoming trona production. In 1958, the Wyoming soda ash "tail" started wagging the soda ash "dog." This is when the ammonia-soda industry initiated a price increase which was not followed by the Wyoming producer.

In the author's opinion, if Westvaco Chemical had selected a refining process which did not preserve the then existing selling price differential between light and dense ash, there might not be a Wyoming soda ash industry. The ammonia-soda industry could not absorb the extra cost of producing dense ash without a selling price differential (although the differential slowly disappeared, as did the ammonia-soda plants), and by 1958, Wyoming did not need a price increase to expand, and each expansion resulted in decreased production costs.

The third process

In 1962, Stauffer Chemical, which operated a soda ash plant at Searles Lake, California, started up a plant in Wyoming. The refining process selected for their plant was one of the processes examined but not selected by FMC for the first trona-to-refined-soda-ash plant. This process, commonly referred to as the monohydrate process, incorporated calcination of the trona near the beginning of the processing steps. This converts the trona into a crude soda ash which still contains all of the insoluble materials. The crude soda ash is then dissolved in water, and the insolubles are removed from the solution in the same manner as in the sesquicarbonate process. Because soda ash has a nearly constant solubility in water (throughout the temperature range where monohydrate is the stable crystal form), the soda ash solution is evaporated, and the resulting sodium carbonate monohydrate crystals are heated to form dense soda ash. Most of the water vapor from the crystallization step is condensed and returned to the dissolvers. The final soda ash product from the monohydrate process is dense ash, with the bulk density being about 63 pounds per cubic foot (1.009 g/cc).

The surface processing cost difference between the soda ash produced via the sesquicarbonate or the monohydrate process is minor. In plants of comparable size, using the best selection of equipment and other parameters, the operating cost of producing the medium density 50-pounds-per-cubic-foot (0.801 g/cc) ash via the sesquicarbonate process would have a several dollar per short ton cost advantage, primarily because this process involves only one heating or calcination step. The energy difference between the two processes is about one million Btus (1,054,180 Kjoules), which is the energy for drying the monohydrate crystals. However, the capital cost for the sesquicarbonate process is somewhat higher because of the larger amount of solution processed per short ton of product, and the need for alloy steel piping. This increased capital cost nullifies the energy processing cost advantage of the sesquicarbonate process. The heat densification step of the sesquicarbonate process results in higher total dense ash production cost when compared to the monohydrate process. These surface processing/manufacturing cost differences are not a significant factor in determining selling prices, since other factors such as mining costs, energy costs, royalty rates, etc., are more important in total production cost comparisons.

Secondary products

The ammonia-soda process soda ash plants have utilized their basic position in soda ash to manufacture other sodium products. Several of the Wyoming trona processing plants have done likewise, and these products have contributed greatly to the size and scope of the present-day trona industry. One of the advantages available to the production of these additional products is that they can be produced from precursor materials rather than the more expensive final soda ash. In the sesquicarbonate process this is the centrifuge cake consisting of purified trona crystals before the calcination step. In the monohydrate process, this is the monohydrate crystal centrifuge cake before the final drying step. As pointed out above, the sesquicarbonate process centrifuge cake is inherently less costly to produce than the equivalent monohydrate process centrifuge cake. Because this sesquicarbonate material also contains a higher ratio of carbon dioxide to sodium than does monohydrate, it is the preferred starting material for making sodium sesquicarbonate, sodium bicarbonate, sodium phosphates, and sodium sulfates. The monohydrate material is better for making caustic soda (sodium hydroxide) and products derived from caustic, such as sodium cyanide and tri-

sodium phosphate. However, the cost advantages of using either of the two centrifuge products is not sufficient to preclude the manufacture of secondary products from refined soda ash by either non-trona producers, or at non-Wyoming locations.

The fourth process

Although the first attempt at Wyoming trona solution mining in the 1940s failed, FMC continued to be interested in the probability that solution mining would be safer and substantially less costly than mechanical mining. From 1955 to 1959 a solution mining field test was conducted northeast of the FMC plant site. The goal was to use the resulting brine in the sesquicarbonate process. This objective was not realized. From 1983 to 1993, another trona solution mining field test was conducted 16 miles (25.7 km) south of the FMC plant site. This time the goal was to utilize the resulting brine in the monohydrate process plant. This objective was only partially successful.

In 1987 FMC started to design a process of placing the insoluble tailings from the plant back into the underground voids created by mechanical mining. The process selected was designed to solution mine the pillars left to support the roof and other trona not recovered via mechanical mining. The FMC underground tailings disposal project was started in 1989, and the resulting brine pumped back to the surface contained sufficient volume and alkali concentration to support a sizable processing plant. The exit brine had a bicarbonate concentration of about 4 wt.% and a carbonate concentration of about 15 wt.%, which was the expected value. However, the brine also has a "high" level of soluble impurities, such as chloride, sulfate, and organics, because the carrier for the injected tailings is the waste solution from the surface plant processing. In order to produce a high purity soda ash product from this heavily contaminated feed stock, a double crystallization process was devised.

The process chosen involves evaporation, filtration, and conversion of the bicarbonate values into carbonate. The concentrated brine is then cooled to produce sodium carbonate decahydrate crystals. The crystals recover a substantial amount of the water and most of the sodium carbonate values. The crystals are melted and the solution is evaporated to form monohydrate crystals, which are separated from the liquor by centrifuges; the crystals are then heated to form dense ash. Recovery of both water and alkali is good. The plant is currently producing at the design rate of 700,000 TPY (635,028 mt) of high quality product at a total soda ash cost substantially below that produced by the other two plants using the sesquicarbonate and monohydrate processes. This patented solution mining processing facility is called the Evaporation Lime Deca Mono plant, or ELDM plant, based on the primary processing steps involved.

Conclusion

In conclusion, during the past 50 years, there have been four different basic processes used to convert Wyoming trona into soda ash. Three of the processes use mechanically mined ore, and one is based on solution mining of ore abandoned after mechanical mining. The advantages of solution mining in virgin territory are obvious and will not be repeated here, and although several large-scale solution mining tests have been conducted, this aspect of trona processing awaits a different process technology which has yet to be installed. Since most of the trona deposit is not amenable to mechanical mining, it is only a matter of time before solution mining in virgin areas will become a necessity, if Wyoming soda ash production is to continue growing during the next 50 years. The basic philosophical factor which FMC has determined from its past experimental experience with Wyoming trona solution mining, is that the surface processing must be tailored to handle the brine that any solution mine will produce and not visa versa. In other words, the needs of a successful solution mine come first, and the surface processing will be designed accordingly. Don't design the solution mine to produce a brine for a preconceived or a pre-built surface process.

The Wold Benetron® process

Wayne Hazen
Hazen Research, Incorporated
Golden, Colorado 80403

Abstract

The Wold Benetron® (beneficiated trona) process produces soda ash from trona by dry separation methods. It is based upon the characteristics of the mineral impurities associated with the trona and the degree of liberation as a function of particle size. This paper discusses the mineral associations for bed 17 trona and how they impact dry separation methods.

Introduction

The Wold Trona Company has extensive deposits of trona under lease in the Green River Formation in southwestern Wyoming. In 1992, Ralph Tacoma, consultant to John Wold, asked Hazen Research, Inc. to conduct an experimental program to determine the potential for making a high-grade soda ash product by dry beneficiation methods. If this could be done, the resultant product, after calcining, might find a market which did not require the high-purity soda ash currently produced by the Wyoming trona industry using chemical methods.

Roland Schmidt of Hazen Research led the effort to investigate the possibilities for physical upgrading of trona ore, through study of the mineralogy of the trona. By the end of 1994, a small-scale method was deemed successful enough to justify building a demonstration plant using commercial-size separation equipment. This plant, with a nominal capacity of 1500 pounds per hour, was operated successfully in early 1995, producing ton-size quantities for customer evaluation.

The purpose of this paper is to present the basic characteristics of trona and associated minerals from the Wyoming trona deposit that make a physical separation of trona and gangue possible and to provide the technical understanding for a plant to make a product of consistent quality and known specification. The trona samples studied were all from trona bed 17, including many from drill cores and others from various mines.

Minerals in trona

According to the literature, strata immediately below and above trona beds consist of oil shale and a marlstone in which the carbonate is chiefly a fine-grained dolomite. Mineable trona beds are generally quite pure and locally assay as much as 97% trona, with the central parts of the bed usually purer than those parts near the roof and floor of the mined bed. Trona beds also contain thin layers, mostly less than $^1/_4$ inch thick, of interbedded shale or marlstone. Therefore, the first part of the study was concerned with the liberation characteristics of the trona bed minerals.

Obviously, separation by physical means is not possible unless the trona is liberated from impurity minerals at a coarse enough size to use commercially available separation equipment. The first significant fact that soon became clear is that the impurities which accompany the trona crystals are fairly well liberated at about 6 mesh. These impurity minerals are largely dolomitic shale, shortite, and clays. A detailed study was made of the nature of the liberated non-trona minerals in a sample of bed 17 ore, with the results shown in **Table 1**.

Table 1. Water-insoluble materials associated with trona in bed 17.

Mineral	Chemical formula	Approximate weight %
Dolomite	$CaMg(CO_3)_2$	32
Shortite	$Na_2Ca_2(CO_3)_3$	21
Searlesite	$NaBSi_2O_5(OH)_2$	1.6
Northupite	$Na_3Mg(CO_3)_2Cl$	4.1
Norsethite	$BaMg(CO_3)_2$	0.15
Quartz	SiO_2	7
Pyrite	FeS_2	1.2
Carbon	organic	3
Feldspars and clays[1]		31
		101

[1]Clays are the major component of this fraction.

Dry separation

Magnetic, electrostatic, and air tabling methods were investigated most thoroughly for separation of trona from the other minerals. The properties of the minerals involved with respect to these separations are listed in **Table 2**.

The possibilities for dry separation clearly lie in the use of magnetic separation and density difference. There are many kinds of magnetic separators commercially available, but not many dry density separators. We chose an air table, which uses a gently sloping screen deck with a vibrating action like a Wilfley table. Separation is achieved by an air stream blowing upward through the screen. The denser particles next to the screen are conveyed uphill by the vibrating action, while lighter particles slide downhill, thus separating the light and heavy fractions. It operates on a completely different principle than an air classifier. For clean separation, particles should be of about the same size. Therefore, the first step in processing is to screen the trona ore into separate size fractions.

Performing test work with a laboratory-size air table requires a large quantity of material, since its capacity is high. However, comparable results can be achieved by heavy liquid separation. Therefore, work with small quantities of sample from drill cores used heavy liquid separation, which predicts air table results.

Dry physical separations are not usually practical for particle sizes finer than minus 150 mesh. Because the crushing of the ore, grinding to less than 6 mesh, and calcining all produce dust and fines which are removed from the system, a complete process must include recovery from fines. Part of the research included an unusual means for producing high-purity soda ash from the fines by crystallization. The long story of that development is not part of this presentation.

By studying the separation of trona from its accompanying impurities at different screen sizes using combinations of separation devices, including heavy

Table 2. Physical properties of trona and significant impurities present in trona.

Mineral component	Specific gravity	Magnetic susceptibility	Electrical properties
Trona	2.14	Nonmagnetic	Nonconductor
Shortite	2.60	Nonmagnetic	Nonconductor
Dolomitic shale	2.10 - 2.13 (apparent)	Paramagnetic	Conductor
Dolomite	2.85	Nonmagnetic	Nonconductor
Illite-glauconite	2.4 - 3.0	Paramagnetic	Conductor?
Fe-northupite	2.34	Paramagnetic?	Nonconductor
Quartz	2.66	Nonmagnetic	Nonconductor
Pyrite	5.0	Nonmagnetic	Conductor
Sepiolite/loughlinite	~2	Nonmagnetic	Nonconductor

liquid, magnetic, and electrostatic separation, we were able to physically remove impurities from trona with the overall results shown in **Figure 1**.

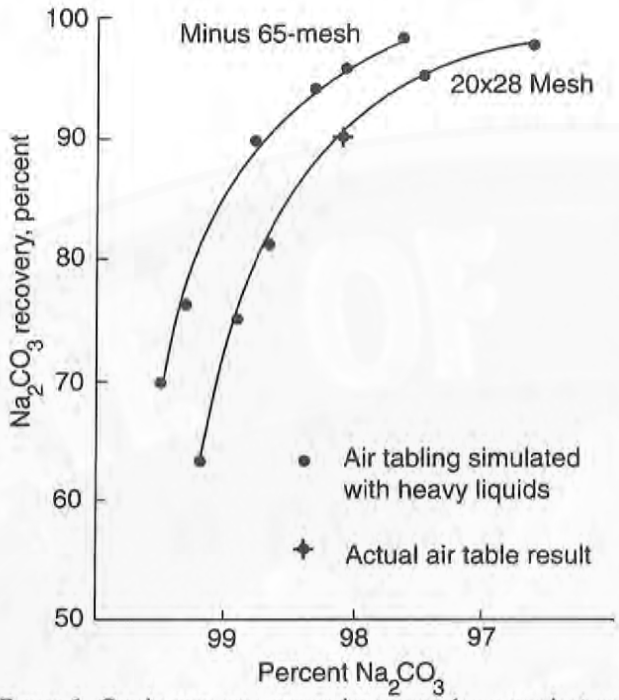


Figure 1. Grade recovery curves for trona of two mesh sizes.

The fact that liberation of trona is not as complete at 20 mesh as it is at 65 mesh is evident. Also, there was sufficient bed 17 material in this case, so that the grade-recovery curve was verified in one run with the laboratory air table.

For some kinds of glass manufacture, the iron content of soda ash product is of particular importance. Because the iron is present partly in the shale and partly as pyrite, a more complete removal of iron could be achieved by sacrificing some recovery. This is clearly shown in **Figure 2**.

The recoveries shown are based on the feed to process, and therefore do not include the fines. Air tables are not useful for this separation below about 100 mesh. Also, any dust generated by handling or during calcining is not amenable to dry separation.

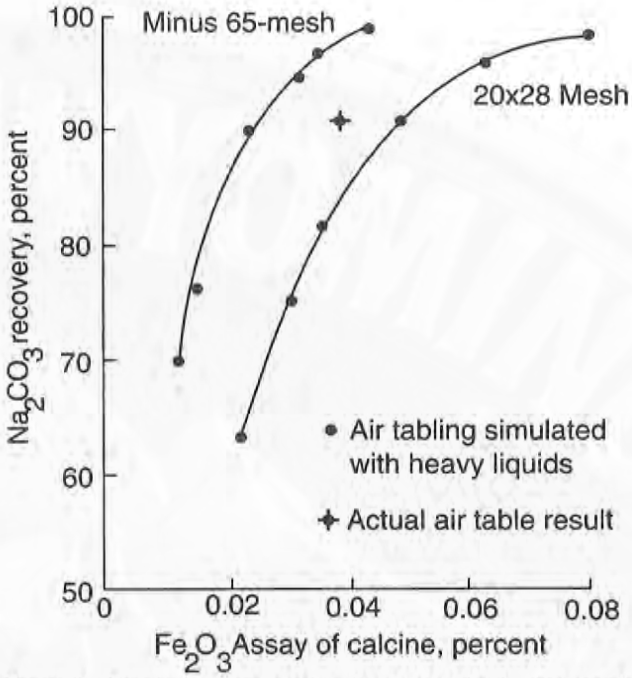


Figure 2. Grade recovery curves for trona of different mesh sizes with varying amounts of iron.

Pilot plant

After the small-scale work was completed, a pilot plant was constructed for calcining, air tabling, and magnetic separation to produce tonnage quantities of the product. The air table and magnetic separator were commercial-size machines, so there is no risk in scale-up to larger capacities.

The plant operation was directed by Rudy Pruszko of Wold Trona Company, under whose direction many improvements were made. One of particular importance from an operating standpoint was the development of an on-stream iron analyzer for controlling the magnetic separator. This assured uniformity of grade so either a product of 0.07% or 0.04% Fe_2O_3 could be made at will. A reason for spending so much effort on gaining an understanding of the nature and abundance of the impurities is that to be successful, a plant must be controllable so that a uniform product of consistent grade can be delivered. One of the demonstration plant runs gave the following results for about 50 tons of product (**Table 3**).

Figures 3 and 4 show the air table and the three-roll rare earth magnetic separator in the pilot plant.

Table 3. Trona and iron recoveries from pilot plant, in wt.%. Analyses on calcined basis.

Screen size Tyler mesh	Grade Na_2CO_3	Recovery Na_2CO_3	Fe_2O_3
20 x 28	96.8	95.8	.077
28 x 35	97.0	97.3	.070
35 x 48	96.1	92.9	.066
48 x 65	96.4	91.3	.060
65 x 100	96.1	88.0	.070
Average	96.5	93.5	.068



Figure 3. Air table used in pilot plant.

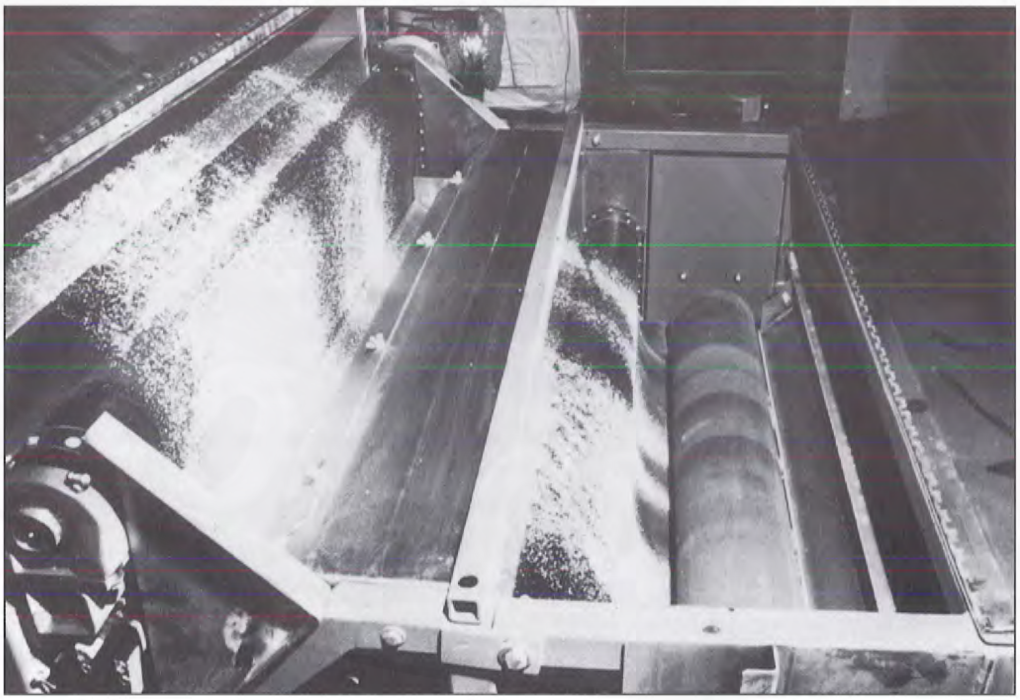


Figure 4. Magnetic separator used in pilot plant.

Calcining the trona was accomplished in a low-temperature fluid-bed calciner operating at 200°C. Since the decomposition products are carbon dioxide and water, the fluidizing gas can be the carbon dioxide which is recirculated through a dust collector and water condenser. Thus only carbon dioxide is vented, because heating is accomplished by coils in the bed. Trona feed and products of the pilot plant are shown in **Figures 5, 6,** and **7**.

The question is raised as to why the concentrate produced by dry separation does not have high purity without a big loss in recovery. It was observed that there is a marked variation in color of the trona particle. A portion of clean trona concentrate was hand-picked with tweezers under a microscope to give three fractions which were then analyzed, with the results shown in **Figure 8**.



Figure 5. Trona feed (28 x 35 mesh) to calciner at pilot plant.



Figure 6. Trona product (28 x 35 mesh, 98% Na_2CO_3) after calcining in pilot plant.

Surprisingly, 80% of the trona in the concentrate was 99% pure with only 0.01% Fe_2O_3, which is suitable for glass manufacturing. This work meant that some trona contains shale and clay impurities at much higher levels than other trona particles. A detailed microscopic analysis using oil immersion techniques revealed the situation shown in **Figure 9**, a photomicrograph of a sample of trona concentrate.



Figure 7. Magnetic separator (28 x 35 mesh) discard. These particles are magnetic because of the clay and shale impurities (dark color) present.

Significantly, the clear particles are of a very high grade that can yield as pure a commercial soda ash as that made by crystallization. A careful study of the impurities within the particles revealed that, like the liberated particles, they are largely dolomite and clay, except that they are generally very fine grained and are deposited along grain boundaries and fracture planes of the trona crystals.

Figures 10 and **11** are photomicrographs of particles of trona containing a high level of impurities. These are photographs of polished sections examined by microprobe.

Figure 12 shows a comparable photograph of a polished section of the clean trona.

Summary

In summary, the fundamental research undertaken for the Wold Trona Company has provided the knowledge for making a dry separation of trona, capable of producing a soda ash product of 97% purity with low iron content. In contrast, recovery of soda ash using standard commercial equipment is 90 to 95%.



Figure 8. Hand-picked trona (6 x 8 mesh) sorted by color. Trona on left contained 0.019% Fe_2O_3 and represents 80% of the trona concentrate. Trona in center contained 0.122% Fe_2O_3 and represents about 16% of the concentrate. Trona on right contained 0.40% Fe_2O_3 and represents about 3% of the concentrate.

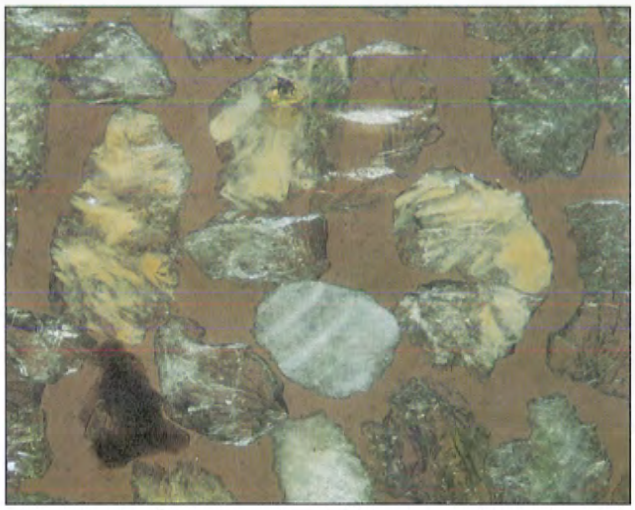


Figure 9. Photomicrograph of clean trona, 38 x 35 mesh fraction.

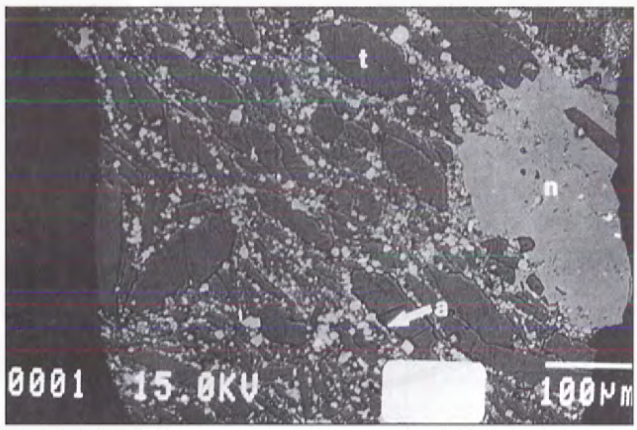


Figure 10. Photomicrograph of a polished section of impure trona. t=trona; a=complex silicates; and n=northupite, $Na_3Mg(CO_3)_2Cl$, analyzing about 1.3% Fe_2O_3.



Figure 11. Photomicrograph of a polished section of impure trona. t=trona; b=glauconite; and a=white inclusions thought to be khanneshite and burburbankite.

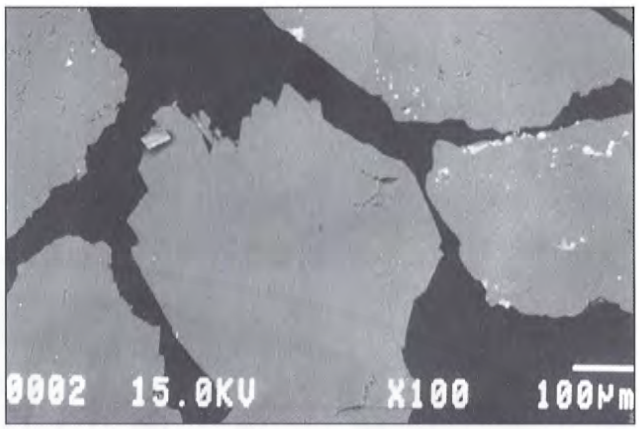


Figure 12. Polished section of clean trona.



Aerial view of General Chemical's trona mine and refinery complex in the Green River Basin, Wyoming.

Microwave-induced wet calcination of trona

Robert D. Streuber
Hydrocarbon Technologies, Incorporated
Lawrenceville, New Jersey 08648
and
Chang Yul Cha
University of Wyoming
Laramie, Wyoming 82071-3295

Abstract

We investigated the technical feasibility of a microwave-based trona process in various laboratory experiments. The results of these experiments are discussed below. We found that this process allows the trona to be directly calcined while in solution without the need for high temperature or pressure. Some of the advantages of this technique when compared to conventional processing methods are: 1) decrease in decomposition reaction bulk fluid temperature; 2) greatly decreased apparent activation energy (102 kJ/mole vs. 4.2 kJ/mole); and 3) increased rate constant at 100°C (0.0006 s^{-1} to 0.154 s^{-1}).

Microwave-induced wet calcination of trona has the potential to eliminate many of the steps currently necessary in the conventional processing of trona into soda ash. This includes crushing and high temperature calcination, with the goal of improving economics and simplifying the process.

Introduction

Trona processing

Conventional production of soda ash from trona ($Na_2CO_3 \cdot NaHCO_3 \cdot 2H_2O$) is a complex process with several steps. There are two leading methods by which sodium carbonate (soda ash) can be recovered from trona ore. The most widely practiced method is the monohydrate process which involves a calcination step followed by dissolving, washing, filtering, and recrystallization into the sodium carbonate product, monohydrate.

The second method, the sesquicarbonate process, differs from the monohydrate process in that the calcination step is the final step in the process rather than the first. The product also differs and is called sesquicarbonate (light soda ash), which is distinct from monohydrate (heavy soda ash). The density of the sesquicarbonate is less than that of the monohydrate, and the crystal morphology of the sesquicarbonate is elongated and slender whereas the monohydrate crystal is long as well, but swells towards the center into a football shape.

Solution mining

With the commonly practiced room-and-pillar method of trona mining, large portions of the ore must be left in place to support overlying strata. A promising method for recovering this remaining trona, as well as previously inaccessible deposits in shallow beds is solution mining. Water or a brine solution is flooded through the deposit and a trona-rich solution is recovered for processing. The economic and mining efficiency benefits of solution mining make it an attractive future option.

As solution mining becomes more popular, current methods which are geared to accept dry trona will need to be re-evaluated. It would be possible to alter existing systems to accept the slurry, but the added

drying costs would make these options economically unattractive. An alternate possibility, called wet calcination, actually completes the decomposition with the trona remaining in solution. The focus of this project is wet calcination performed by application of microwave energy. Whereas conventional processes require the soda ash to be crystallized out of solution before calcination to decompose the trona, the University of Wyoming microwave wet calcination process decomposes trona in solution by application of microwaves to soda ash without the need for drying. Furthermore, the unique way in which microwaves are able to specifically heat the trona makes microwave wet calcination more efficient than application of conventional heat in wet calcination.

Microwave fundamentals

Microwaves are electromagnetic energy characterized by frequencies between 300 megahertz (MHz) and 300 gigahertz (GHz), and wavelengths of 1 mm to 1 meter. This range of frequency and wavelength has found application in various industries from communications to food preparation. The chemical industry has long known of the ability of microwaves to provide quick and precise heating; however, the misconceptions about the benefits of microwave application to certain reactions have precluded common utilization aiding chemical reactions until very recently. Certain substances which contain charged particles (ions) or which contain molecules, such as silicon carbide, with a charge gradient (dipole moment) across the molecule can be preferentially heated.

In a microwave field, the electromagnetic flux of the microwaves as they pass through the sample causes a local distribution of charge along the sample. This charge causes dipolar molecules to try to align with the field and causes ions to try to separate with the positive ions moving towards the negative part of the field and with the negative ions towards the positive area. However, as the field oscillates, it changes the charge distribution periodically so that the ions and dipoles can never quite line up and are continually readjusting to the field. This continuous readjustment causes the ions to essentially vibrate with the field, and the dipoles to rotate. Both of these movements cause friction among the ionic or dipolar particles resulting in rapid localized heating.

Particles that can be heated in this way are called microwave absorbents. A good microwave absorbent is extremely efficient at converting electromagnetic field energy to heat, while a poor absorbent is less efficient. There are also non-absorbers such as quartz and glass which are essentially invisible to microwaves, and are commonly used, as in this case, as reactor vessels. The benefit of microwaves in certain reactions is that they may be precisely applied to good microwave absorbents and those absorbents will be heated preferentially to extremely high temperatures. They will be provided with a very large activation energy for reactions, while the bulk fluid (such as air or water) will remain relatively cool. To heat particles to such high temperatures conventionally is often impossible due to materials considerations, or is otherwise very expensive and often time consuming.

Project goals

The goals of this project are to: 1) explore the feasibility of producing soda ash from trona solution using a microwave process; 2) investigate the best possible process for converting the final 2% of the sodium bicarbonate in trona into sodium carbonate or soda ash; 3) study the kinetics of the reaction, i.e., reaction rate, pre-exponential factor, and activation energy; and 4) express energy requirements for the system.

Experimental methods

In order to determine the feasibility of wet calcination of trona in solution, a series of experiments was conducted. This included characterization of trona solution versus water alone as a microwave absorbent. During these preliminary experiments, the reactor system used (**Figure 1**) was a typical continuous microwave reactor setup consisting of a microwave generator, a wave-guide, an impedance-matching device (tuner), a directional coupler, a circulating reactor bed, and a cooling system. Quartz was chosen as the reactor material for its invisibility to microwaves and its high temperature durability. The microwave generator used for the continuous experiments was manufactured by Cober Electronics Inc. This particular model produces microwaves at a fixed frequency of 2.45 GHz, with an adjustable power output between 0 and 3000 watts.

The second phase of this work consisted of an in-depth study of the decomposition reaction. The first experiments were intended to compare effects of microwave heating versus conventional heating and were carried out in a batch reactor system. A series of identical experiments was conducted with both con-

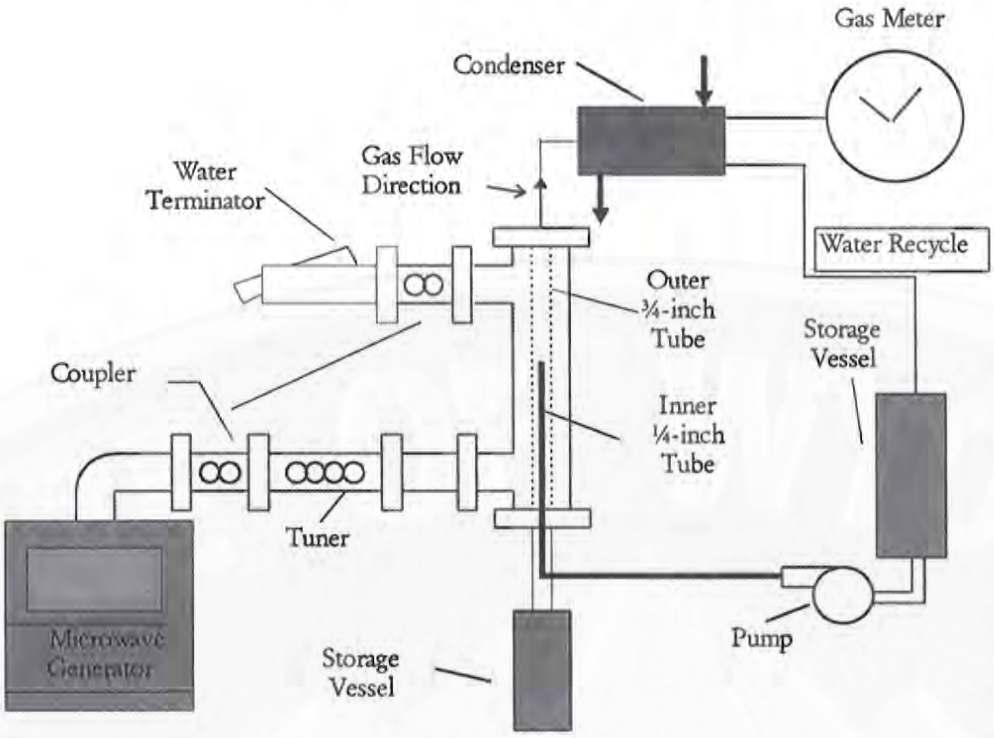


Figure 1. Typical microwave reactor setup.

ventional and microwave heating. A batch reactor kinetic study was also completed to evaluate the reaction order, activation energy, and pre-exponential factor of the decomposition reaction.

The batch reactor experiments were all performed in a glass 1000-ml round bottom flask. The microwave portion of the experiments was performed in a modified 1000-watt Tappan® home microwave oven. The conventionally heated experiments were performed by two different methods, with a fluidized sand bath as the heating medium, and a round bottom variable current controlled electrical resistance heater. A simple schematic of the microwave reactor setup is shown in **Figure 2**.

The microwave energy source for the batch reactions was a Tappan® 1000-watt home microwave oven with a fixed frequency of 2.45 GHz. The reaction chamber used for these experiments was a round bottom 1000-ml ground glass flask. The flask was equipped with a water-cooled condenser that extended out past the heating zone and was used to separate the evolved CO_2 and the steam. The condensed steam was recycled and the product gas, CO_2, was passed through a dry test gas meter. The production of CO_2 was measured as a function of time throughout the experiment. Periodically, a product gas sample was analyzed by a Hewlett Packard® model 5890 gas chromatograph to determine composition. The conventionally heated system was very similar to the microwave setup except that the heat source was a fluidized pre-heated sand bed.

The following procedures are general and apply to both the conventional and the microwave heating experiments. The 1000-ml round bottom flask was cleaned, dried, and the weight of the flask recorded. The desired concentration of solid sodium bicarbonate and sodium carbonate was weighed out and mixed with distilled water to produce a fixed solution volume of 250 milliliters.

For each run, the total weight of the solution and flask, the starting temperature, and starting time were noted. The experiment was started immediately upon energy introduction, whether microwave or conven-

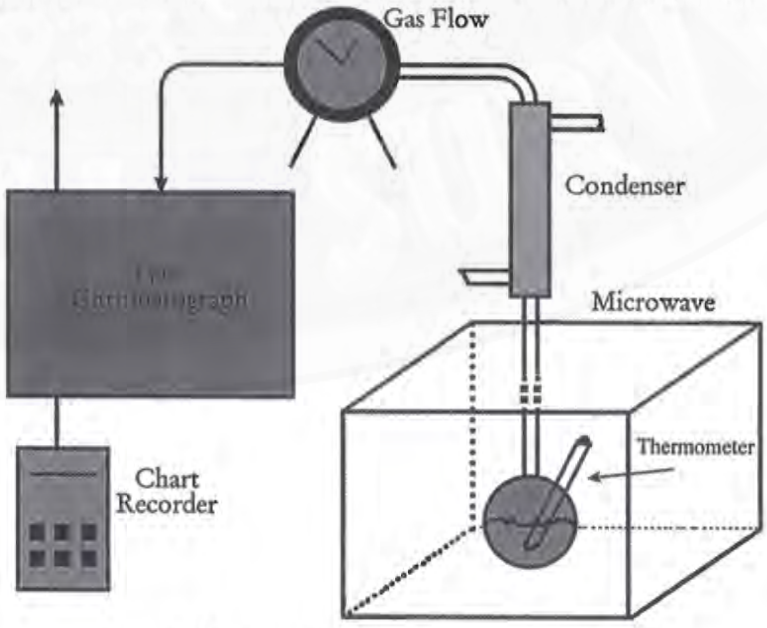


Figure 2. Microwave configuration batch reactor system.

tional energy. The temperature of the solution and production of gas were measured as a function of time to 10 minutes. At this time the application of energy was terminated and the solution weighed. The conversion of the sodium bicarbonate was then determined by both weight loss and gas production. It was eventually concluded that calculation of the conversion by weight loss or gas production was not very accurate, so a titration procedure to detect final sodium carbonate concentration was developed and utilized thereafter.

A series of batch microwave heated experiments was completed in a 1000-watt microwave oven. An experimental plan was developed that varied different controllable parameters of the experiment including starting solution concentration, use of microwave absorbents, and residence time. To determine the kinetic parameters for the decomposition of sodium bicarbonate, experiments were performed in the batch reactor at a fixed concentration of 20% sodium bicarbonate with conversion and the final percentage of sodium bicarbonate determined at the end of each experiment by titration.

The data obtained from the batch reactor experiments were analyzed and various conditions were chosen for corresponding tests in the continuous reactor. Various experimental setups were tested in order to determine the configuration that would best allow for scale-up of the continuous reactor. The parameters varied were power input, residence time, and flow direction as well as presence of a microwave absorbent within the reaction zone. All setups were very similar to that setup shown in **Figure 1**.

Results and discussion

Initially it was necessary to determine if a microwave process could be utilized for catalyzing the conversion of trona in solution to sodium carbonate (wet calcination). For microwave heating to be of benefit, it was imperative that either dry trona or trona in solution absorb microwaves better than the solvent alone. To test this, absorption experiments were performed. Dry trona was placed in an empty $^{3}/_{4}$-inch quartz reactor that was placed inside the waveguide. In order to calculate the amount of microwave energy that the dry trona absorbed, measurements were of input power (directly from the generator), reflected power (back to the generator from the load), and transmitted power (through the load). The power absorbed by the trona was then calculated by subtracting the transmitted and reflected power from the input power. Next, the same experiment was performed with a 9.94% trona solution, and with water. Both were pumped through the reaction zone of the waveguide. Finally, an empty reactor was tested to determine the amount of energy that the reactor system absorbed. The results of this experiment are shown in **Figure 3**.

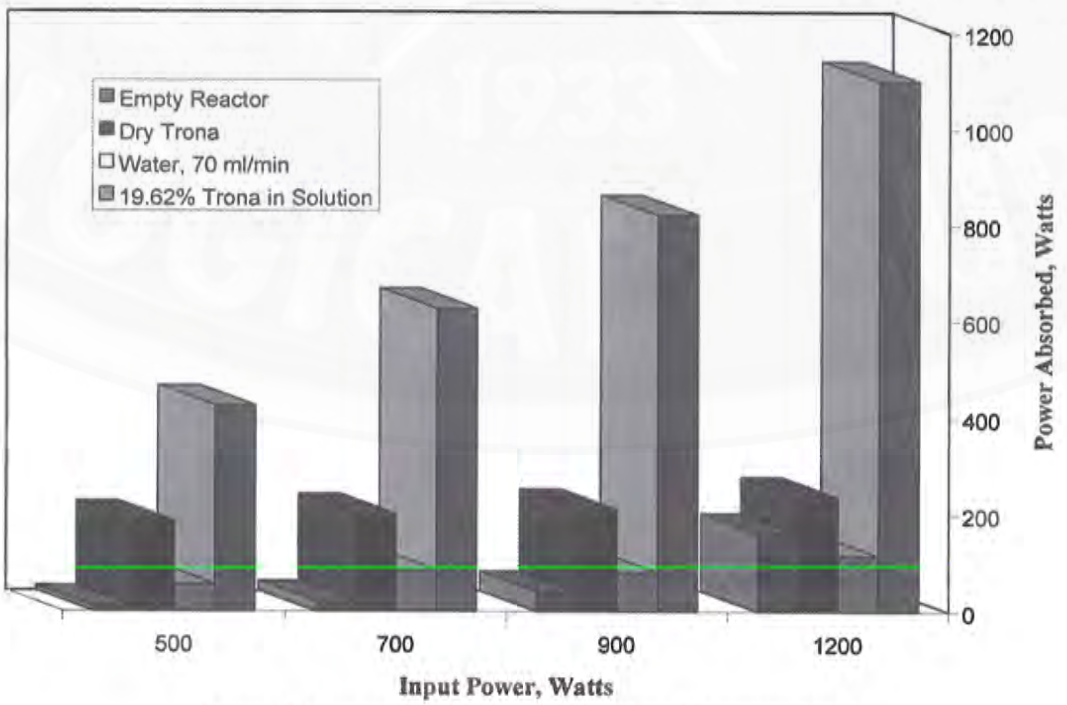


Figure 3. Comparison of power absorbed by different materials.

The four different tests were completed and it was found that only the trona in solution was capable of absorbing most of the input power. The dry trona was tested to determine the feasibility of calcining dry trona in a microwave field, but did not prove to be a very good absorbent alone. It is interesting to note that pure water only absorbed approximately a tenth of the power that the trona in solution absorbed, and the reactor's load was near zero in comparison. This is conclusive evidence that trona in solution is a very good microwave absorbent and an excellent candidate for decomposition in a microwave field.

The results of the batch microwave versus conventional heating experiments are clearly shown in **Figure 4** as conversion of sodium bicarbonate versus solution temperature.

In order to provide an equivalent comparison between the heating methods, all the experiments were performed with a 10% sodium bicarbonate solution and were only analyzed up to the boiling point of water. It was determined that past this point the extent of reaction was influenced by the rate of energy input. At the boiling point, the rate of water vaporization is a direct function of energy supply rate, and evaporation of the water removes produced CO_2 as it vaporizes which drives the reaction to sodium carbonate production. The microwave-heated solution outperformed all the conventionally heated experiments by roughly 200% or more. This implies that the microwaves enhance the reaction rate. It should be emphasized that the time required to reach the boiling point, approximately 4 minutes, was the same for both the microwave reactor and the 130°C fluidized bed reactor.

The results of the batch reactor experiments show that the decomposition of trona in a microwave field is possible. Furthermore, microwave energy is far superior in decomposition of sodium bicarbonate to comparable conventional heating, with decomposition of the sodium bicarbonate through conventional heating at 100°C being much slower than at 100°C in a microwave field. **Figure 4** shows that to get the same rate of decomposition utilizing conventional heating, it was necessary to radiate the batch reactor with a fluidized bed that was at 180°C whereas microwave decomposition began to proceed rapidly at a bulk temperature of only 80°C.

It was further shown that the decomposition reaction began almost immediately under microwave energy with over half of the CO_2 production occurring within 4 minutes of exposure to the microwave energy at which time the bulk temperature was only 80 to 85°C. To further explore the possibilities of microwave application, experiments were completed that utilized added microwave absorbents. It was found that this addition greatly enhanced the conversion of sodium bicarbonate, in some cases yielding a 35% higher conversion. The experiment, which utilized a 10% silicon carbide (SiC) additive, produced the best results with conversion of over 80% of the initial

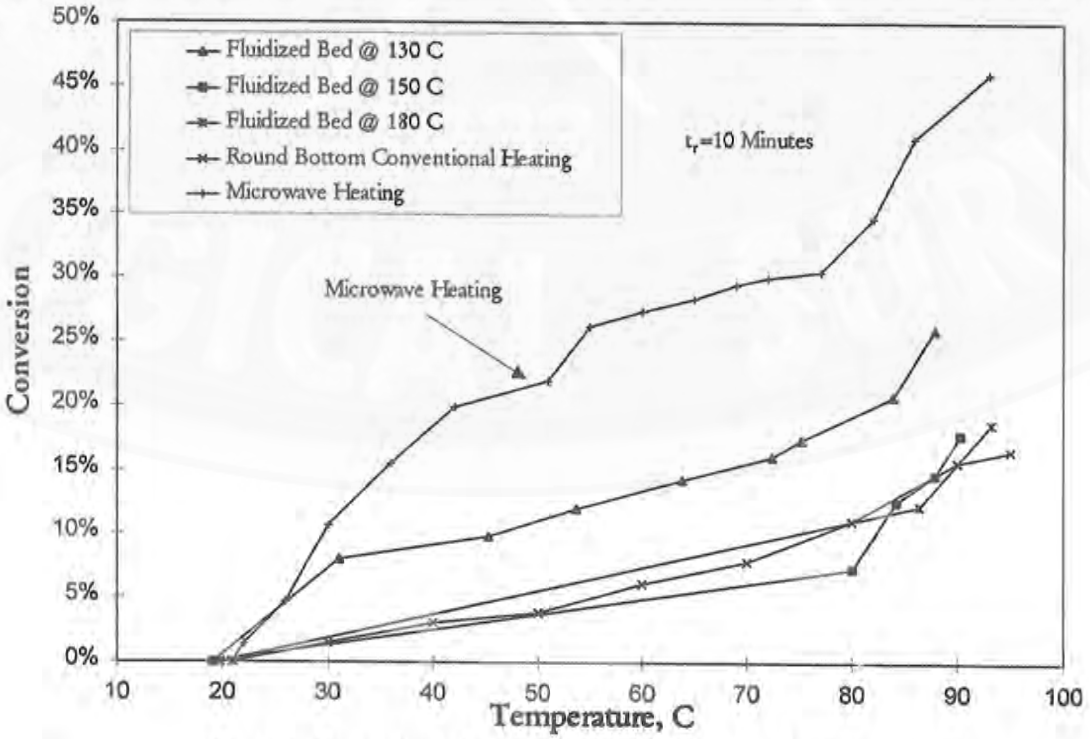


Figure 4. Comparison of conventional and microwave heating.

sodium bicarbonate in 10 minutes. The experimental results are summarized in **Figure 5**.

Experiments to analyze the reaction kinetics were conducted in half-minute intervals with a titration performed at the end of each experiment to obtain the conversion of $NaHCO_3$ (**Figure 6**). A 20% SiC microwave absorbent additive was used.

The region considered isothermal for the order determination test (4 to 12 minutes) is also shown in **Figure 6**. To determine the order of the reaction the integral method, as outlined below, was used.

Consider the reaction: $NaHCO_3 \rightarrow Products$ (1).

First order rate equation: $-r_A = -\frac{dC_A}{dt} = k_d C_A$ (2).

Separated and integrated obtains: $-\ln(1-X_A) = k_d t$ (3).

Definition: $X_A = C_a / C_{Ao}$ (4).

The data were then plotted accordingly, with $-\ln(1-X_A)$ on the y-axis and time on the x-axis. Data regres-

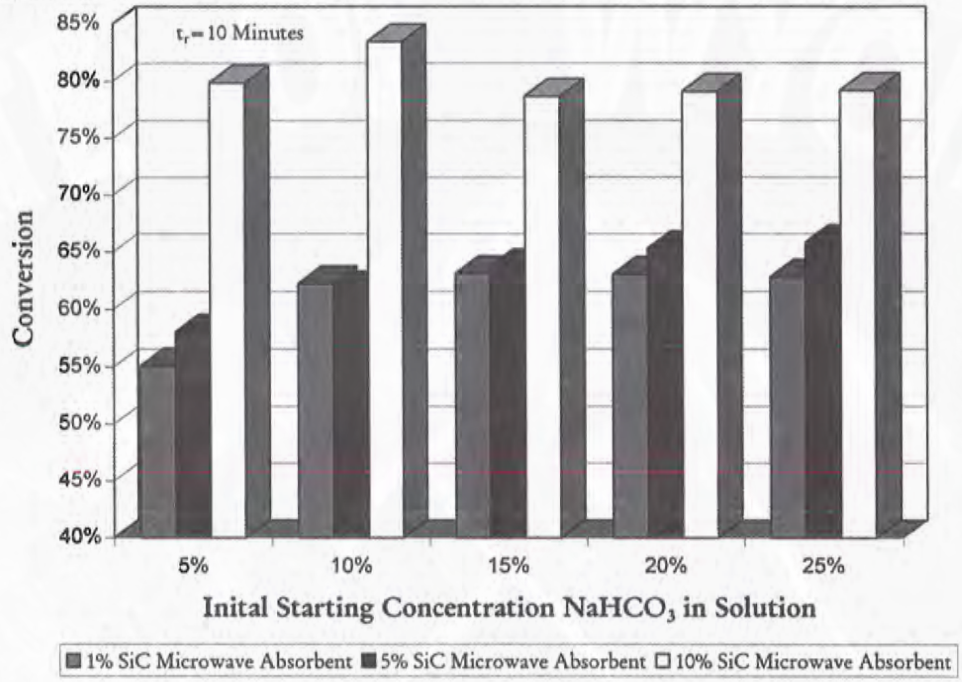


Figure 5. Benefits of using silicon carbide in a microwave field.

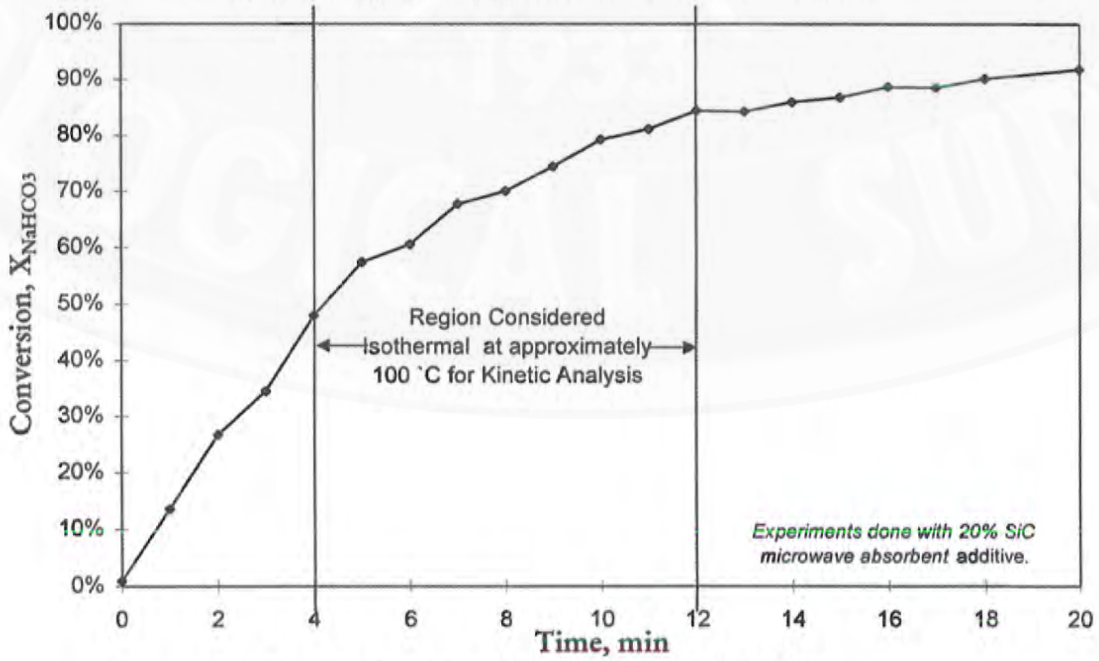


Figure 6. Conversion of $NaHCO_3$ as a function of time.

sion was performed to determine the slope, k_d, which is the rate constant. The results are shown in **Figure 7**.

Upon plotting the data it was determined the reaction was first order with a reaction constant of $0.154 s^{-1}$ at system temperatures ranging from 80 to 100°C. The apparent activation energy and the rate constant were determined by utilizing Arrhenius' equation. **Figure 8** illustrates the method for determining the apparent activation energy and the rate constant, in this case a plot of $\ln(k_d)$ vs. 1/T where 1/T is inverse temperature in Kelvin, and k_d is

$$\left(\frac{dX_A}{dt}\right)\left(\frac{1}{(1-X_A)}\right) \quad (5)$$

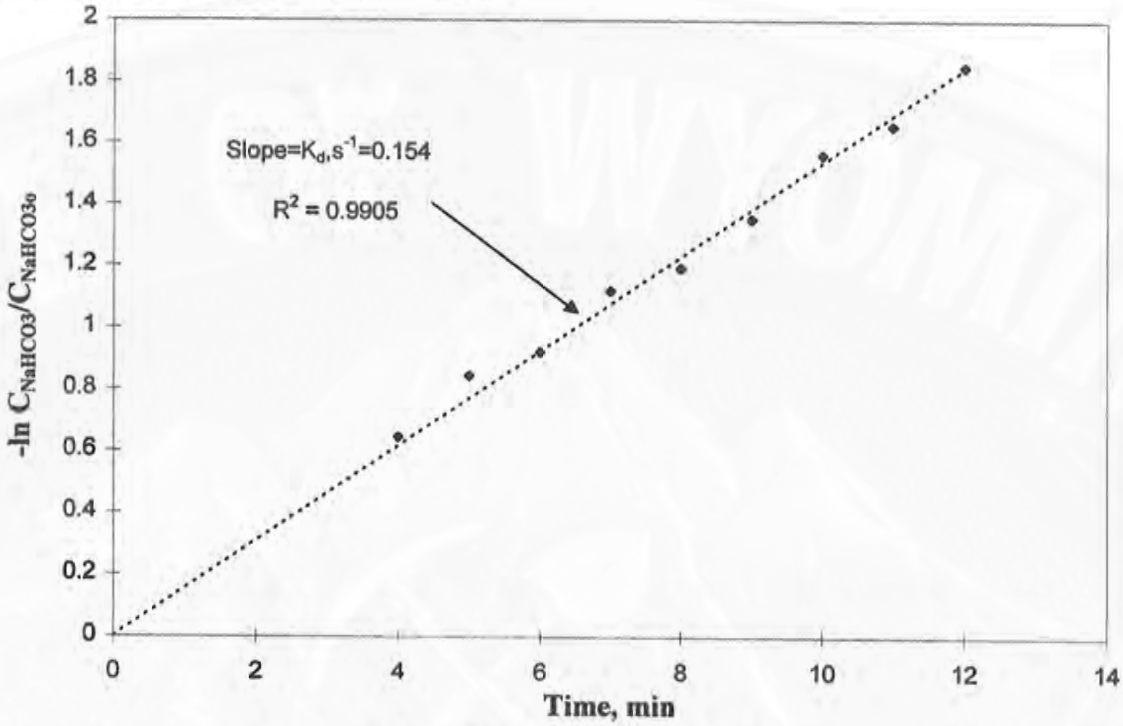


Figure 7. Graph to determine reaction order.

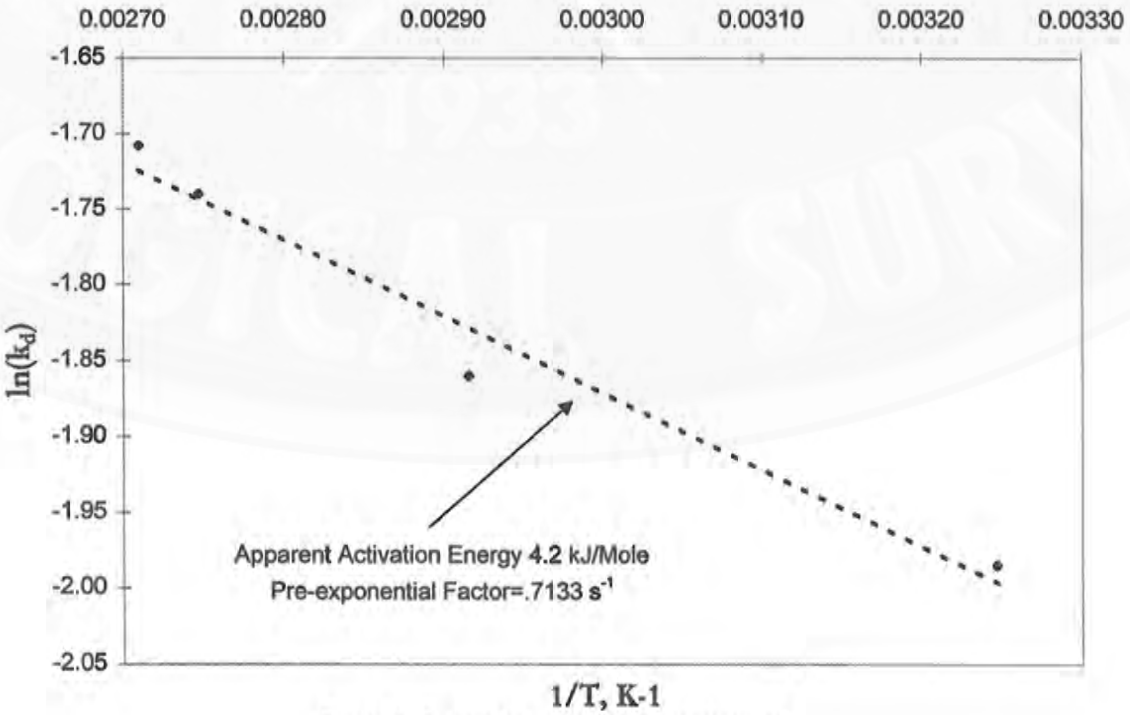


Figure 8. Determination of kinetic parameters.

The apparent activation energy from this plot was determined to be 4.2 kJ/mole and the pre-exponential factor was 0.7133 s^{-1}.

The observed activation energy, as determined from the bulk fluid temperature (4.2 kJ/mole), proved to be an order of magnitude lower than the reported activation energy (102 kJ/mole) for the solid decomposition of sodium bicarbonate. This means that the temperatures of the $NaHCO_3$ molecules would have to be much higher than the surrounding solution. The hypothesis is physically consistent with the findings that the solution absorbs microwaves better than water alone, and the site of the reaction should be at a much higher temperature than that measured in the bulk fluid.

Although particle temperature is impossible to measure, we attempted to validate the hypothesis by experiments intended to determine the heat of reaction. A known amount of water was heated and its weight loss and temperature were monitored. After the temperature of the water reached the boiling point, it was assumed to be constant. The experiment was then repeated using a solution containing sodium bicarbonate. Temperature, conversion, and weight loss were monitored as a function of time. The results are shown in **Figures 9** and **10**.

The results of the energy balance experiments indicate that the heat of reaction associated with the decomposition of the sodium bicarbonate in solution was calculated to be 121.6 kJ/mole, which is comparable to values that have been reported in the literature. The fact that the bulk temperature was lower than this, at 80-85°C confirms that the microwaves were able to enhance the reaction significantly by creating a higher temperature at the trona reaction site, as was suggested by the discrepancy between the apparent and published activation energies.

Additionally, it was determined that only about 23%, or 231 watts of the incident power was actually used to drive the decomposition reaction. The remaining 77% was used to heat the solution from room temperature up to the desired operation temperature and vaporize the water. In order to maximize the effectiveness of the microwave energy to drive the decomposition reaction at low temperatures, it would be possible to raise the temperature of the bulk solution to the operating temperature by inexpensive conventional means before applying microwaves to rapidly drive the reaction.

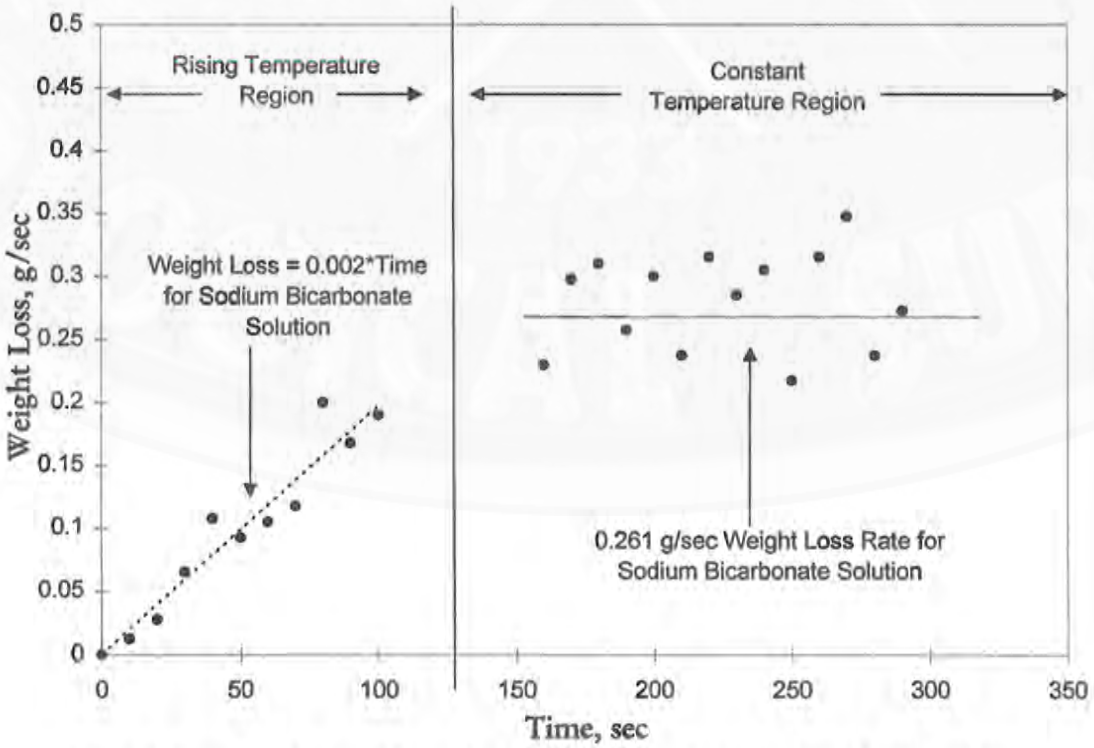


Figure 9. Summary of the weight loss for sodium bicarbonate solutions as a function of time.

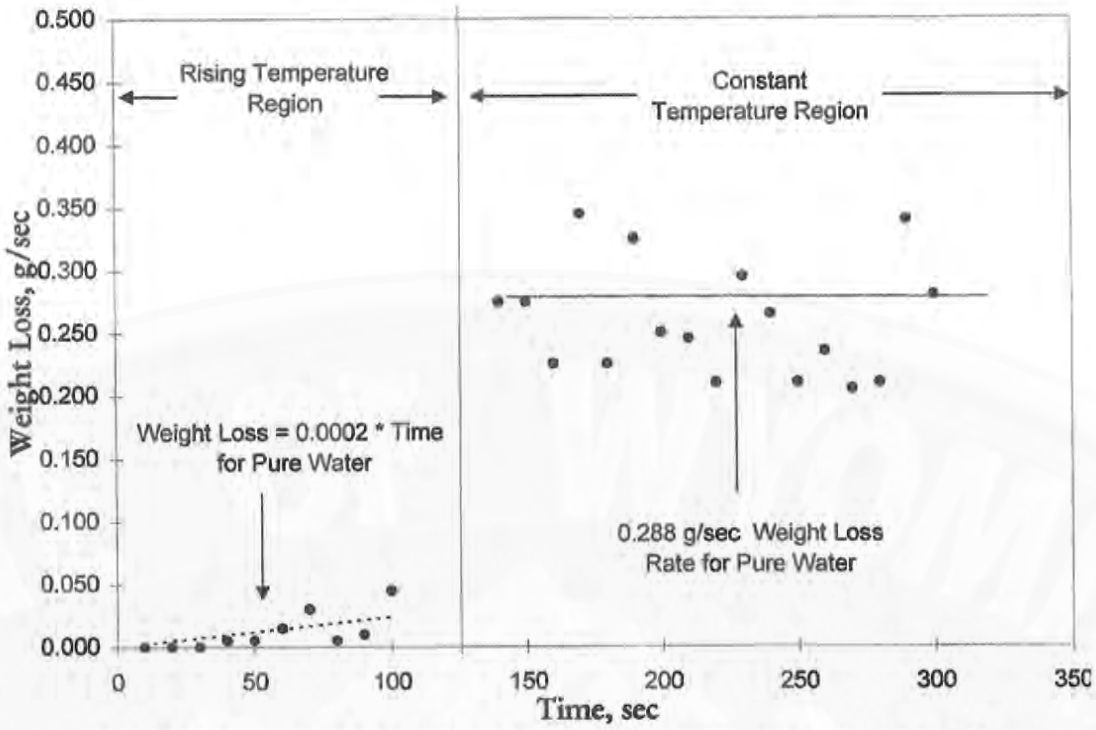


Figure 10. Summary of the weight loss for the water experiment as a function of time.

Conclusions

The microwave induced wet-calcination of trona is a feasible process with advantages over conventional methods of soda ash production from solution.

Trona in solution absorbs microwaves better than dry trona or water.

Decomposition of bicarbonate in a microwave field exceeded all conventional methods in the 10-minute batch series.

Over half of the conversion of the sodium bicarbonate occurring in the 10-minute microwave experiments occurred before the solution reached the boiling point of water.

Attempts to further increase the decomposition of sodium bicarbonate by utilizing the microwave absorbent silicon carbide were successful.

Wet calcination of sodium bicarbonate was found to be a first order reaction.

The apparent activation energy was 4.2 kJ/mole for this process, while the reported activation energy of the solid decomposition of sodium bicarbonate was 102 kJ/mole.

The energy balance calculation yielded a heat of reaction for the decomposition reaction of 121.6 kJ/mole, which suggests that internal trona temperatures are much higher than the bulk solution due to preferential microwave absorbency.

The rate constant for this process was 0.154 s^{-1}, while the rate constant of the solid phase decomposition at 100°C was only 0.0006 s^{-1}.

Only about 23% of the input power is actually used to drive the reaction, with the remaining 77% either lost or used to heat the water from room temperature.

Acknowledgments

The authors would like to express their sincere appreciation to Heather Rothfuss for her patience in editing and reviewing the paper. She has done an excellent job in improving the content and writing of the text.

References cited

Ball, M., and others, 1992, Thermal decomposition of solid sodium sesquicarbonate: Journal of the Chemical Society, Faraday Transactions, v. 88, no. 4, p. 631-636.

Cheung, W., and others, 1985, Microwaves made simple: principles and applications: Artech House, Inc., Dedham, Massachusetts, 365 p.

Ekmekyapar, A., and others, 1996, Nonisothermal decomposition kinetics of trona: Industrial Engineering Chemical Research, v. 35, no. 1, p. 258-262.

Frint, R., 1985, FMC's newest goal: commercial solution mining of trona: Engineering and Mining Journal, September, p. 26-35.

Gardiol, F.E., 1984, Introduction to microwaves: Artech House, Inc., Dedham, Massachusetts, 503 p.

Metexas, R.C., and Meredith, R.J., 1983, Industrial microwave heating: Peter Peregrinus Ltd., London, UK, 370 p.

Rucinski, C., 1996, Microwave-char technology for SO_2 abatement: M.S. Thesis, University of Wyoming, Laramie, 189 p.

Wu, Y., and Shih, S., 1993, Intrinsic kinetics of the thermal decomposition of sodium bicarbonate: Thermochimica Acta, v. 223, p. 177-186.

Overview of air pollution issues facing the trona industry

David Gaige
Woodward-Clyde Consultants
Denver, Colorado 80237

Abstract

Several developments concerning air pollution issues will affect the trona industry. Internationally, the issue of greenhouse gases, and the actions that will result from the Kyoto Protocol, are the most critical. In the United States, several regulatory changes may have an impact on the cost of producing soda ash. The Environmental Protection Agency (EPA) has recently proposed a revision to the National Ambient Air Quality Standards (NAAQS) that will tighten the controls on fine particulates. In addition, several new regulations have been developed in accordance with the 1990 Clean Air Act Amendments.

Determining the effect of new and existing regulations requires defining and quantifying the emissions currently resulting from the trona industry. One of the most interesting and troubling factors is the realization in the last three years that significant quantities of volatile organic compounds (VOCs) are released when trona ore is heated. In the next decade, these VOCs could potentially affect some of the existing and proposed regulations imposed on the trona industry. It is this combination of new regulations and new revelations that will present some of the most significant challenges to environmental managers in the trona industry.

The VOC emissions may affect the applicability of several regulations, ranging from the prevention of significant deterioration (PSD) to the maximum available control technology (MACT) standards for hazardous air pollutants. Of equal concern, however, are the developing regulations that will affect the emissions of fine particulates, nitrogen oxides (NO_x), and possibly even carbon dioxide (CO_2).

Introduction

Some of the new regulations that will affect the operation of facilities in the trona industry during the next five years include: Compliance Assurance Monitoring, Credible Evidence, section 112(r) and the prevention of an accidental release, section 112(g) Hazardous Air Pollutant MACT standards, new Ambient Air Quality standards for Fine Particulate and Ozone, New Source Review reform, and greenhouse gas emission reductions. Title VII of the 1990 Clean Air Act (CAA) Amendments added a new section 114(a)(3) that requires the EPA (Environmental Protection Agency) to promulgate rules on enhanced monitoring and compliance certifications. The 1990 amendments also revised section 114(a)(1) of the Act to provide additional authority concerning monitoring, reporting, and record keeping requirements. As amended, that section provides the Administrator (of EPA) with the authority to require any owner or operator of a potential pollution source to provide the following monitoring information on a one-time, periodic or continuous basis:

(A) establish and maintain records;

(B) make reports;

(C) install, use, and maintain monitoring equipment;

(D) sample emissions in accordance with procedures or methods, at locations, at intervals, during periods and in a manner as the Administrator shall prescribe;

(E) keep records on control equipment parameters, production variables, or other indirect data when direct monitoring of emissions is impractical;

(F) submit compliance certifications in accordance with section 114(a)(3); and

(G) provide other information as the Administrator may reasonably require.

Taken together, these statutory provisions prescribe a set of measures, including monitoring and compliance certification, that owners or operators must follow in order to provide an assurance of ongoing compliance with the Act. The Compliance Assurance Monitoring (CAM) rules are not final yet, but are expected to be signed in July 1998 and will be implemented over the next five years depending on the status of the Title V permit applications. The requirements of CAM will become an integral part of the Title V permits that the State of Wyoming's Department of Environmental Quality (DEQ) will be developing for the trona industry.

Compliance Assurance Monitoring (CAM) and Credible Evidence (CE)

The CAM rule includes two basic categories. The first category, in subpart B of part 64, applies to emission units that use active control devices to achieve compliance. The second category refers to other control measures, such as process modifications, material substitution, and other control options.

Basically, this regulation (CAM) requires some type of monitoring be provided to demonstrate that any major pollution source with a regulated emission limit, and a control measure (active or not) is operating in compliance. Where continuous emission monitors currently exist the monitoring requirement will be satisfied. This rule is important in areas where emission limits have been established, but monitoring is not currently in place. This may include mass emissions for particulates from boilers, calciners and dryers, and ore crushers. This may also include NO_x emissions from the calciner and dryer and potential VOC emissions from new calciners.

Most sources have historically used opacity monitors to provide assurance that the systems are working and the limits are being met. Opacity, however, is not a reliable measurement of mass emissions, and to satisfy CAM requirements, new techniques may be needed to demonstrate compliance. This regulation may also require monitoring to assure that the low NO_x burners are operating correctly.

The final element of CAM that applies to monitoring under both subparts B and C is the concept of a quality improvement plan (QIP). A QIP is required if the cumulative duration of excursions a) from indicator ranges or b) from emissions that exceed limits where direct monitoring is involved, meets or exceeds a threshold to be established in the part 70 permit. The threshold is to be set at a level where the cumulative duration of excess emissions is unacceptable and improvements are necessary to assure ongoing compliance. An example of this is the New Source Performance Standards for Opacity from coal-fired boilers. In this example, if the opacity limit is exceeded more than 5% of the boiler operating time, corrective action is required. Similar to this standard, the QIP includes both a "problem investigation" phase and a "corrective action" phase.

The Credible Evidence (CE) rules that were signed in 1997 may have significant consequences on major sources. The provisions that were proposed in 1993 would have amended 40 CFR parts 51, 52, 60, and 61 to allow data gathered by enhanced monitoring to be used as "preemptively credible evidence" in enforcement actions. The rule also would have modified parts 51, 52, 60, and 61 to specifically provide for the use of "credible evidence" other than compliance test method data to prove noncompliance in an enforcement action. It would eliminate any potential ambiguity regarding the use of data other than compliance or reference test method data as a basis for Title V compliance certifications. EPA eliminated the "preemptively credible evidence" categories, and promulgated the remaining portions of the October 22, 1993 revisions separately from CAM.

The determination of opacity is an example where credible evidence can have a significant effect. The regulations require a certified opacity observer to perform the opacity compliance test (EPA Method 9), but under credible evidence rules, the opacity instrument which can read 20.1% opacity day or night can be used for determining continuous compliance. The rules that have now been developed establish that any reasonable evidence can be used by the regulatory agency, EPA (or the public in the case of third party suits), to determine compliance. The rules apply not only to the opacity data, or other continuous emission monitoring data, but can include parametric data which may indicate that a standard has been exceeded. The rules may also apply to other areas where there may be evidence that a regulatory requirement was not met, including permitting requirements. The issue of hydrocarbons in the ore, and the appropriate permitting and reporting requirements, should again be considered.

Although CAM and other part 70 data likely will be the most significant source of potential CE data for sources with CAM requirements, other types of information may also be important. Furthermore, given that excursions from CAM indicator ranges will not necessarily indicate noncompliance, the value of CAM data as potential CE will depend on specific circumstances. A key to minimizing the risk of the unknown in this area is to establish in the Title V permit exactly what will be used to demonstrate compliance. Especially where parametric monitoring is required, the specific limits of the parameters being monitored will need to be established in the permit.

Even though the CE and CAM rulemakings are distinct regulatory actions, there are complementary aspects to the two rules. As noted above, the CE rule will have the effect of eliminating any potential ambiguity regarding the use of non-compliance test data as a basis for Title V compliance certifications. Most importantly, the CE rulemaking affects the potential consequences of identifying deviations in a compliance certification based on CAM data instead of data from the compliance or reference test method.

The current implementation schedule for CAM is after promulgation of the standard (which could be any time). All permits issued 18 months following promulgation must comply with CAM requirements. Wyoming DEQ plans to issue the trona plant permits prior to this so that the initial permits may not need to define the CAM compliance plan. Under this scenario, a CAM compliance plan will need to be implemented in the second round, or implemented in the application that will be submitted in 2002. This should allow time to develop a compliance plan. Where parametric monitoring is the best answer, a significant amount of data may be required to establish parameters that accurately monitor performance and allow the establishment of enforceable limits for the parameters.

Hazardous air pollutants (HAP) (section 112(g))

Under the Clean Air Act Amendments of 1990, EPA is required to regulate large or "major" industrial facilities that emit one or more of 188 listed hazardous air pollutants (air toxics). Air toxics are those pollutants that are known or suspected of causing cancer or other serious health effects. On July 16, 1992, EPA published a list of industrial source categories that emit one or more of these hazardous air pollutants. This list does not currently contain the trona plants, but EPA is required to develop standards for industrial categories of "major" sources (those that have the potential to emit 10 tons/year or more of a listed pollutant or 25 tons/year or more of a combination of pollutants). Based on the recent PSD applications, EPA will need to address the availability of stringent controls, known as maximum achievable control technology (MACT).

Section 112(g) is designed to ensure that emissions of toxic air pollutants do not increase if a facility is constructed or reconstructed before EPA issues a MACT or air toxics regulation for that particular category of sources or facilities. In effect, 112(g) is a transitional measure to ensure that facilities adequately protect the public from toxic air pollutants until EPA issues a MACT standard that applies to the facility in question.

EPA proposed the 112(g) regulation in April, 1994. EPA delayed issuing the final 112(g) regulation in order to work out a number of complex issues, including defining construction and reconstruction of major sources, and to develop the best way to integrate the program with existing state programs.

EPA's final rule streamlines the process by limiting the 112(g) requirements to the construction of new facilities, and the reconstruction (rebuilding) of large sources of toxic air emissions at existing facilities. For example, an existing facility would only be subject to 112(g) requirements if it added or rebuilt a large production line or process that emitted toxic air pollutants above the "major" source threshold (e.g., above 10 tons annually for any single listed pollutant, or above 25 tons annually for a combination of listed pollutants).

Section 112(g) is primarily a transitional provision designed to operate until EPA issues air toxics or MACT standards. EPA anticipates that most MACT standards will be in place by the year 2000. Therefore, EPA believes that section 112(g) will yield the most public health and environmental benefits by requiring stringent controls on newly constructed or rebuilt large sources of toxic air pollutants (where uncontrolled emissions are likely to be the highest), where an applicable air toxics regulation has yet to be issued.

Sources or facilities subject to 112(g) will be subject to stringent air pollution control requirements, referred to as "new source MACT." Under the Clean

Air Act, new source MACT control is required to be no less stringent than the best controlled similar source or facility. Section 112(g) requirements apply to new major process or production units at existing sites. A new addition qualifies as a discrete process or production unit if the collection of equipment or structures produces an intermediate or final product independently, in substantial degree, from the existing equipment or structures.

EPA anticipates that the new source MACT requirements will be equally or more stringent than the requirements in the air toxics or MACT standard that EPA will later issue for the industrial source category in question. However, should the new source MACT requirements prove to be less stringent than the air toxics regulation that EPA later issues, the source or facility will be provided additional time to comply with the air toxics or MACT standard.

EPA's final rule provides an 18-month transition period for states to make adjustments in their programs to comply with 112(g) requirements. For states that are unable to adopt these requirements within the designated time-frame, the EPA will basically provide the review and approval of case-by-case MACT determinations.

Relative to the recognized emissions of VOCs, including some HAPs, EPA has requested the Wyoming DEQ to develop a MACT standard. A review of the available control technology for controlling the VOC emissions from the trona industry will likely be undertaken by DEQ or EPA in the near future.

Accidental release (section 112(r))

In response to environmental disasters such as the release of toxic gases near Bhopal, India and others, Congress added the 112(r) requirements in the Clean Air Act Amendments of 1990. Regulations have now been developed which affect every facility storing large quantities of chlorine, ammonia, sulfuric acid, and many other chemicals. The regulations require a process safety management (PSM) plan, an emergency response plan, and an "off-site consequence analysis." There are some similarities of this program to the Process Safety Management requirements found in OSHA. A key difference, however is the requirement to communicate the risk to the public.

A critical part of this program is the off-site consequence analysis. The regulations require that the analysis be performed on a "worst case" basis. Under this scenario the assumption is made that all of the material stored is released in less than 10 minutes. Standard dispersion models are then used to predict the worst case consequences. This has a potential to over-predict the real potential for an accident. Water treatment plants storing chlorine, for example, could have the worst case off-site consequence analysis result in a predicted limit of severe environmental risk several miles from the source.

If the worst case prediction appears to be unacceptable, an alternative can be presented. This alternative is based on the most likely event resulting in a severe accident. Passive and active controls such as chlorine scrubbers, can be part of the alternative scenario. An objective of this program is to inform the public of the potential risk. The "worst case" information may not present a realistic picture, and it is likely that most facilities will need to develop alternative scenarios to adequately provide enough information for the public to make an informed judgment concerning the potential risk. If a plant is affected by this program, early planning, review of the risk management procedures, and allowing time to adequately consider alternative scenarios will be important.

Fine particulates and ozone

The new proposed standards for fine particulates and ozone may affect the trona industry in a number of ways. First, Sweetwater County is likely to exceed the ambient air quality standards, requiring the DEQ to develop a plan to bring the county into compliance. This plan would likely require emission reductions from trona industry sources. In addition to potential requirements for reductions in primary particulates, there is an even greater potential for rules to reduce NO_x and SO_2 emissions.

The technology of this rule is developed in parts of the country where nitrates and sulfates contribute significantly to fine particulates, and the aim of the legislation is to reduce NO_x and SO_2 emissions. The City of Denver has already developed a rule that requires new source tradeoffs of NO_x and SO_2 emissions in the Denver particulate non-attainment area. Although the trona industry is not responsible for large amounts of sulfur dioxide, there are significant emis-

sions of NO_x. The NO_x emissions are the subject of several investigations including the Green River Visibility Study. Emissions of nitrogen oxides are a concern of the Federal land managers in the region in regard to the effect of NO_x on regional haze and pH of mountain lakes. Although not a target of the regulation, another source of fine particulates may be condensable hydrocarbons, again raising the issues of VOC emissions from the processing of trona ore.

The impact of the proposed revisions on the ozone standard is less predictable, and possibly less onerous. The Wyoming standard is currently more stringent than the Federal standard, and is based on a 1-hour averaging period. Key provisions of the proposed standard include revisions of the averaging time and the manner in which the concentrations in a region can be averaged. The result may be a relaxation of the Wyoming standard.

New Source Review (NSR) reform

The New Source Review regulations have not substantively changed since the late 1970s. EPA is now responding to the requirement to periodically review existing regulations and has proposed to reform the NSR rules. A major aspect of the NSR is to increase the role of the Federal land manager (FLM) in the permit review process. One of the problems has been that the FLM's comments were received relatively late in the permit review process (usually during the public comment period). This has lead to delays and has placed the permit review agency in a difficult position. The reform proposal formalizes the involvement of the FLM early in the process. In the Western United States where there is so much Federal land, the FLM's concerns must be considered during the preparation of the permit application. The issues will probably not change, but the procedures and the role of the FLM will be better defined. The primary areas of concern are referred to as Air Quality Related Values (AQRVs) and include visibility, the potential for acid rain, and other impacts to wildlife or vegetation.

Greenhouse gases

The control of greenhouse gases, including emissions of CO_2, has been discussed for several years. Control of CO_2 from fuel combustion sources is best achieved through increased combustion and process efficiencies. In July, 1996 the United States presented an outline for negotiation of the next steps under the Framework Convention on Climate Change. In December, 1996, the U.S. further elaborated its ideas by describing key elements that should be included for discussion in a protocol to guide the reduction of greenhouse gas emissions in the post-2000 period.

The broad framework resembles the concept of emission trading developed for the reduction of acid rain. Basically, each country will be issued emission allowances and a time schedule for reductions of emissions. These reductions could be accomplished either through actual reductions or through purchase of excess reductions from another country.

The proposal calls for periodic review of the agreement as scientific knowledge and information increase; it also requires the parties to establish long-term goals for atmospheric greenhouse gas concentrations.

Although the protocol reached at Kyoto called for a 12% reduction in carbon-equivalent emissions in the United States by 2005, it has not yet been ratified by Congress. However, a consensus that global warming and climate change are of real concern is beginning to develop. Several connections have been made between global climate change and storms, typically blamed on El Niño, or other forms of severe weather, which should increase pressure to reduce the production of greenhouse gases, including CO_2.

Summary

In summary, several new and proposed regulations will create additional challenges for the trona industry as soda ash production continues to grow and as additional resources are developed. As emissions of VOCs from the heating of trona ore are better defined, the applicability of existing and proposed regulations will need to be reviewed. As the Kyoto Protocol is implemented into regulations, reduction in the generation of CO_2 may be required to offset emission increases associated with facility expansion. One of the critical issues in the near future will be to establish adequate compliance demonstration meth-

ods during the development of Title V permits. Planning ahead for the CAM and CE requirements will minimize the impact of these regulations, and minimize the impact to the cost of production.

Tailings disposal methods

David H. Scriven
Western States Mining Consultants, P.C.
Casper, Wyoming 82601

Abstract

Trona is currently being produced from beds 17, 20, 24, and 25 in the Green River Basin. These trona beds are composed of sodium sesquicarbonate (trona), oil shales, mudstones, and claystones. They are underlain and overlain by oil shales, mudstones, and claystones. The trona beds are mined occasionally with portions of the underlying floor and overlying roof rock. The resultant feedstock to the refineries ranges in purity from a low of 75% to a high of nearly 95% trona.

Each of the five operating plants uses a process to dissolve the trona. The portion which is non-soluble, (oil shale, mudstone, and claystone) is referred to as insols or tailings and must be disposed of. The methods to dispose of the tailings differ for each of the operations. Both surface and underground methods are used and range from rather simple to highly sophisticated processes. Basically, five disposal methods are used in the basin:

Surface – non-managed. This method transports tailings via slurry pipelines to a tailings reservoir and deposits the tailings in a single-point discharge.

Surface – managed. Tailings are transported via slurry pipelines to a tailings reservoir using a multi-point discharge system for controlled deposition.

Underground – non-managed. Tailings are pumped down blind drill holes into mined-out, inaccessible areas of the mine.

Underground – managed. Tailings are pumped into the mine through a pipeline installed in the shaft and then into a mined-out accessible area of the mine. Retaining walls are constructed to contain the tailings in the mined-out rooms.

Underground – highly managed. Tailings are converted to a low-liquid paste and pumped into mined-out accessible areas of the mine.

Introduction

One of the big challenges of processing trona as well as other minerals is handling the solid waste material known as tailings. This paper describes why tailings exist, how they are separated from the ore, and several methods used for their disposal.

Trona is a naturally occurring evaporite mineral which formed in Lake Gosiute (of the Green River Basin) during the Eocene Epoch when the basin was subsiding and the Uinta Mountains were rising. At times, conditions existed when water was unable to flow out of Lake Gosiute, causing the lake to become brackish, then saline. Sodium sesquicarbonate (trona) was precipitated in the lake, especially during periods when water inflow was restricted and evaporation occurred, ultimately forming beds of trona. This evaporation and trona deposition cycled with periods of heavy inflows and abundant algal growth (vegetation) in the lake. During these periods, oil shale, mudstone, claystone, and sandstone were deposited.

During trona deposition, other sediments were also deposited with the sodium sesquicarbonate, including clay, silt, and organic materials. This caused impurities in the trona which constitute the tailings.

Trona processing

Simply stated, in the five operating plants in the Green River Basin, trona is processed by dissolving the sodium sesquicarbonate and recrystallizing the salt in the form of soda ash (sodium carbonate). The insoluble portions of the ore are removed from the process by various types of classifiers. These insolubles, which are principally claystone and oil shale, are referred to as tailings. These insolubles account for 6 to 25% of the ore mined, with an average of about 12%. Over 10 million short tons of soda ash produced in the Green River Basin each year require mining over 18 million short tons of trona. This equates to production of nearly two and a half million short tons per year of insolubles or nearly seven thousand short tons per day of tailings requiring disposal.

Disposal methods

Soda ash has been produced in the Green River Basin since the 1940s, but large-scale production really started in the 1960s. In the early days, most of the soda ash producers used the same basic method for tailings disposal. A pond was built away from their plant and the tailings were pumped through slurry pipelines to the pond. Some of the companies recovered the water for reuse in the plant, others just allowed the water to evaporate. One company cleaned the ponds out when they filled up, others just raised the embankments so they could hold more. They were all more or less non-managed facilities. This seemed like a fairly simple and inexpensive way to handle the problem. It turned out to be neither simple nor inexpensive. Now there are as many disposal methods utilized in the basin as there are trona mines. Disposal methods can be classified into two major categories–surface disposal methods and underground disposal methods.

Surface methods

All of the plants still use surface methods to some degree. They range from totally non-managed facilities to managed facilities with controlled deposition. In a non-managed facility, which is still the most common type of surface facility, tailings are slurried to an impoundment, sometimes at great distance from the plant, and deposited through a single-point discharge with sub-aqueous deposition of the tailings. This means the tailings are allowed to settle out under water. The tailings are just allowed to run into the pond, forming a poorly consolidated beach. The transport water is allowed to evaporate.

In a managed system, multiple offtakes are utilized (**Figure 1**). This system is used by General Chemical Corporation. This is a sub-aerial depositional method in which the tailings are allowed to settle out under air. A spray bar reduces the energy of the tailings as they are discharged, forming a consolidated beach. Ideally,



Figure 1. Surface managed trona tailings at General Chemical Corporation's trona plant. Note multiple outtakes being used.

the offtakes are rotated on a daily basis, laying down a thin layer of tailings. As the tailings drain and dry, a large negative pore pressure is induced which causes further consolidation. Under-drains aid in the drying and consolidation process. Water from this system is decanted (from the tailings cell) into an adjacent pond where it is returned to the plant for reuse. Further advantages are seen when enlargements are made to the facility.

By building a solid beach, upstream construction methods (**Figure 2**) can be used to raise embankments. The cost advantage is clearly seen by using this

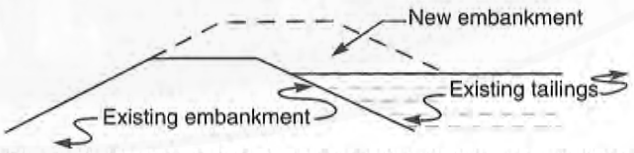


Figure 2. Upstream construction methods for raising tailings embankments.

type construction rather than the more common downstream construction methods as shown in **Figure 3**. In addition, the fill material requirement is less with the upstream method because it forms a solid, well-drained beach.

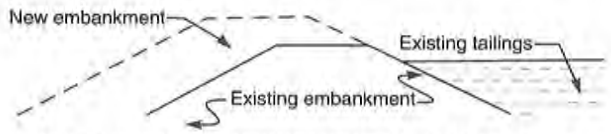


Figure 3. Downstream construction methods for raising tailings embankments.

Tailings can be used as borrow material to construct the embankment. This has two distinct advantages: the borrow material is close by, which reduces construction costs, and pond volume is created in the process of building the embankment. This upstream construction system does create a low-permeable facility, but an erosion blanket is required under the offtake system to prevent slope erosion.

The depositional technique used in the upstream construction method results in a drained, consolidated deposit of laminated tailings which provides strict control of seepage during operation, and, since the tailings are fully drained and consolidated at all times, allows for relatively easy reclamation and the elimination of long term environmental concerns.

Underground methods

Four of the plants in the Green River Basin currently use underground methods to dispose of tailings. These methods also range from non-managed to managed facilities. As opposed to the surface disposal methods, a managed system is not necessarily favored over a non-managed system. They both have their place depending on the particular mine and the configuration of the mined-out areas.

The non-managed facilities simply drill an injection hole into their mined-out workings and pump tailings into the mine. **Figure 4** is a schematic of an injection well similar to the method used by FMC. This technology initially developed by the U.S. Bureau of Mines for backfilling abandoned coal mines is a good system for putting tailings underground. As the cone or donut, as it is called, builds up in the abandoned mine workings, the cross-sectional area of the flow is decreased which increases the flow velocity to carry tailings farther into the old mine workings. The water is collected at a low point in the mine and pumped back to the surface. To operate a system such as this requires extensive mined-out workings which after 50 years of operation, FMC has, and a low point in the mine accessible to install a pump station. These systems typically require a water content of 80 to 90%. Multiple wells must be drilled with pressure valves which automatically switch the flow to another injection well when the well being used fills or plugs up. This is rather simple since the injection well operates at negative pressure and any pressure in the line is an indication the well is plugging.

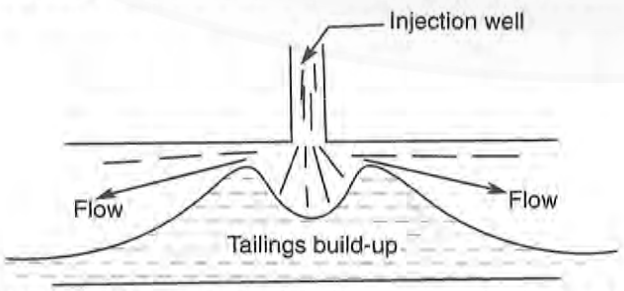


Figure 4. Underground schematic diagram of a blind hole (non-managed) tailings disposal system.

Tg Soda Ash also uses a non-managed system; however, it is dynamically different from the FMC method in that blind holes are not drilled into the mined-out workings but into the gob pile resulting from their shortwall operation. The gob pile is the rubbilized area created from the roof failing behind the mining operation. Holes are more difficult to complete in the gob pile but the system appears to be working fairly well. The company initially drilled five holes and has been pumping into the first one since 1993. They put only a part of the waste stream underground, however.

The managed systems slurry their tailings down a pipe installed in the shaft, then to a mined-out panel where the tailings are deposited. At the Solvay mine, the mined-out panel to receive the tailings is divided into sections as shown in **Figure 5**. Dams are constructed across all three entries, in a cross cut. The first three dams are constructed of a biaxial geogrid with filter fabric heat-bonded to it (**Figure 6**). The dams are supported by cables anchored at both ends of the cross cuts and in the roof. These dams hold back the solids yet allow all the excess water to seep out. Tailings are transported to the panel via 4-inch diameter steel pipe. The water is collected at a low point in front of the dam and pumped to a sump which is located at the center entry of a submain.

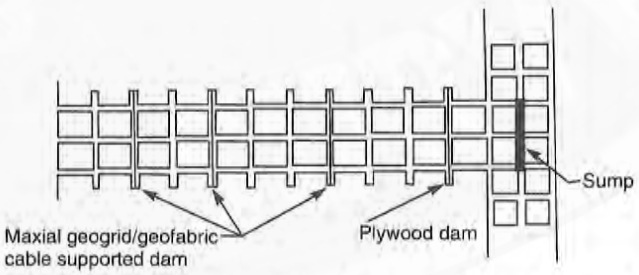


Figure 5. Schematic diagram of a managed underground tailings disposal system, as used by Solvay in a tailings panel.



Figure 6. Biaxial geogrid fabric dam used in Solvay's underground tailings panel.



Figure 7. Plywood dam in Solvay's underground tailings panel disposal system.

The final dam in the panel is constructed with plywood (**Figure 7**). From the sump, the water is pumped to a tank at the pump station where it is returned to the surface. The pump station has a series of positive displacement pumps used to return the supernatant liquid back to the surface. The optimum water-to-solids ratio in the slurry has been determined to be approximately 2:1.

OCI's Tailings Returned to Mine (TRM) system has been in operation for the past few years. Approximately 90% of the tailings are sent back to the mine. The TRM system makes a low-water-content paste which is pumped down the shaft to mined-out panels and deposited. Laboratory tests indicted a water content of 42% would create a stable colloidal mixture but actual operations require a water content closer to 47%. The tailings create a little bleed water which has to be collected and returned to the surface.

Conclusion

Tailings disposal is not the most popular capital project the trona plants in the Green River Basin have to deal with because their return on investment is not as favorable as something which aids production. However, a penny saved is a penny earned and opportunities are still available to save money (such as recovery of Na_2CO_3 from waste water returns). Most of the operators, however, are now working hard to make their systems as efficient as possible as they are beginning to realize that 7000 tons a day of waste will be a larger expense if not dealt with properly.

I would like to offer special thanks to the staffs at General Chemical Corporation, Solvay Minerals, and Tg Soda Ash for their hospitality and help in preparing this paper.

Road log for the geology field trip of June 13, 1997

Geology and outcrops of the trona-bearing rocks of the Green River Formation

William C. Culbertson,
Field trip leader
U.S. Geological Survey
Denver, Colorado 80225

Segment I – Firehole Canyon

Enter U.S. Interstate Highway I-80 from Dewar Drive, Exit 102. To the northwest is White Mountain where all three members of the Eocene Green River Formation are exposed. The Tipton Shale Member is at the base, then the Wilkins Peak Member, and Laney Shale Member at the top. All of the trona beds in the Green River Basin occur in the Wilkins Peak Member (**Figure 1**). Take Exit 99 to State Highway 191 southbound (the East Flaming Gorge road). Mileage starts where Highway 191 crosses I-80.

Cumulative Mileage	Incremental Mileage	
0.0	0.0	The next 19 miles are on the fluviatile Eocene Wasatch Formation, which is dipping westward (off the western flank of the Rock Springs uplift) into the Green River Basin. Massive lenticular sandstones and channel-fill sandstones can be seen in road cuts and outcrops.
4.5	4.5	The highest peak to the right (west) is Wilkins Peak, the type locality of the Wilkins Peak Member of the Green River Formation.
11.4	6.9	Turnout on road gives excellent view of the Green River Formation in Middle and Little Firehole Canyons. Red beds of the Wasatch are in the foreground. The base of the Tipton Shale Member is halfway up the barren hill. Conspicuous red ledges at top of hill result from the burning of the rich oil shale in the Tipton.
13.7	2.3	Turn right (west) on road to Firehole Campground.
19.2	5.5	The contact between the Green River and Wasatch Formations is on the slope in the foreground. In the distance is Chimney Rock, where a sandstone caprock overlies about 180 feet of oil shale in the Laney Member.
20.1	0.9	On right are the ledging oil shale beds of the upper part of the Tipton Shale Member, overlain by platy marlstone of the Wilkins Peak Member.
20.8	0.7	Sandstone-mudstone Unit A exposed in road cut. Near its base, it contains a persistent 4-foot-thick lacustrine sequence consisting of interbedded oil shale, marlstone, limestone, a tuff, and basinward, a thin trona bed.
21.3	0.5	**Stop 1.** An excellent exposure of the lacustrine sequence from Unit B to Unit C, which includes the stratigraphic positions of trona beds 17 and 18 (**Figure 2** and **Table 1**). If present, bed 17 would be about at the white layer, and bed 18 would be near the top, just below a tuff bed. This sequence includes alternating thin beds of oil shale, marlstone, and thin layers of limestone. Abundant calcite pseudomorphs after shortite occur throughout these beds.

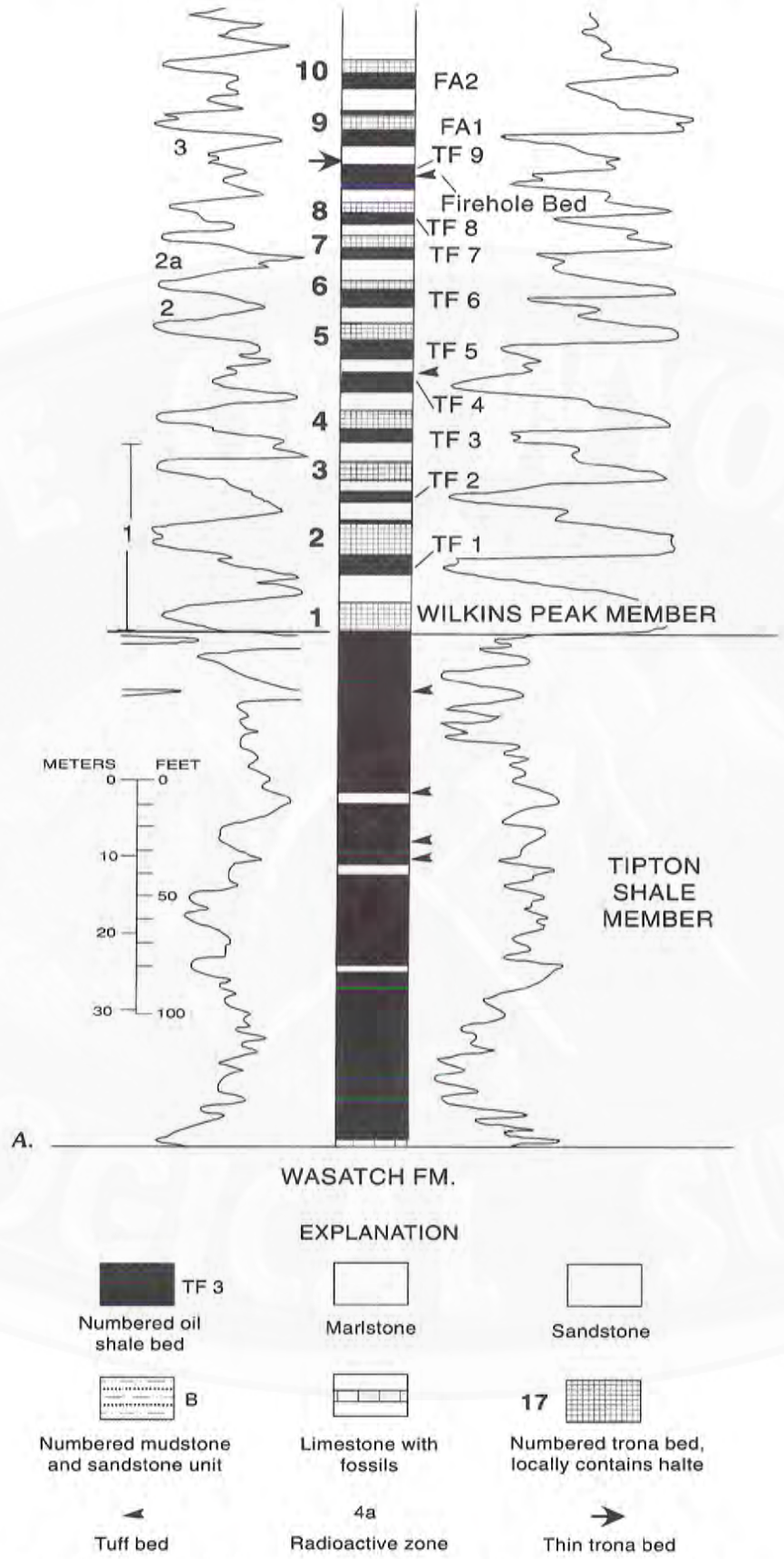


Figure 1. Generalized columnar section of the Green River Formation. A, Tipton Shale Member and lower part of Wilkins Peak Member; B, middle part of Wilkins Peak; C, upper part of Wilkins Peak and lowermost Laney Shale Member.

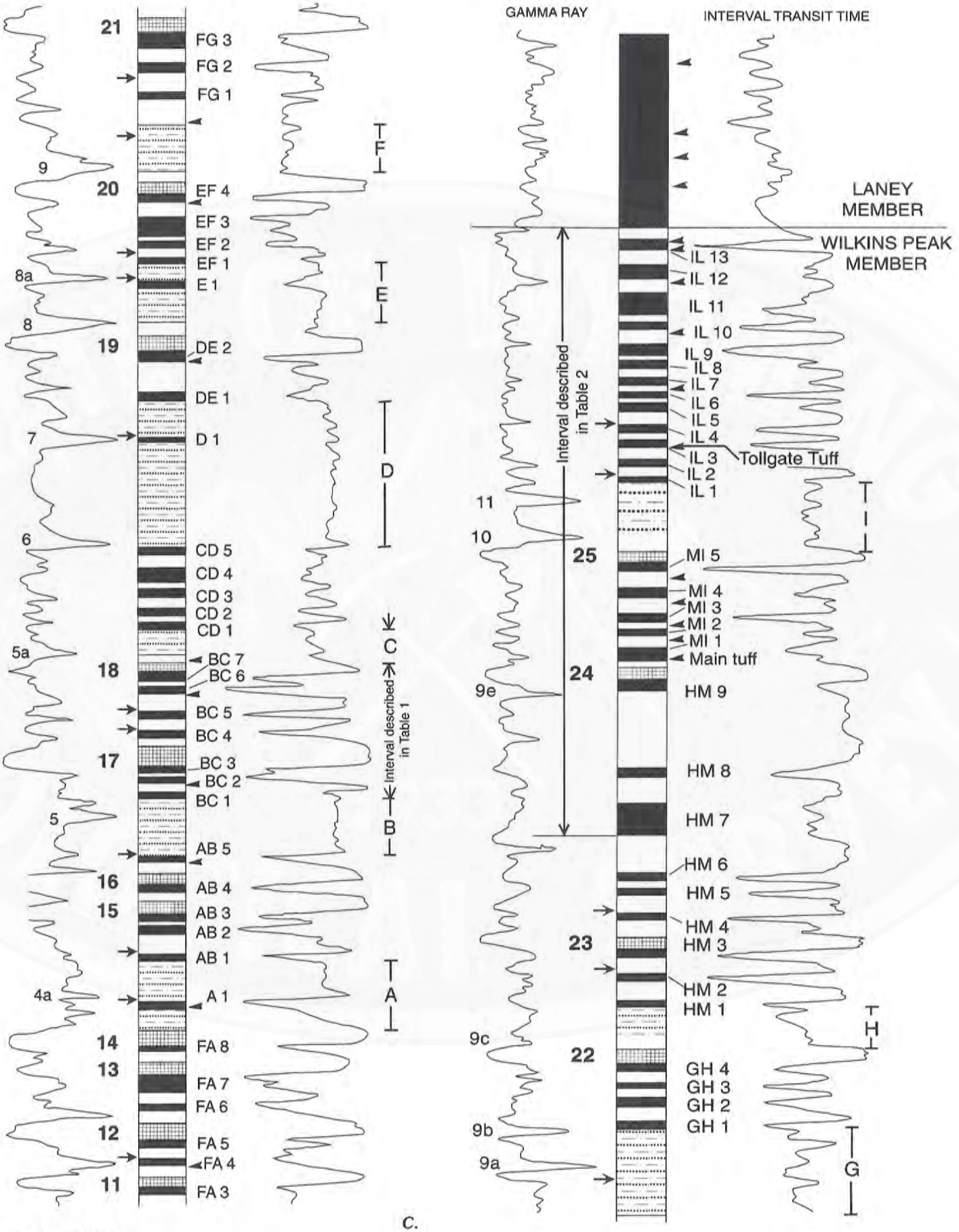


Figure 1 continued.

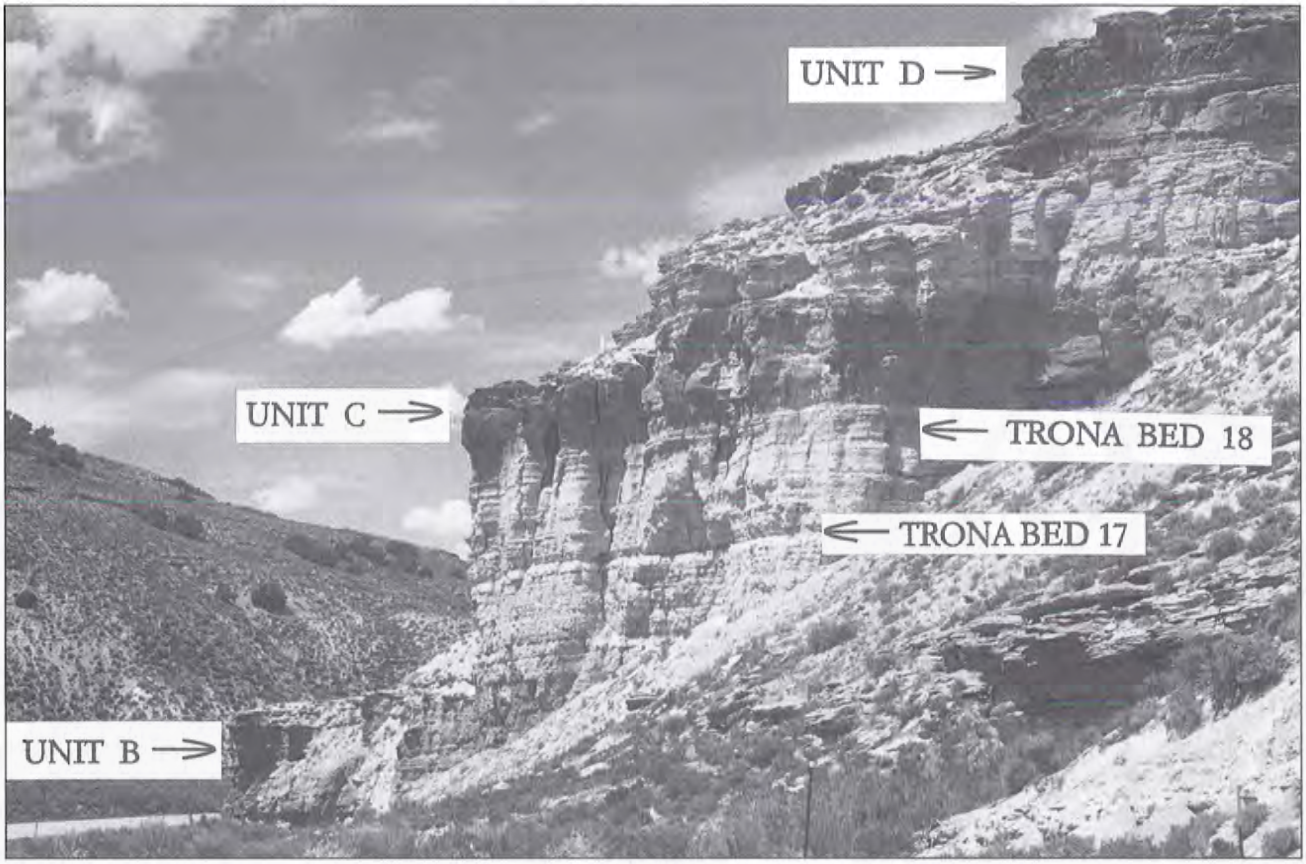


Figure 2. View of Firehole Canyon measured section.

Cumulative Mileage	Incremental Mileage	
22.3	1.0	Unit D at roadside, the thickest and most extensive of the nine sandstone-mudstone units, A through I (**Figure 1**).
24.1	1.8	Entrance to campground. This place provides an excellent view of the upper half of the 1100-foot-thick Wilkins Peak Member. The sequence from Units D through H contains ledging beds of sandstone alternating with slope-forming lacustrine beds. Above Unit H is a 290-foot-thick slope-forming sequence, principally of lacustrine beds, except for the fluviatile Unit I in the middle. Above this are brownish ledges of the varved oil shale beds of the Laney Member. Return to Interstate I-80 via East Flaming Gorge road.

Segment 2 – Tollgate Rock

0.0	0.0	At Exit 99 take I-80 westbound towards Green River.
0.2	0.2	To the right, the contact between the Tipton Shale Member and the underlying Wasatch Formation is about 30 feet above the highest red bed. The contact is marked by a thin bed of fossiliferous limestone, the *Goniobasis* marker. The Tipton is 145 feet thick here, and the upper 40 feet is ledging oil shale capped by silty marlstone beds of the Wilkins Peak that form a conspicuous bench.

Cumulative Mileage	Incremental Mileage	
2.5	2.3	Road cut in upper oil shale of the Tipton Shale Member.
3.8	1.3	Road cut in the lower Wilkins Peak Member, exposing horizons of trona beds 5 through 8. Just above the road cut is the Firehole bed, an orange brick-like bed of altered tuff.
7.2	3.4	Road cut in Unit D, which displays crossbedding and scour structures. Above are the white-weathering beds that gives White Mountain its

Table 1. Partial measured section of the Wilkins Peak Member that includes stratigraphic positions of trona beds 17 and 18 (see Figure 1B for details). From Firehole Canyon measured section C70-16. Located in NE¼ SW¼ sec. 19, T16 N, R106 W; measured by W.C. Culbertson

Cumulative thickness (feet)	Interval thickness (feet)	Lithologic description
		Unit C
47.4	1.8	Marlstone, silty
45.6	2.0	Limestone, thin bedded with 0.2' calcite layer
43.6	0.4	Tuff
43.2	1.3	Limestone, thin bedded with 40% calcite layer
41.9	2.4	Marlstone. With 0.5' oil shale in middle
--	--	(Position of trona bed 18)
39.5	0.6	Oil shale, lean **(BC-7)**
38.9	0.9	Marlstone, recess
38.0	4.6	Calcite crystals in 50% marlstone matrix
33.4	1.5	Oil shale **(BC-6)**
31.9	1.2	Limestone, thin bedded
30.7	2.0	Marlstone
28.7	1.5	Oil shale **(BC-5)**
27.2	2.9	Limestone, thin-bedded
24.3	0.6	Interbedded marlstone and limestone
23.7	1.2	Oil shale **(BC-4)**
22.5	0.4	Marlstone pebble conglomerate
22.1	2.0	Marlstone, lower 1' recess
20.1	2.1	Marlstone, white band on cliff
--	--	(Position of trona bed 17)
18.0	1.4	Oil shale **(BC-3)**
16.6	1.3	Marlstone
15.3	2.8	Oil shale **(BC-2)**
12.5	4.8	Marlstone
7.7	5.8	Oil shale **(BC-1)**
1.9	1.9	Limestone, silty, platy ledge, 0.2 foot algal limestone at top
0.0		Unit B

Notes: Abundant calcite pseudomorphs after shortite throughout section. **BC-1**, etc., are laterally persistent beds of oil shale in the Wilkins Peak Member. Their stratigraphic positions are shown on the generalized stratigraphic section of the Wilkins Peak Member (Figure 1B).

Cumulative Mileage	Incremental Mileage	
		name. Although the fluviatile Units E through H can be identified here, they do not make the conspicuous ledges as they do in Firehole Canyon.
7.3	0.1	Take Exit 91 to the town of Green River. Continue to the west edge of town.
10.2	2.9	Continue straight ahead on service road 374 (old U.S. Highway 30).
10.5	0.3	Turn right into parking area just east of Tollgate Rock.
		Stop 2. Tollgate Rock has excellent exposures of the sequence that includes the horizons of trona beds 24 and 25, including the Main tuff, Unit I, and the Tollgate (layered) tuff (**Figure 3** and **Table 2**). The sequence consists mainly of alternating beds of oil shale and marlstone, which contain abundant pseudomorphs of calcite after shortite. The tuffs are excellent marker beds. In particular, because of its unique layering, the Tollgate tuff can be recognized in outcrops and cores across more than 3000 square miles in the Green River Basin, ranging in thickness from 2.3 inches in the south to 6.9 inches in the north.
		End of field trip. Return to Rock Springs via I-80 eastbound.

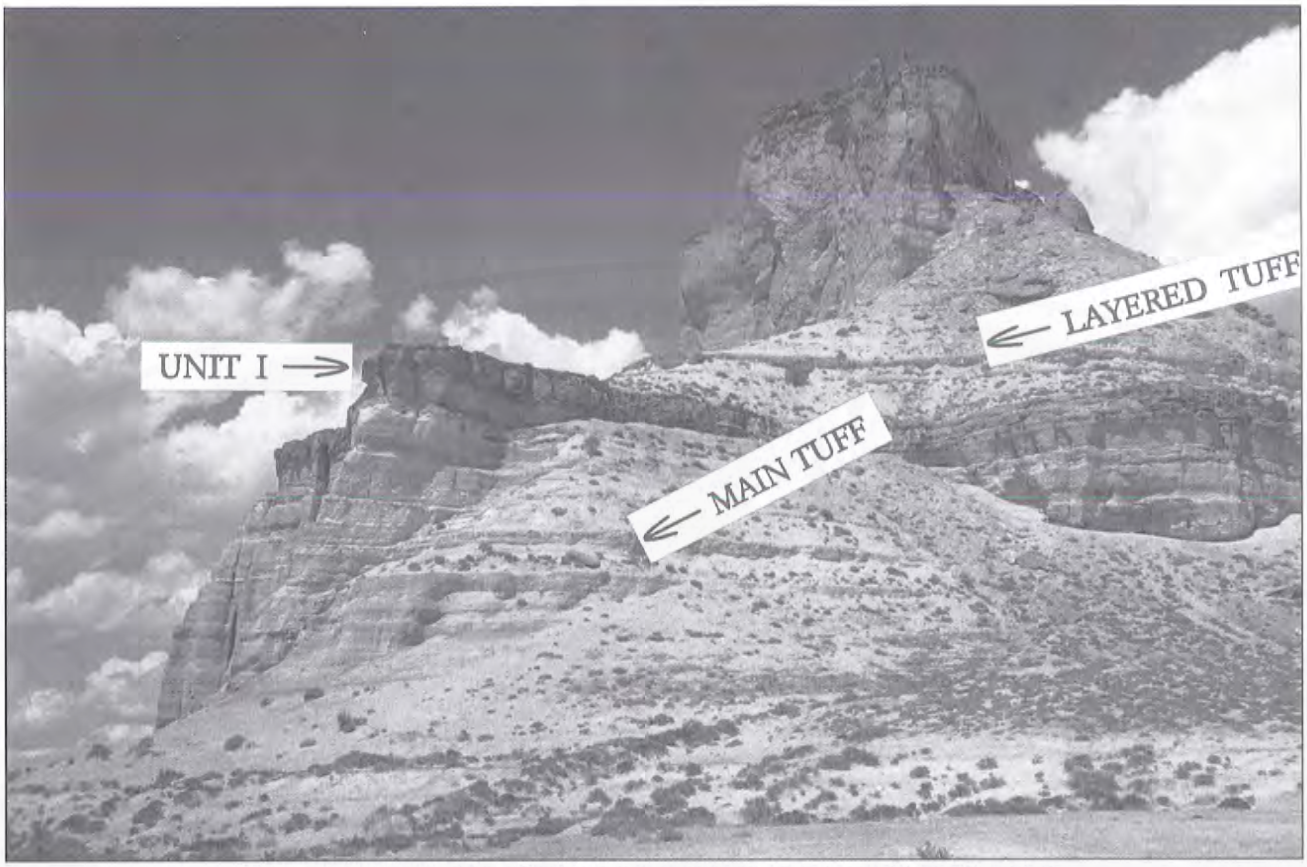


Figure 3. View of Tollgate Rock measured section near Green River, Wyoming.

Table 2. Partial measured section of upper part of Wilkins Peak Member that includes stratigraphic positions of trona beds 24 and 25 (see Figure 1C for details). From Tollgate Rock measured section at Green River, Wyoming. Located in NW¼ sec. 15, T18N, R107W, this section starts at base and on south side of cliff exposure; measured by W.C. Culbertson, July 1970.

Cumulative thickness (feet)	Interval thickness (feet)	Lithologic description	
		Top of Wilkins Peak Member (Laney Shale Member above)	
196.3	82.0	Marlstone with 5 beds of oil shale and 10 tuffs	
114.3	2.5	Oil shale, flaky, forms ledge **(IL-3)**	
111.8	0.2	Tuff, layered (Tollgate layered tuff)	
111.6	3.4	Marlstone, with stringers of shortite	
108.2	3.0	Limestone and limy marlstone, forms ledge	
105.2	1.5	Oil shale, rich, few shortite crystals, forms ledge **(IL-2)**	
103.7	0.07	Marlstone pebble conglomerate	
103.7	5.0	Marlstone, limy at base, forms ledge	
98.7	0.4	Oil shale, rich, forms ledge **(IL-1)**	
98.3	0.1	Marlstone pebble conglomerate	
98.2	8.0	Marlstone, 3-10% shortite, 0.1' tuff, forms slope	
90.3	1.3	Marlstone, oil shale, and layers of calcite, 0.07' tuff	
89.0	0.35	Tuff	
88.7	0.8	Marlstone with thin layers of oil shale, weak ledge	
87.9	2.0	Marlstone, limy, white spots	
85.9	4.0	Mudstone and siltstone	
81.9	8.5	Sandstone, very fine-grained, cross-bedded up to siltstone, forms ledge	**(UNIT I)**
73.4	3.4	Mudstone, silty, up to siltstone	
70.3	4.6	Marlstone, 20% shortite, with 0.06' tuff	
65.7	2.8	Marlstone with layers of calcite pseudomorphs	
--	--	(Position of trona bed 25)	

Table 2 continued.

Cumulative thickness (feet)	Interval thickness (feet)	Lithologic description	
62.9	1.3	Oil shale, rich, 10% shortite **(MI-5)**	
61.6	5.6	Marlstone, 50% shortite, in bands of crystals, 0.11 tuff	
56.0	3.3	Marlstone, white to greenish-gray, 20% shortite	
52.7	0.6	Tuff	
52.1	5.1	Marlstone, 50% shortite	
47.0	1.5	Oil shale, 20% shortite, algal bed? **(MI-3)**	
45.5	2.5	Marlstone, with 0.05' tuff	
43.0	0.9	Tuff	
42.1	1.2	Oil shale, 20% shortite	**(MI-2)**
40.9	0.8	Marlstone	
40.1	1.4	Oil shale, 60% shortite	
38.7	0.15	Tuff	
38.5	2.0	Marlstone, abundant shortite	
36.5	0.4	Oil shale	
36.1	0.2	Tuff	
35.9	3.6	Oil shale, 60% shortite **(MI-1)**	
32.3	0.75	Tuff (Main Tuff)	
31.5	5.6	Marlstone, 25-40% shortite, 0.09' tuff	
--	--	(Position of trona bed 24)	
25.9	4.0	Marlstone, 30-50% shortite, 0.06' tuff	
21.9	0.3	Oil shale	**(HM-9)**
21.6	1.4	Marlstone, 50% shortite	
20.2	0.8	Oil shale, 15% shortite, forms weak ledge	
19.4	10.4	Marlstone, 30-60% shortite	
9.0	0.4	Oil shale, shortite **(HM-8)**	
8.6	3.7	Marlstone, 50% shortite, forms slope	
4.9	4.9	Oil shale and marlstone, abundant shortite, 0.04' tuff **(HM-7)**	
0.0	0.0	Base of exposure	

Note: All shortite seen on the outcrop is actually calcite pseudomorphs after shortite. **HM-9**, etc., are laterally persistent beds of oil shale in the Wilkins Peak Member. Their stratigraphic positions are shown on the generalized stratigraphic section of the Wilkins Peak Member (Figure 1C).



Frontispiece: Aerial view of the trona mine and processing plant operated by OCI Wyoming, L.P. northwest of Green River, Wyoming. In 1997, this operation produced about 3.4 million net short tons of trona from the underground mine and refined about 2.0 million short tons of soda ash (data from Wyoming State Inspector of Mines, Annual Report for 1997). Photograph by John R. Dyni, July, 1998.

Luncheon talk of June 11, 1997
A new entrant's perspective of the Wyoming soda ash industry

John Wold
Wold Trona Company
Casper, Wyoming 82601

Abstract

Wold Trona Company's entry as the sixth Green River Basin soda ash producer is the culmination of 30 years' acquisitions of prospecting permits and sodium leases. The large investment requirements of the conventional monohydrate mine/plant operations has led the Wold approach to conventional underground mining and dry beneficiation of trona ore to 98% purity soda ash (Benetron® process) acceptable to a major portion of world markets.

The fines and rejects of the dry process has led Hazen Research to pursue the successful development of a revolutionary "Crystaltron®" process, a 99.5+% soda ash product, which has significant economic and physical advantages over the current Green River monohydrate product.

When Jack Kennedy was campaigning for the presidency in 1960, he came to Rock Springs and told us, in his Boston accent, what a great future lay ahead for us in "Soder Rash." Well, "soder-rash" is a contagious ailment and I would guess that most of us here have the itch.

Thank you for your flattering introduction. They say that flattery is good for you if you don't inhale it. Look what that man in Washington has got away with by not inhaling–so I won't inhale, but simply ask your indulgence and patience for some reminiscing and comments from one who has been an active player for almost fifty years in several of Wyoming's major minerals. I was launched as a professional geologist with the old Standard Oil Company of New York in 1939 in the Mid-continent and Gulf Coast. During the 58 years since, I have participated in the rise and now the decline of our domestic oil business–as well as participating in several cyclical phases of the uranium game–and the development of our sensational, unmatched coal resources.

Some 30 years ago a Casper friend of mine, Gene Simons, interested me in Green River Basin trona deposits as a passive investor. We filed on sodium prospecting permits and drilled some wells under what is now the Flaming Gorge Recreation Area. After Rogers Morton, as Secretary of the Interior, froze the issuance of federal preferential right sodium leases, I decided that our efforts with the U.S. Bureau of Land Management (BLM) to transfer those prospecting permits to leases, was like tilting with windmills. I made a business judgement and bowed out. Gene, God bless him, fought on–often pleading his own case in federal district court. He finally won some preferential rights after 29 years–that's persistence!

Well, while I bowed out of that one, I still had soder rash itch. In the late 1980s and early 1990s, experience in solution mining of uranium in Wyoming and Texas provoked me to speculate on the pros and cons of trona solution mining. That was not a new idea–FMC had made quite an investment in a trona solution mining program. Vulcan Materials and Allied Chemical spent several million apiece in the Green River Basin on unsuccessful solution mining. As we studied their activities, it appeared that their attempts to link up injection wells with producing wells by hydro-fracing presented some serious difficulties. Below 1000 to 1500 feet of overburden, it is difficult to keep hydrofractures in a horizontal plane–they tend to orient in the vertical plane. That orienting and caving can present real problems when you have multiple halite-bearing trona beds, vertically just a few feet from mineable trona beds. We felt that sophisticated horizontal drilling, developed by the oil and gas industry in the 1980s, could be the answer for linking injection and producing wells. That technology has been used successfully in the Piceance Creek Basin of Colorado for solution mining of nahcolite.

However, we have abandoned solution mining in our project at this time for several reasons. The Wold

sodium leases in our logical mining unit (LMU) are located south of the five present producers toward the depositional center of the basin. We have 15 trona beds to shoot at instead of 1, 2, or 3 that are available to the present operators to the north. While some of the multiple beds under our LMU carry halite, many significant halite-free beds give us exceptional conventionally mineable reserves. We will first be working trona bed 17 at depths comparable to the mines operated by FMC, Solvay, and General Chemical.

These impressive multiple-bed trona resources which we acquired from Occidental Chemical, Olin, and Vulcan–plus the shallow depth to bed 17, led two of our consultants, Gale Peters and Ralph Tacoma, to urge us to go to conventional underground mining and dry beneficiation of our ore. We determined that the high capital cost of a grass roots monohydrate facility puts a new entrant into the Green River Basin at an almost insurmountable economic disadvantage with the established producers in the trona district. Dry beneficiation might give us a way around that economic disadvantage for a start-up operation.

Our research indicated that significant soda ash markets do not require a 99.5% monohydrate ash. But they do require consistency of product, particularly in the glass market. Simple calcined trona yields an ash which is currently being marketed for animal feed. It has an inconsistent quality because the ore contains variable impurities due to geological conditions and unselective mining. Our dry beneficiated product which we call "Benetron®" has the consistency which almost all of the glass market requires.

Dry beneficiation sounds fine, but the grinding and handling of dry trona generates sizeable percentages of dust and rejects, which are called fines and middlings. You can dump them back underground, send them to a monohydrate plant, sell them in the limited low-grade markets, or try to develop a new technology. We decided on the latter option, one which had been chased unsuccessfully for many years in a number of major research efforts by the established industry.

Hazen Research of Golden, Colorado, has developed for us a proprietary crystallization process that produces "Crystaltron®," a soda ash product directly competitive or superior in certain respects to the monohydrate product. It has been characterized as a "technology breakthrough equivalent to the monohydrate improvement over the Solvay synthetic process." However one may wish to characterize it, our financial projections show the Wold "Crystaltron®" program has economics similar to our dry Benetron® process but yields a higher purity soda ash. Wayne Hazen and his staff have done a remarkable job for us with the help of Jim Herickoff (our Chief Operating Officer), Wayne Mortensen, Barbara Stuckert, and Rudy Pruszko, all key members of the Wold Trona team.

The capital investment in a start-up dry beneficiation or Crystaltron® mine/plant is roughly 1/3 that of a grass roots monohydrate installation of equivalent capacity. Per ton operating costs are 40 to 50% lower than the monohydrate process for a number of reasons, one of which is we don't have to evaporate 2 tons of water for every ton of ash.

The development of a new "mousetrap" in an established industry is not always welcome. It can invite negative rumors and obstructionism. Two Green River soda ash producers submitted the only appeals of our Environmental Assessment. Wyoming BLM reviews of those two appeals characterized them as "a transparent and egregious misuse of the appeals process" to stifle competition. The appeals were dismissed by the Interior Board of Land Appeals as having no merit.

We were pleased that our mine and plant permitting provoked no negative responses from environmental groups. Under the guidance of Gene George's Energy Compliance Corporation, permitting has gone smoothly. Our reception from all governmental agencies and the support of Governor Geringer has been most rewarding. But more than that, we have always felt welcome in Rock Springs and Green River. Those splendid people like new ideas and new business.

Peter Drucker has pointed out that "all great changes in business have come from outside, not from within" and "when an idea is right, you can't stop it–you may slow it down but you can't stop it."

Now, from a newcomer's perspective: there are many studies in our judgement, which could be undertaken beneficially on a cooperative basis by the producers here in the basin–producers who turn out almost 1/3 of the world's soda ash.

For instance, the surface and subsurface geology of the Green River Basin deserves more detailed attention than it has received in the past. What is the significance at depth, underground, of the extensive shear zones and fracture systems so apparent on the surface of the basin? How do fracture systems, which may run for miles, affect the migration of solutions

which may be introduced in large volumes by nature or by man? Do these fracture systems have a serious affect on mine planning, mine flooding, and solution mining of old workings? Can they threaten the safety of personnel working underground? We know that there is tectonic movement in the basin–induced both by nature and by mining. Should industry or governmental agencies sponsor multiple seismic monitoring for our better knowledge of those forces as they may affect mine safety and economics? These are questions that should be answered, perhaps best on a cooperative basis.

In the final analysis, we cannot overdo the beneficial exchange of information and geological mining knowledge–knowledge with its almost infinite variation and refinement. Knowledge is the key to economic growth and knowledge is the key to fulfillment of dreams.

STATE OF WYOMING
1933
GEOLOGICAL SURVEY

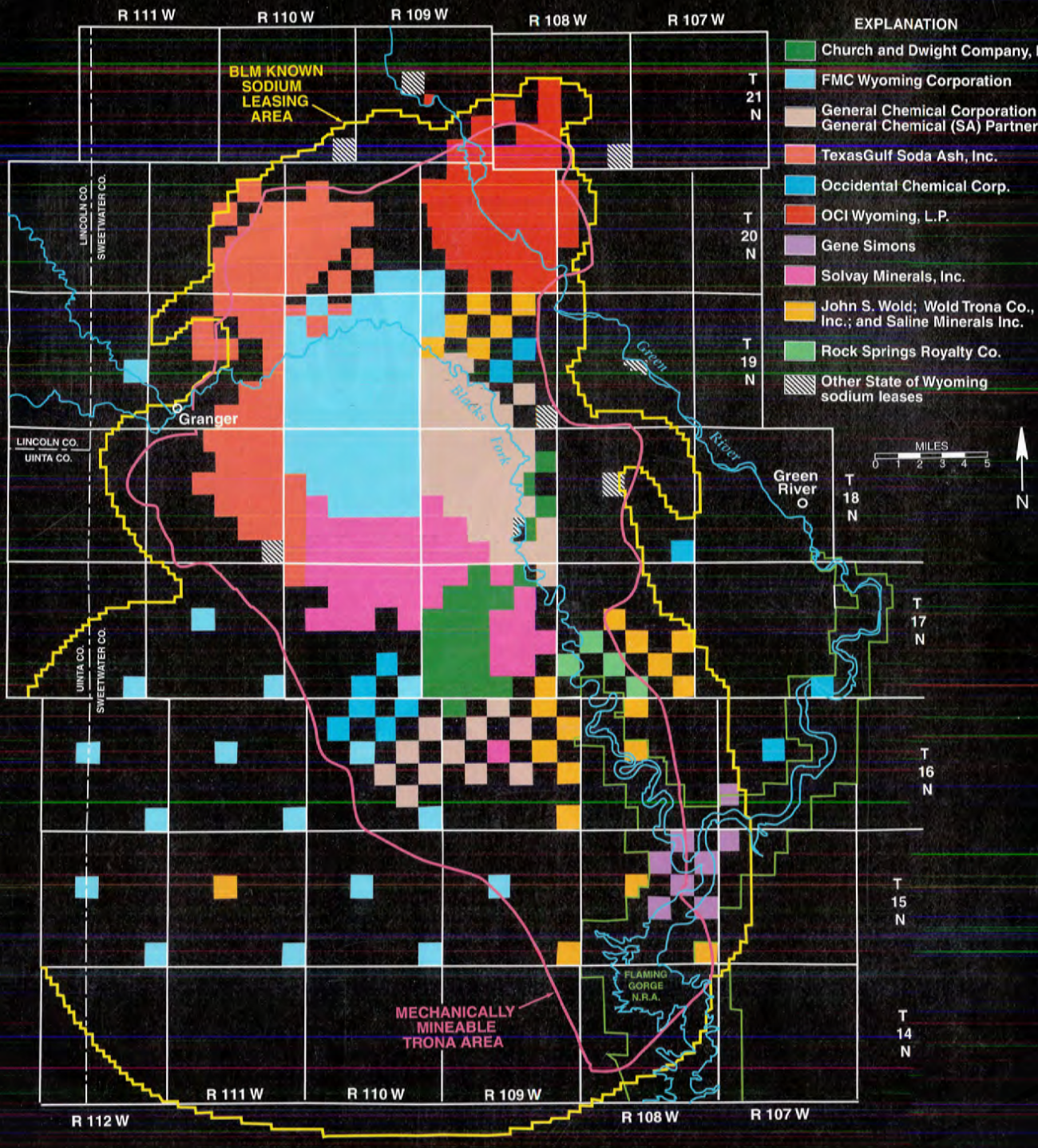
Selected conversion factors*

TO CONVERT	MULTIPLY BY	TO OBTAIN	TO CONVERT	MULTIPLY BY	TO OBTAIN
Length			**Pressure stress**		
inches, in	2540	centimeters, cm	lb in^{-2} (=lb/in^2), psi	7.03×10^{-2}	kg cm^{-2} (=kg/cm^2)
feet, ft	3.048×10^{-1}	meters, m	lb in^{-2}	6.804×10^{-2}	atmospheres, atm
yards, yds	9.144×10^{-1}	m	lb in^{-2}	6.895×10^{3}	newtons (N)/m^2, N m^{-2}
statute miles, mi	1.609	kilometers, km	atm	1.0333	kg cm^{-2}
fathoms	1.829	m	atm	7.6×10^{2}	mm of Hg (at 0°C)
angstroms, Å	1.0×10^{-8}	cm	inches of Hg (at 0°C)	3.453×10^{-2}	kg cm^{-2}
Å	1.0×10^{-4}	micrometers, µm	bars, b	1.020	kg cm^{-2}
Area			b	1.0×10^{6}	dynes cm^{-2}
in^2	6.452	cm^2	b	9.869×10^{-1}	atm
ft^2	9.29×10^{-2}	m^2	b	1.0×10^{-1}	megapascals, MPa
yds^2	8.361×10^{-1}	m^2	**Density**		
mi^2	2.590	km^2	lb in^{-1} (=lb/in^3)	2.768×10^{1}	gr cm^{-3}(=gr/cm^3)
acres	4.047×10^{3}	m^2	**Viscosity**		
acres	4.047×10^{-1}	hectares, ha	poises	1.0	gr $cm^{-1}sec^{-1}$ *or* dynes cm^{-2}
Volume (wet and dry)			**Discharge**		
in^3	1.639×10^{1}	cm^3	U.S. gal min^{-1}, gpm	6.308×10^{-2}	1 sec^{-1}
ft^3	2.832×10^{-2}	m^3	gpm	6.308×10^{-5}	m^3 sec^{-1}
yds^3	7.646×10^{-1}	m^3	ft^3 sec^{-1}	2.832×10^{-2}	m^3 sec^{-1}
fluid ounces	2.957×10^{-2}	liters, l *or* L	**Hydraulic conductivity**		
quarts	9.463×10^{-1}	l	U.S. gal day^{-1} ft^{-2}	4.720×10^{-7}	m sec^{-1}
U.S. gallons, gal	3.785	l	**Permeability**		
U.S. gal	3.785×10^{-3}	m^3	darcies	9.870×10^{-13}	m^2
acre-ft	1.234×10^{3}	m^3	**Tansmissivity**		
barrels (oil), bbl	1.589×10^{-1}	m^3	U.S. gal day^{-1} ft^{-1}	1.438×10^{-7}	m^2sec^{-1}
Weight, mass			U.S. gal min^{-1} ft^{-1}	2.072×10^{-1}	1 sec^{-1} m^{-1}
ounces avoirdupois, avdp	2.8349×10^{1}	grams, gr	**Magnetic field intensity**		
troy ounces, oz	3.1103×10^{1}	gr	gausses	1.0×10^{5}	gammas
pounds, lb	4.536×10^{-1}	kilograms, kg	**Energy, heat**		
long tons	1.016	metric tons, mt	British thermal units,	2.52×10^{-1}	calories, cal
short tons	9.078×10^{-1}	mt	BTU	1.0758×10^{2}	kilogram-meters, kgm
oz mt^{-1}	3.43×10^{1}	parts per million, ppm	BTU lb^{-1}	5.56×10^{-1}	cal kg^{-1}
Velocity			**Temperature**		
ft sec^{-1}(=ft/sec)	3.048×10^{-1}	m sec^{-1} (=m/sec)	°C + 273	1.0	°K (Kelvin)
mi hr^{-1}	1.6093	km hr^{-1}	°C + 17.78	1.8	°F (Farenheit)
mi hr^{-1}	4.470×10^{-1}	m sec^{-1}	°F - 32	5/9	°C (Celsius)

Divide by the factor number to reverse conversions.

Exponents: for example 4.047×10^{3} (see acres) = 4,047; 9.29×10^{-2} (see ft^2) = 0.0929.

Back Cover: Lands leased for trona in the Green River Basin, Wyoming as of July, 1998. Includes federal, state, and Union Pacific Resources leases. For more detailed maps of this same area, see articles in this volume by Kemp and Harris, pages 105 to 108; Murphy, pages 109 to 112; and See and Brown, pages 113 to 119. Map modified from Murphy, 1998, page 110 (this volume).



STATE OF WYOMING GEOLOGICAL SURVEY 1933

Geology -- Interpreting the past to provide for the future

ISBN 1-884589-14-6